Gene Poe

SPECIAL SENSOR MICROWAVE/IMAGER USER'S GUIDE

NAVAL
RESEARCH
LABORATORY

WASHINGTON, D.C.

ACKNOWLEDGEMENT

The authors wish to thank CDR D. McConathy, now retired who played a large role in developing and supporting the procurement of the SSM/I instrument, CDR F. Wooldridge, Space and Naval Warfare Systems Command, who initiated this calibration/validation effort and made it possible, CDR T. Piwowar, Office of the Chief of Naval Research, and LCDR L. Burgess, Navy Space Systems Activity, who continued the Navy effort, and Colonels S. McElroy and A. Curtis, Directors of the Defense Meteorological Satellite Program Office, for their direction and strong support throughout the project. Special thanks are due Ms. L. Ridgely and Ms. M. Spangler who typed, proofread and assembled this report.

TABLE OF CONTENTS

1.0 INTRODUCTION

The first Special Sensor Microwave/Imager (SSM/I) was launched 19 June 1987 aboard the Defense Meteorological Satellite Program (DMSP) Block 5D-2 Spacecraft F8. The SSM/I represents a joint Navy/Air Force operational program to obtain synoptic maps of critical atmospheric, oceanographic, and selected land parameters on a global scale. These include detection and measurement of rain storms over land, measurement of the local and large scale variability of ocean surface windspeed for ridge, front, and storm weather systems, mapping of sea ice concentration and ice/water boundaries for routing of ships as well as mapping of land surface parameters. Table 1.1 presents a summary of the primary environmental parameters to be retrieved from the SSM/I along with the spatial resolution, parameter range, and measurement accuracy.

The Block 5D-2 spacecraft is in a circular sun-synchronous near-polar orbit at an altitude of 833 km with an inclination of 98.8 degrees and an orbit period of 102.0 minutes. The orbit produces 14.1 full orbit revolutions per day and has an 0612 am local ascending node equatorial crossing. Figure 1.1 shows the SSM/I in the early morning orbit. The SSM/I swath width is 1400 km and results in a high ground track repeat coverage on successive days as shown in Figure 1.2. Small unmeasured circular sectors of 2.4 degrees occur at the North and South Poles. Figures 1.3 and 1.4 present typical SSM/I sub-satellite track and swath width coverage for successive orbits.

The SSM/I is built by Hughes Aircraft Company under the direction of the Naval Space Systems Activity (NSSA) and the Air Force Space Division. The Space Sensing Branch of the Naval Research Laboratory (NRL) has served as technical consultant to the NSSA since 1982 and in this capacity has performed numerous studies and analyses requested by NSSA [1],[2], prepared a SSM/I calibration/validation plan, and currently is leading the DMSP calibration/validation effort with a team of sensor scientists.

The purpose of this document is to provide in a single volume descriptions of the radiometric performance of the SSM/I and definitions of the algorithms used to calibrate the SSM/I and retrieve the environmental parameters. These algorithms are currently employed in the SSM/I software at the Fleet Numerical

Table 1.1 SSM/I Environmental Products

Parameter	Geometric Resolution (km)	Range of Values	Quantization Levels	Absolute Accuracy
Ocean Surface Wind Speed	25	3 to 25	1	$\pm$2 m/s
Ice				
o Area Covered	25	0 to 100	5	$\pm$12%
o Age	50	1st Year, Multiyear	1 yr,>2 yr	None
o Edge Location	25	N/A	N/A	$\pm$12.5 km
Precipitation Over Land Areas	25	0 to 25	0, 5, 10, 15, 20, $\geq$25	$\pm$5 mm/hr
Cloud Water (<100μm Diameter)	25	0 to 1	0.05	$\pm$1.0 kg/m^2
Liquid Water (>100μm Diameter)	25	0 to 60	0.10	$\pm$2.0 kg/m2
Integrated Water Vapor	25	0 to 80	0.5	$\pm$3.0 kg/m^2
Precipitation Over Water	25	0 to 25	0, 5, 10, 15, 20, $\geq$25	$\pm$5 mm/hr
Soil Moisture	50	0 - 60%	1	None
Land Surface Temperature	25	180 - 340K	1	None
Snow Water Content	25	0 - 50 cm	1	$\pm$3 cm
Surface Type	25	12 Types	N/A	N/A
Cloud Amount	25	0 - 100%	1	$\pm$20%

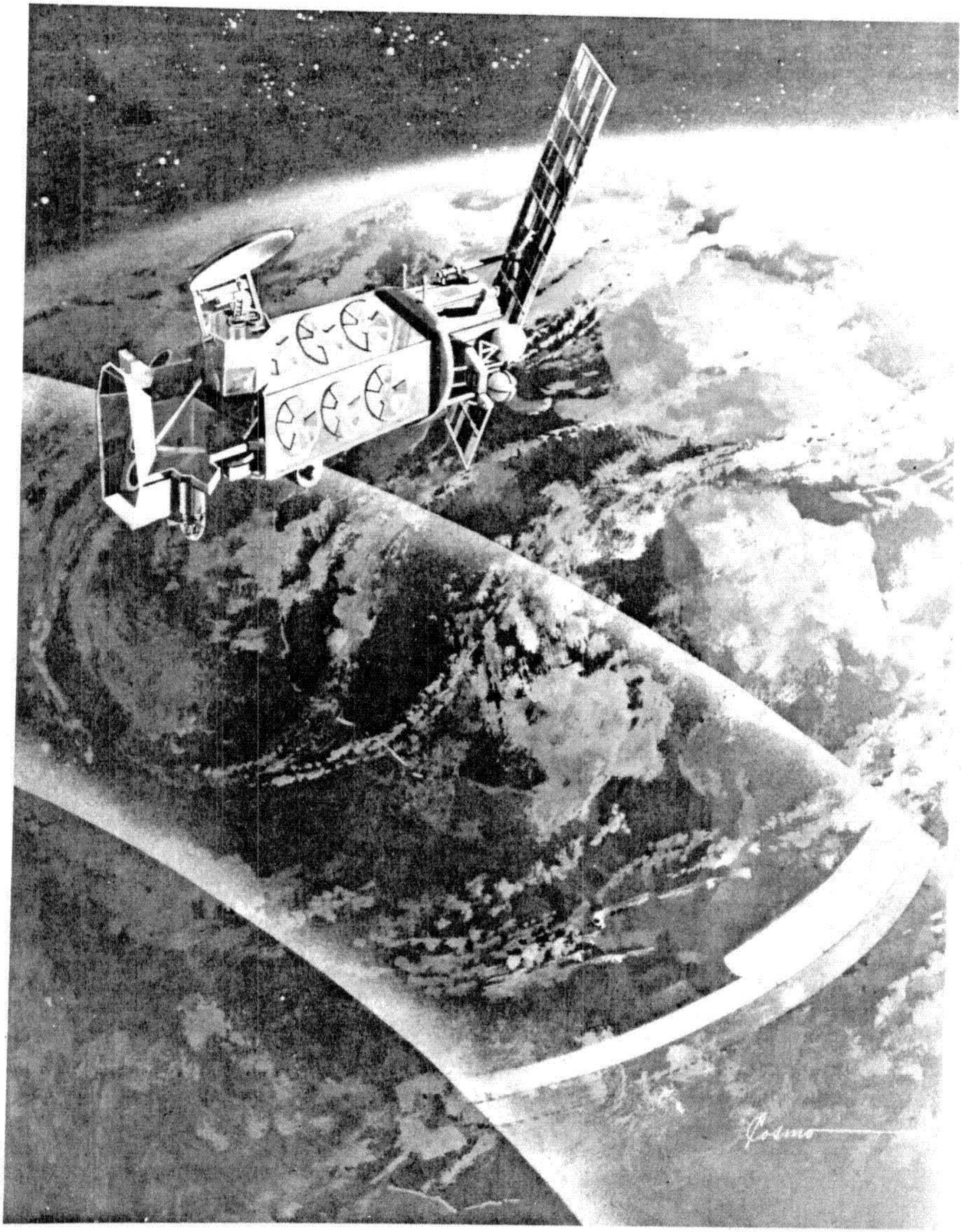

Figure 1.1 DMSP Block 5D-2 Satellite

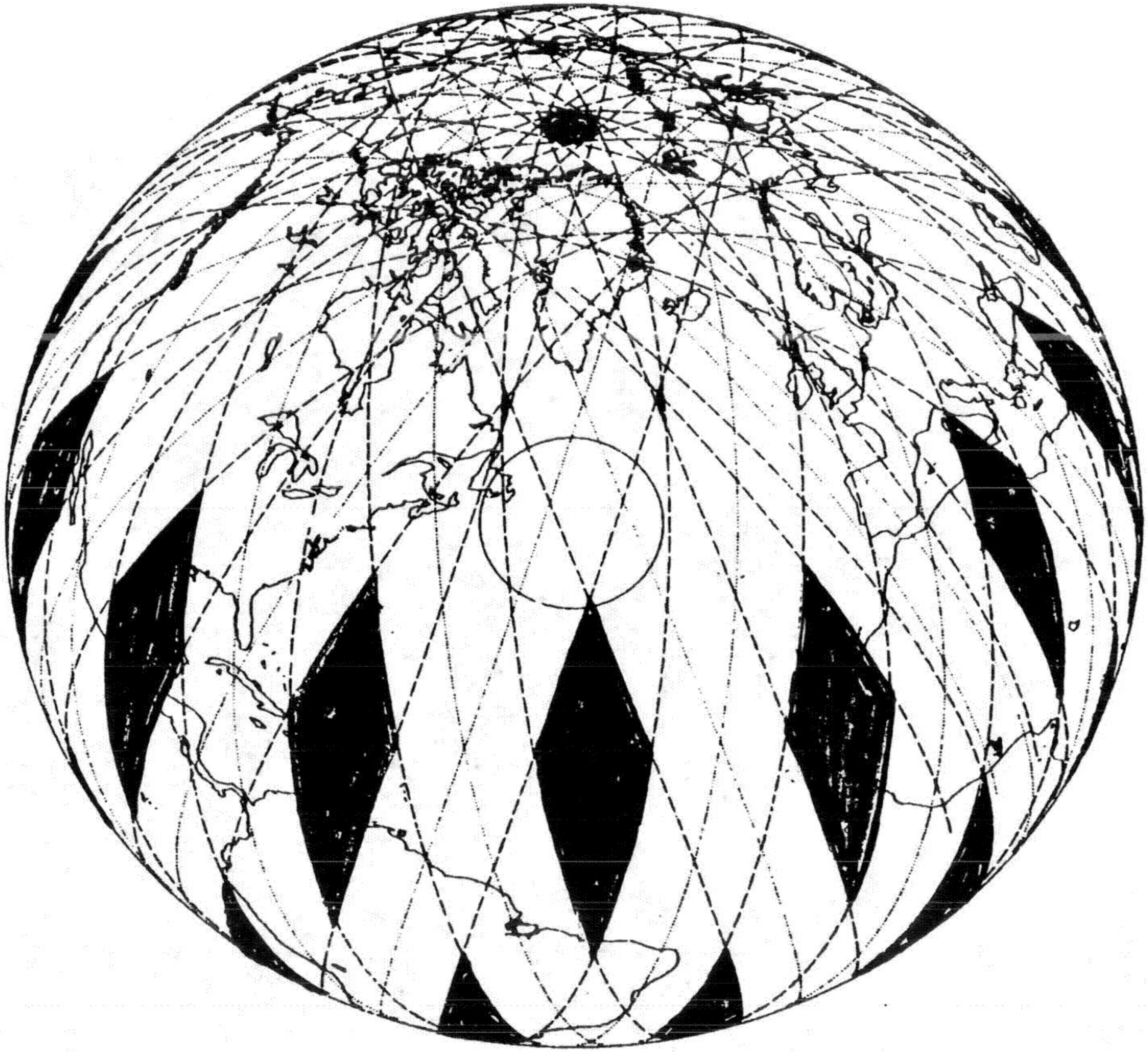

1400 kM SWATH

Figure 1.2 Coverage of SSM/I in 24 Hours

Figure 1.3 Equatorial View of Successive Orbits

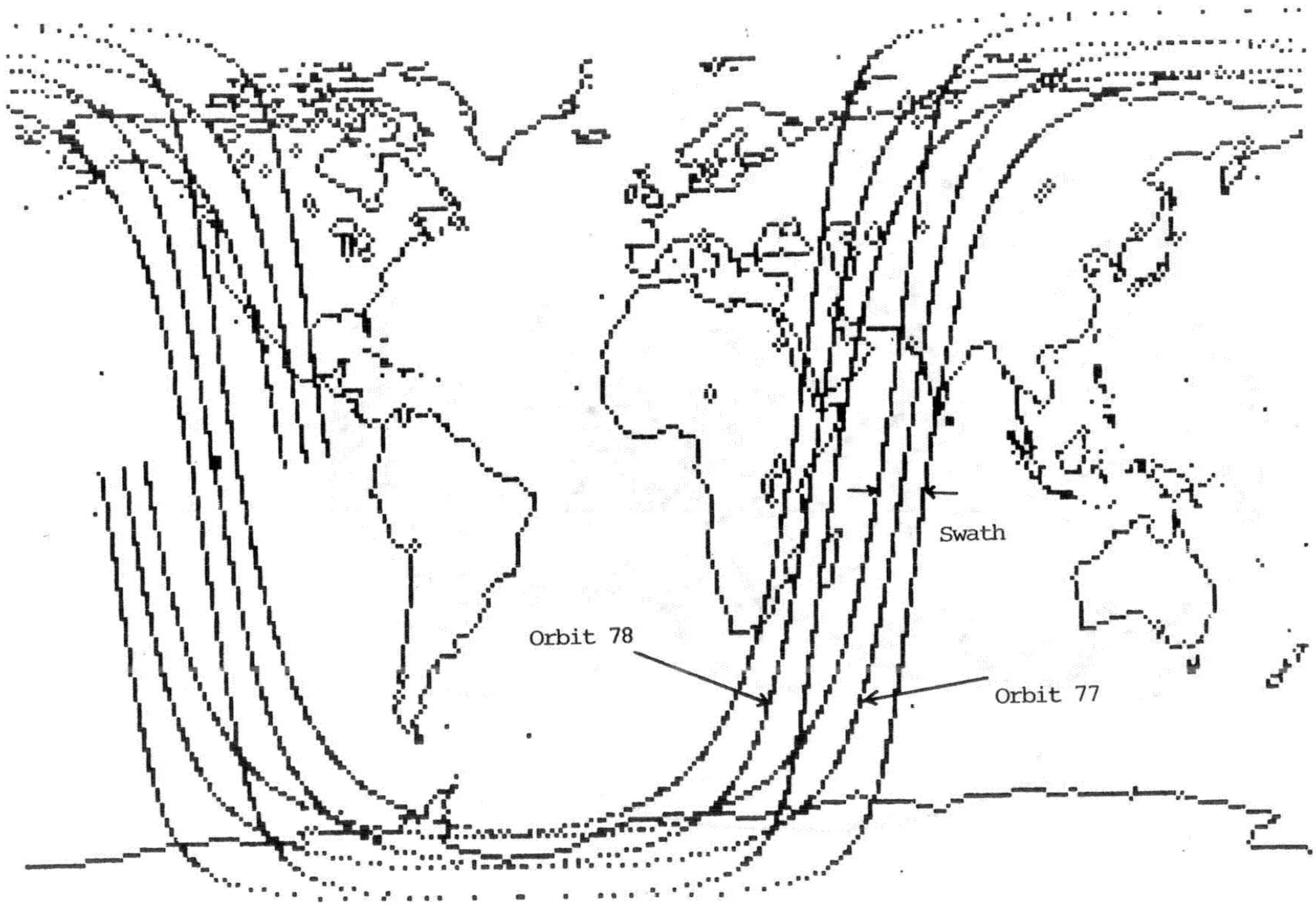

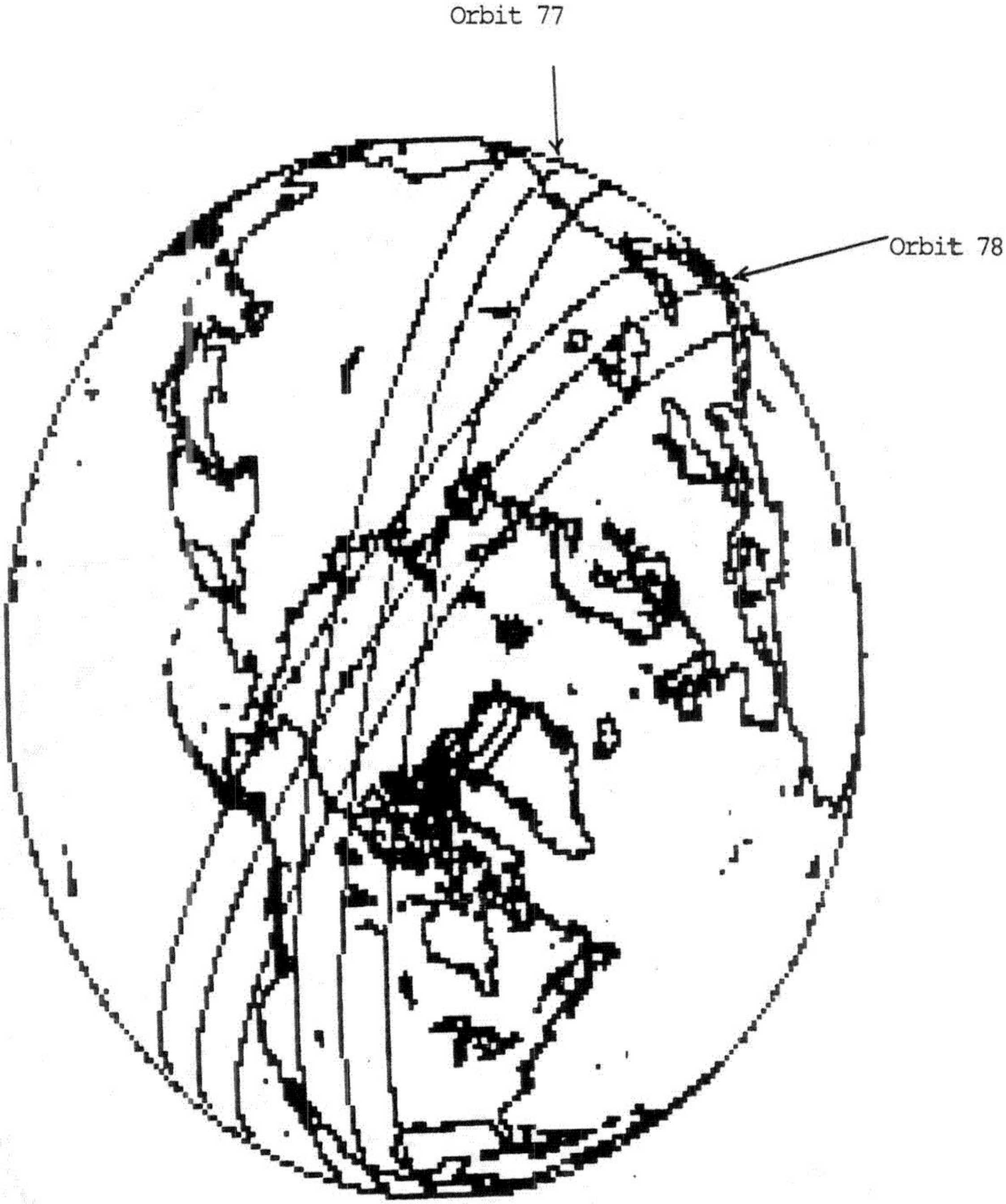

Figure 1.4 Polar View of Successive Orbits

Oceanography Center and at the Air Force Global Weather Center. Also included herein are the coefficients employed in the computations of the sensor brightness temperatures and environmental parameters as well as any logical decision tests occurring prior to computation of environmental parameters. Since the SSM/I software has a highly modular structure, it is appropriate to also discuss the flexibility and full capability of the software to accommodate changes in coefficients, structure of the decision tests, and mathematical expressions used to compute the parameters.

A description of the SSM/I instrument is presented in Section 2.0. Section 3.0 contains a description of the algorithms used to calibrate the output of the SSM/I in terms of brightness temperature incident on the antenna aperture. Section 4.0 presents the algorithms used to retrieve the environmental parameters from the calibrated brightness temperatures. Section 5.0 contains a description of the sensor health statistics computed by the SSM/I software to monitor the stability of the sensor. Section 6.0 presents a brief description of the data format used in archiving the SSM/I data products with the National Environmental Satellite, Data and Information Service (NESDIS).

2.0 INSTRUMENT DESCRIPTION

2.1 Overview

The SSM/I is a seven channel, four frequency, linearly polarized, passive microwave radiometric system. The instrument measures atmospheric/ocean surface brightness temperatures at 19.35, 22.235, 37.0, and 85.5 GHz. These data will be processed by the Fleet Numerical Oceanography Command and the Air Force Weather Center to obtain near real time global precipitation maps, sea ice morphology, marine surface wind speed, columnar integrated liquid water, and soil moisture percentage. In addition, Navy and Air Force DMSP tactical sites will be capable of receiving this same data directly from the satellite to satisfy their unique customer mission requirements.

The DMSP Block 5D-2 satellite and the SSM/I are depicted in Figure 1-1. The instrument consists of an offset parabolic reflector of dimensions 24 x 26 inches, fed by a corrugated, broad-band, seven-port horn antenna. The reflector and feed are mounted on a drum which contains the radiometers, digital data subsystem, mechanical scanning subsystem, and power subsystem. Figure 2.1 presents an overview of the major subsystems. The reflector-feed-drum assembly is rotated about the axis of the drum by a coaxially mounted bearing and power transfer assembly (BAPTA). All data, commands, timing and telemetry signals, and power pass through the BAPTA on slip ring connectors to the rotating assembly.

A small mirror and a hot reference absorber are mounted on the BAPTA and do not rotate with the drum assembly. They are positioned off axis such that they pass between the feed horn and the parabolic reflector, occulting the feed once each scan. The mirror reflects cold sky radiation into the feed thus serving, along with the hot reference absorber, as calibration references for the SSM/I. This scheme provides an overall absolute calibration which includes the feed horn. Corrections for spillover and antenna pattern effects from the parabolic reflector are incorporated in the data processing algorithms.

The SSM/I rotates continuously about an axis parallel to the local spacecraft vertical at 31.6 rpm and measures the upwelling scene brightness

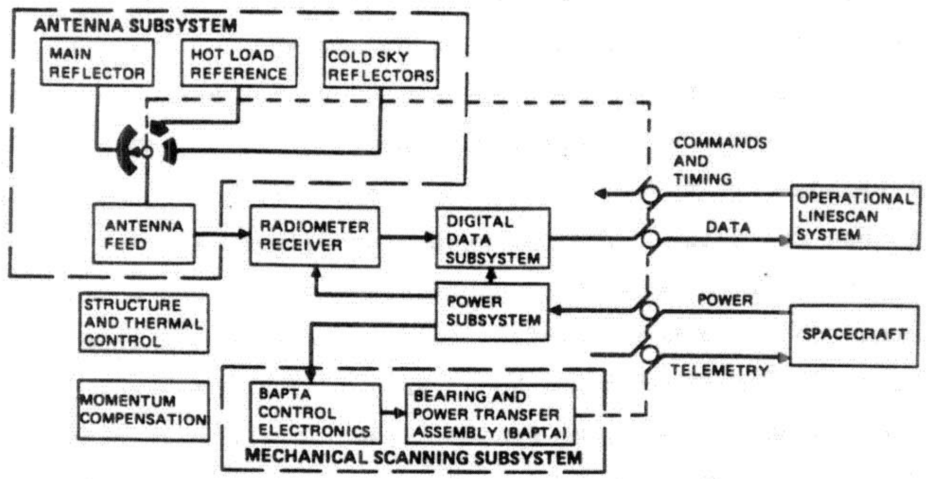

Figure 2.1 Sensor Overview

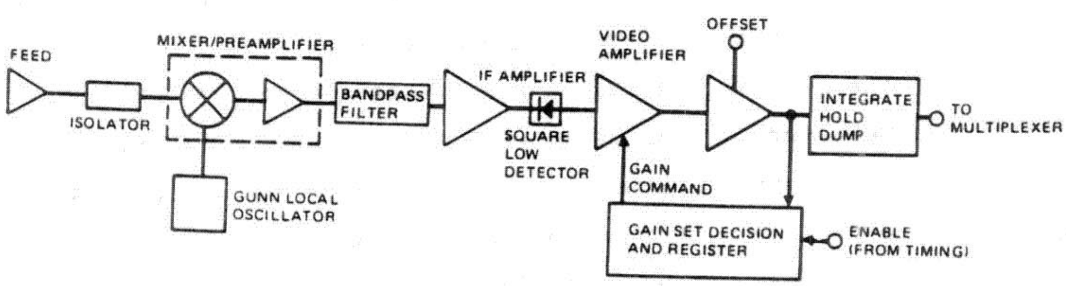

Figure 2.2 Radiometer Block Diagram

temperatures over an angular sector of 102.4° about the sub-satellite track. The scan direction is from the left to the right when looking in the aft direction of the spacecraft with the active scene measurements lying $\pm 51.2^{\circ}$ about the aft direction. This results in a swath width of 1400 km. The spin rate provides a period of 1.9 seconds during which the spacecraft sub-satellite point travels 12.5 km. Each scan 128 discrete uniformly spaced radiometric samples are taken at the two 85.5 GHz channels and on alternate scans 64 discrete samples are taken at the remaining five lower frequency channels.

A total-power radiometer configuration is employed in the SSM/I. A functional block diagram of a typical radiometer is shown in Figure 2.2. The signal from the output of the feedhorn is down converted by a balanced mixer, amplified by IF amplifiers, and converted to a video voltage with a square-law detector. The bandpass filter is used to define the receiver passband and to improve out-of-band rejection. The detected video signal is then amplified and offset to remove part of the component of receiver output due to receiver noise. The output of the video amplifier is integrated by an integrate and dump filter for 3.89 msec at 85.5 GHz and 7.95 msec for the remaining channels and delivered to the data processing system. The time between radiometer output samples is 4.22 msec at 85.5 GHz and is the same time required for the antenna beam to scan 12.5 km in the crosstrack direction. The time between samples at the remaining frequencies is 8.44 msec.

The data processor multiplexes the seven radiometer output signals with an analog multiplexer and samples and holds the signals before being digitized into 12-bit words. In addition, twelve channels are multiplexed with the radiometer data. These channels contain three hot target temperature measurements, two temperature sensor measurements within the radiometer, reference voltage, and reference return data. A microprocessor supervises instrument timing, control, and data buffering with the DMSP Optical Line Scanner (OLS) instrument which records all SSM/I data. The average data rate of the SSM/I including zeros required to match the OLS interface is 3276 bps.

The prototype of the SSM/I instrument is shown in the stowed position in Figure 2.3 and deployed in Figure 2.4. The feedhorn antenna may be seen in Figure 2.3 and the calibration reflector in Figure 2.4. The hot calibration

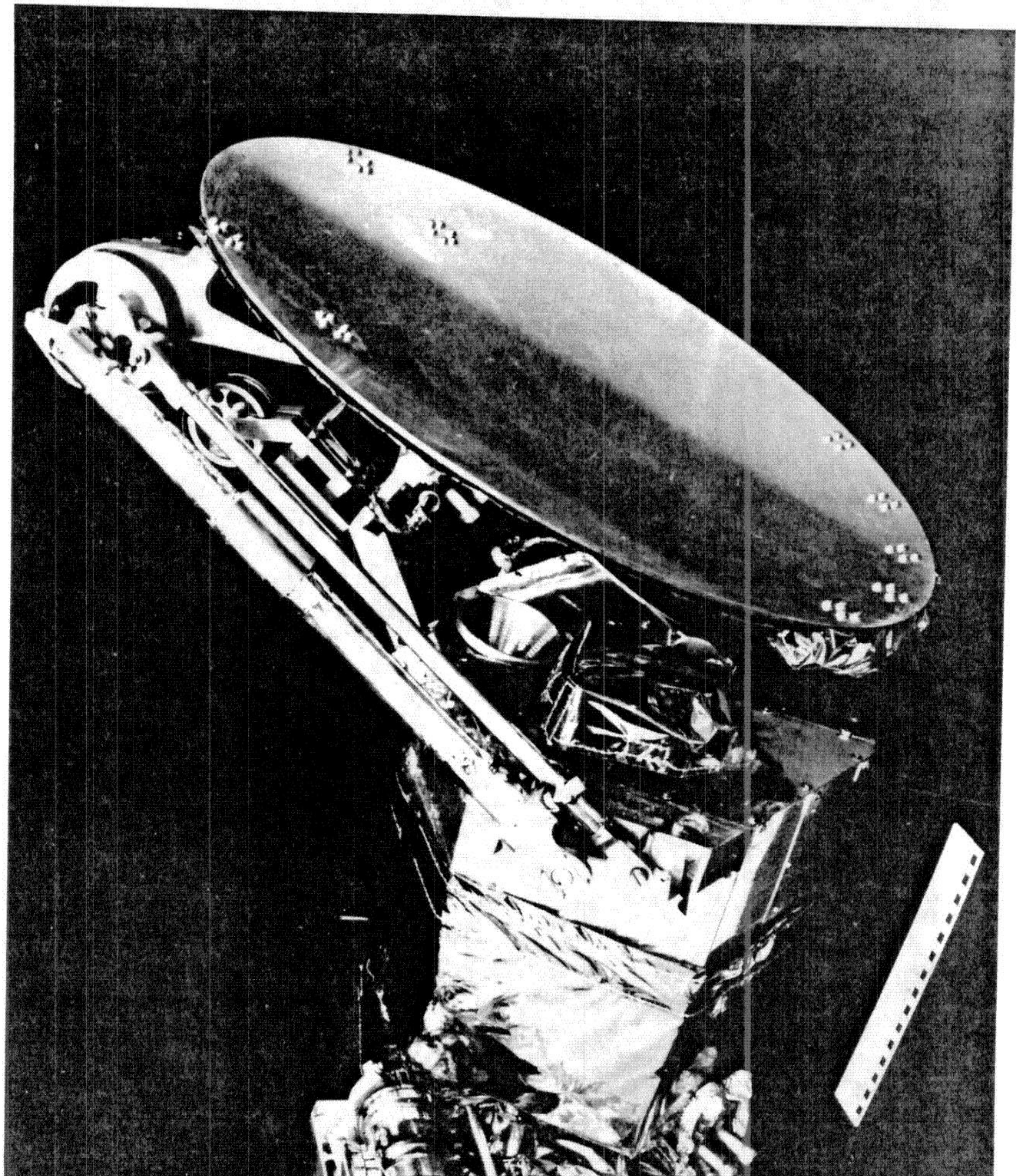

Figure 2.3 Prototype of SSM/I in Stowed Position

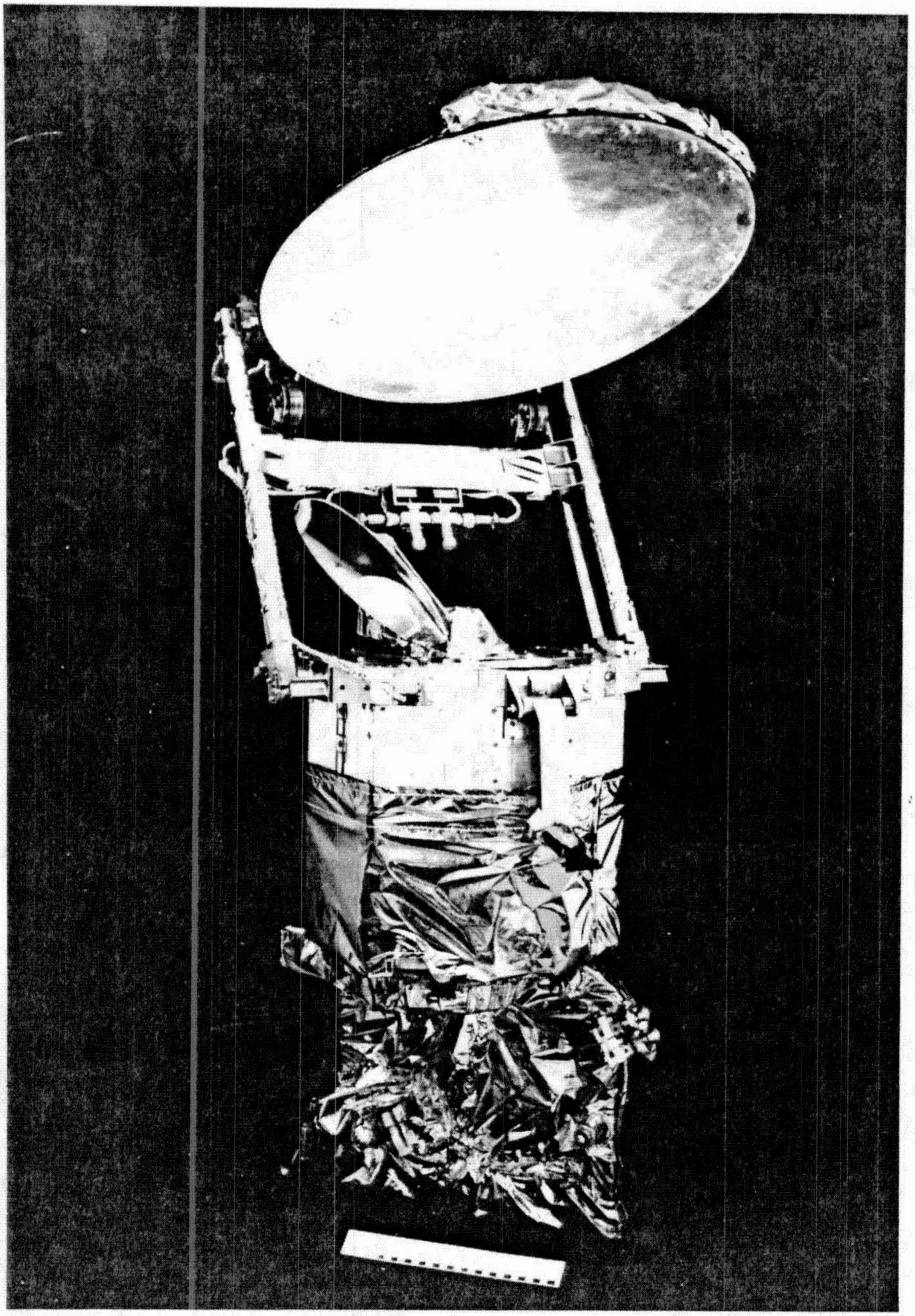

Figure 2.4 Prototype of SSM/I in Deployed Position

target is hidden by the thermal blanket in both figures. Photographs of the feedhorn, calibration reflector, and hot target are presented in Figures 2.5 through 2.7. The SSM/I sensor weighs 107 lbs. A high speed momentum wheel weighing 16 lbs is mounted inside the spacecraft. The SSM/I system consumes 45 watts.

2.2 Scan Geometry

Figure 2.8 presents the instantaneous field of view (IFOV) of the SSM/I for the channel frequencies during the scan region of the scene sector. The ellipses denote projections of the 3 dB beamwidths of the earth's surface. The SSM/I spins about an axis parallel to the local spacecraft vertical unit vector, the X direction in Figure 2.8, at a rate of 31.6 rpm as the sub-satellite track moves along the -Y direction at 6.58 km/sec. This results in a separation between successive scans of 12.5 km along the Y which is nearly equal to the resolution of the 85 GHz beams. On each scan 128 uniformly spaced samples of the 85.5 GHz scene data are taken over a 102.4 degree scan region. The sampling interval is 4.22 msec and equals the time for the beam to travel 12.5 km in the cross track direction. Radiometer data at the remaining frequencies are sampled every other scan with 64 uniformly spaced samples having an 8.44 msec interval. Scan A denotes scans in which all channels are sampled while Scan B denotes scans in which only 85.5 GHz data are taken. The start and stop times of the integrate and dump filters at 19.35, 22.235, and 37.0 GHz are selected to maximize the radiometer integration time and achieve concentric beams for all sampled data. Figure 2.9 presents the beam sizes and sampling grid for a region near the ground track of the sub-satellite point and near the edge of the swath. The effect of the radiometer integration times is to increase the effective along scan beam diameter and make the beams at 37 and 85 GHz nearly circular. Note the greater overlapping of beams near the edge of the swath.

2.3 Antenna Beam Characteristics

Table 2.1 presents measurements of the IFOV 3-dB beamwidths of the secondary radiation patterns as a function of channel frequency and polarization for SSM/I. The data apply to Sensor S/N 002 and are based on

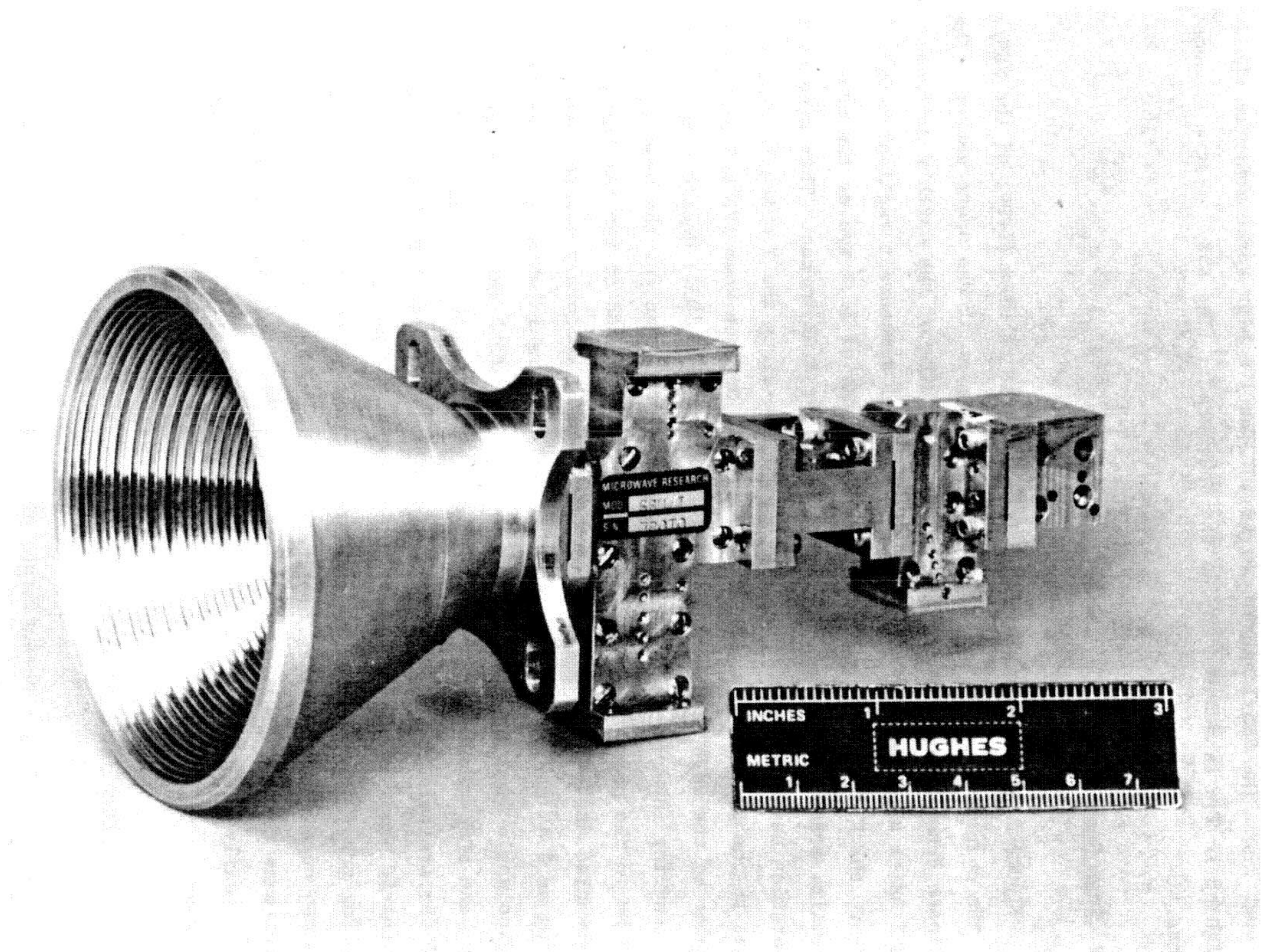

Figure 2.5 Prototype SSM/I Feedhorn

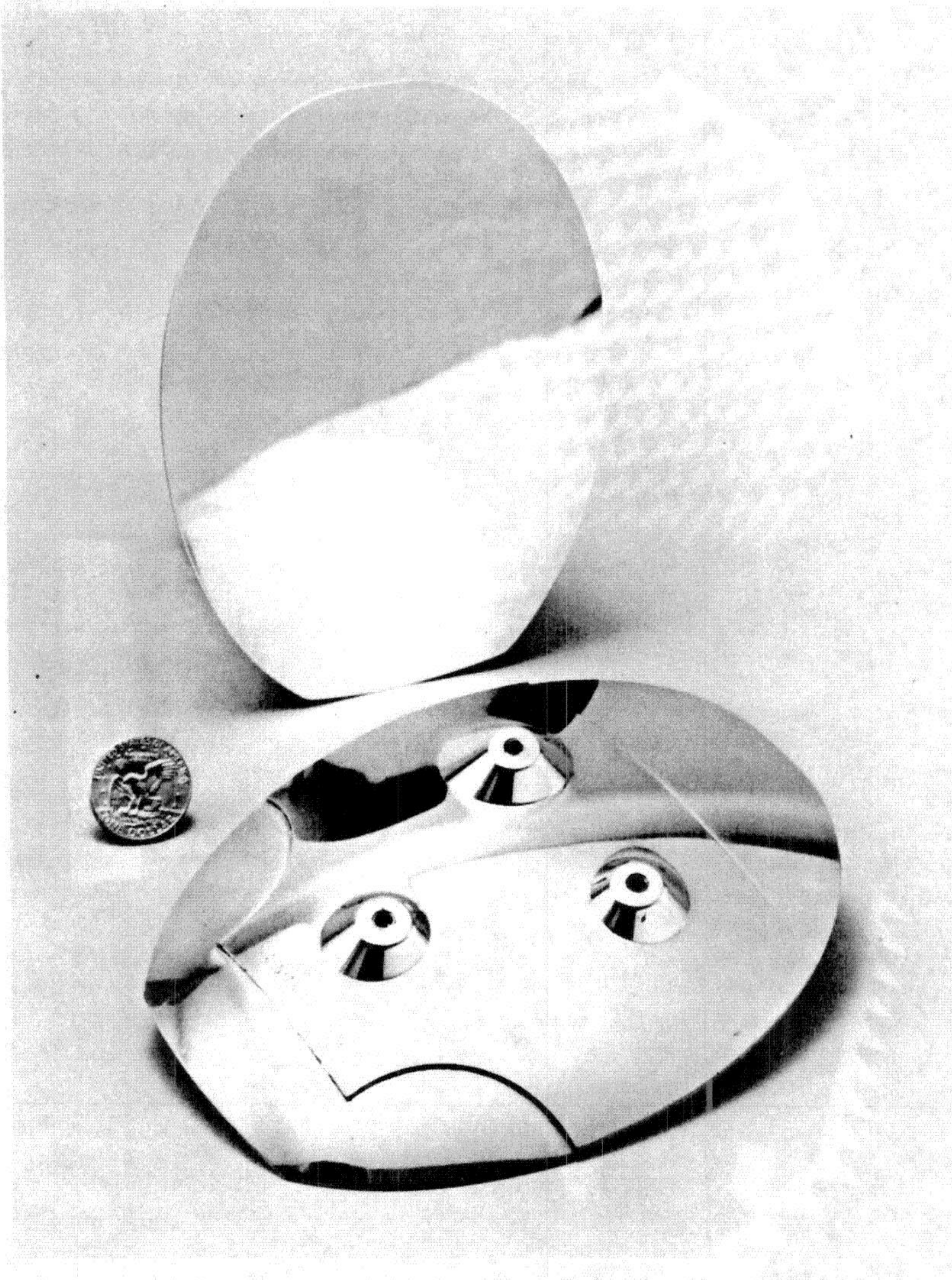

Figure 2.6 Prototype SSM/I Cold Sky Calibration Reflector

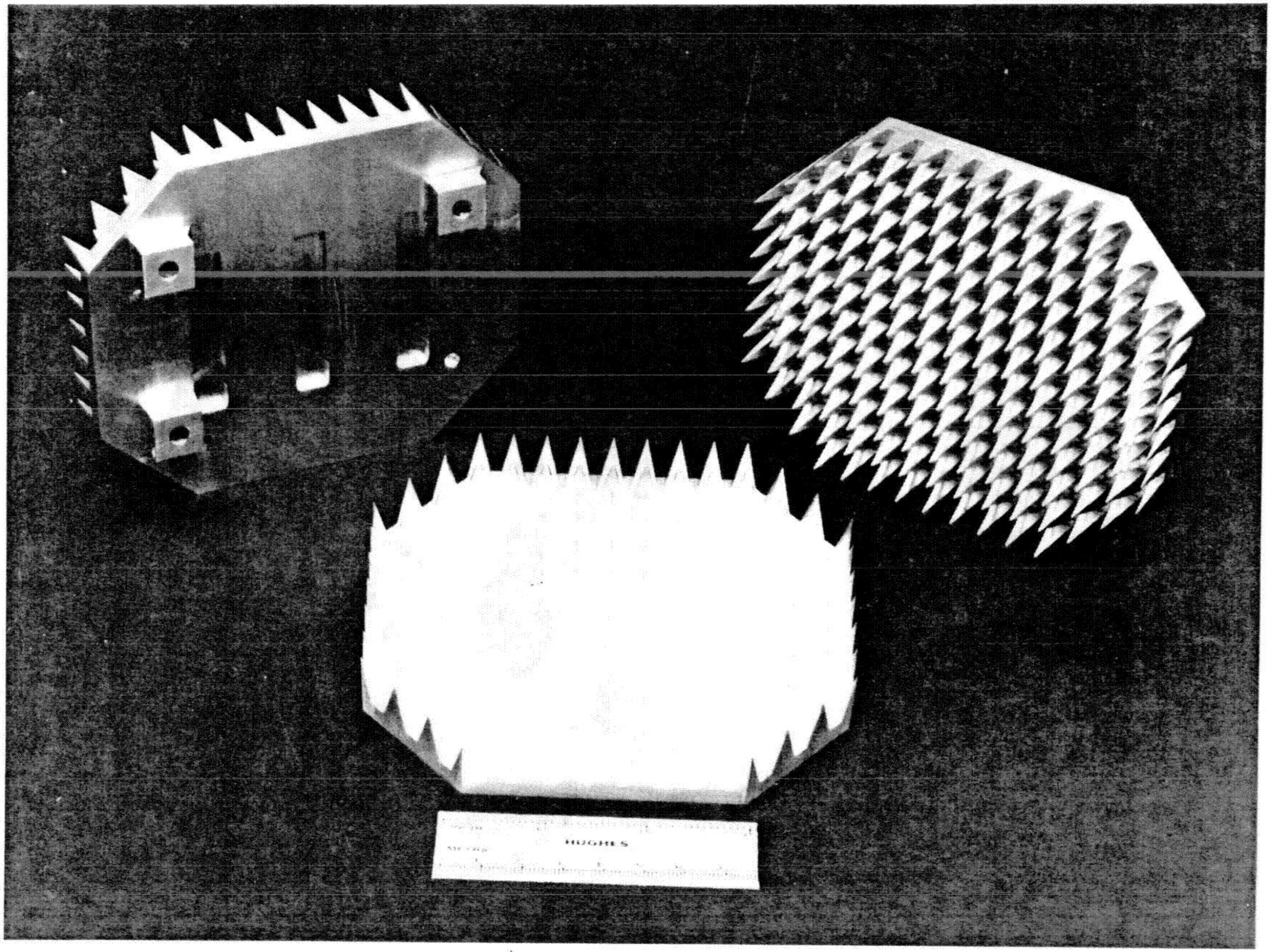

Figure 2.7 Prototype SSM/I Hot Load Calibration Target

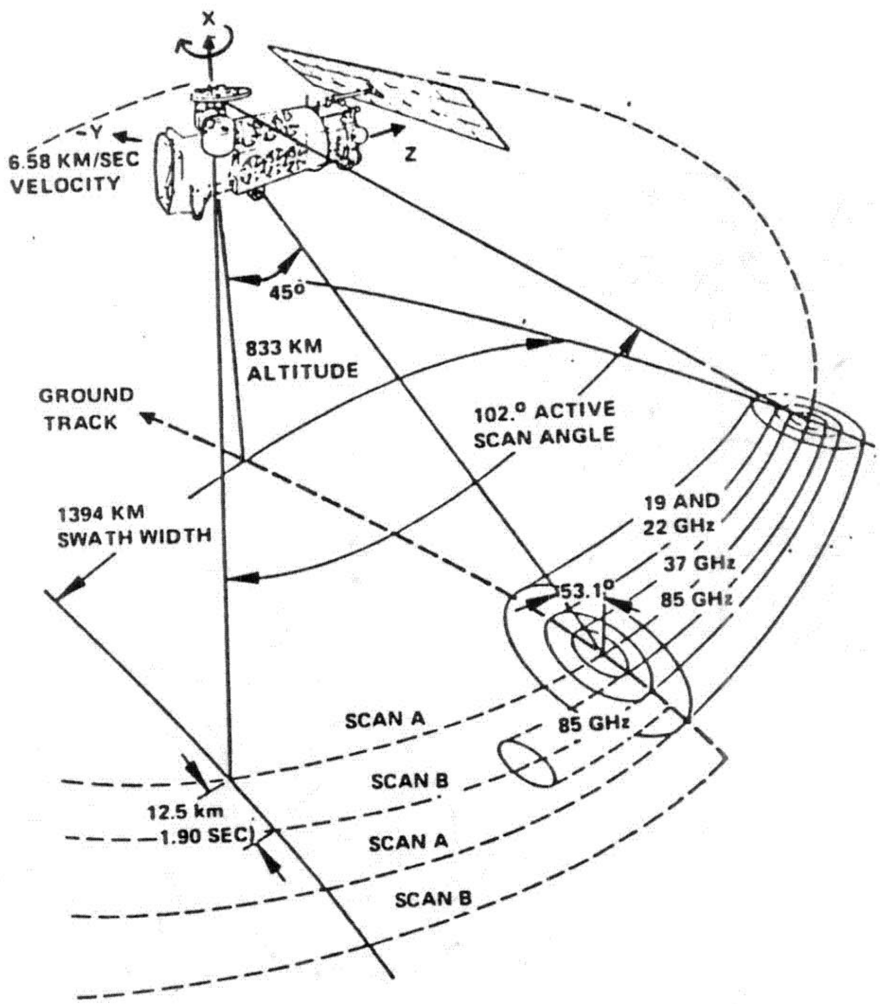

SCAN A	
SCENE STATIONS/SCAN	128
PIXELS/SCAN	576
SCAN B	
SCENE STATIONS/SCAN	128
PIXELS/SCAN	256
SCENE STATIONS/ORBIT	404,224
PIXELS/ORBIT	1,313,728

Figure 2.8 Scan Geometry

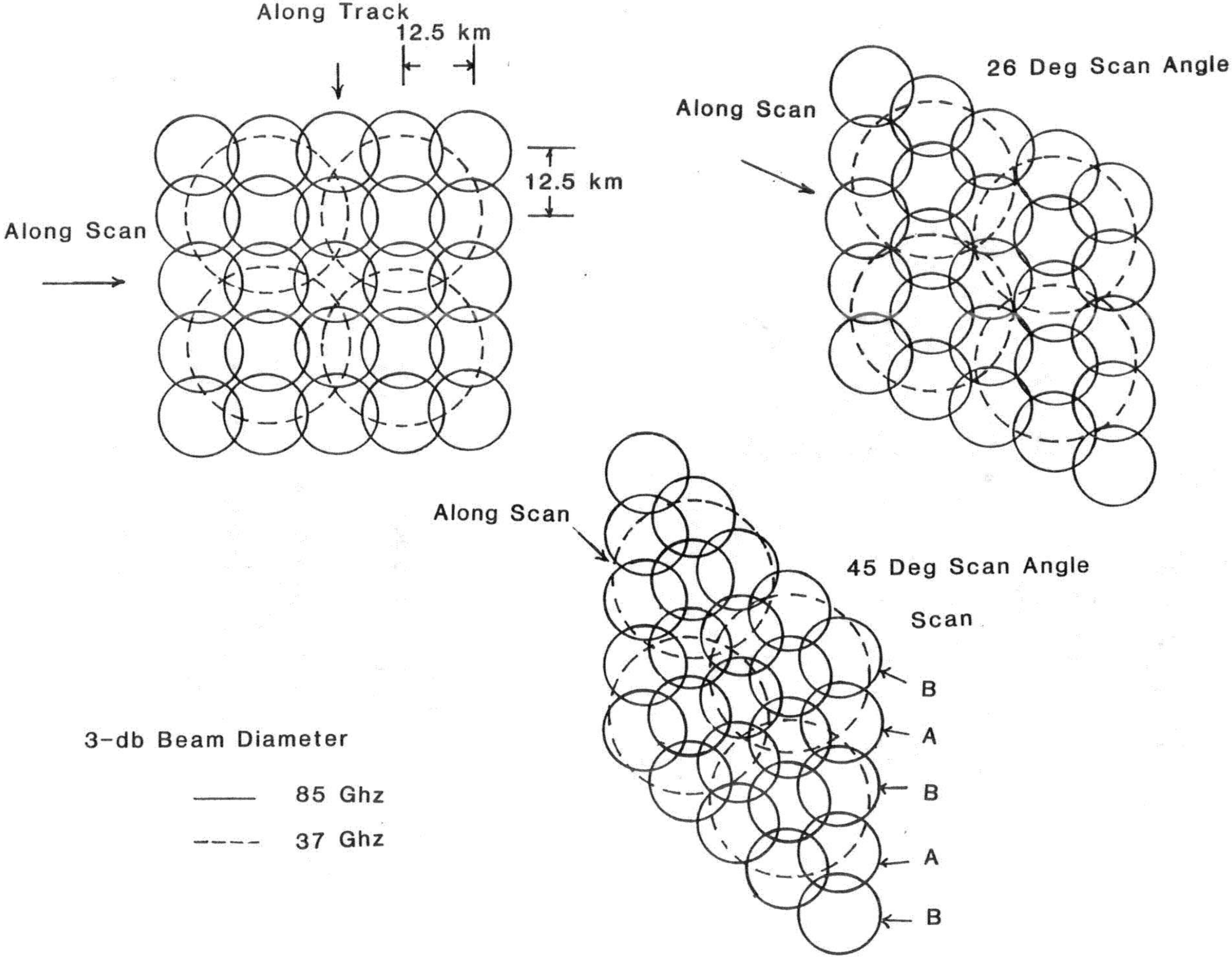

Figure 2.9 Spatial Sampling

antenna pattern measurements which have been averaged over the RF passbands. Similar beamwidths apply to other sensor serial numbers. Since the radiometer integrate-and-dump filter integrates the instantaneous radiometer output over 3.89 msec at 85.5 GHz and 7.95 msec at the remaining channels, an effective field of view (EFOV) may be defined for each sampled radiometer brightness temperature which takes the integration time into account. (As noted earlier the time between samples is 4.22 msec for 85 GHz and 8.44 msec for 19/22/37 GHz channels which includes both the integration time and time to sample and dump the data.) The EFOV is significantly larger than the IFOV in the crosstrack direction (or, H-plane direction) and essentially the same in the alongtrack direction. Table 2.1 presents the EFOV 3-dB beamwidths next to the IFOV beamwidths. Also shown are the alongtrack and crosstrack dimensions of the EFOV beamwidths when projected onto the earth's surface.

Table 2.1 SSM/I Antenna Beamwidths
(S/N 002)

Channel Frequency (GHz)	Pol. V/H	IF Pass-Band (MHz)	Beamwidth (Deg) E-Plane IFOV	H-Plane IFOV	H-Plane EFOV	EFOV on Earth Surface (km) Along-Track	Cross-Track
19.35	V	10-250	1.86	1.87	1.93	69	43
19.35	H	10-250	1.88	1.87	1.93	69	43
22.235	V	10-250	1.60	1.65	1.83	50	40
37.0	V	100-1000	1.00	1.10	1.27	37	28
37.0	H	100-1000	1.00	1.10	1.31	37	29
85.5	V	100-1500	0.41	0.43	0.60	15	13
85.5	H	100-1500	0.42	0.45	0.60	15	13

Another important antenna performance parameter is the main beam efficiency and is defined as the percentage of energy received within the main beam of the far-field radiation pattern in the desired polarization within the prescribed bandwidth to the total energy received. The far-field antenna pattern is the combination of the radiation patterns of the feedhorn antenna and the parabolic reflector antenna. Table 2.2 presents antenna beam efficiencies as a function of channel frequency and polarization for instrument S/N 002. The data are based on antenna range measurements of both the feedhorn patterns and the radiation patterns from the reflector. The antenna sidelobe column denotes the percentage energy lying outside 2.5 times the 3-dB beamwidth of the far-field pattern when normalized to the sum of the co- and cross-polarization energies. The cross-polarization column is the percentage of cross-polarized energy appearing at the output of the feedhorn and includes contributions from both the reflector and feedhorn. The feedhorn spillover loss refers to the loss of energy in the far-field pattern not intercepted by the reflector. Thus the feedhorn spillover loss is a multiplicative factor in the computation of beam efficiency. Slightly different values of sidelobe and cross-polarization energies occur for the other sensor serial numbers with beam efficiencies all greater than 90%. The beam efficiencies in the table may be improved with an antenna pattern correction algorithm and is discussed in Section 3.1.

Table 2.2 SSM/I Beam Efficiencies
(S/N 002)

Channel Frequency (GHz)	Pol. V/H	Antenna Sidelobe (%)	Cross-Polarization (%)	Feedhorn Spillover Factor	Beam Efficiency (%)
19.35	V	0.8	0.35	0.969	96.1
19.35	H	0.4	0.30	0.969	96.5
22.235	V	2.0	0.65	0.974	95.5
37.0	V	7.3	1.80	0.986	91.4
37.0	H	4.7	1.20	0.986	94.0
85.5	V	5.7	0.60	0.988	93.2
85.5	H	7.8	1.40	0.988	91.1

Although not shown in Table 2.2, the loss in beam efficiency due to small scale surface roughness of the reflector surface is very small at all frequencies. The rms surface roughness is less than 1.0 mils, and translates to a loss of 0.8% at 85.5 GHz and less than 0.15% at the remaining frequencies. Figures 2.10 through 2.16 show the effective far-field antenna reception patterns which result from the use of an integrate and dump filter with the actual antenna pattern. The filter smoothes out the sharp nulls of the sidelobes and widens the patterns in the along scan direction. The co- and cross-polarized antenna patterns in the cardinal E- (along view) and H- (along scan) planes are shown for each channel.

The location of the boresights of the antenna beams depends on (1) the repeatability of the deployment of the reflector with respect to feedhorn, (2) the alignment accuracy of the SSM/I sensor coordinates with the spacecraft

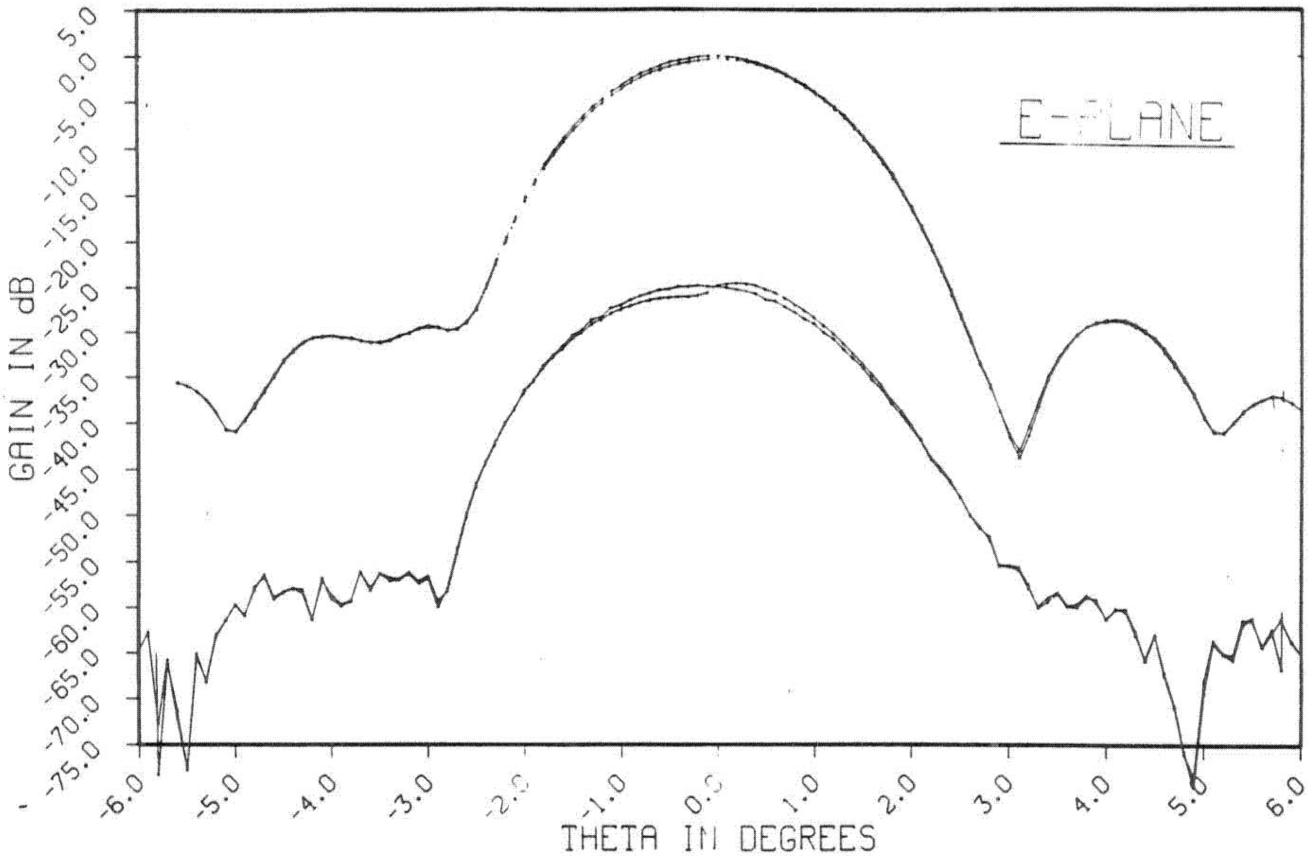

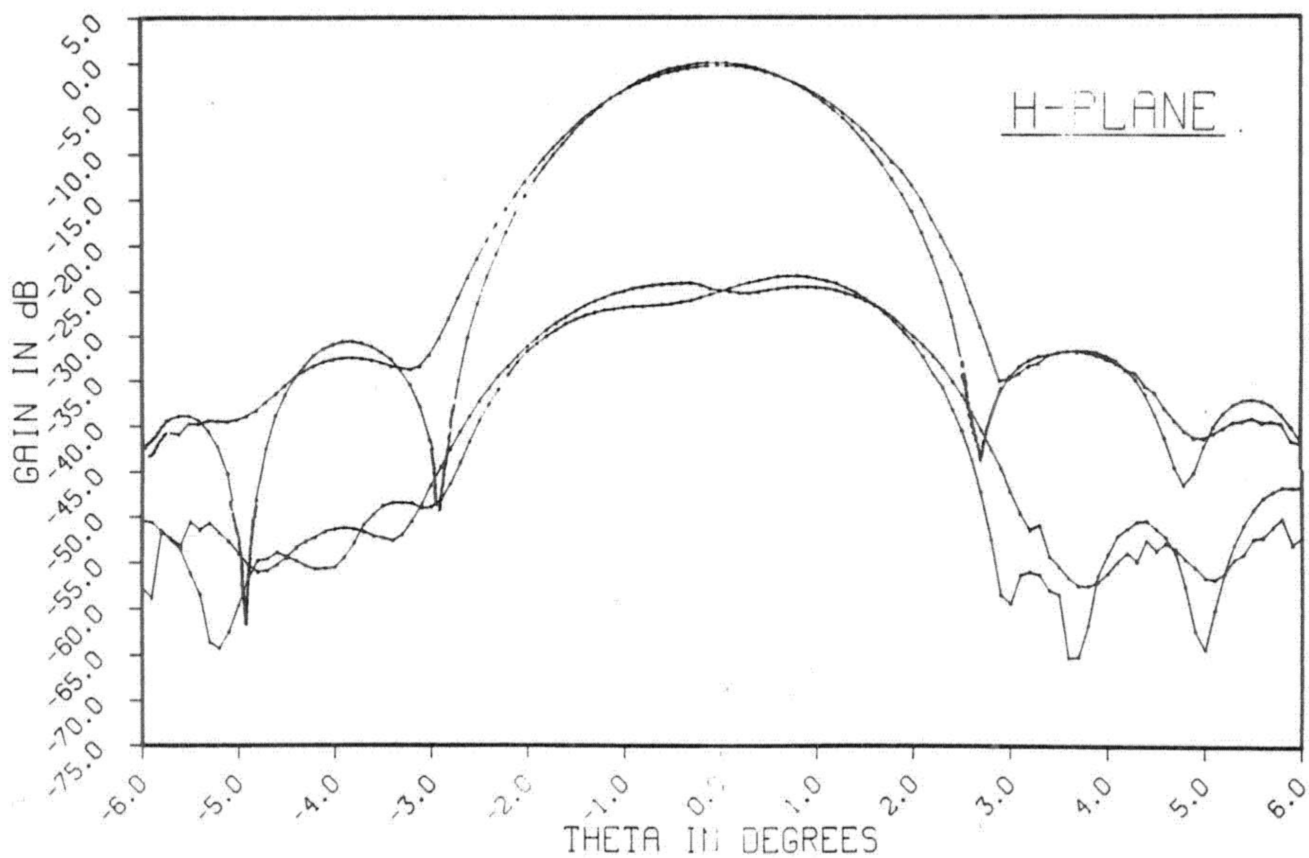

Figure 2.10 19.35 Ghz Vertical Pol.

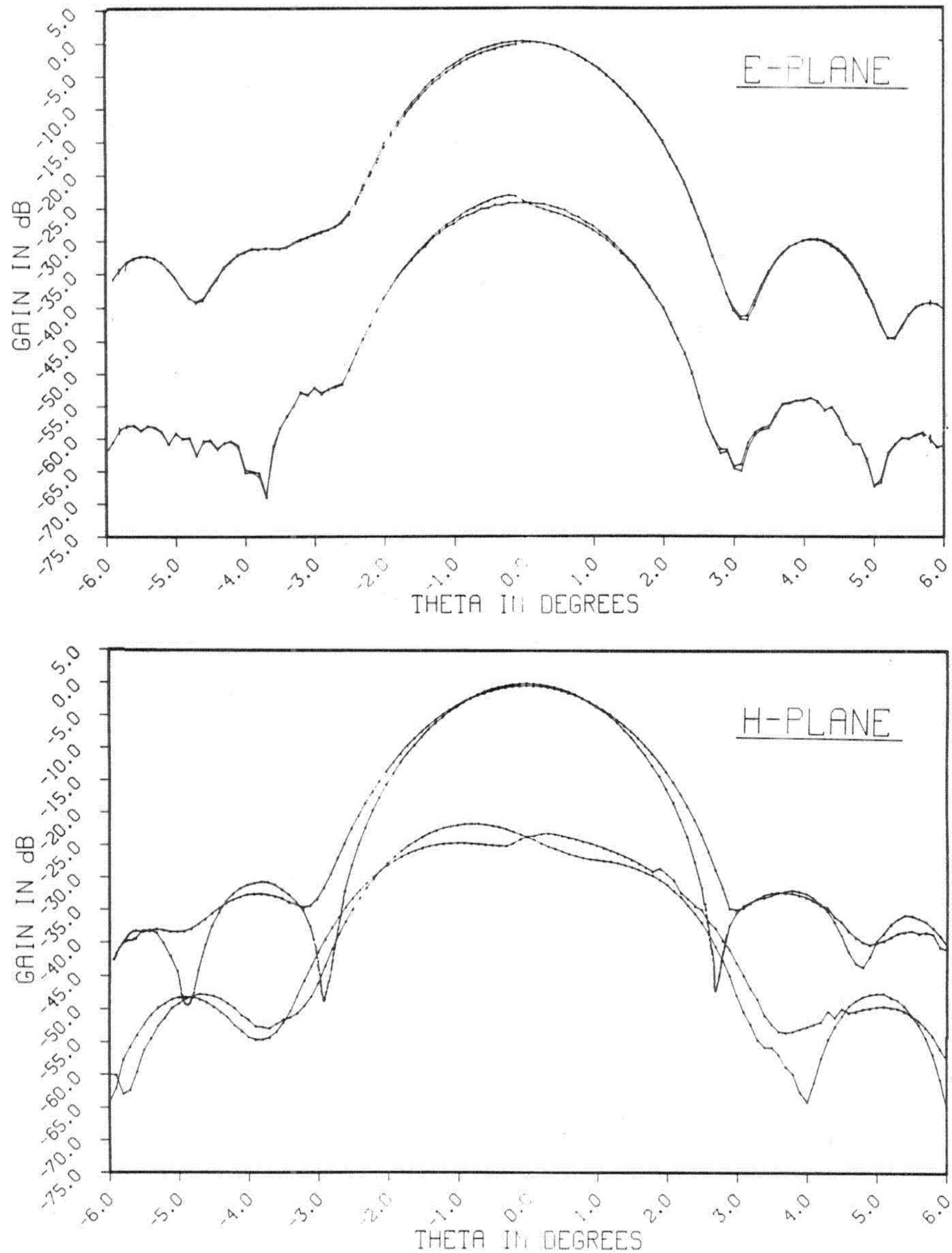

Figure 2.11 19.35 Ghz Horizontal Pol.

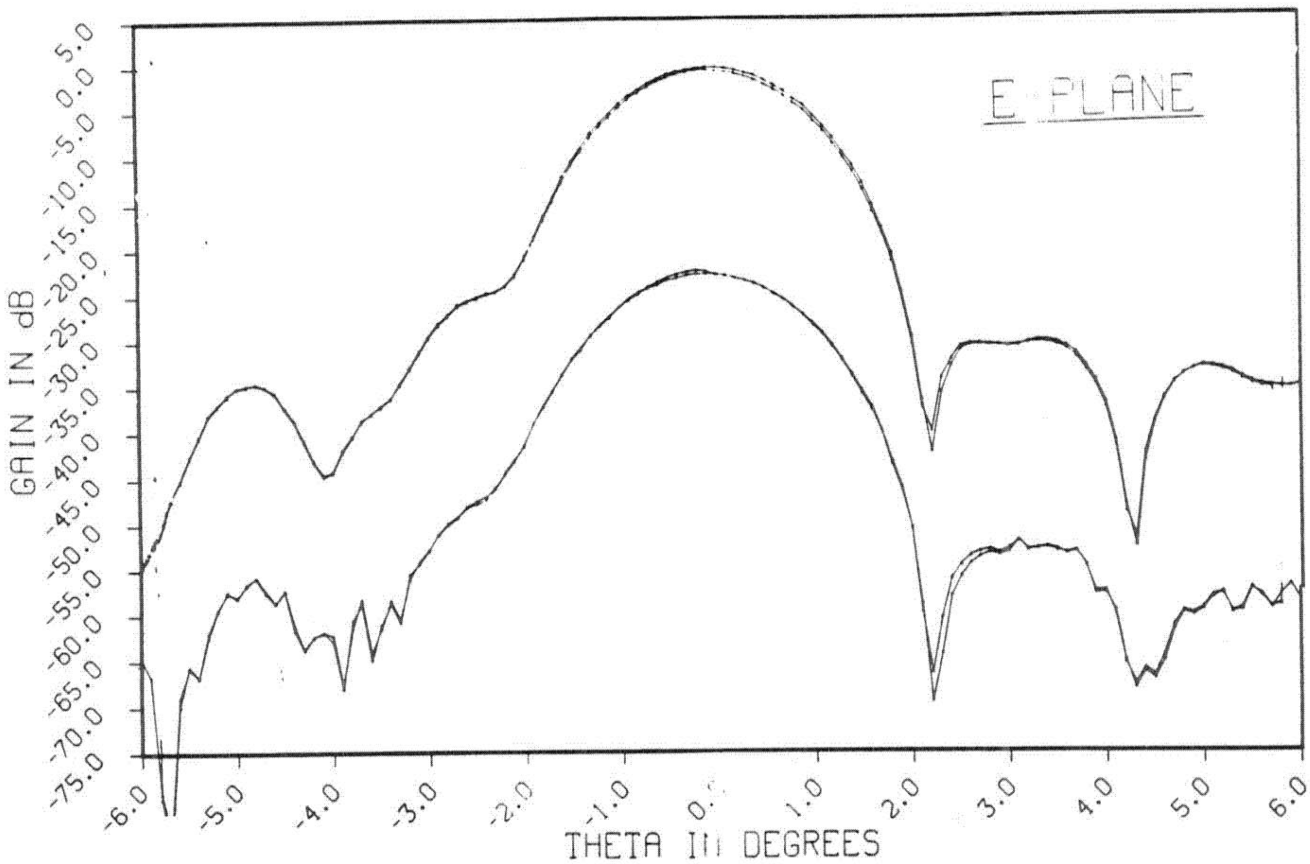

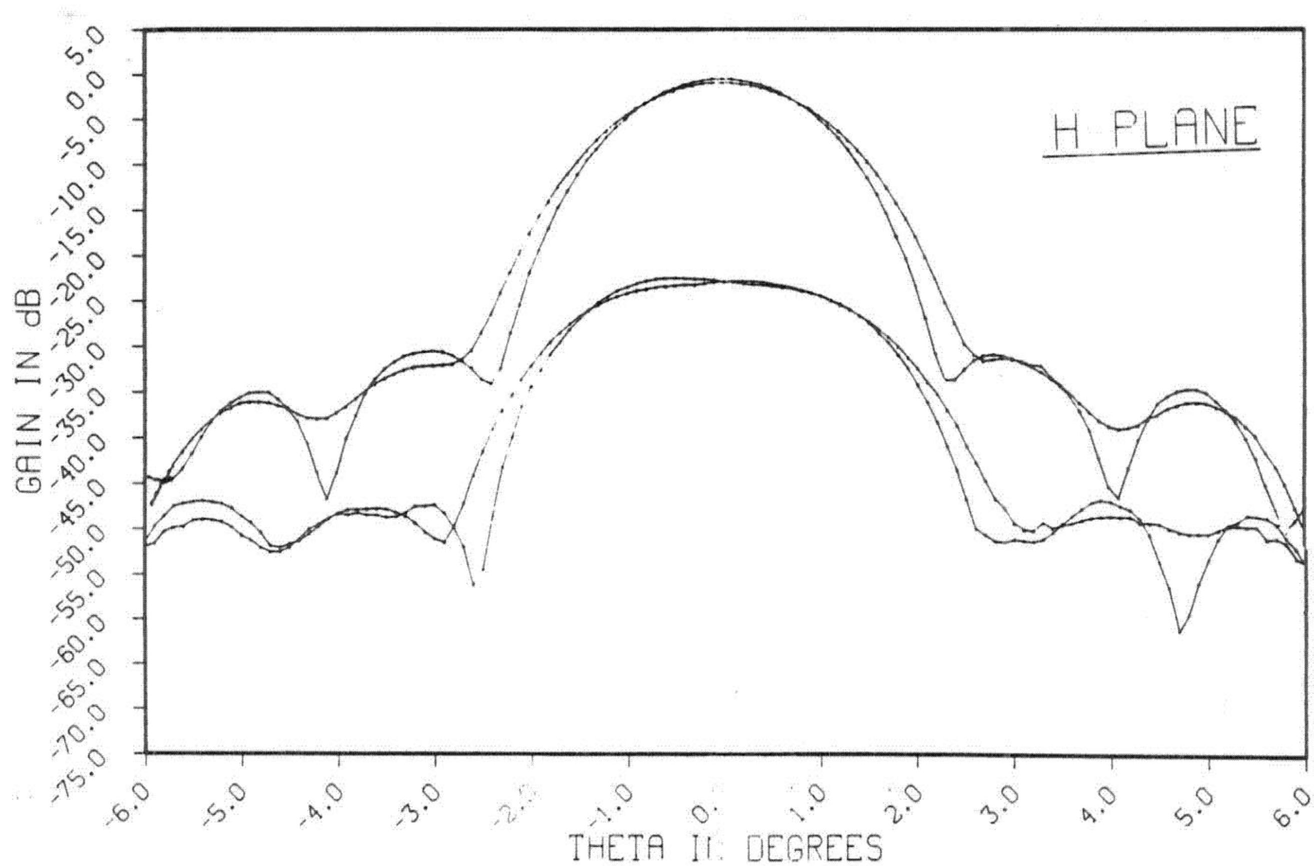

Figure 2.12 22.235 Ghz Vertical Pol.

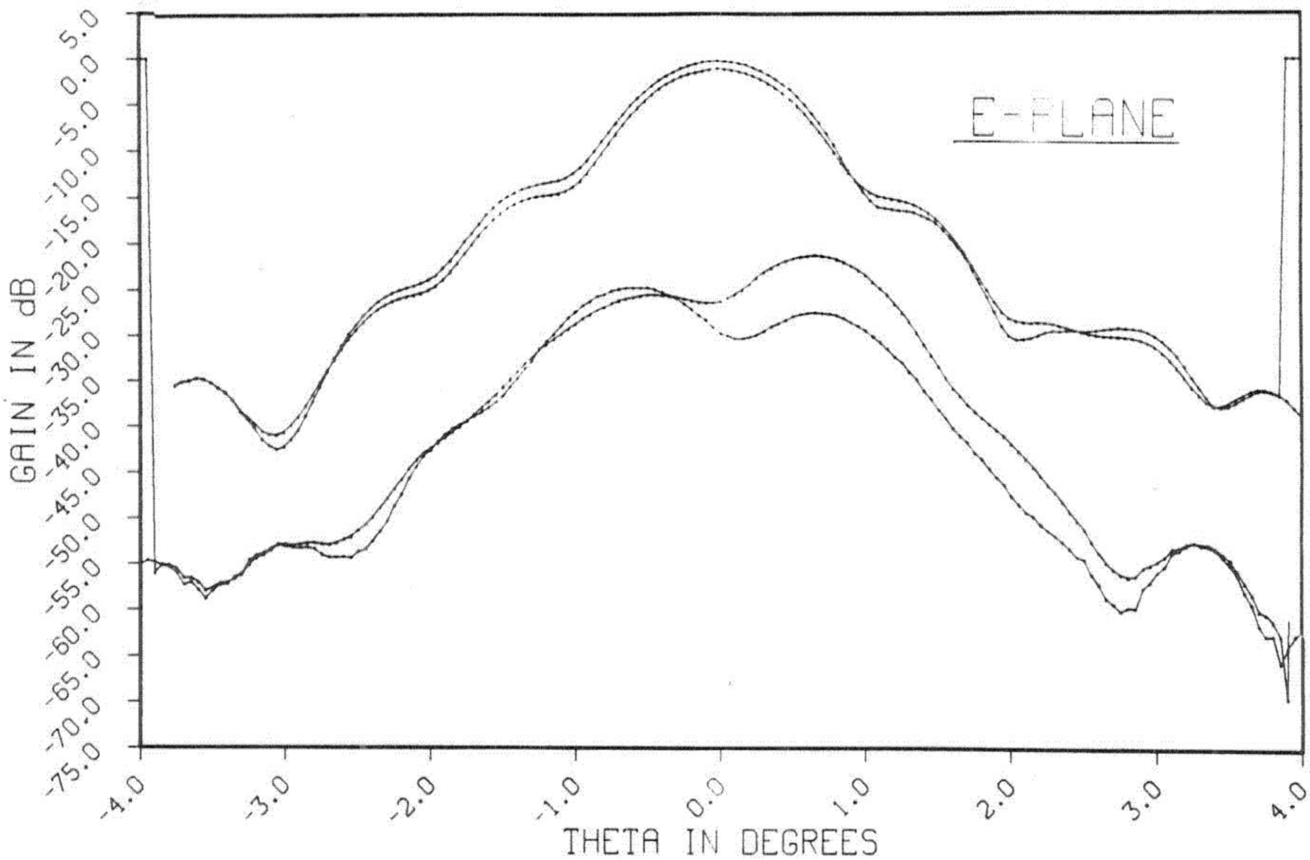

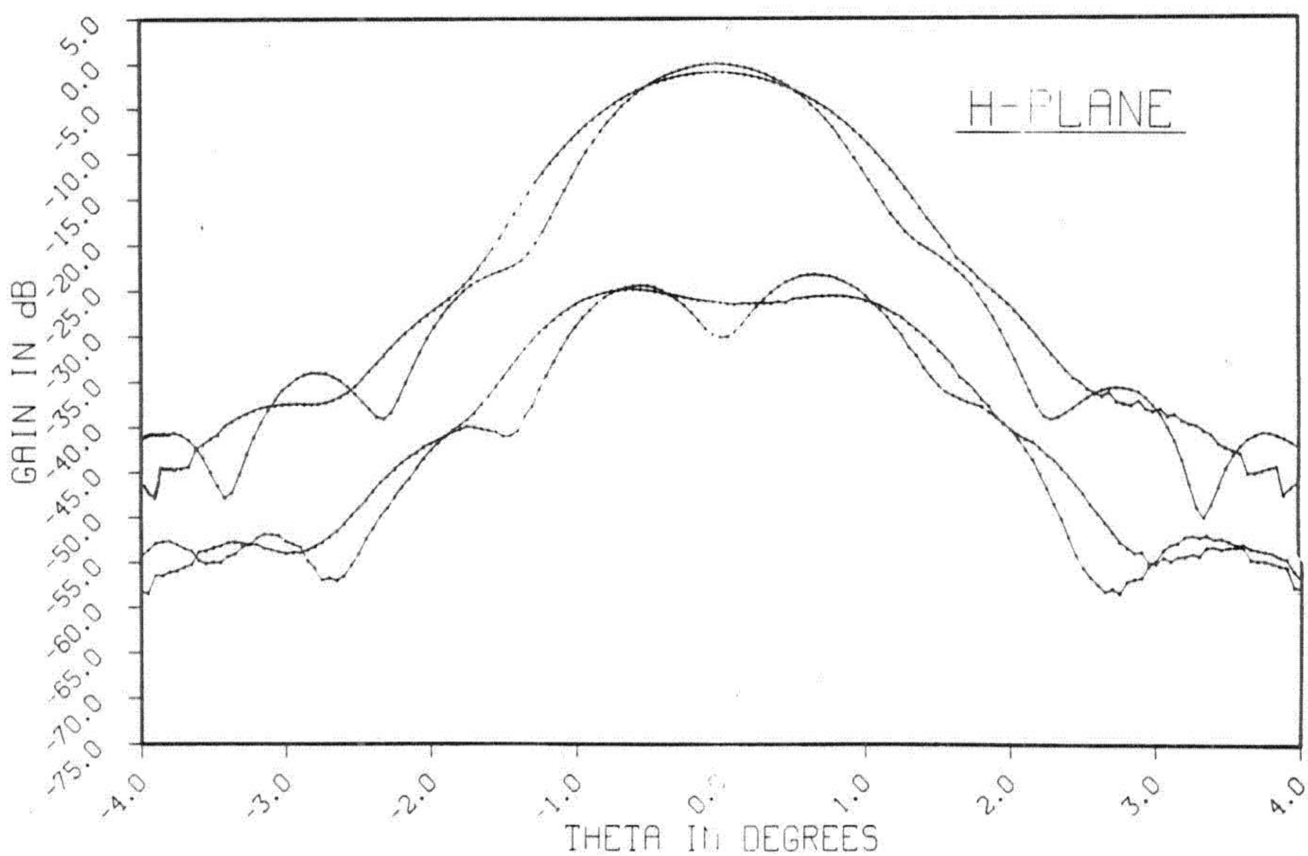

Figure 2.13 37 Ghz Vertical Pol.

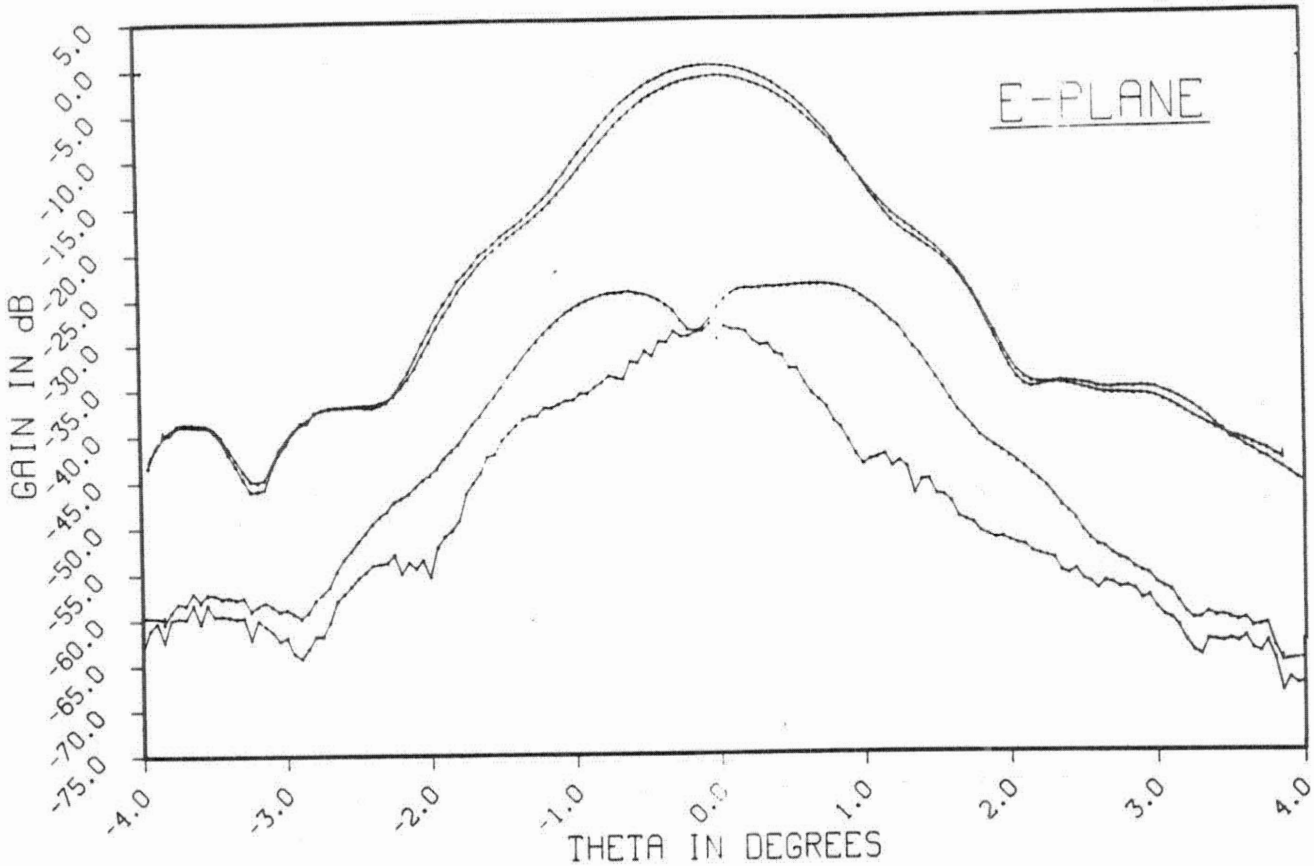

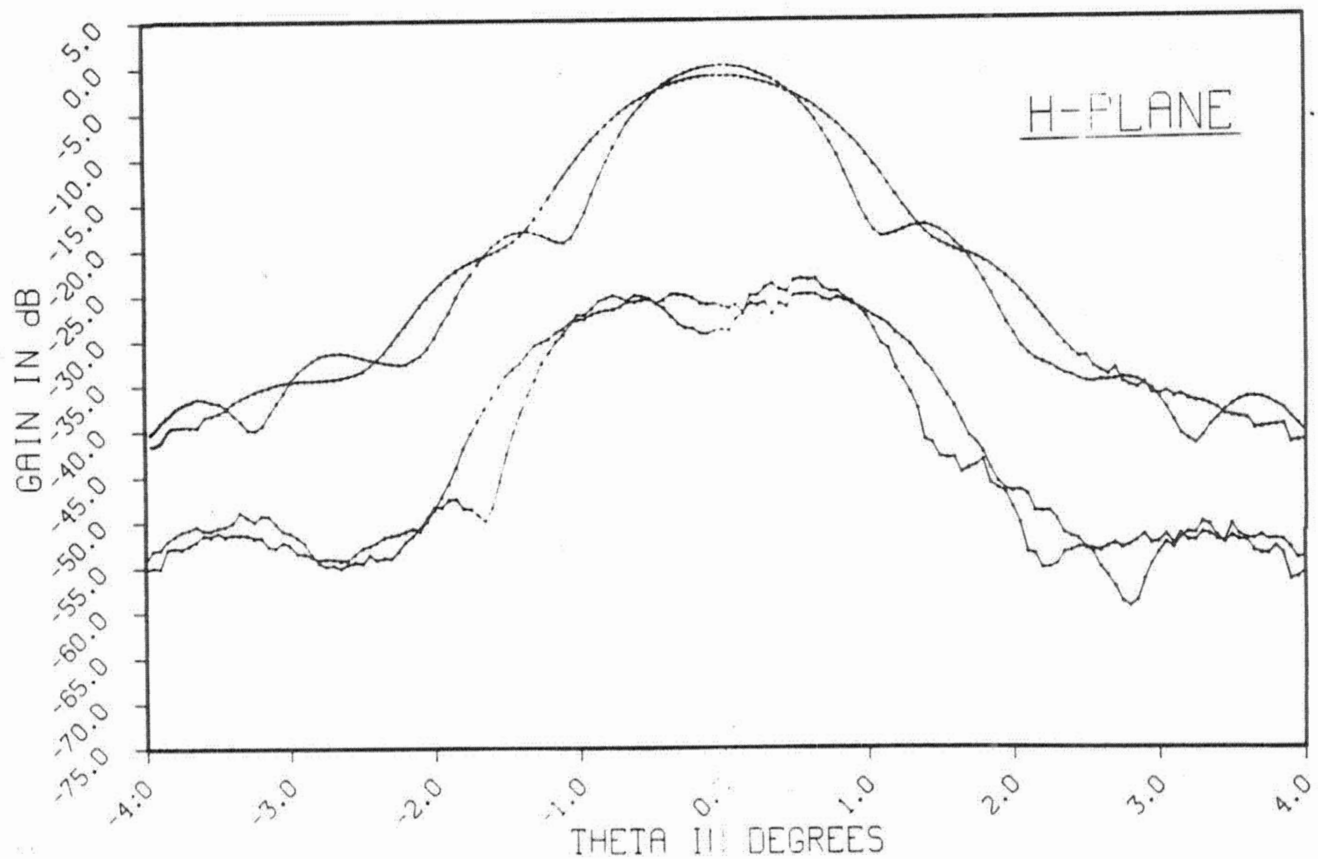

Figure 2.14 37 Ghz Horizontal Pol.

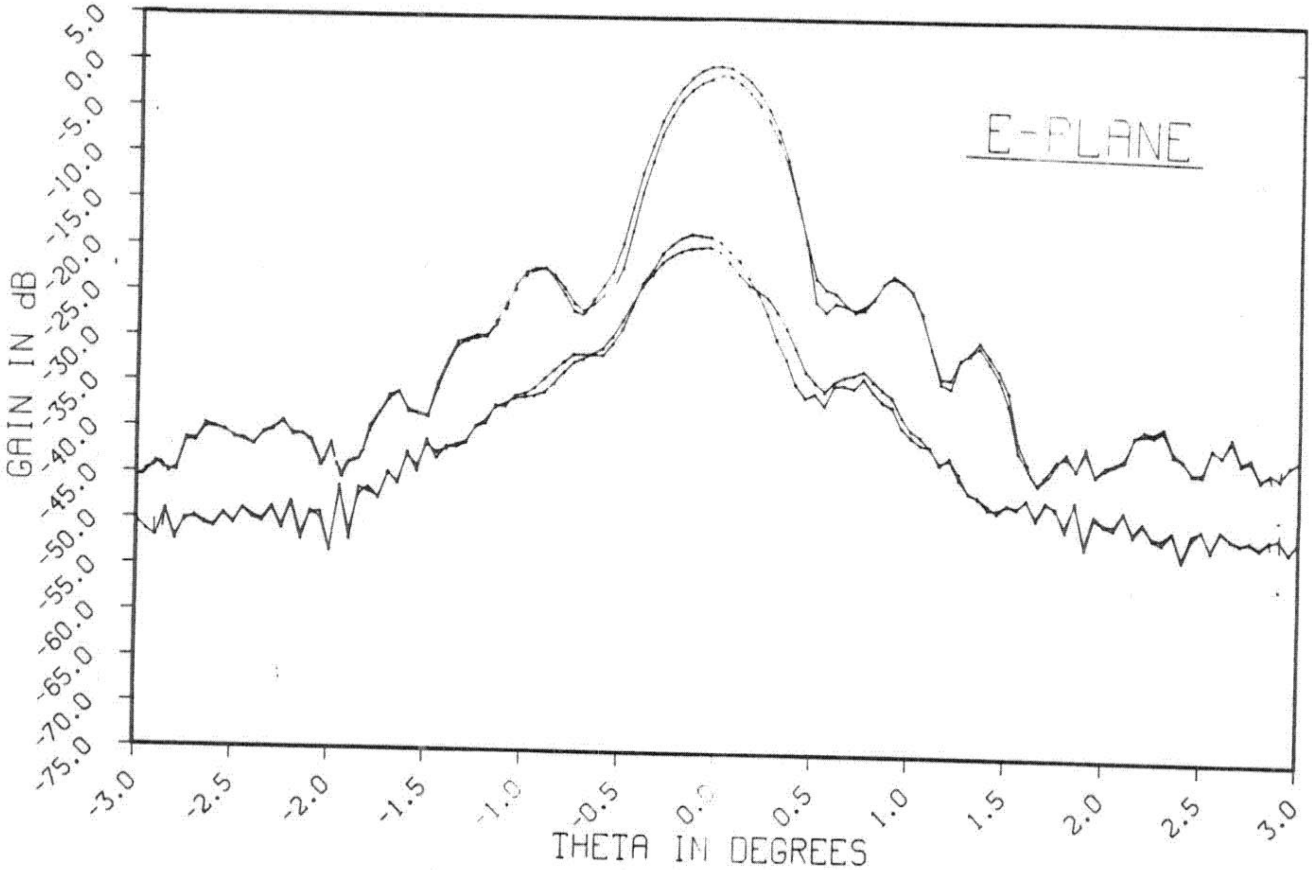

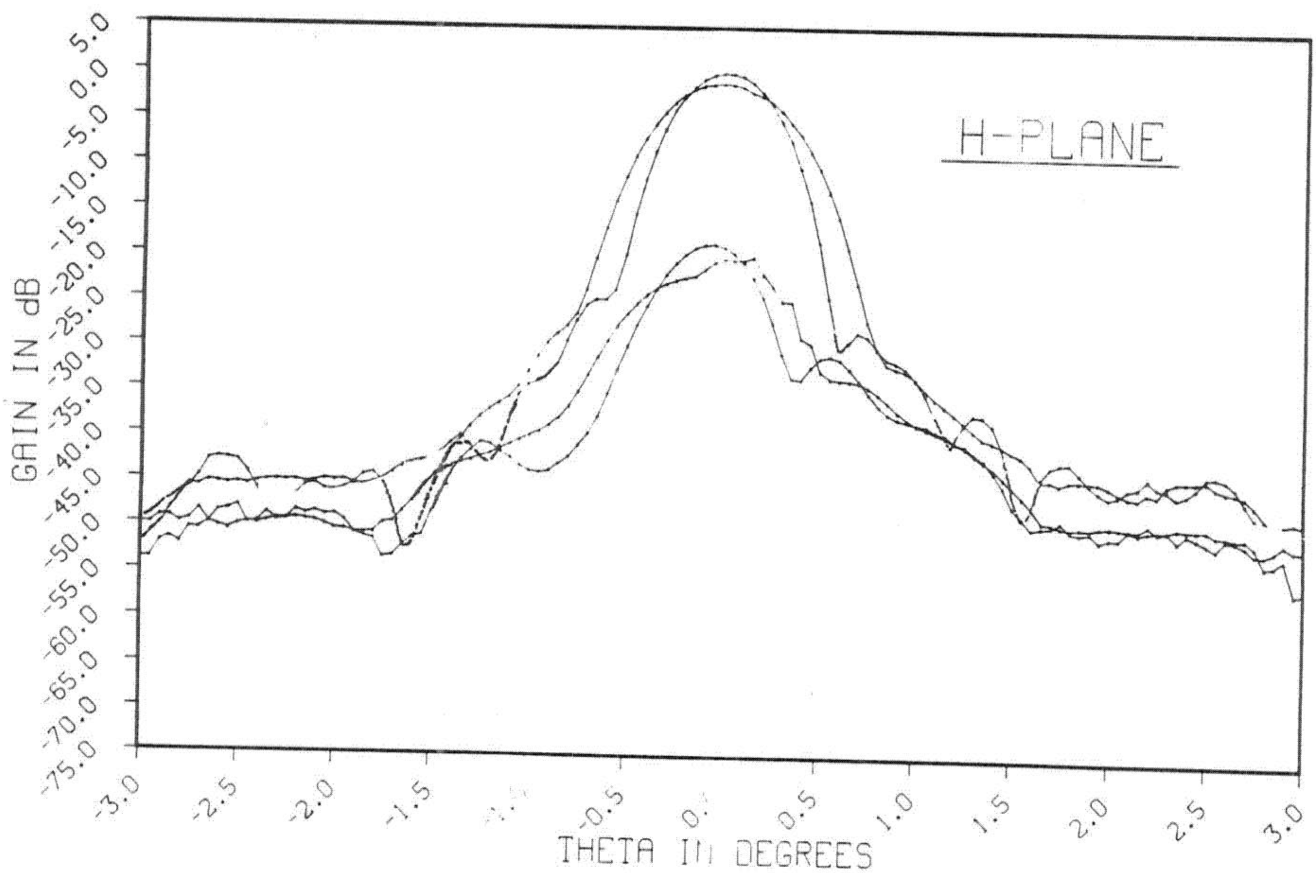

Figure 2.15 85.5 Ghz Vertical Pol.

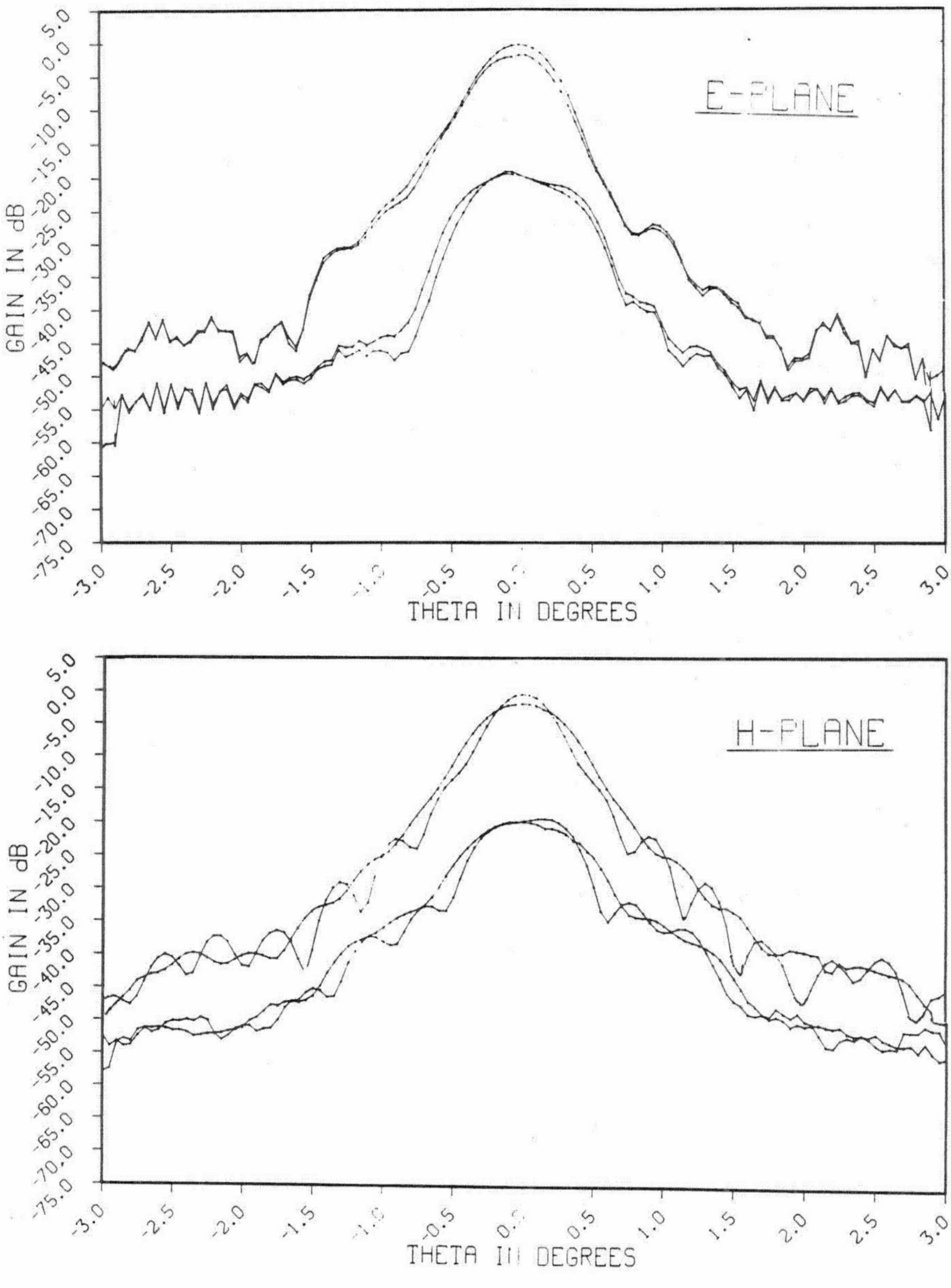

Figure 2.16 85.5 Ghz Horizontal Pol.

coordinates (3) the alignment of the sensor spin axis with the spacecraft local vertical axis and (4) the ability to design a wideband feedhorn to achieve co-axial beams for all channel frequencies and polarizations. Table 2.3a presents the beam pointing accuracy budget for the SSM/I which include both systematic and random components. The errors are defined in the spacecraft coordinate system and include spacecraft attitude control contributions. As shown the beam pointing error is less than half the 85 GHz 3db beam width (6.5 km). Known systematic errors may be taken into account in the earth location algorithm. For example the azimuth and elevation offsets of the antenna boresight as determined from contours of the antenna range pattern measurements and as shown in Table 2.3b are taken into account in the SSM/I pixel location software module.

Table 2.3a Beam Pointing Accuracy (Deg)

	Along Track		Cross Track	
A. Sensor Spin Axis	Systematic	Random	Systematic	Random
RDM Mounting	.014	----	.010	----
Deployment Repeatability	----	.030	----	.021
RDM Stiffness	----	.017	----	.012
BAPTA to RDM	.036	----	.025	----
Top Ring to BAPTA	.054	----	.038	----
Scan Accuracy - Elec	----	----	----	.030
Scan Accuracy - Mech	----	----	.073	----
S/C Attitude Error	----	.014	----	.012
B. Antenna Boresight				
Antenna to Top Ring	.079	----	.062	----
0 g Uncertainty	.036	----	----	----
SUBTOTAL	.109	.037	.107	.040
RSS	.146 (5.3. km)		.147 (3.2 km)	

Table 2.3b Beam Center as Determined from Contour Plots of Antenna Pattern Data (S/N 002)

Frequency GHz	Polarization V/H	Beam Center (Deg) Relative to Optical Boresight Az	EL	Relative to Sensor Coordinate Az	EL
19.35	V	-0.02	-0.25	-0.03	135.25
19.35	H	-0.02	-0.26	-0.03	135.26
22.235	V	-0.03	-0.275	-0.04	135.28
37.0	V	-0.05	-0.26	-0.07	135.26
37.0	H	0.0	-0.19	0.0	135.19
85.5	V	-0.04	-0.26	-0.06	135.26
85.5	H	-0.02	-0.265	-0.03	135.26

2.4 Radiometric Performance

2.4.1 Radiometer Sensitivity

The radiometer sensitivity or noise equivalent temperature differential NEΔT is the standard deviation of the radiometer output referenced to the energy of the waveform incident on the antenna aperture. For a total-power radiometer, the sensitivity may be written as

$$\Delta T = T_{SYS}\sqrt{\frac{1}{B_C \tau} + \left(\frac{\Delta G}{G}\right)^2}$$

$$T_{SYS} = T_S + T_R$$

where

T_{SYS} = System noise temperature

T_R = Receiver noise temperature

T_S = Scene brightness temperature

B_C = Convolutional pre-detection bandwidth

τ = Radiometer integration time

$\frac{\Delta G}{G}$ = rms radiometer gain fluctuation and drift

Although the receiver gain fluctuation contributes directly to the NEΔT, due to the frequent radiometric calibration of the SSM/I every 1.9 seconds and the development of amplifiers and detectors with low 1/f noise, the effect of the fluctuations are negligible over the calibration period. This enables a factor of 2 improvement of signal-to-noise for the total-power SSM/I system over a conventional "Dicke" switched radiometer system which was employed on previous satellite radiometers.

Table 2.4 presents laboratory measurements of the NEΔT (K) taken during selected performance tests over a period of a year for instrument S/N 002. The results apply to a scene temperature of 300 K. It should be noted that the results presented include the noise due to all sources including the contributions of post-detection amplifiers, quantization noise of the 12-bit A/D converter as well as insertion loss of the feedhorn.

Table 2.4 SSM/I ΔT with T_s = 300K (S/N 002)

Date of Measurement	19V	19H	22V	37V	37H	85V	85H
2 April 1984	0.42	0.44	0.75	0.36	0.43	0.61	0.73
16 April 1984	0.45	0.41	0.77	0.34	0.40	0.64	0.66
8 March 1985	0.45	0.42	0.72	0.37	0.36	0.69	0.75
25 March 1985	0.47	0.40	0.73	0.39	0.35	0.66	0.78
26 April 1985	0.45	0.42	0.73	0.41	0.34	0.63	0.73
5 June 1985	0.46	0.41	0.76	0.36	0.40	0.80	0.71
10 June 1985	0.44	0.43	0.75	0.33	0.39	0.77	0.74
Average	0.45	0.42	0.74	0.37	0.38	0.69	0.73

2.4.2 Radiometer Calibration

The radiometer calibration accuracy budget, exclusive of antenna pattern correction effects, which are discussed in Section 3.2, is composed of three major contributors: (1) hot load reference error, (2) cosmic background reference error, and (3) radiometer/calibration test nonlinearity. The calibration error of the hot load is measured during the thermal vacuum calibration by comparison to the variable reference target when the temperature of the variable target equals the temperature of the hot load. Since the temperature of the variable target is believed to be extremely accurate (temperature gradients over the surface of the target are negligible and the emissivity is >0.9999) it serves as a primary standard calibration reference for the in-orbit hot-load and cold targets used in thermal vacuum calibration. Examination of the thermal vacuum calibration data shows the error of the hot load to be $\leq$0.05K rms, which is at the fluctuation level of the temperature sensor measurements. In effect, no systematic calibration error of the hot load is detectable.

The radiometric temperature of the cosmic background is consistent with a blackbody radiator at 3°K. The SSM/I calibration reflector is designed to reflect the cold cosmic background into the feedhorn and minimize the possible reception of extraneous energy from the spacecraft, the earth and other undesired sources of radiation. An analysis of the calibration reflector antenna patterns when the SSM/I is in the calibration position reveals that the reception of earth and spacecraft radiation is extremely small; less than a few tenths of a degree. Figure 2.17 shows the broadest calibration antenna patterns which occur at 19.35 GHz. Note that essentially all of the antenna pattern energy lies within ~28° of boresight, except for the feedhorn spillover energy. The spillover energy views the cosmic background since the SSM/I is located on top of the spacecraft and since the calibration reflector completely occults the primary reflector during the calibration measurements. Thus it is believed that the SSM/I calibration reflector provides a clear view of the cosmic background to the feedhorn and hence provides a highly accurate blackbody calibration reference at 3°K.

Finally, nonlinearities in the calibration measurements (due to radiatively induced thermal gradients in the targets by the radiometer) and in the radiometer receiver (due to imperfect operation of the square law detector and IF amplifier compression) may be expected to appear in the calibration data. At measurement temperatures equal to the hot load and cosmic background calibration references, the calibration uncertainty is simply the accuracy of the reference. At intermediate temperatures, radiometer nonlinearity and calibration reference temperature errors contribute to the total uncertainty with the errors weighted according to the temperature difference between the input and the calibration references. These errors are included in the total

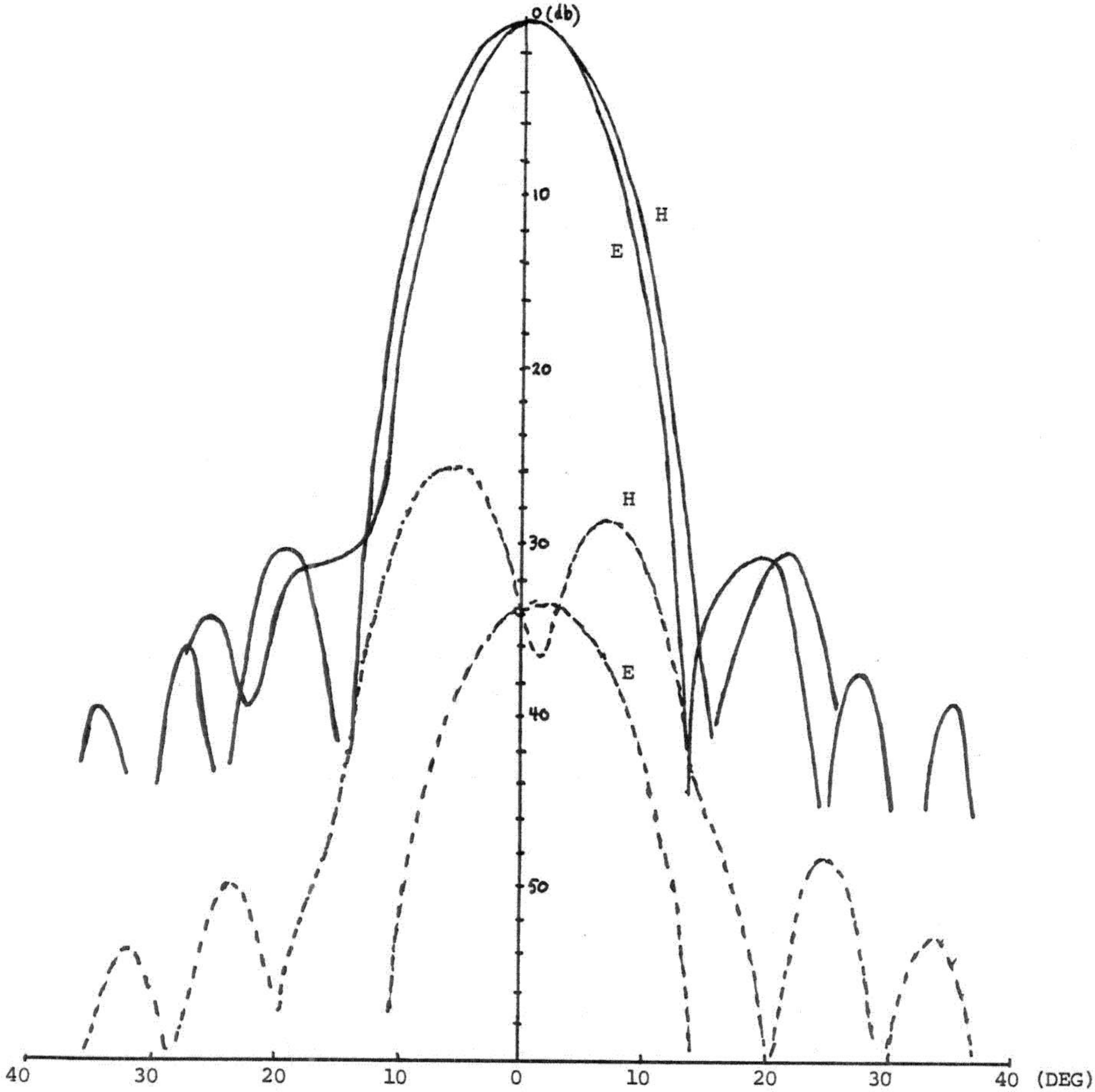

Figure 2.17 Antenna Patterns of E and H Plane of Cold Calibration Reflector at 19.35 GHz Vertical Polarization (—— Co, --- Cross Pol)

system calibration accuracy results obtained during the thermal vacuum calibration tests.

Thermal vacuum radiometer calibration is accomplished using two precision microwave reference targets in addition to the spacecraft hot load to simulate an operational configuration. A liquid nitrogen cooled precision target is substituted for the cold sky reflector, and a variable precision target which is controllable through the radiometer operating range of 100K to 375K is positioned over the feed during part of the active scan to simulate active scan data. The spacecraft hot target is used as the calibration hot reference, and is calibrated by comparison to the variable target during the calibration procedure.

The precision microwave reference targets are each instrumented with eight precision platinum temperature sensors, and the spacecraft hot reference is instrumented with three flight platinum temperature sensors.

Calibration data are taken for ten variable target temperatures over the instrument range of 100K to 375K, and for three instrument physical temperatures at the low, nominal, and high points of the qualification temperature range. At each combination of variable target temperature and instrument physical temperature, 40 frames of calibration data are taken and the average radiometric brightness temperature measured for the variable target, T_B, and the instrument error, ϵ, are computed using the relationship

$$T_B = T_C + (T_H - T_C)\frac{V_B - V_C}{V_H - V_C}$$

$$\epsilon = T_B - T_{var}$$

where T_H, T_C, T_{var} are the hot, cold, and variable target temperatures from the platinum temperature sensors, and V_H, V_C, V_B are the hot, cold, and variable radiometer output voltages (in digital counts) corresponding to the target measurements. Thus the calibration error is the difference between the computed variable target radiometric brightness temperature and the average physical temperature of the variable target.

Figures 2.18 and 2.19 present the total radiometer calibration error measured during thermal vacuum calibration for all channel frequencies and polarizations as a function of target temperature for three sensor temperatures: hot (38°C), ambient (28°C) and cold (0°C). As shown the largest errors occur at the cold temperatures and in all cases are less than 1.2°K.

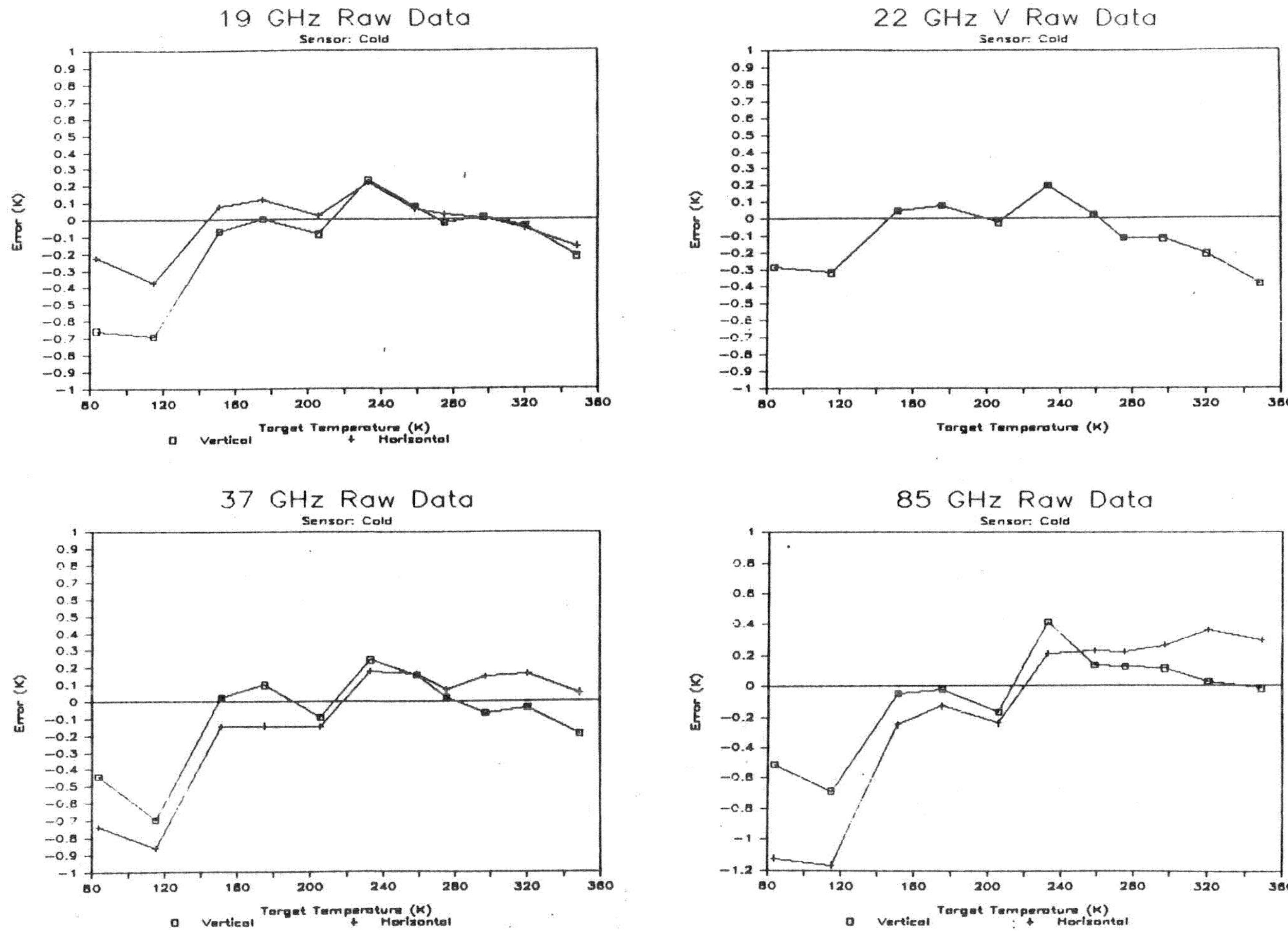

Figure 2.18 Thermal/Vacuum Calibration at 0 c Sensor Temperature

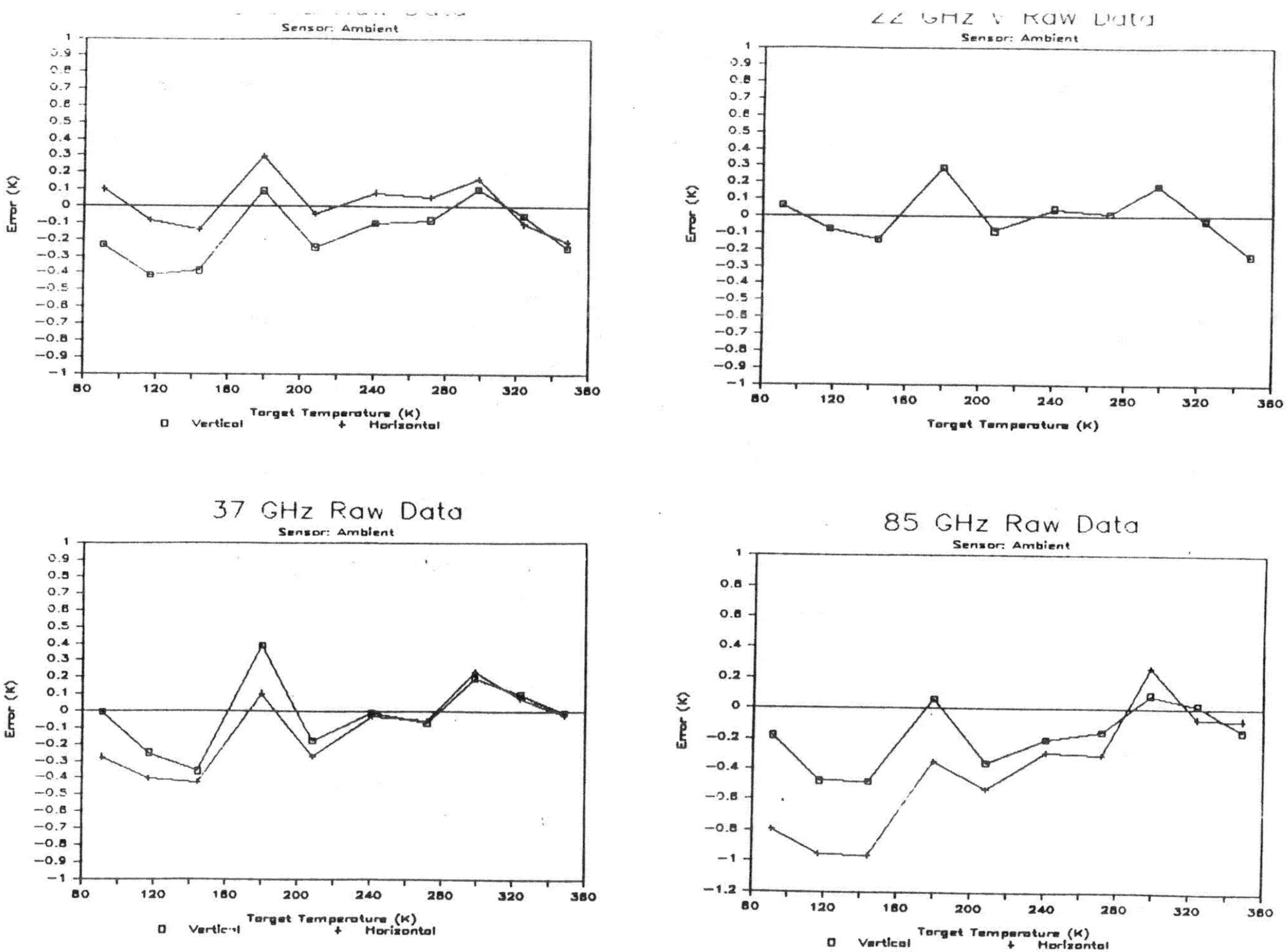

Figure 2.19a Thermal/Vacuum Calibration at 27 C Sensor Temperature

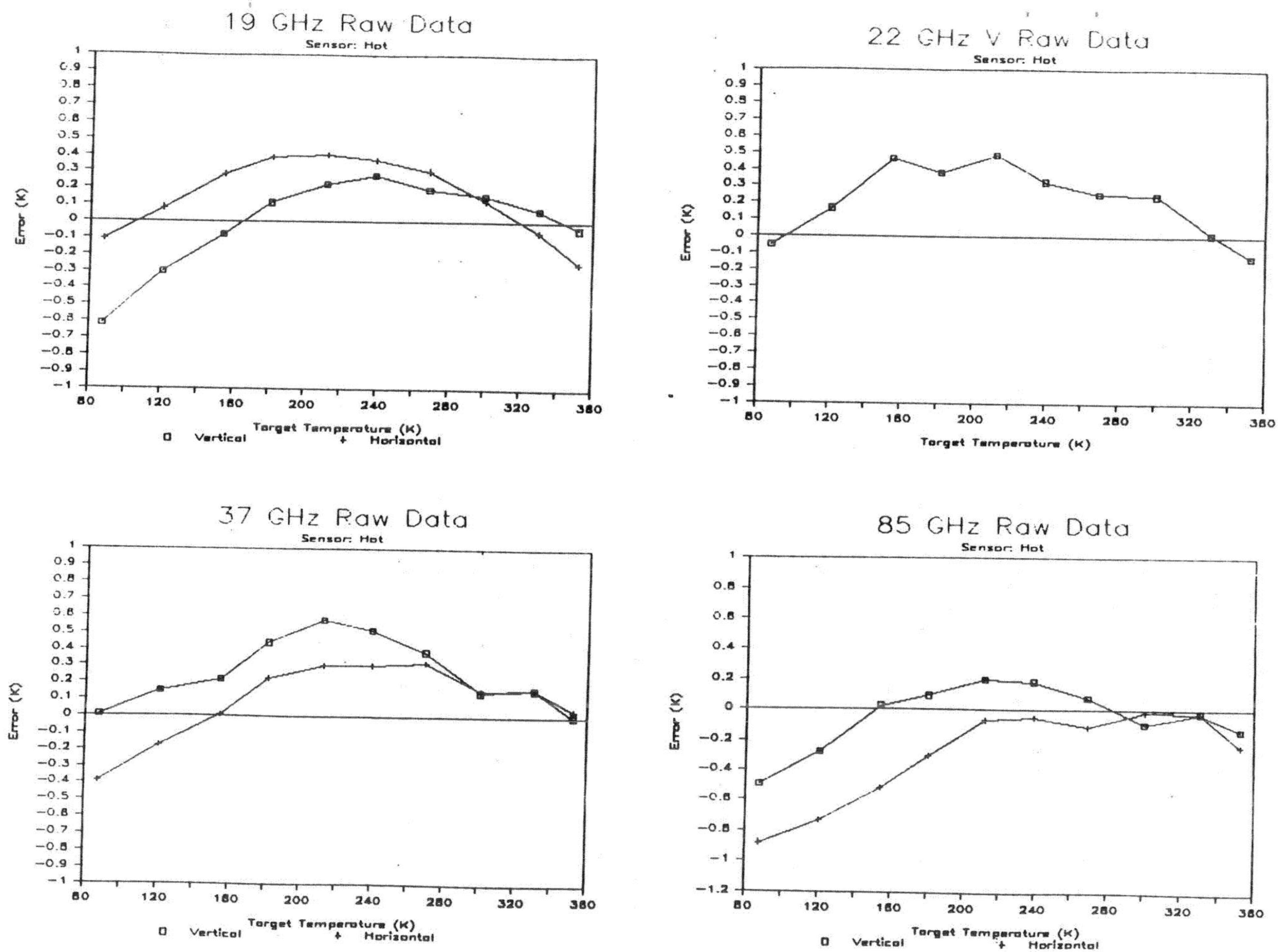

Figure 2.19b Thermal/Vacuum Calibration at 38 C Sensor Temperature

3.0 SENSOR DATA RECORD ALGORITHM

The absolute brightness temperature of the scene (T_B) incident upon the antenna is received and spatially filtered by the antenna to produce an effective input signal or antenna temperature (T_A) at the input of the feedhorn antenna. Section 3.1 presents the overall radiometer calibration algorithm used to convert the measured output of the A/D converter into absolutely calibrated antenna temperatures which are contained in the temperature data record (TDR) file. To obtain an estimate of T_B from T_A it is necessary to apply an antenna pattern correction (APC) to correct for spurious energy received in the antenna side lobes, cross-polarization coupling and feedhorn spillover loss. The estimates of the main-beam brightness temperature derived from T_A using the APC are contained in the sensor data record (SDR) file. The APC algorithm is discussed in Section 3.2.

3.1 Temperature Data Record Algorithm

As discussed in Section 2.0, the SSM/I is calibrated each scan from the input to the feedhorn through the output of the A/D converter. This is accomplished by passing the feedhorn beneath two fixed calibration reference targets: a hot-load black-body radiator at 300K and a small calibration reflector which reflects the cold cosmic background radiation of 3K into the feedhorn field-of-view. A linear function is used to model the radiometer transfer function which relate the digitized output voltage to the temperature incident at the feedhorn. Letting V_H and V_C denote the A/D output voltages associated with viewing the hot-load and cosmic background brightness temperatures, then the brightness temperature of the scene incident at the feedhorn T_A is expressed in terms of the measured output voltage V_S at time t by

$$T_A = \hat{T}_C + \left(\hat{T}_H - \hat{T}_C\right) \frac{\bar{V}_S - \hat{V}_C}{\hat{V}_H - \hat{V}_C}$$

where

$\hat{V}_H$ = estimate of the radiometer calibration voltage of the hot-load at time t which is based on the set of measured hot-load calibration voltages

$\hat{V}_C$ = estimate of the radiometer calibration voltage of the cosmic background at time t which is based on the set of measured cosmic-background calibration voltages.

$\hat{T}_H$ = estimate of the effective brightness temperature of the hot-load at time t from the set of measured temperatures of the hot-load.

$\hat{T}_C$ = estimate of the effective brightness temperature seen by the feedhorn when viewing the calibration reflector.

The bar on V_S denote the time average over the radiometer integration time. Figure 3.1 presents a time series of calibration and scene voltages that occur each scan.

Five samples of V_{Hi} and V_{Ci} ($i = 1,\ldots 5$) are taken each scan and averaged to reduce the sensor noise in the estimates $\hat{V}_H$ and $\hat{V}_C$

$$\hat{V}_H = \frac{1}{5}\sum_{i=1}^{5} V_{H_i}$$

$$\hat{V}_C = \frac{1}{5}\sum_{i=1}^{5} V_{C_i}$$

Three high resolution temperature sensors are used to estimate the average surface temperature of the hot-load

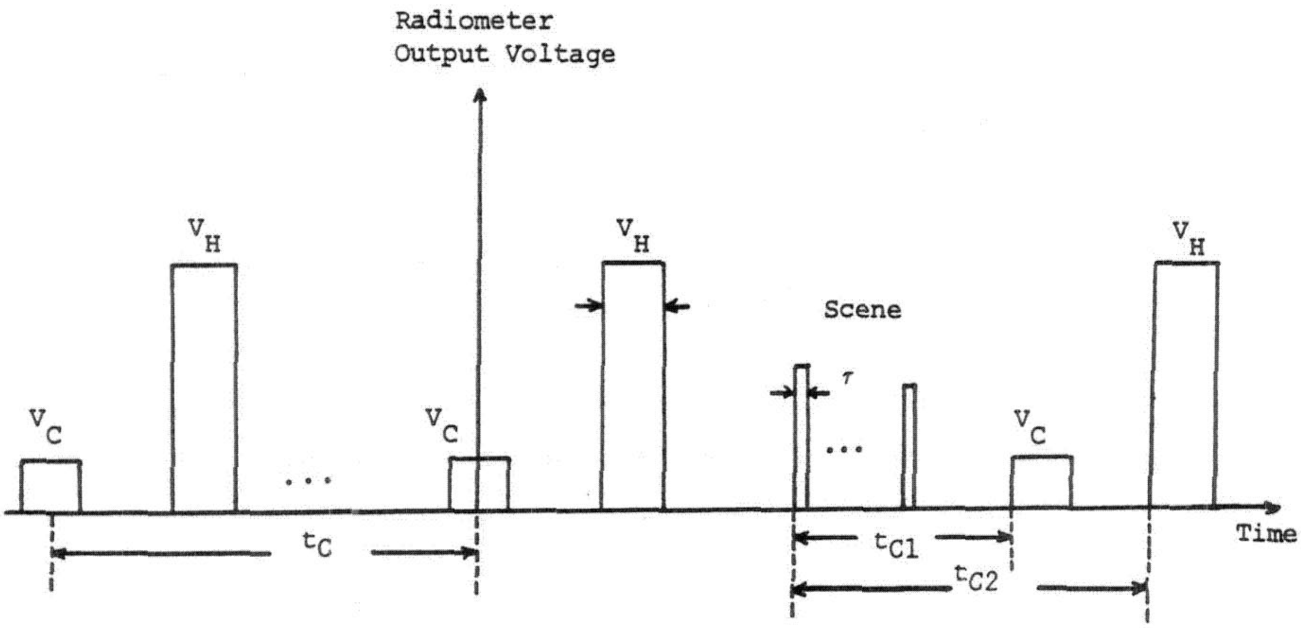

τ = Radiometer integration times:

3.89 msec at 85 GHz

7.95 msec at 19/22/37 GHz

t_C = Calibration period 1.9 sec

V_C = Calibration voltage of cosmic background

V_H = Calibration voltage of hot load

t_{C1} = Time from start of scene voltages to cold calibration

0.925 sec (175 Deg rotation)

t_{C2} = Time from start of scene voltages to hot calibration

1.376 sec (260 Deg rotation)

$\hat{T}_C$ = Effective radiometric temperature of cold calibration target

$\hat{T}_H$ = Effective radiometric temperature of hot calibration target

Figure 3.1 Sequence of Calibration and Scene Measurements

$$T_H = \frac{\sum_{i=1}^{3} x_i T_{H_i}}{\sum_{i=1}^{3} x_i}$$

where x_i is either 1 or 0 depending on whether the temperature sensor is functioning properly or not. This temperature is used for all frequencies and polarizations.

To account for radiative coupling between the hot-load and the top plate of the rotating drum assembly which faces the hot-load when not being viewed during calibration, a correction is applied to the average hot-load temperature T_H

$$\hat{T}_H = T_H + \alpha(T_P - T_H)$$

where

$\hat{T}_H$ - effective hot-load temperature

α - empirical correction determined from thermal-vacuum calibration

T_P - temperature of the plate facing the hot-load.

Based on calibration data taken during thermal-vacuum testing

α = 0.01. A temperature sensor measures T_P.

The effective radiometric temperature of the cosmic background seen by the feedhorn when viewing the calibration reflector may be expressed as

$$\hat{T}_C(\hat{k}) = \oint_{4\pi} d\Omega' G(\hat{k}, \hat{k}') T_{inc}(\hat{k}')$$

where G is the far-field antenna power pattern which weights the angular distribution of the brightness temperature T_{inc} incident in direction $\hat{k}'$ on the antenna (reflection and feedhorn) when the antenna is pointed in direction $\hat{k}$. As noted earlier by appropriate design of the calibration reflector and selection of calibration regions, $T_{inc} \simeq T_{cosmic}$ where T_{cosmic} is the radiometric temperature of the cosmic background which is consistent with a blackbody radiator at 3^oK. Analysis of the antenna pattern G shows that the effects of energy received from the spacecraft and earth are extremely small, less than 0.1 - 0.2K. Thus, T_c may be determined solely on the basis of the radiometer temperature of the cosmic background:

Frequency (GHz)	T_c (K)
19.35 - 22.235	2.7
37.0	2.8
85.5	3.2

The values presented include a correction to the Rayleigh-Jeans approximation which becomes important for very cold radiators at mm-wave frequencies.

It should be noted that T_C is an adjustable parameter and the validity of the current value will be examined during the early orbit calibration/ validation effort of the SSM/I. The calibration parameters T_H, V_H, V_C are up-dated each scan to compute the scene brightness temperatures T_A before the next calibration occurs. Since the radiometers are expected to exhibit extremely good stability over a number of calibration data sets, it is very probable that T_H, V_H, and V_C may be averaged over many scans to reduce the effects of sensor noise. Although this is not done presently, the number of scans to be used will be determined during the early orbit calibration/validation effort of the SSM/I. Based on the stability achieved with other satellite sensors, it should be possible to average the calibration data over periods of 30 to 60 seconds.

3.2 Antenna Pattern Correction

3.2.1 Background

The antenna temperature T_A (i.e. the TDR of Section 3.1) may be expressed in terms of an integral of the scene brightness temperature distribution T_S incident on the antenna reflector and the effective co- and cross-polarized far-field antenna power patterns. For channel center frequency ν_o, polarization p, and with the antenna pointed in direction $\hat{k}$, T_A may be written as

$$T_A(p,\hat{k}) = \int_{Earth} d\Omega' \left[G_{pv}(\hat{k},\hat{k}') T_S(v,\hat{k}') + G_{ph}(\hat{k},\hat{k}') T_S(h,\hat{k}') \right] + (1-\eta_p) T_{cosmic}$$

where $G_{pq}(\hat{k},\hat{k}')$ is the effective far-field antenna power pattern which weights the angular distribution of the brightness temperature incident in direction $\hat{k}'$ in polarization q when the antenna is pointed in direction $\hat{k}$ and measuring polarization p.

The term effective identifies the fact that the effects of the radiometer integrate and dump low pass filter are included in G_{pq}. As noted earlier the filter widens the beam in the along scan direction and leaves the beam essentially unaltered in the along track direction. See Figures 2.10 - 2.16.

The vertical or horizontal polarizations as measured on an antenna range are not the same as the local vertical and horizontal polarizations on the earth's surface over the antenna field of view. For narrow antenna beams such as the SSM/I, they may be considered to be the same to an excellent approximation.

The feedhorn spillover factor η_p is defined by the fraction of energy received from the reflector in polarization p to the total energy received by the feedhorn. For clarity the dependence of G_{pq}, T_S, η_p, and T_A on the channel center frequency is not shown but it should be understood that G_{pq} and η_p are averaged over the receiver passband.

Figure 3.2 presents the geometry of the integration variables: the angular integration $d\Omega'$ is taken over the earth field of view and T_{cosmic} is the brightness temperature of the cosmic background. When $p = q$, G_{pp} is the defined as the co-polarized patterns (i.e., G_{vv}, G_{hh}) and when $p \neq q$ G_{pq} is defined as the cross-polarization patterns (i.e., G_{vh}, G_{hv}). In practice G_{pq} and η_p are determined from antenna pattern measurements over 4π steradians on an antenna range. η_p is essentially the integrated feedhorn pattern over the solid angle subtended by the reflector.

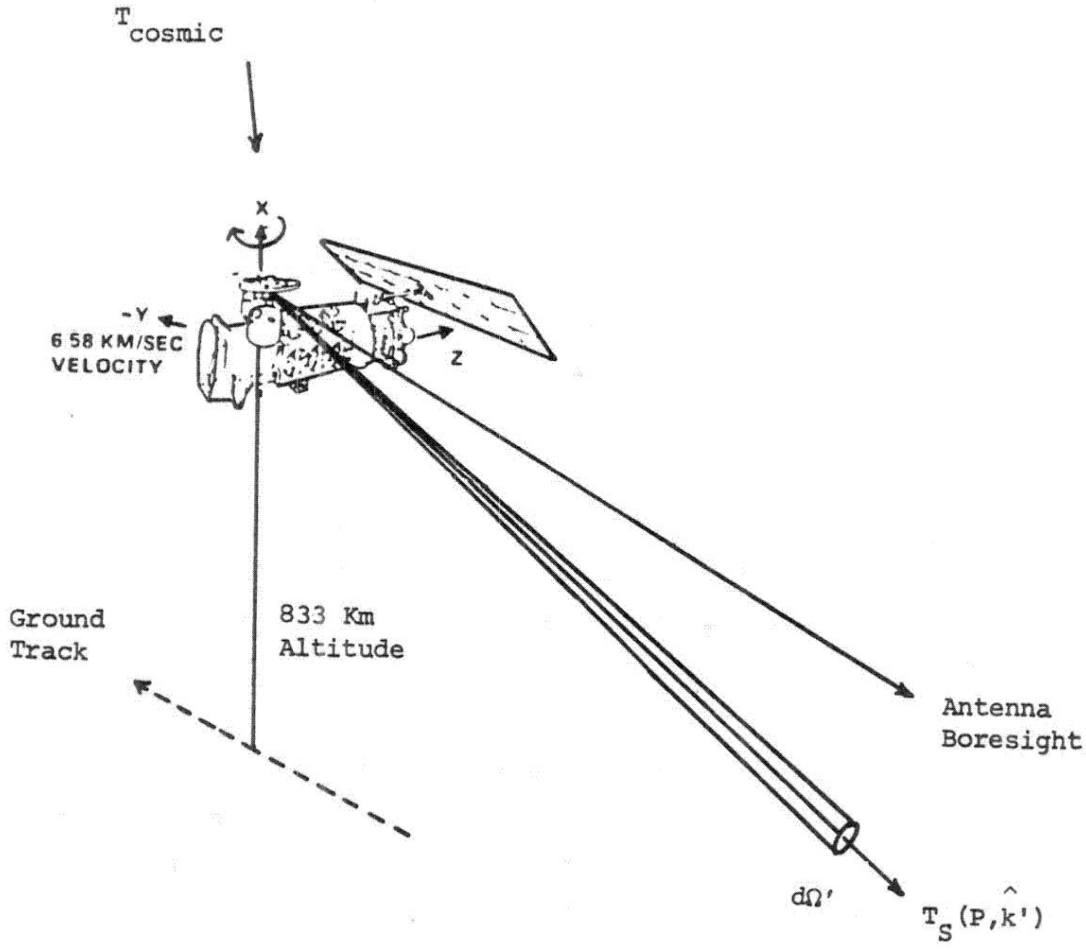

$$T_A(p,\hat{k}) = \int_{Earth} d\Omega' \left[G_{pv}(\hat{k},\hat{k}') T_S(v,\hat{k}') + G_{ph}(\hat{k},\hat{k}') T_S(h,\hat{k}') \right] + (1-\eta_p) T_{cosmic}$$

where

η_p = Feedhorn spillover factor

G_{pq} = Far-field antenna pattern

T_S = Scene brightness temperature incident on antenna

v,h = Vertical or horizontal polarizations

Figure 3.2 Geometry for Antenna Temperature Definition

Proper normalization requires for p = v or h polarizations:

$$\int_{Earth} d\Omega' \left[G_{pv}(\hat{k},\hat{k}') + G_{ph}(\hat{k},\hat{k}') \right] = \eta_p$$

The above expression for T_A assumes that the time variation of the scene brightness temperature over the integration time T_s is negligible and is a valid approximation for the SSM/I.

In principle the accuracy of the scene brightness temperatures incident on the reflector T_s may be improved by making antenna pattern corrections (APC). These corrections are intended to remove the effects of:

(a) Feedhorn spillover loss η_p
(b) Cross-polarization coupling G_{pq} $(p \neq q)$
(c) Sidelobes contributions of G_{pp}.

For convenience corrections (a) and (b) are denoted as Level 1 and correction (c) as Level 2. Level 1 corrections are applied first to T_A and can be inverted, if desired, to obtain the original temperatures T_A. In general, Level 2 corrections cannot be inverted and usually require significantly more data processing than Level 1.

In addition the benefits of Level 2 corrections are considerably more difficult to evaluate since, as will be discussed below, they depend on the spatial variations of T_S over the sidelobe regions of G_{pp}. Each of the corrections are discussed separately below. For clarity the corrections are presented for the vertical polarization p = v. Similar equations apply for the case p = h.

3.2.2 Level 1 Corrections

Based on the antenna pattern results presented in Section 2.3 and the expression for T_A, the correction for feedhorn spillover loss and cross-polarization coupling is written as

$$\hat{T}_S(v,\hat{k}) = \frac{1}{\eta_v(1-b_v)}\left[\hat{T}_A(v,\hat{k}) - b_v\hat{T}_A(h,\hat{k})\right]$$

where $\hat{T}_A(v,\hat{k})$ and $\hat{T}_A(h,\hat{k})$ are the antenna temperatures (i.e. TDRs) for the vertical and horizontal polarizations for antenna boresight direction $\hat{k}$. The justification for this algorithm is based on the fact that the spillover factor η_p is essentially the same for the v- and h-polarization at each frequency and that the cross polarization coupling occurs primarily within the mainbeam of G_{pp}. Note that the term b_V includes contributions from all sources. Although the primary contribution is expected to arise from the antenna pattern which is discussed in detail below, some contribution may arise from interchannel cross-talk. The total b_V will be evaluated during the SSM/I Cal/Val effort. Also note that the form of the correction uses the fact that η_V is close to unity for all channels and hence the cosmic background contribution may be neglected.

Since the horizontally polarized brightness temperature is not measured for the 22.235 GHz channel, it is estimated using the horizontally polarized temperature at 19.35 GHz:

$$\hat{T}_A(22.235,\ h,\hat{k}) = 96.6 + 0.653\ \hat{T}_A\ (19.35,\ h,\hat{k})$$

This relationship is derived by correlating simulated radiometer data at the two channels for a wide range of environmental conditions over land, sea, and ice surfaces.

The antenna pattern portion of b_V is a measure of the integrated cross polarized coupling for the v-polarization and is selected on the basis of eliminating the cross-polarization coupling when the vertical and horizontal scene temperatures are uniform but not necessarily equal over the antenna field-of-view.

$$b_V = \frac{\int_{Earth} d\Omega' G_{vh}}{\int_{Earth} d\Omega' G_{hh}}$$

Based on antenna range measurements and computations to account for the action of the radiometer integrate and dump lowpass filter Table 3.1 presents η_p and b_p for SSM/I instrument S/N 002.

Table 3.1 Coefficients for Feedhorn Spillover and Cross Polarization Coupling Corrections (S/N 002)

Center Frequency (GHz)	Polarization p = v/h	η_p	b_p
19.35	v	0.969	0.00473
	h	0.969	0.00415
22.235	v	0.974	0.01070
37.0	v	0.986	0.02170
	h	0.986	0.02612
85.5	v	0.988	0.01383
	h	0.988	0.01947

The accuracy of the algorithm to remove cross polarization coupling depends on the spatial variability of the incident cross-polarized scene brightness temperature. For a temperature distribution essentially uniform over the main beam, the correction is extremely accurate. The accuracy degrades slightly in the event significant cross-polarized variations occur within the main beam.

The accuracy of the algorithm to remove the feedhorn spillover loss depends on the accuracy of the spillover loss factor η_p which is currently obtained by integrating the feedhorn antenna pattern over the solid angle subtended by the reflector. Accurate knowledge of η_p is important since a 1 % error in η_p can result in a 2°K error in the estimate of T_s. An evaluation of the Level 1 APC correction will be conducted during the early-orbit SSM/I calibration/validation effort.

3.2.3 Level 2 Correction

The task of attempting to improve the spatial resolution of G_{pp}, i.e., correcting for the imperfect spatial filtering of the antenna, or, more generally of inverting the integral relation between measured T_A and the up-welling scene temperature T_s contains mathematical features common to a large number of remote sensing problems. In particular the problem may be shown to be mathematically equivalent to the problem of inverting microwave or infrared measurements to obtain atmospheric temperature profiles in remote sounding data [3]. A great deal of literature published on the latter subject has shown that it is not desirable to attempt to obtain fine details in the sounding because of amplification of noise in the sensor data. This arises from the numerical instability of the Fredholm integral equation of the first kind which must be solved and the attendant amplification of errors that occurs in the inversion process.

In view of this situation, it is desirable to restruct the Level 2 algorithm for the SSM/I which minimizes the antenna sidelobe energy contributions outside the main beam and, if possible, not significantly alter the antenna pattern within the mainbeam. To this end, the Level 2 algorithm considered herein estimates the average scene brightness temperature over the main beam weighted by the antenna gain. Other estimates, such as the true spatial average over the main beam, could be used but the discontinuity at the edge of the main beam introduces significant amplification of sensor noise.

The current Level 2 algorithm is expressed as a linear combination of antenna temperature measurements T_A in the immediate vicinity of the measured antenna temperature to be corrected. Other approaches for Level 2 corrections have been investigated [4]-[7] but require extensive data processing which is not available for the SSM/I. The restriction of antenna temperature samples to a small region surrounding the temperature to be corrected is not severe since as shown in antenna pattern data presented in Section 2.3 essentially all of the sidelobe energies lies within the region defined by the set of 5 x 5 neighboring samples of brightness temperature surrounding the temperature to be corrected.

To reduce energy contributions in the sidelobes, antenna temperature samples are selected which lie outside the main beam. Furthermore since the spatial samples of brightness temperature overlap at the 3-dB points (except at 19.35 and 22.235 GHz) the samples in the algorithm should be separated by approximately one sample to avoid significant overlapping of the main beams of the measurement samples.

The current SSM/I Level 2 APC software module permits a maximum of four antenna temperature samples to be employed in a 5 x 5 matrix of neighboring samples and the selection may be changed in five angular sections across the scan as shown in Figure 3.3. Following the rationale discussed above, Figure 3.4 shows a reasonable selection of antenna temperature samples which may be used in the Level 2 APC as shaded for several positions across the scan for the 85 GHz channels. The circles indicate 3 dB contours. A similar geometry applies to the 37 GHz channels.

Due to the extremely high beam efficiencies achieved for the 19.35 and 22.235 GHz antenna patterns, little change occurs in the antenna temperature when performing Level 2 corrections at these frequencies. In view of this fact Level 2 corrections are not performed for these channels. The improvement in main beam efficiency is incorporated into the Level 1 correction which uses only the co- and cross-polarized central measurement samples.

To determine the relative merit of the Level 2 APC for 37 and 85 GHz channels the APC is written as

$$\hat{T}_S(\upsilon,\hat{k}) = a_o\left[\hat{T}_A(\upsilon,\hat{k}) - \sum_{n=1}^{4} a_n \hat{T}_A(\upsilon,\hat{k}_n)\right]$$

where $\hat{k}_n$ define the antenna bore-sight directions for the shaded beams in Figure 3.4.

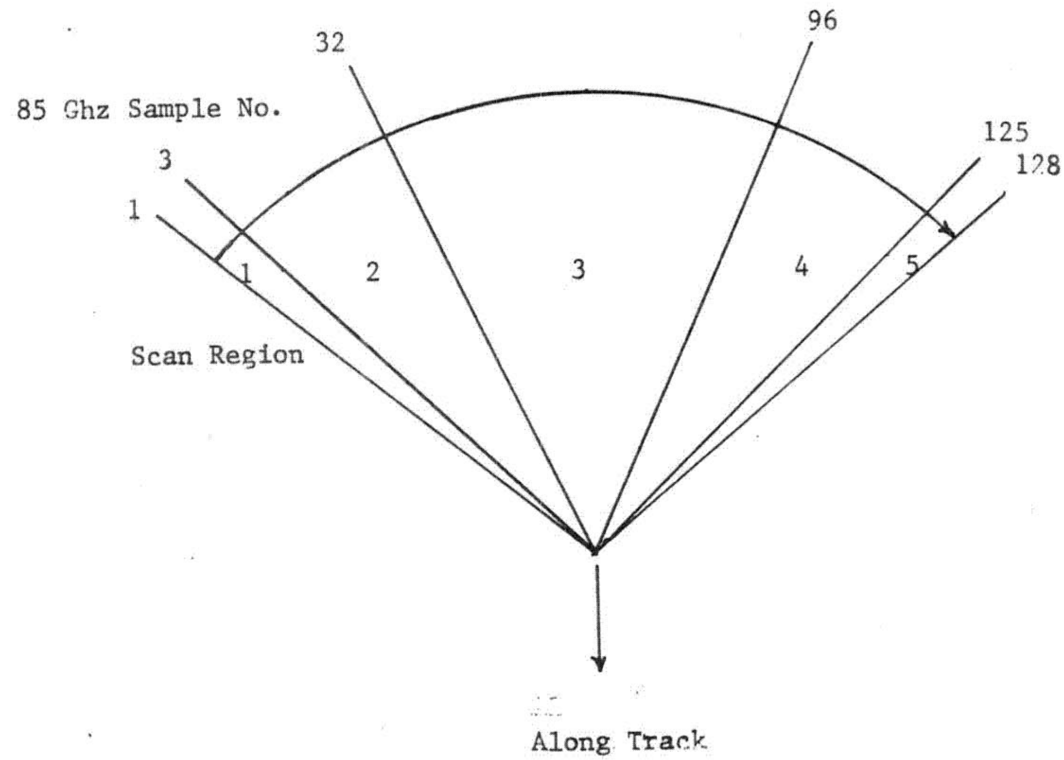

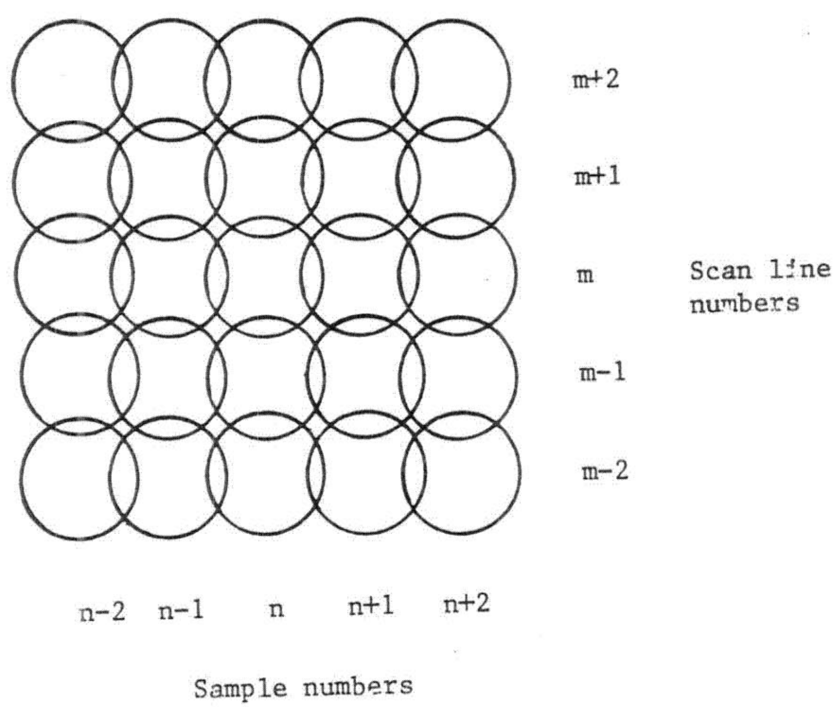

Scan line m and sample number n identify pixel to be corrected in Level 2 APC

Figure 3.3 Scan Regions to Vary a_n and Selection of Samples in Level 2 APC

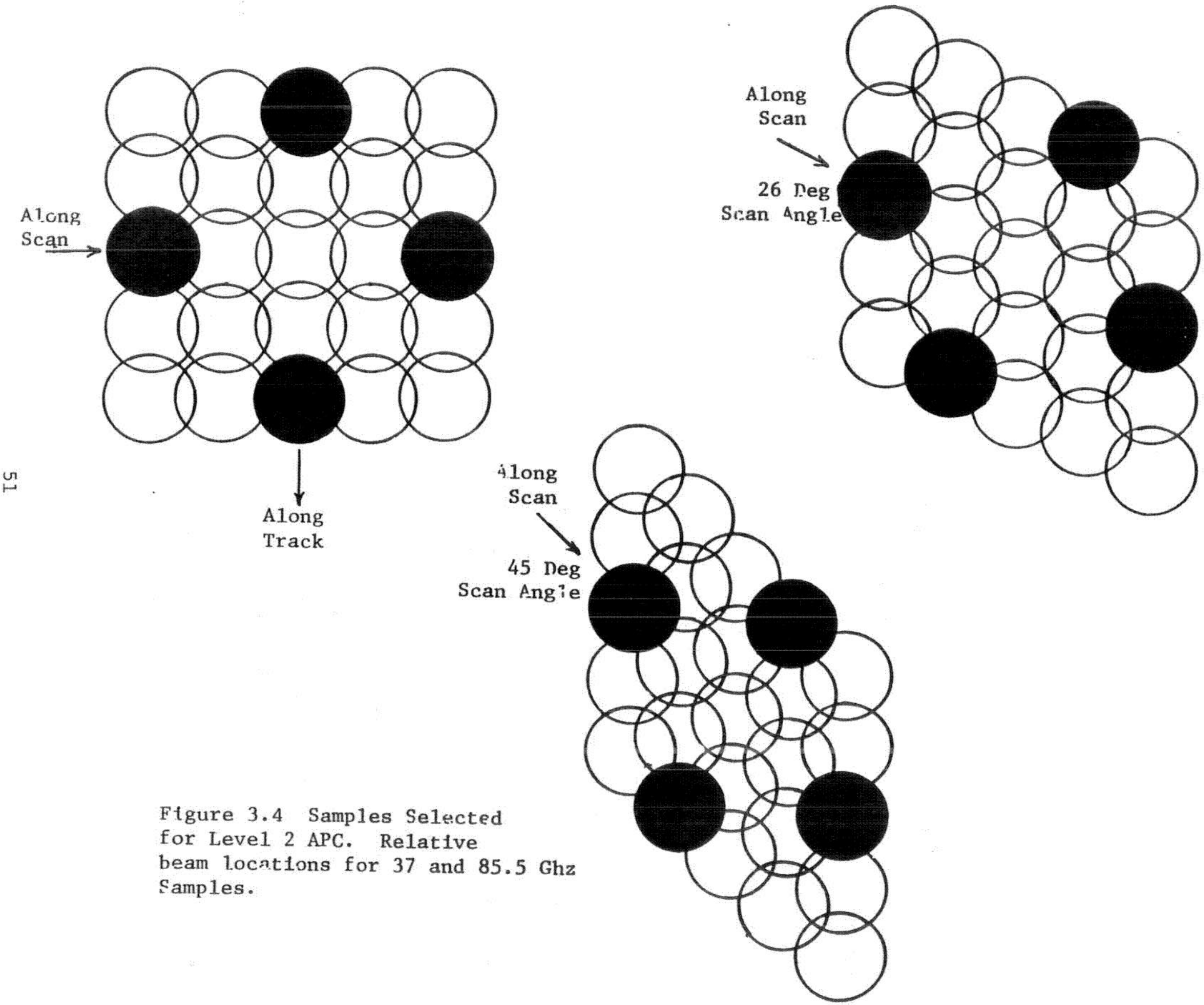

Figure 3.4 Samples Selected for Level 2 APC. Relative beam locations for 37 and 85.5 Ghz Samples.

The selection of the weighting coefficients a_n depends on the spatial distribution of energy lying outside the mainbeam. Qualitatively, a_n is a measure of the sidelobe energy lying within the angular region defined by the mainbeam of the samples selected in Figure 3.3. More precisely, the set a_n may be determined by solving the system of equations which requires the minimization of the integral

$$\int_{MB} d\Omega' \left[\frac{G_{vv}(\hat{k},\hat{k}')}{c} - \sum_{n=1}^{4} a_n G_{vv}(\hat{k}_n,\hat{k}') \right]^2$$

where

MB = angular region defined by the main beam. As noted earlier the main beam is defined by 2.5 times the 3 db beamwidth.

The coefficient a_o is determined by noting that proper normalization requires

$$a_o = \frac{1}{1 - \sum_{n=1}^{4} a_n}$$

Table 3.2 presents computations of coefficients $\{a_n\}$ which minimize the above integral over E_c for the set of shaded pixels shown in Figure 3.4. Results are shown for both polarization at 37 and 85 GHz. The scan regions are identified in Figure 3.3.

To test the effectiveness of the current Level 2 correction algorithm a simulated brightness temperature map was generated at 37 and 85 GHz using a scaled NOAA AVHRR IR image over the eastern coast of the United States. The SSM/I antenna patterns were convolved with the IR image in a scan geometry identical to the SSM/I. Although the simulated 37 and 85 GHz images cannot be expected to contain real responses to environmental conditions, they do provide a means to test the effectiveness of the current Level 2 APC. In particular the sharp contrast of the IR land-water boundary allows a stringent test of the

Table 3.2
Coefficients for Level 2 APC (See Figure 3.3 for Scan Regions)

Scan Region 5: $125 < n \leq 128$

Freq. (GHz)	Pol					
Scan Line		m	m	m+2	m	m-2
Sample No.		n	n+2	n+1	n-2	n-1
		a_0	a_1	a_2	a_3	a_4
37	V	1.0327	--	--	0.0083	0.0234
	H	1.0300	--	--	0.0146	0.0144
85.5	V	1.0216	--	--	0.0085	0.0126
	H	1.0395	--	--	0.0163	0.0217

Scan Region 4: $96 < n \leq 125$

Scan Line		m	m	m+2	m	m-2
Sample No.		n	n+2	n+1	n-2	n-1
		a_0	a_1	a_2	a_3	a_4
37	V	1.0723	0.0129	0.0228	0.0083	0.0234
	H	1.0623	0.0164	0.0132	0.0146	0.0144
85.5	V	1.0444	0.0080	0.0134	0.0085	0.0126
	H	1.0819	0.0276	0.0101	0.0163	0.0217

Scan Region 3: $32 \leq n \leq 96$

Scan Line		m	m	m+2	m	m-2
Sample No.		n	n+2	n	n-2	n
		a_0	a_1	a_2	a_3	a_5
37	V					
	H					
85.5	V	Same coefficients as Scan Region 2				
	H					

Scan Region 2: $3 \leq n < 32$

Scan Line		m	m	m+2	m	m-2
Sample No.		n	n+2	n-1	n-2	n+1
		a_0	a_1	a_2	a_3	a_4
37	V					
	H					
85.5	V	Same coefficients as Scan Region 2				
	H					

Scan Region 1: $1 \leq n < 3$

Scan Line		m	m	m+2	m	m-2
Sample No.		n	n+2	n-1	n-2	n+1
		a_0	a_1	a_2	a_3	a_4
37	V	1.0377	0.0129	--	--	0.0234
	H	1.0318	0.0164	--	--	0.0144
85.5	V	1.0210	0.0080	--	--	0.0126
	H	1.0519	0.0276	--	--	0.0217

Level 2 correction. Further description of the simulated images and general discussion of the APC problem for the SSM/I are available upon request.*

The effectiveness of the current Level 2 APC may be viewed by comparing the resultant APC corrected image with a simulated image in which the antenna pattern used to convolve with the IR image has all sidelobe energy removed. If the current Level 2 APC did its job perfectly, the corrected image would be identical to the image generated with antenna patterns having no sidelobe energy. Two errors may be defined:

(1) T_B (APC corrected image) - T_B (image with no sidelobe energy)

(2) T_B (uncorrected image) - T_B (image with no sidelobe energy)

Error (1) defines the difference between the brightness temperature resulting from an application of the current Level 2 APC and the brightness temperature associated with a "perfect" antenna pattern having no sidelobe energy outside the mainbeam. Error (2) defines the difference between the original brightness temperature without any APC and the brightness temperature having the "perfect" pattern.

A comparison of errors (1) and (2) provide a measure of the effectiveness of the Level 2 APC. Figures 3.5 and 3.6 present histograms of errors (1) and (2) for Port 5 (37 GHz V-pol) and Port 7 (85 GHz V-pol). The solid line corresponds to error (1) and the dashed line to error (2). The upper histograms in the figures apply to the open ocean where the radiometric variation in the simulated images occur over distances that are large in comparison with the antenna beamwidth. The bottom histograms apply to the transition region associated with land/water boundaries.

The results presented in both figures show that there are many occasions in which the correct Level 2 APC offers an improvement in the absolute brightness temperature of the simulated imaged. At the same time numerous occasions arise

---

*J. Dunn, "Antenna Pattern Correction for the SSM/I," Naval Research Laboratory Report (in press), NRL, Washington, DC.

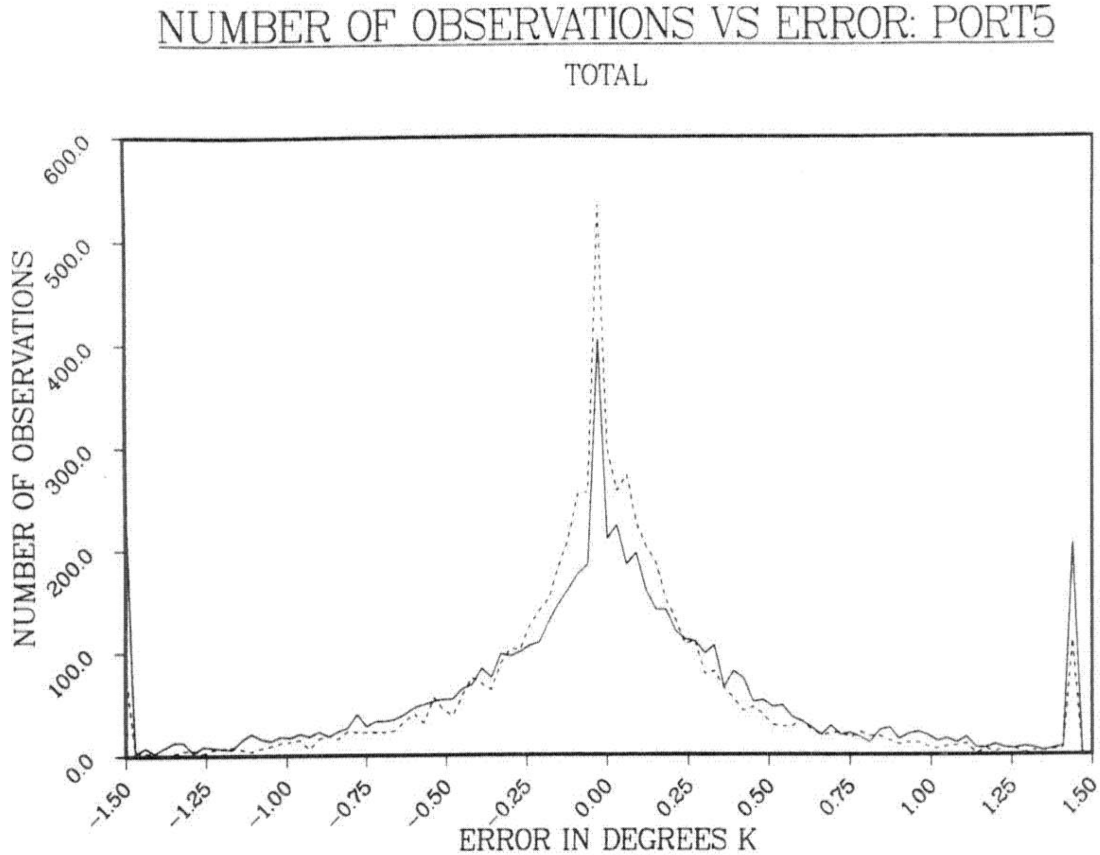

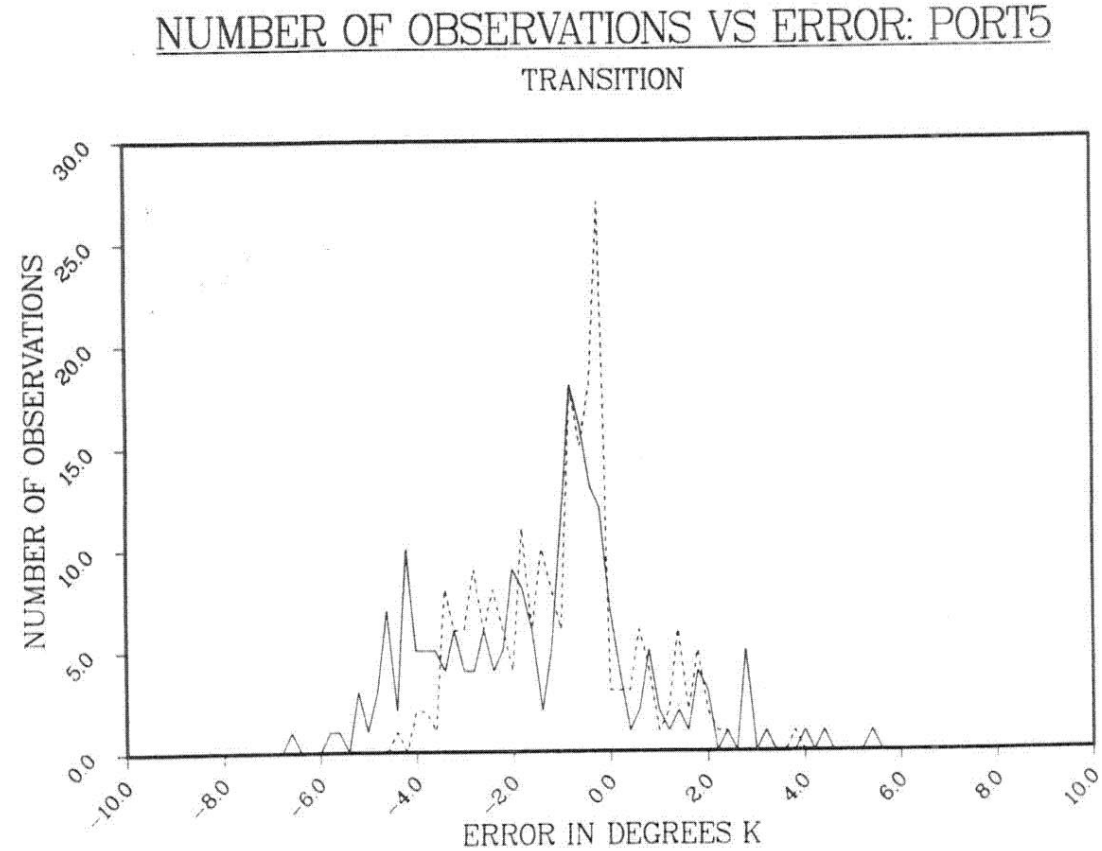

Figure 3.5 Histogram of Level 2 APC Errors at 37 GHz

—— Current APC

--- No APC

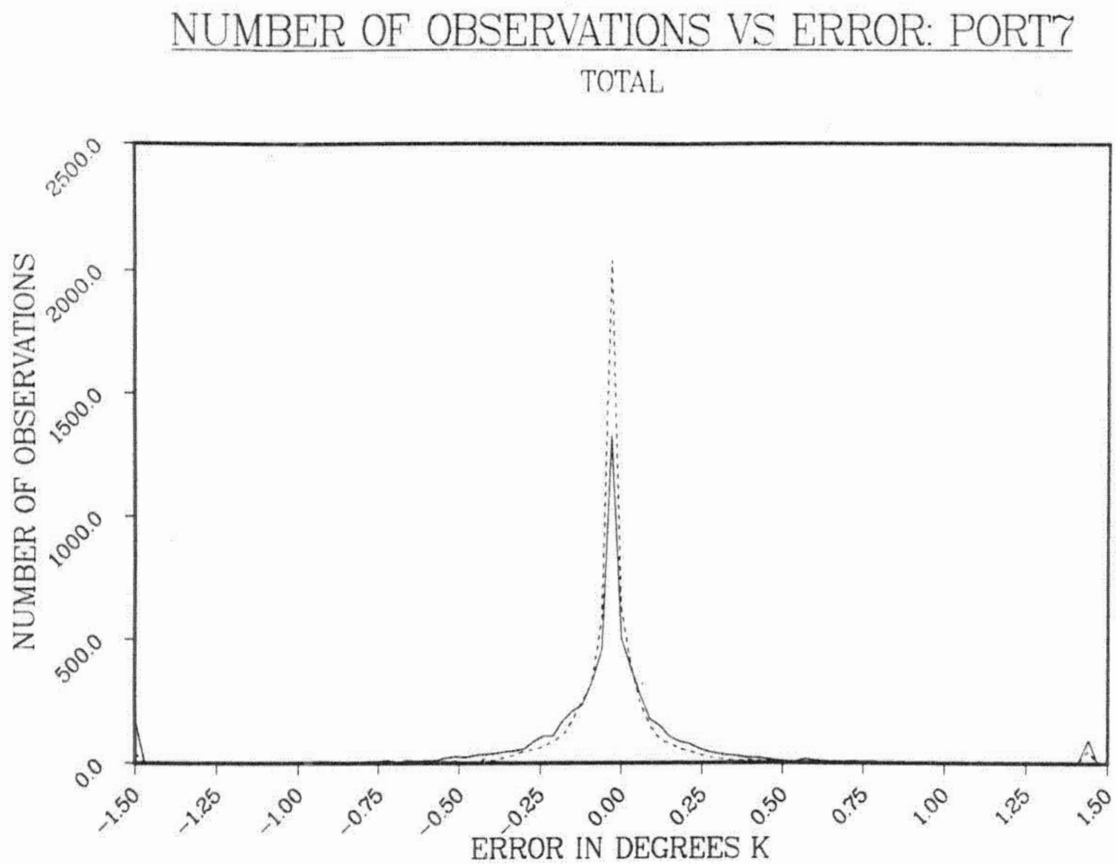

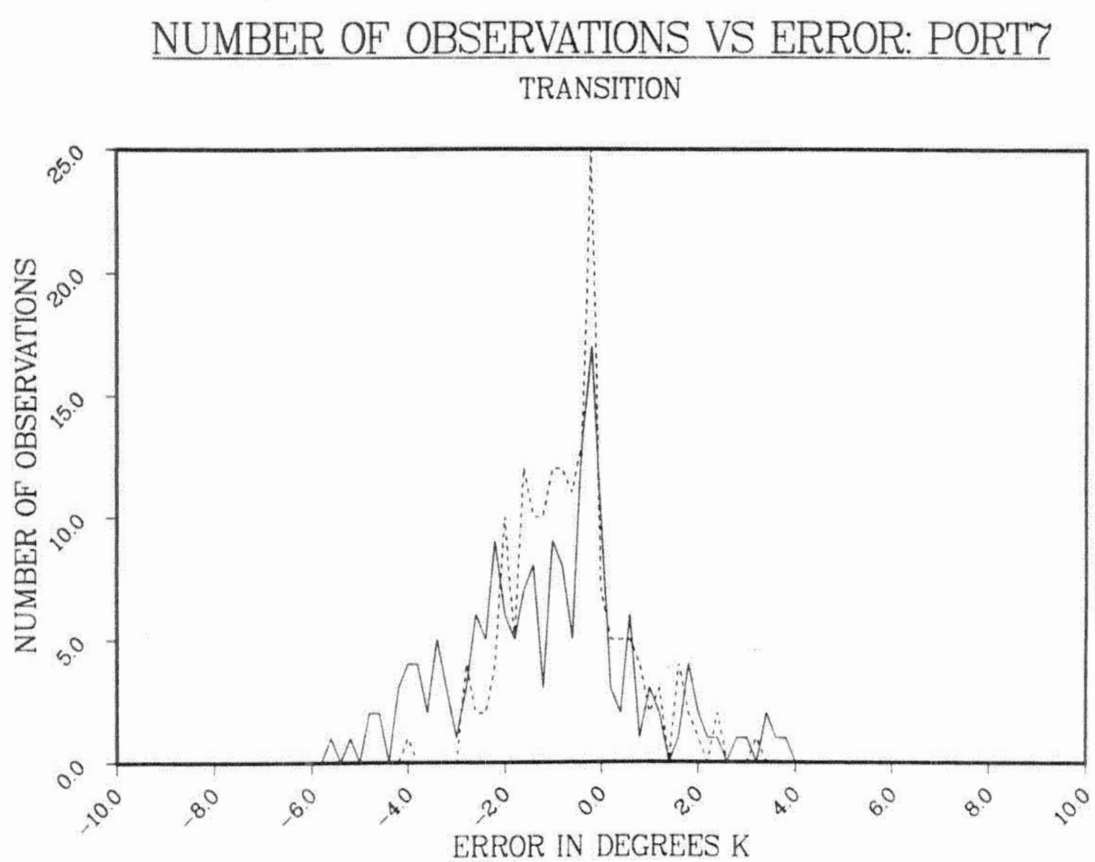

Figure 3.6 Histogram of Level 2 APC Errors at 85 GHz

—— Current APC

--- No APC

in which the APC actually degrades the radiometric image. This is a disturbing result that occurs for both the 37 and 85 GHz data and is apparent in both the transition regions and in the open ocean. These results indicate that caution must be exercised in applying the current Level 2 APC to SSM/I data. On the other hand, these results should not be interpreted to mean that all Level 2 APC algorithms will yield results similar to those of Figures 3.5 and 3.6. Further effort is needed in the evaluation of a suitable Level 2 APC for the SSM/I. This will be conducted during the SSM/I calibration/validation effort.

3.2.4 Antenna Pattern Matching

A third level antenna pattern correction may be envisioned which would attempt to match the higher resolution beams, e.g., at 85 GHz, to the lower resolution beams, e.g., at 19.35, 22.235 or 37 GHz. This level would be applied to the scene brightness temperatures estimated from the Level 1 and Level 2 APC algorithms presented above. This correction may be viewed in terms of a spatial filter which smoothes the higher resolution sampled brightness temperatures to a level commensurate with the lower resolution data.

One of the simplest filters is to numerically average the set of brightness temperatures whose boresights lie within the coarser 3 dB beam cell. This estimate of the average brightness temperature at 85 GHz over a beam cell that is comparable to the 37 GHz beam may be improved upon using the theory developed by Stogryn [3]. In short this approach permits the determination of a set of coefficients $\{c_n\}$ which are optimum in the sense that

$$\int_{Earth} d\Omega' \left[G_{pp}(\nu_1, \hat{k}, \hat{k}') - \sum_{n=1}^{N} c_n G_{pp}(\nu_2, \hat{k}_n, \hat{k}') \right]^2$$

is minimized. The higher resolution antenna patterns at frequency ν_2 have boresights defined by vectors $\hat{k}_n$, n=1, ..., N. The lower resolution antenna pattern at frequency ν_1, has boresight at $\hat{k}$. Once the set $\{\hat{k}_n\}$ is selected, it is straight forward to solve for the set of coefficients $\{c_n\}$ which minimizes the above integral. A constraint is need to insure proper normalization of results

$$\sum_{n=1}^{N} c_n = 1$$

To demonstrate the efficacy of this approach to data smoothing, computations were made to determine the set of coefficients of a 3 x 3 matrix of 37 GHz pixels surrounding a 19 GHz pixel. Figure 3.7 presents the 19 GHz antenna pattern along with the resultant smoothed 37 GHz pattern defined by the sum

$$\sum_{n=1}^{N} c_n G_{pp}\left(\nu_2, \hat{k}_n, \hat{k}'\right)$$

Computations were made for a scan region near the SSM/I ground-track and the results are presented in terms of distance on the surface of the earth. Note that the smoothed 37 GHz patterns are in remarkably good agreement with the 19 GHz patterns with the exception of the region where the antenna pattern is 30 db below the maximum gain. Similar results were obtained for the intercardinal pattern cuts in this example. The values of the coefficients $\{c_n\}$ varies somewhat across the SSM/I scan, but, in all cases studied using at least a 3 x 3 array the resultant smoothed patterns are similar to those of Figure 3.7.

Similar computations were made to smooth the 85 GHz data to the resolution of the 37 GHz data. In this case a 5 x 5 array of 85 GHz pixels surrounding a 37 GHz pixel near the ground track was used. Figure 3.8 presents the 37 GHz antenna pattern and the resultant smoothed 85 GHz pattern. Again, good agreement occurs in the H-Plane cut (i.e. in the along scan direction) but appreciable disagreement occurs in the E-Plane cut (i.e., in the along track direction) when the pattern power lies 7 db below the peak. Since the other patterns (i.e. the intercardinal cuts) gave results which closely resembled the results of the H-Plane cut, the disagreement in the single E-Plane cut is not expected to introduce an appreciable effect in the smoothed brightness temperature data. As in the case of matching the 37 GHz data to the 19 GHz data, the values of the coefficients of a 5 x 5 array of 85 GHz data vary across the SSM/I scan. The resulting smoothed patterns display good agreement with 37 GHz pattern in all regions across the SSM/I swath.

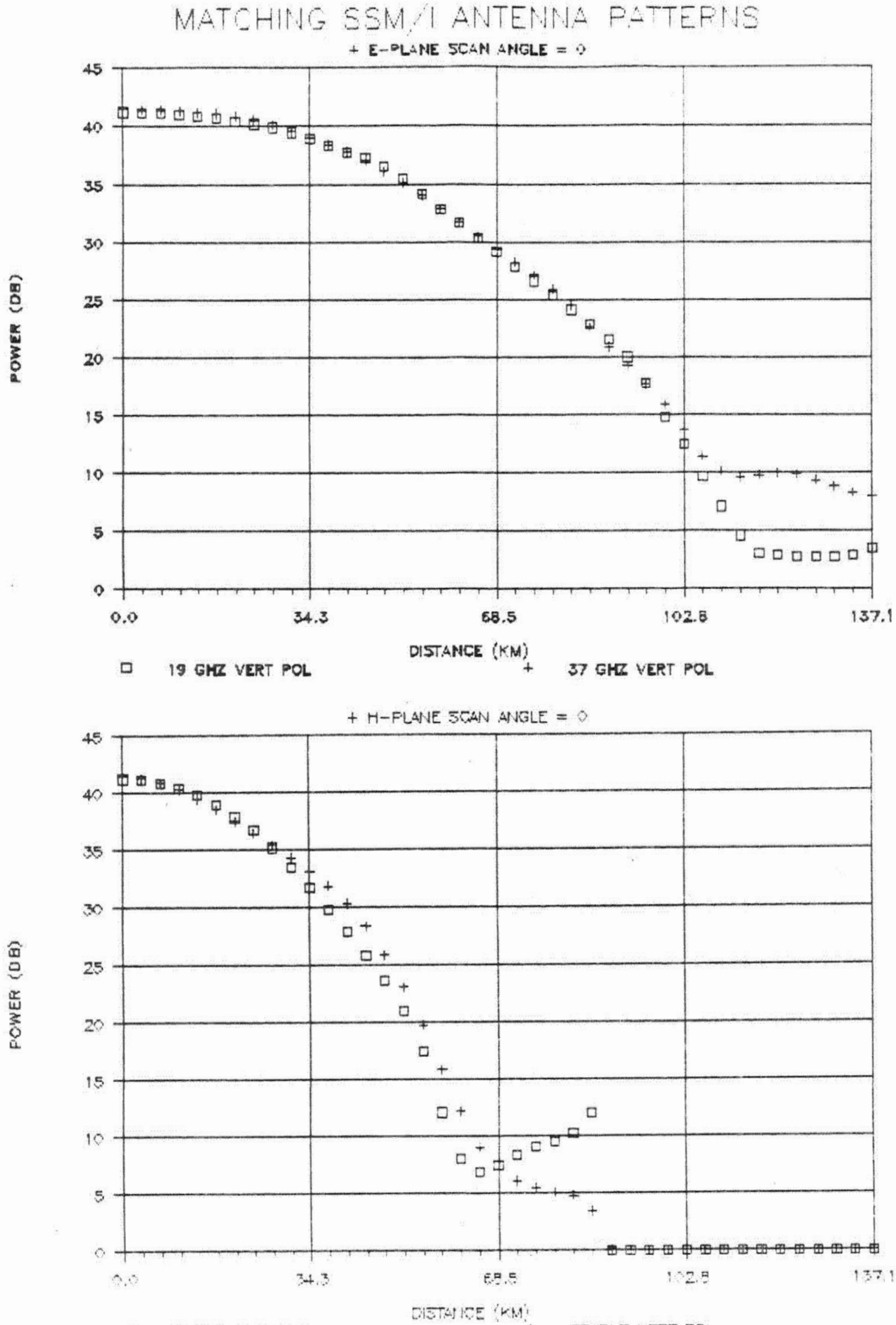

Figure 3.7 Smoothed 37 GHz Antenna Pattern and 19 GHz Pattern

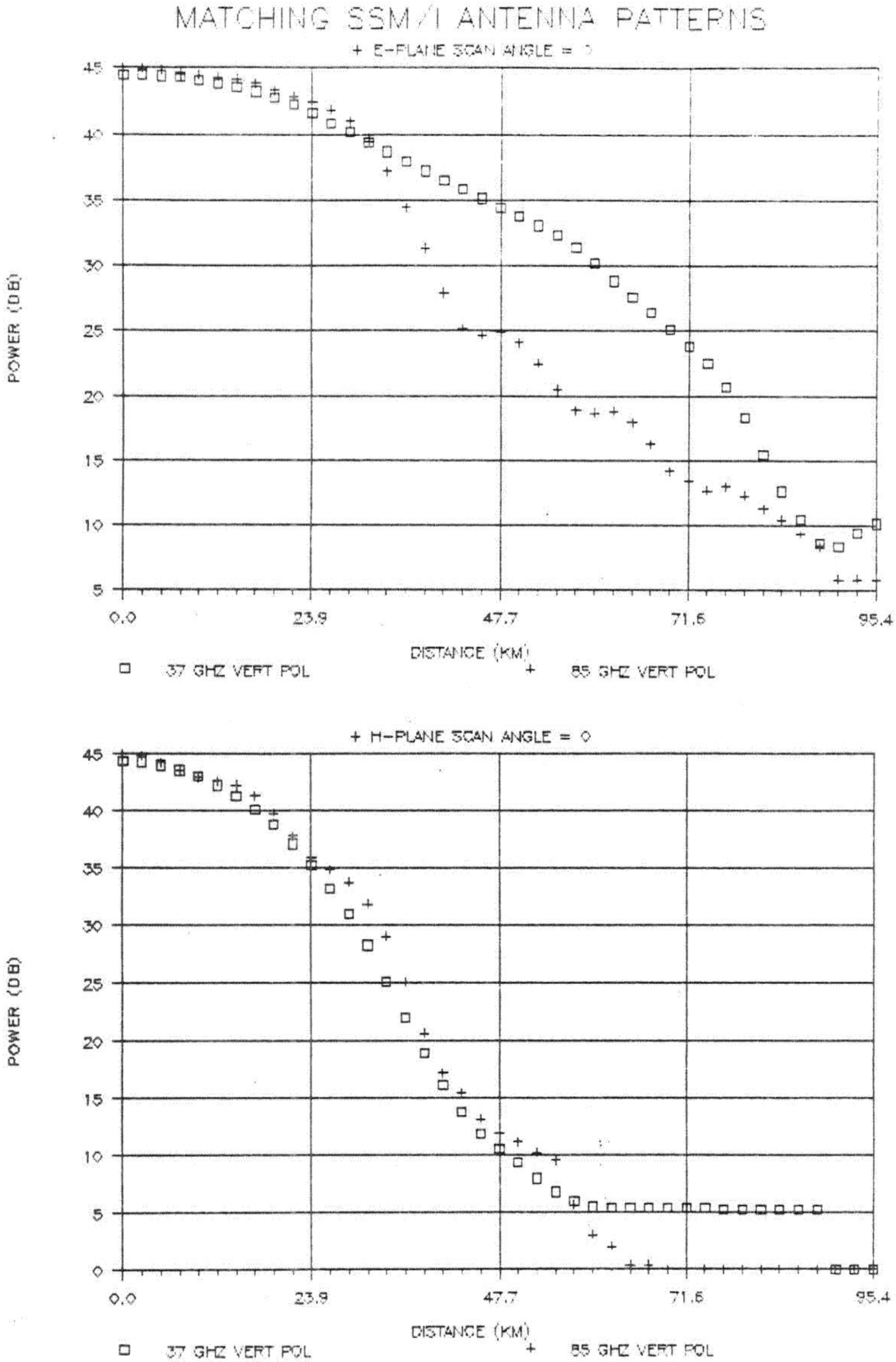

Figure 3.8 Smoothed 85 GHz Antenna Pattern and 37 GHz Pattern

Antenna pattern matching is not currently being exercised in the estimate of SSM/I scene brightness temperatures. This process may be performed with a modification to the current SSM/I SDR software module. The benefits of matching higher resolution SSM/I data to the lower resolution data will be examined further during the SSM/I calibration/validation effort.

It should be noted that a reduction of sensor noise occurs in the process of smoothing the data. For the examples discussed above the rms noise in the smoothed 37 GHz data (3 x 3 array) is reduced by a factor of 0.45 and the noise in the smoothed 85 GHz data (5 x 5 array) is reduced by 0.25.

It should also be noted that the technique of selecting the set of coefficients $\{c_n\}$ to match an antenna pattern at frequency ν_1 is sufficiently general to cover the problem of data interpolation. For example if frequency ν_1 is set to ν_2 (i.e., the high and low resolution patterns are the same) then the coefficients determined in the above antenna matching problem provides a means of interpolating the temperature at $\hat{k}$ from the set of temperatures at $\{k_n\}$, n=1, ..., N. Figures 3.9 - 3.11 present computations at 19, 37 and 85 GHz of the desired pattern at a prescribed $\hat{k}$ (which is the actual pattern centered at a point not sampled) and an "interpolated" pattern associated with the interpolated data point which is based on samples at $\{\hat{k}_n\}$. The scan region for interpolation is taken to lie near the satellite ground track and the point of interpolation $\hat{k}$ is selected as a worst case situation, i.e., midway between successive scans and midway between samples. A 4 x 4 array of samples surrounding point $\hat{k}$ is selected for the interpolation.

The results appear very good at 19 GHz and not so good at 37 and 85 GHz. This situation arises from the fact that the 19 GHz data are spatially sampled near the Nyquist rate (i.e., approximately two samples per 3 db beam diameter) while the 37 and 85 GHz are undersampled. To sample the 85 GHz at the Nyquist rate would require the SSM/I to spin at approximately twice the current rate and to sample at four times the present the sampling rate. (This option was not possible during the design of the SSM/I due to the data rate limitations imposed by the spacecraft data acquisition system.) In any event the above technique of selecting coefficients is an attractive procedure to obtain accurate interpolated 19 GHz data and, if smoothed to match the lower resolution, interpolated 37 and 85 GHz data as well.

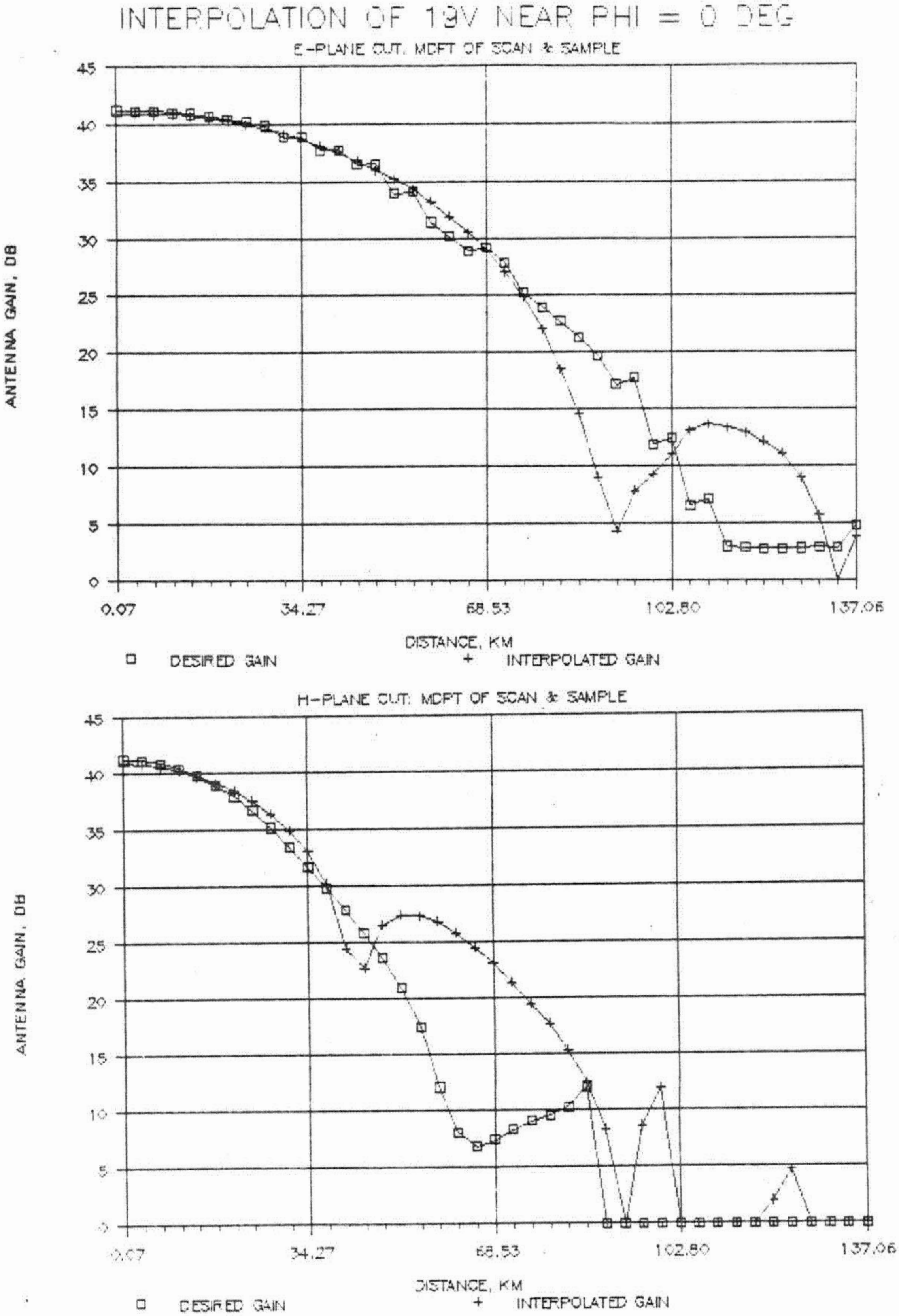

Figure 3.9 Interpolated Patterns of 19 GHz Data (Midpoint between scans and samples)

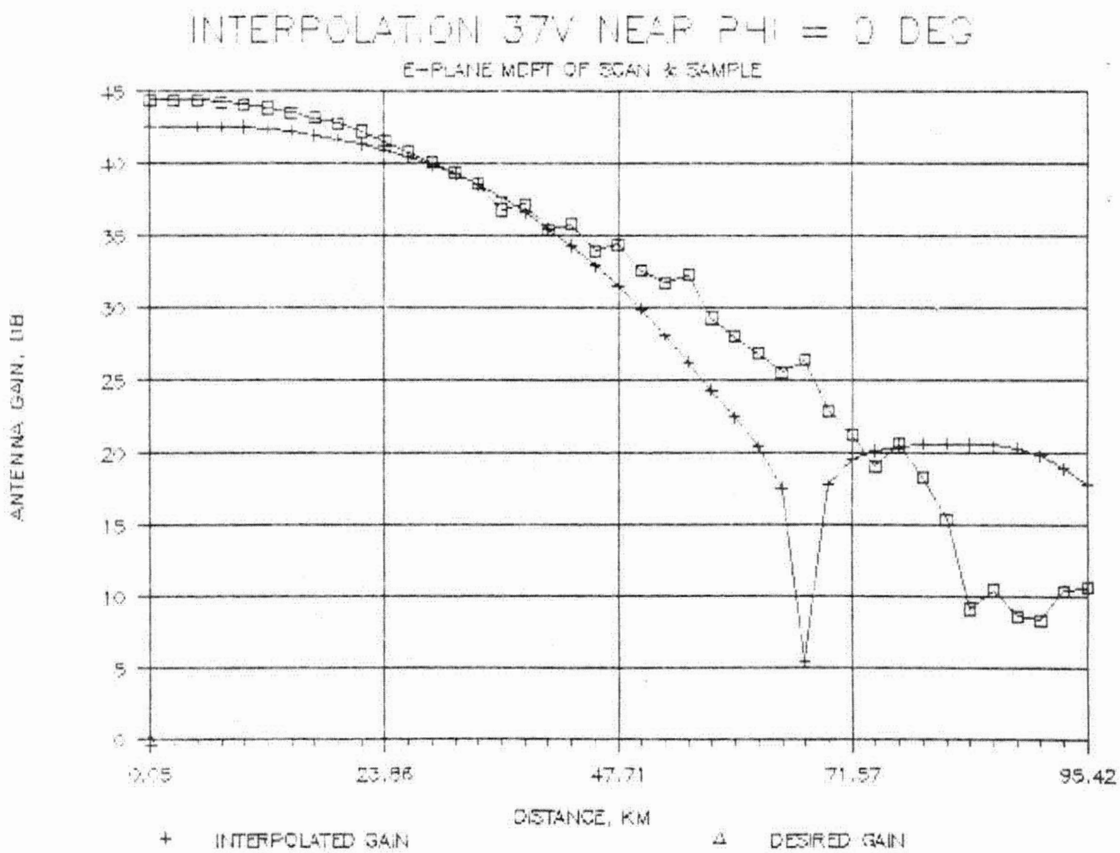

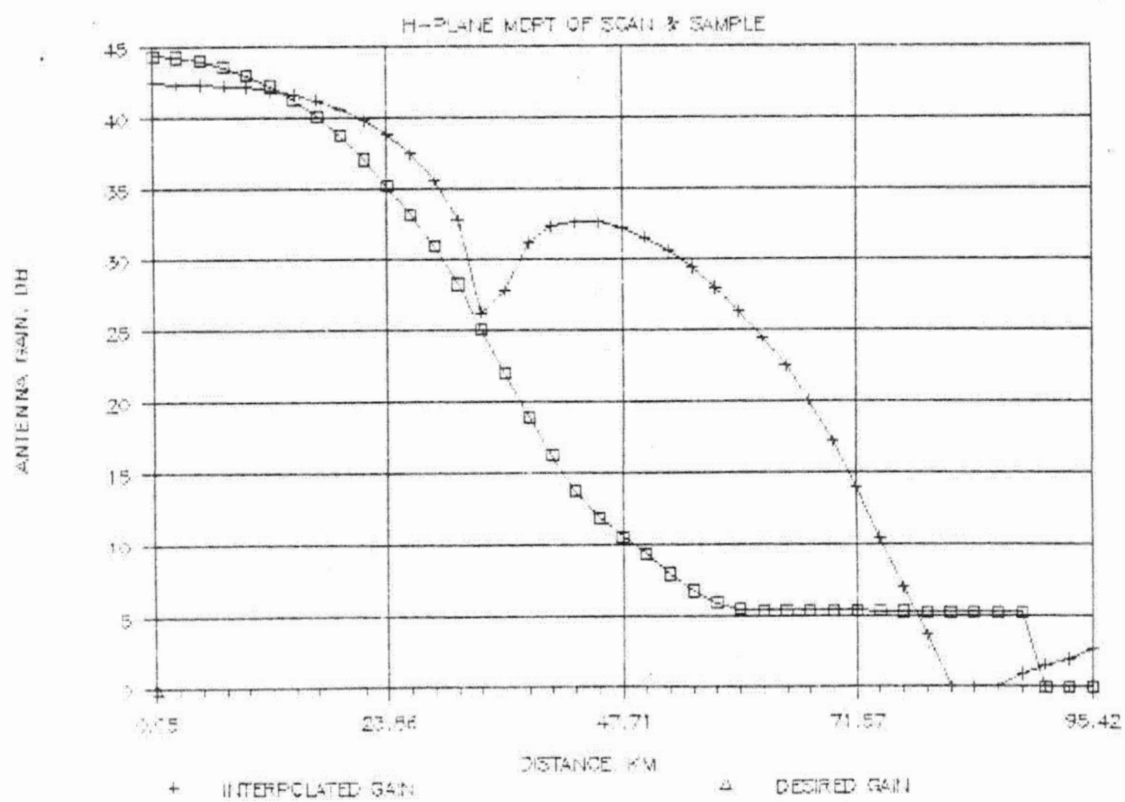

Figure 3.10 Interpolated Patterns of 37 GHz Data
(Midpoint between scans and samples)

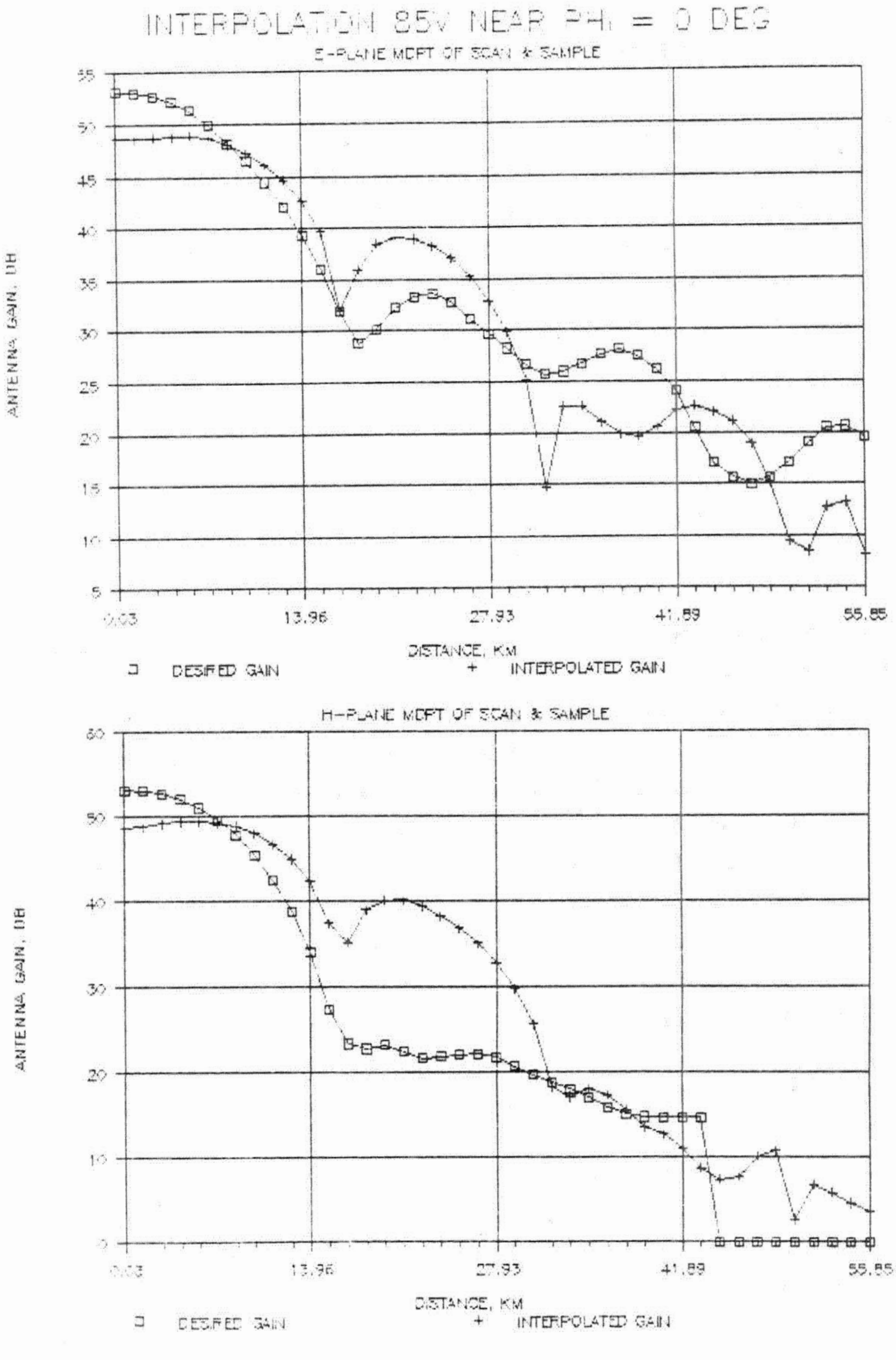

Figure 3.11 Interpolated Patterns of 85 GHz Data (Midpoint between scans and samples)

4.0 ENVIRONMENTAL PARAMETERS

The previous section described processing done to create calibrated brightness temperatures (Sensor Data Records, SDRs) from the raw sensor data. In this section we will discuss the use of the SDRs and other input data in a system to derive environmental parameters (Environmental Data Records, EDRs). A detailed description of the development of the retrieval algorithms and their exact form is given in Appendix A.

4.1 Input Data and Processing System

Figure 4.1-1 is a diagram of the SSM/I processing software at Fleet Numerical Oceanography Center (FNOC). The first processing module, SMISDP, creates TDRs and SDRs from the raw data (digitized voltages), as discussed in Section 3.0. Note that after locating each SSM/I footprint, SMISDP assigns a surface type identification, read from the surface type file, SMISURFTYP. This surface type identification is passed in the SDR file to the next processing module, SMIEPE, which estimates EDRs. This a priori surface identification can be one of eight categories, as listed below. Depending on the categories, certain further classification and processing may be done by SMIEPE. Note that the TDRs, SDRs, and EDRs along with the Quality Data Records (QDRs), and the Sensor Calibration File (SENCAL) are written to archived tape by SMIARK. The QDRs contain statistical and sensor health information and are described in Section 5.0. SENCAL contains all of the constants and information used to create the TDRs and SDRs from the raw sensor data file. Not shown in Figure 4.1-1 but presently planned for inclusion in the archival tape is the Parameter Extraction Coefficients File used by SMIEPE which contains all of the constants used to generate the EDRs from the SDRs.

It is important to recognize that there are several logical steps involved in producing an EDR value before an estimation equation is used. The surface categorization is the first of these logical steps. A mistake in SMISURTYP will almost certainly result in a meaningless calculation later in SMIEPE. For example, if an island were mistakenly identified as an ocean location in SMISURTYP, the resulting (large) brightness temperatures would probably lead to an estimate of strong winds occurring at the spot. Every attempt has been made

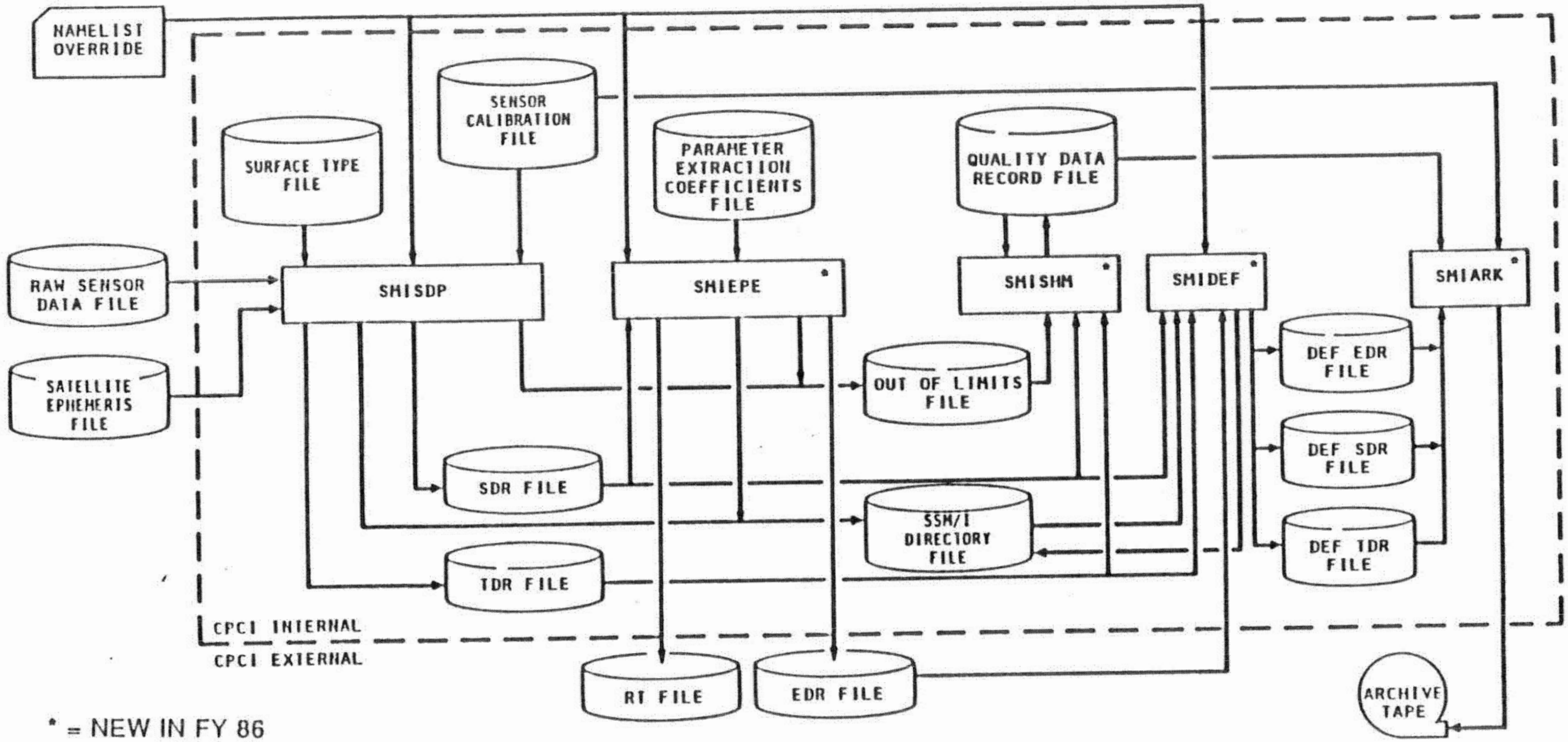

* = NEW IN FY 86

FIGURE 4.1-1 PROCESSING SOFTWARE AT FNOC to screen out such misclassifications, but operational experience is likely to reveal some. They will be dealt with as part of routine software maintenance.

Table 4.1-1 itemizes the further processing resulting from each classification imposed by SMISURTYP.

The coastal zone in SMISURFTYP is one pixel wide at 19.35 GHz. The ocean boundary (one 19 GHz pixel wide) on the ocean side of the coast, and the land boundary (on the land side of the coast) are intended for further investigation, with the hope of deriving useful EDR estimates within them. At the time of initial SSM/I processing, they will be treated like coast and no EDRs will be estimated within those regions.

The remaining software modules, SMISHM (Sensor Health Monitor) and SMIDEF (Data Exchange Formatter) are discussed in Section 5. The remainder of Section 4 will be concerned with the production of EDRs by the SMIEPE module. The structure of SMIEPE is shown in Figure 4.1-2. This structure diagram may be useful in understanding the code that incorporates the SSM/I processing logic.

4.2 Parameter Description

The SSM/I parameters are listed in Table 4.2-1 and are further described in Section 4.3.

4.3 Parameter Estimation Logic (EDREXT)

Parameter values are initially set to "indeterminate" when a pair of scans (type A and type B) are read into EDREXT. The code also checks for negative polarizations (horizontal brightness greater than vertical brightness by more than 2 K).

EDREXT also checks the data to see whether it came from a scene station where all brightness temperatures are available (25 km samples) or an intermediate location where only 85 GHz samples are available. SSM/I code permits estimation of rain intensity and liquid water content over land (RL, LWL) at the intermediate locations. However, all parameter values archived

TABLE 4.1-1 SMISURTYP CLASSIFICATIONS AND PROCESSING

SMISURFTYP CATEGORY	RESULT
Ocean	Process Ocean EDRs
Possible Ice	Check for Ocean/Ice
Ice (multiyear)	Process Ice EDRs
Coast	All EDRs indefinite
Ocean Boundary	All EDRs indefinite
Land Boundary	All EDRs indefinite
Land	Reclassified on the basis of SDRs as snow, arable soil, vegetation, flooded ground, heavy precipitation, glacial, frozen ground/wet snow, desert.
Not Processed	This category is used only at AFGWC to exclude processing of Antarctica.

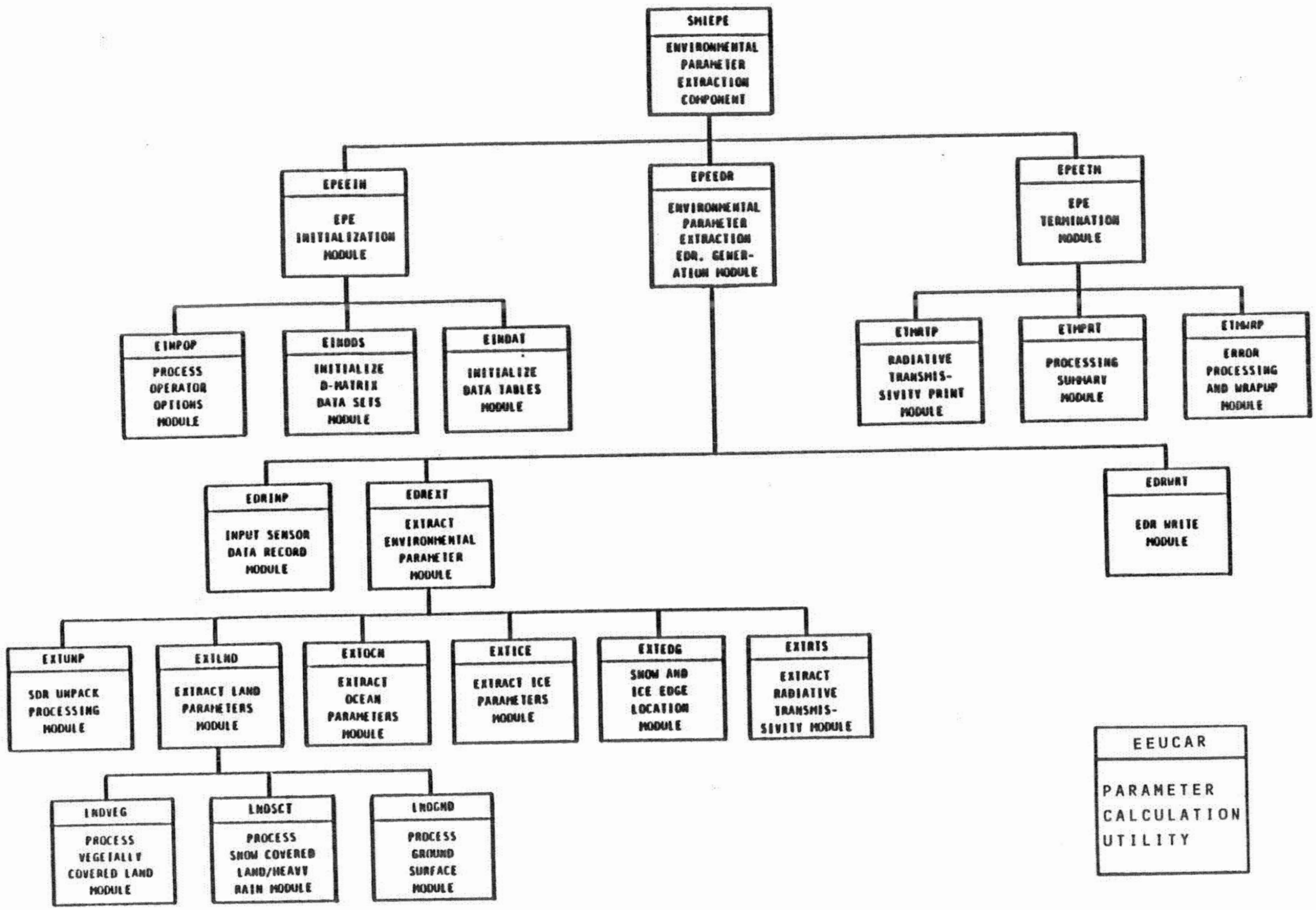

FIGURE 4.1-2 SMIEPE STRUCTURE CHART

Table 4.2-1 SSM/I Environmental Products

PARAMETER	SMIFFE MNEMONICS	DATABASE MNEMONICS	RANGE	UNITS	QUANTIZATION	NUMBER OF BITS	STORAGE RANGE	OUT-OF-LIMITS	INDETERMINATE
ICE AGE	IA	IA	FY, MY	N/A	FIRST YEAR, MULTI-YEAR	2	0,1	2	3
ICE CONCENTRATION	IC	IC	0-100	PERCENT	5.0 PERCENT	6	0-22	62	63
CLOUD WATER	CWI, CWO, CWL, CWS	CW	0-12.6	KG/M•M	0.05 KG/M•M	8	0-252	254	255
SURFACE WIND	SW	SW	0-29	M/S	1.0 M/S	5	0-29	30	31
WATER VAPOR	WVO	WV	0-80	KG/M•M	0.5 KG/M•M	8	0-160	254	255
RAIN	RO, RL	RA	0-61	MM/HR	1.0 MM/HR	6	0-61	62	63
LIQUID WATER	LWO, LWL	LW	0-12.5	KG/M•M	0.1 KG/M•M	7	0-125	126	127
SURFACE MOISTURE	SM	SM	0-61	PERCENT	1.0 PERCENT	6	0-61	62	63
SURFACE TEMPERATURE	STL, STV, STD, STF, STG, STS, TLC, TSC	ST	180-340	DEGREES K	1.0 DEGREES K	8	0-160	254	255
CLOUD AMOUNT	CAL, CAS	CA	0-120	PERCENT	1.0 PERCENT	8	0-120	254	255
SNOW WATER CONTENT	SNW	SN	0-50	CM	1.0 CM	6	0-50	62	63
EDGE	EF	EF	0,1	N/A	N/A	2	0,1	N/A	3
EDR SURFACE TYPE*	TYPE	SC	SEE BELOW	N/A	N/A	6	SEE BELOW	N/A	N/A

* 1 = VEGETATION, 3 = ICE, 5 = OCEAN, 6 = COAST, 7 = FLOODED SOIL, 8 = HEAVY PRECIPITATION, 9 = ARABLE SOIL, 10 = DESERT, 11 = FROZEN GROUND, 12 = GLACIAL GROUND, 13 = SNOW OVER FROZEN GROUND, 14 = SNOW OVER SOIL

into NESDIS records are based on complete (25 km) sets of data, with one exception. The exception is the cloud amount parameter, for which the 37 GHz data (at a 25 km sample location) is deliberately compared with the eight contiguous samples of 85 GHz samples as well as the co-located 85 GHz sample. The NESDIS archive will include all the calibrated brightness temperatures and antenna temperatures including those from the intermediate locations.

4.3.1 Oceanic Parameters

There are five oceanic parameters: surface wind speed (SW), cloud water content (CWO), water vapor content (WVO), rainfall intensity (RO), and liquid water content (LWO). Liquid water content is the columnar density of atmospheric water droplets whose diameter exceeds 100 μm. Cloud water content applies to droplets whose diameter are less than 100 μm. SW and WVO are estimated only over water; the other parameters are estimated over different surfaces as well, using different equations appropriate for the physics of the surface (land, snow, ice, etc.). A different symbol is used in the final character for a parameter over a different surface (e.g., RL for rain intensity over land; CWS for cloud water content over snow).

4.3.1.1 Screening Logic - Oceanic Parameters

As noted above a screening logic is used to identify the surface characteristic before applying an estimation algorithm. For locations identified by SMISURFTYP as ocean, the next step is to check for the presence of seasonal ice - i.e., ice not a part of the multiyear pack ice identified by SMISURFTYP. This zone of possible ice includes all water (including major freshwater lakes) poleward of 45 degrees latitude. The brightness temperatures are checked for the possibility of ice, according to the following logic:

a) IF: TB(19H) and [TB(37V) - TB(37H)] > discriminate
THEN: Perform Ice Concentration (IC) test (b)
ELSE: Surface is OCEAN

b) IF: Ice Concentration (IC) > discriminate (currently 10%)
THEN: Surface is ICE
ELSE: Surface is OCEAN

The above logic is found in module EDREXT. For the remainder of Section 4.3.1, we will assume the surface has been determined to be ocean. The flow of control transfers to the module EXTOCN.

4.3.1.2 Estimation of Oceanic Parameters (RO, LWO, SW, CWO, WVO)

The proper coefficients for these parameters are read from the Parameter Extraction File, based on latitude and season of the SDRs. A formatted printout of the Parameter Extraction File is found in Tables 4.4-1a,b,c at the end of this section.

EXTOCN next checks for possible rain, according to the following logic:

a. IF: TB(19H) > discriminant (initially 190 K)
OR: [TB(37V) - TB(37H)] < discriminant (initially 25 K)
THEN: possible rain exists (b)
ELSE: RO = 0; LWO = 0; calculate SW, CWO, WVO

b. IF: possible rain exists
THEN: calculate RO, LWO; set WVO = indeterminate; calculate SW, CWO if rain is not too heavy. If the rain is heavy, SW and CWO are indeterminate as well

All parameter value calculations take place in the module EEUCAR. This module can use any of the seven brightness temperatures in an equation of the form:

$$p = a0 + a1*TB1 + \ldots + a7*TB7$$

EEUCAR can also compute a non-linear modified parameter value as follows:

$$p' = a8 + a9*p**a10$$

where the coefficients a_i are supplied in a data file which can be updated as needed through SMIFUM, the File Utility Module. Initially no non-linear values are implemented.

In the initial formulation of the coefficients, no more than four brightness temperatures are used in estimation of any parameter. Table 4.3-1 presents the list of channel frequencies and polarizations currently used in estimating the environmental products. The specific coefficients are presented in Table 4.4-1.

This concludes the discussion of estimation of oceanic parameters. The structure of the EXTOCN module is shown in Figure 4.3-1.

4.3.2 Ice Parameters

The ice parameters are ice concentration (IC), ice age (IA), ice edge (EF), and cloud water content over ice (CWI).

4.3.2.1 Screening Logic

The initial screening logic to distinguish ice from ocean was described in Section 4.3.1.1. In Section 4.3.2, it is assumed that the preliminary IC calculation indicates an ice concentration greater than a discriminant value. (The initial discriminant is 10%).

4.3.2.2 Ice Parameter Estimation (IC, IA, EF, CWI)

Estimation of IC, IA, and CWI is made by module EXTICE. The location of the edge is determined by a later processor, EXTEDG, which sets a flag (EF) after doing an area search of IC values.

Table 4.3-1 Channels Used to Estimate Environmental Products

PARAMETER	19V	19H	22V	37V	37H	85V	85H
RL				X		X	
SM	X	X					
LWL				X		X	
CWL	X	X		X		X	
STD		X	X	X			X
STF	X						
STG	X						
STL		X	X	X			X
TLC		X	X	X		X	
STV	X						
CAL					X	X	X
CWS			X		X	X	X
STS	X		X	X	X		
TSC		X	X	X	X		
CAS				X	X	X	X
SNW	X		X	X	X		
RO		X	X	X	X		
SW		X	X	X	X		
LWO		X	X	X	X		
CWO		X	X	X	X		
WVO	X		X	X	X		
IC				X	X		
IA				X			
CWI	X	X		X	X		

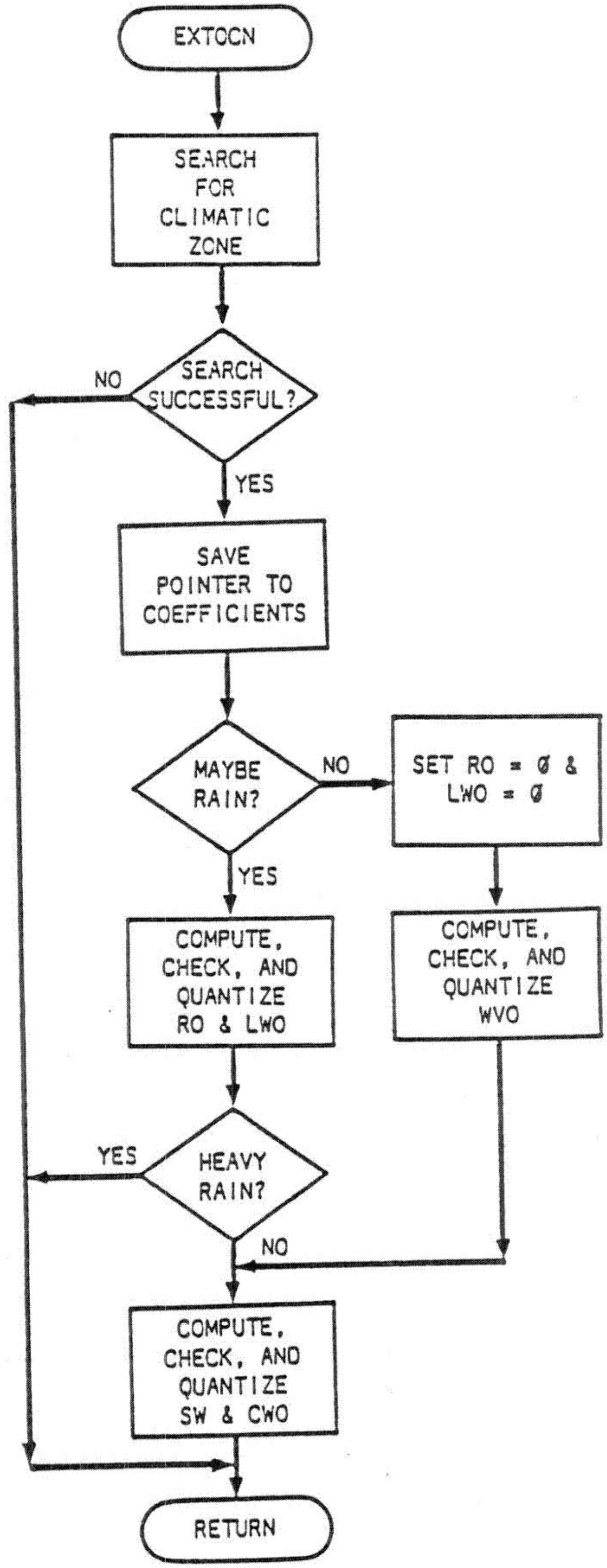

FIGURE 4.3-1 EXTOCN FLOW CHART

EXTICE first determines the proper coefficients from the Parameter Extraction file, based on climatology. IC is calculated in the utility module EEUCAR. If IC is found to be out of limits, the IA parameter is left indeterminate.

If IC is within limits, EXTICE next calculates the intermediate variable TV:

$$TV = (C0 + C1 * TB4) / (IC\% / 100) + C8$$

IF: TV < discriminant
THEN: multi-year ice
ELSE: first year ice.

If IC is greater than a set amount (nominally 90%), EXTICE next calculates CWI in the utility module EEUCAR. Over a mixed background of ice and water, CWI is left indeterminate. The coefficients C0, C1 and C8 are presented in Table 4.4-1.

If ice was found to be present, EDREXT calls the edge processing module, EXTEDG, to mark the ice edge. The same module is also used to mark the edge of snow if found during land surface processing.

This ends the description of the ice parameters. The logic flow of the EXTICE module is shown in Figure 4.3-2.

4.3.3 Land Parameters

The land parameters are rain intensity (RL), liquid water content (LWL), surface moisture (SM), cloud water content (CWx), snow water content (SNW), surface character (TYPE), surface temperature (STx), and cloud amount (CAx). Not all these parameters are simultaneously possible; some are mutually exclusive. The "x" termination may be "L" for land surfaces or "S" for snow-covered surfaces. The naming distinctions are made in order to distinguish in code and documentation between equations for the same parameter that incorporate different coefficients and different physical reasoning. For example, RL and RO are both estimates of rain intensity; a single location in the output record is used to record the value. Necessarily, however, different

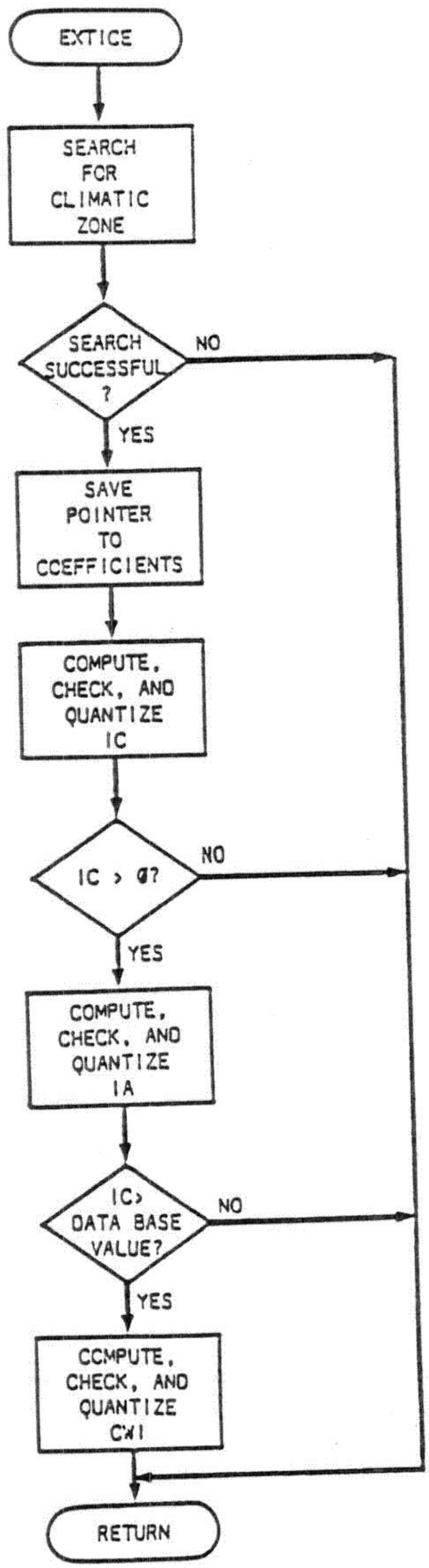

FIGURE 4.3-2 EXTICE FLOW CHART

equations have been used to generate estimates of Rx, depending on physical conditions.

4.3.3.1 Screening Logic

The screening logic begins in the higher level module, EDREXT, where discrimination between ice and ocean was made. In the following material, it is assumed that the SDR surface tag indicates a terrestrial surface (i.e., not ocean, ice, nor coast). Control then goes to the EXTLND module.

EXTLND has the most extensive screening logic, because terrestrial surface exhibit a large variety of conditions. A mid-latitude soil surface may be covered by snow, water, or heavy vegetation; it may be obscured by heavy rain in the atmosphere; it may be frozen, of normal moisture content, or in a desiccated state. These changes are of interest in and of themselves; they also dictate the parameters that can be estimated and the physical principles that should apply. The result of this screening logic is incorporated in the TYPE parameter.

The TYPE categories are: flooded soil, heavy vegetation, snow, heavy rain, glacial surface, frozen ground/wet snow, desert, and arable soil. The logic for making these distinctions is shown in Figure 4.3-3. Note that categorizations are based on the five lowest-frequency channels. The 85 GHz channels are not used for recognition of surface characteristics (at this time) because of their sensitivity to atmospheric characteristics.

EXTLND first considers whether the surface is flooded, by comparing the 22 GHz V and the 19 GHz V channels:

IF: [TB(22V) - TB(19V)] > discriminant (initially 5 K)

THEN: flooded soil. All parameter values (except TYPE) are left indeterminate if the surface is flooded.

ELSE: continue.

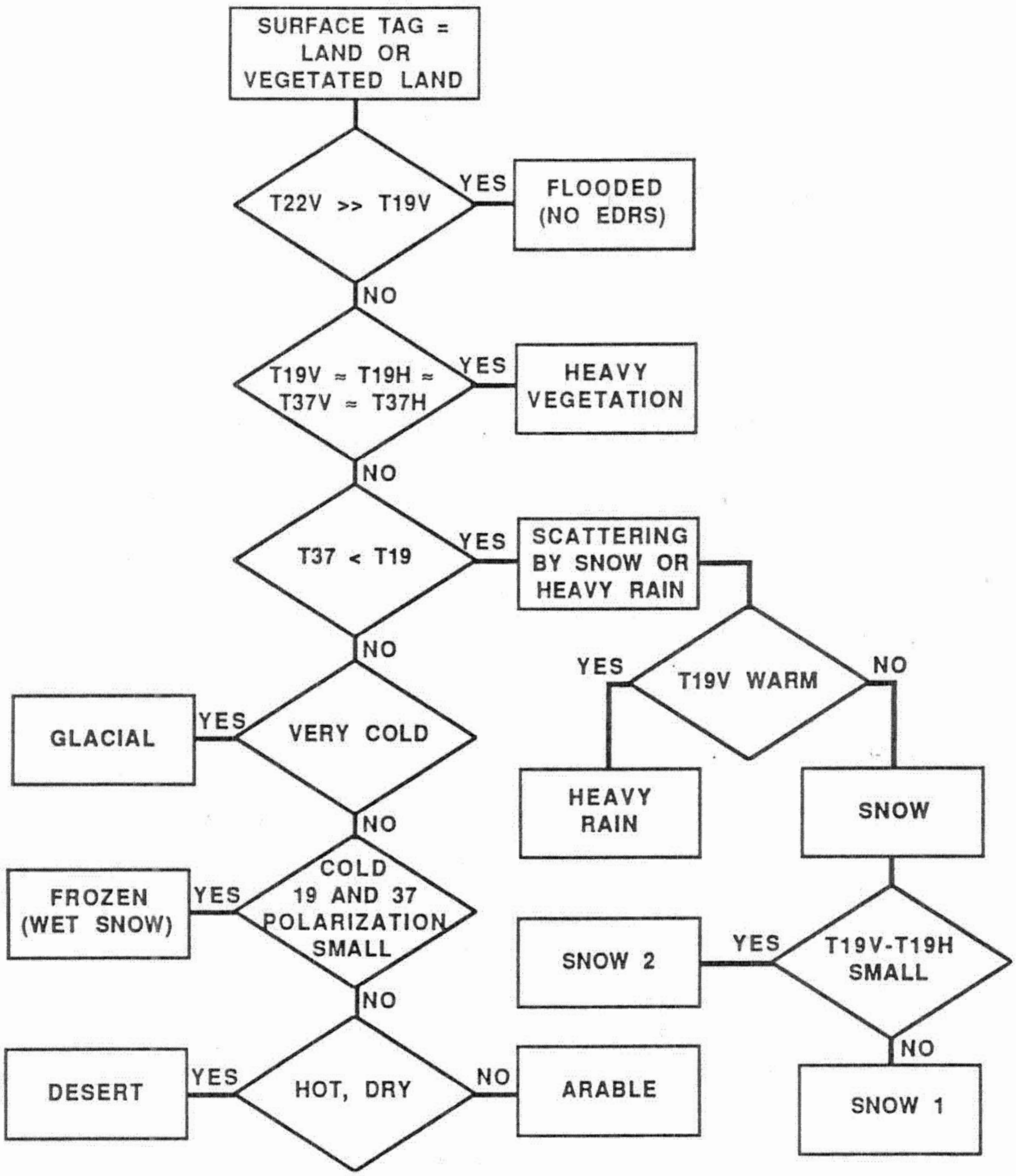

FIGURE 4.3-3 LOGIC TO IDENTIFY SURFACE TYPE

EXTLND next compares the average of 19 and 37 V with the average of 19 and 37 H.

IF: average vertical brightness - average horizontal brightness < discriminant (initially 4 K)

THEN: heavy vegetation. Control passes to module LNDVEG. As shown in Table 4.3-2 only four parameters are estimated in cases of heavy vegetation: surface temperature (STV), rain intensity (RL), liquid water content (LWL), and cloud water content (CWL). However, if rain is present (RL $\neq$ 0), cloud water content is not estimated because the signal from the rain dominates the brightness temperatures. Because the soil surface is masked by the vegetation, no attempt is made to estimate surface moisture.

ELSE: continue.

EXTLND next compares the 19 and 37 GHz channels:

IF 1: [TB(37V) - TB(19V)] < discriminant (initially 0 K)

THEN 1: scattering. Control passes to module LNDSCT. The emissivity of a land surface is normally greater at 37 GHz than at 19. However, snow on the ground, or heavy rain, causes enough scattering at 37 GHz to depress the brightness below that at 19 GHz. These conditions can be separated by considering the magnitude of 19 GHz V brightness.

IF 2: TB(19V) < discriminant (initially 255 K)

THEN 2: snow. The 19 GHz polarization (vertical - horizontal) is checked to decide whether the underlying soil is frozen (SNOW1) or not (SNOW2). If snow is present, the snow parameters are estimated: snow water content (SNW), surface temperature (STS), snow edge

Table 4.3-2 Parameters Calculated per EDR Surface Type

SURFACE TYPE	LAND									OCEAN	ICE
	FLOODED	VEGETATION	HEAVY PRE-CIPITATION	SNOW1	SNOW2	GLACIAL	FROZEN	ARABLE	DESERT		
PARAMETERS											
IA											●
IC											●
IE											●
CWI											●
SW										●	
WVO										●	
RO										●	
CWO										●	
LWO										●	
SM			●		●			●	●		
STL		●				●	●	●	●		
RL		●	●				●	●	●		
CWL		●				●	●	●	●		
LWL		●	●				●	●	●		
CAL			●			●	●	●	●		
SNW				●	●						
STS				●	●						
SWE				●	●						
CWS				●	●						
CAS				●	●						

(SNE), cloud water content (CWS), and cloud amount (CAS). If the underlying soil is unfrozen, an estimate of SM is made.

ELSE 2: heavy rain. The parameters of rain intensity (RL), liquid water (LWL), and cloud amount (CAL) are estimated; the surface moisture (SM) is set to 25%. The actual surface is, of course, invisible because of the heavy rain.

ELSE 1: neither snow nor heavy rain. This is the deduction if the 37 GHz vertical is greater than the 19 GHz vertical. This leads us to believe soil is visible, or perhaps a glacial surface. Control passes to module LNDGND. If the surface is glacial, three parameters are estimated: surface temperature (STG), cloud water (CWL), and cloud amount (CAL). If the ground is frozen, the additional parameters of rain and liquid water (RL, LWL) are estimated. If the ground is arable, surface moisture (SM) is estimated; if the ground is desert, the SM is set to 3%. These alternatives are shown in Figure 4.3-4.

This concludes the description of the screening logic for the land parameters.

4.3.3.2 Land Parameter Estimation

Module EXTLND executes the classification logic described above, resulting in a call to modules LNDVEG (for heavy vegetation), LNDSCT (for snow or heavy rain), or LNDGND (for soil or glacial conditions). If the surface is determined to be flooded, EXTLND sets the surface type (TYPE) appropriately, leaving all other parameters indefinite.

4.3.3.2.1 Heavy Vegetation (module LNDVEG)

The module LNDVEG checks for possible rain by comparing the 85 GHz brightness to that at 37 GHz:

IF: [TB(85V) - TB(37V)] < discriminant (initially 0)

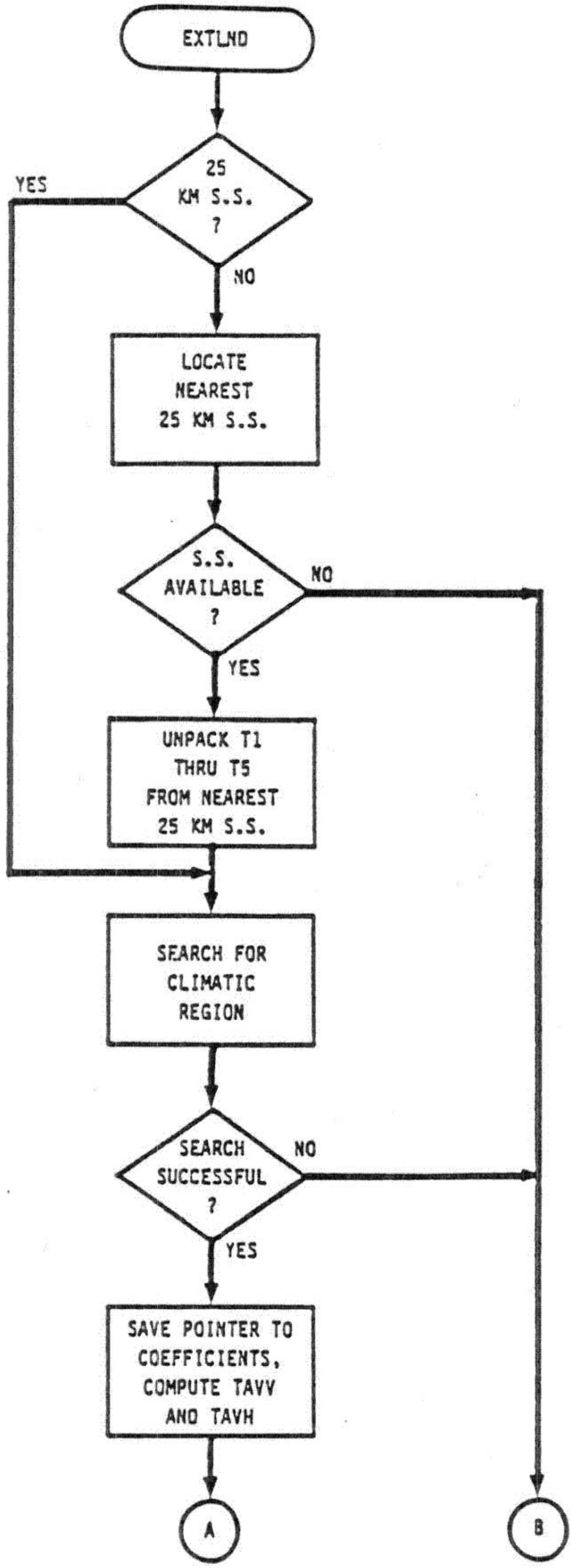

FIGURE 4.3-4 EXTLND FLOW CHART

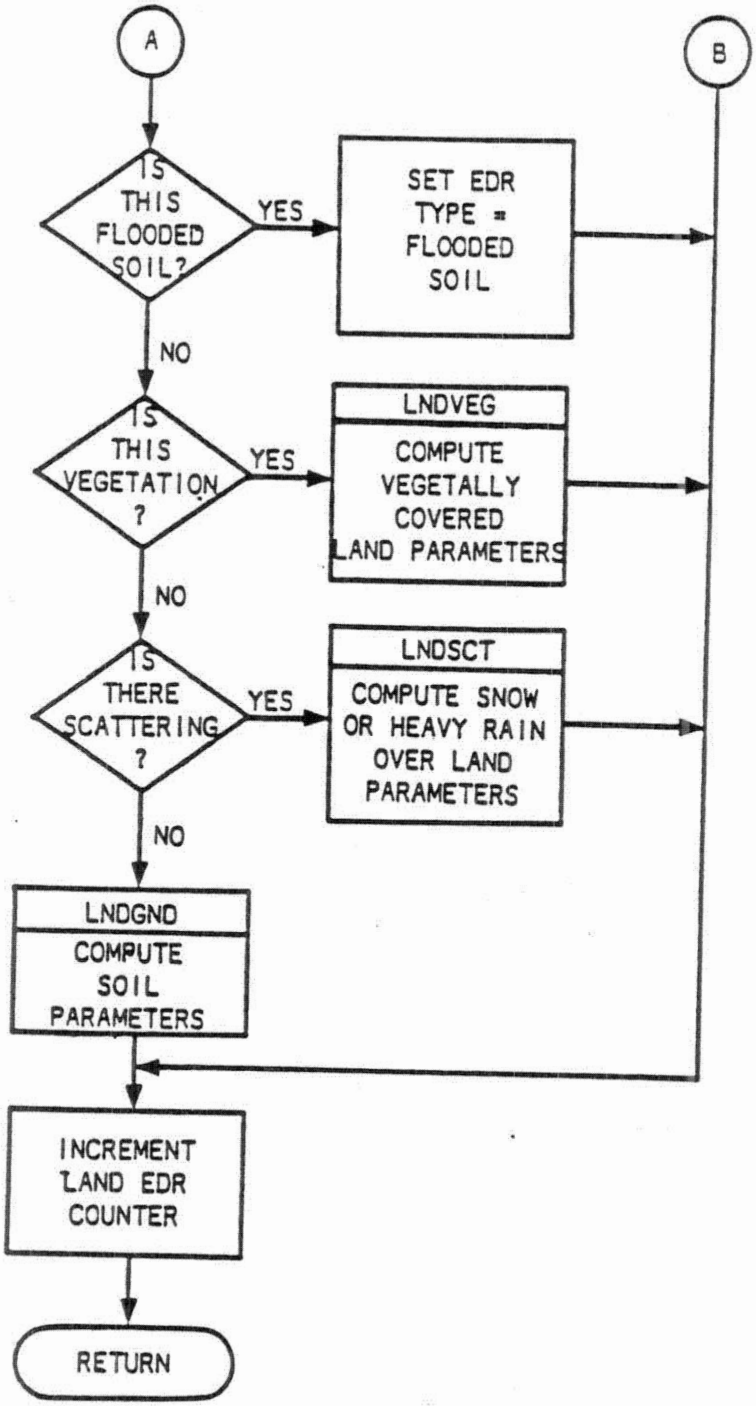

FIGURE 4.3-4 EXTLND FLOW CHART (con't)

THEN: rain exists. Calculate RL, LWL. Cloud water content (CWL) and surface temperature (STV) are left indeterminate.

ELSE: rain is not present. RL = LWL = 0: calculate CWL and STV.

Surface moisture (SM) is not estimated because the soil is masked by the vegetation. Cloud amount (CAL) is not estimated because the vegetation looks similar to a cloud (i.e., a suspension of liquid).

The flow chart for LNDVEG is shown in Figure 4.3-5.

4.3.3.2.2 Scattering by Snow or Rain (module LNDSCT)

LNDSCT first checks the 19 GHz vertical brightness to distinguish between snow and rain:

IF 1: TB(19V) < discriminant (initially 255 K)

THEN 1: the scattering mechanism is snow. LNDSCT next checks the polarization at 19 GHz:

IF 2: [TB(19V) - TB(19H)] < discriminant (initially 5 K)

THEN 2: soil under snow is frozen. The EDR TYPE is set to SNOW 1. Surface moisture (SM) is left indeterminate.

ELSE 2: soil under snow is not frozen; set TYPE to SNOW 2. Estimate surface moisture through utility EEUCAR.

For either snow condition, cloud water and cloud amount (CWS, CAS) are estimated through a call to utility EEUCAR. The presence and amount of cloudiness affects the estimation of remaining parameters:

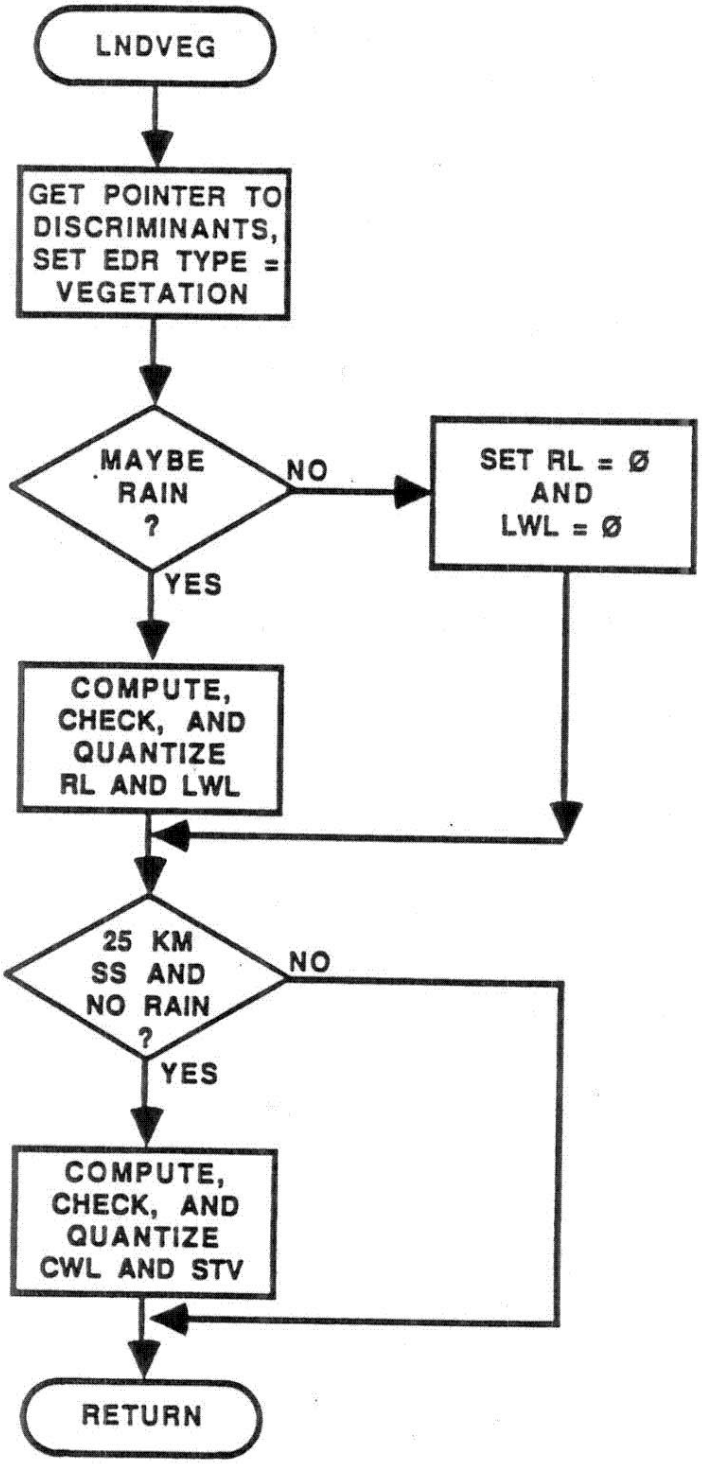

FIGURE 4.3-5 LNDVEG FLOW CHART

IF 3: cloud amount > discriminant (initially 30%)

THEN 3: leave SNW indeterminate. Estimate surface temperature of snow under clouds (TSC) through the utility EEUCAR.

ELSE 3: estimate snow water content (SNW) and surface temperature of snow (STS) through the utility EEUCAR.

ELSE 1: the scattering mechanism is heavy rain. Estimate RL and LWL through EEUCAR; leave CWL and STL indeterminate; set SM to 25%.

The flow chart for LNDSCT is shown in Figure 4.3-6.

4.3.3.2.3 Emission from Soil or Glacial Surface (module LNDGND)

The signature of the brightness temperatures indicates neither heavy vegetation nor a scattering medium such as snow is present. The module first checks for a glacial surface:

IF: TB(19V) < discriminant (initially 200 K)

THEN: the surface is glacial. Surface temperature (STG), cloud water content (CWL) and cloud amount (CAL) are calculated by a call to EEUCAR. No other parameters are estimated over a glacial surface.

ELSE: the surface is either arable soil, desert, or frozen ground/wet snow. Before attempting to distinguish them, LNDGND tests for rain:

IF [TB(85V) - TB(37V)] < discriminant (initially 0 K)

THEN: rain may exist. Estimate RL and LWL through the utility EEUCAR.

ELSE: set RL and LWL to 0.

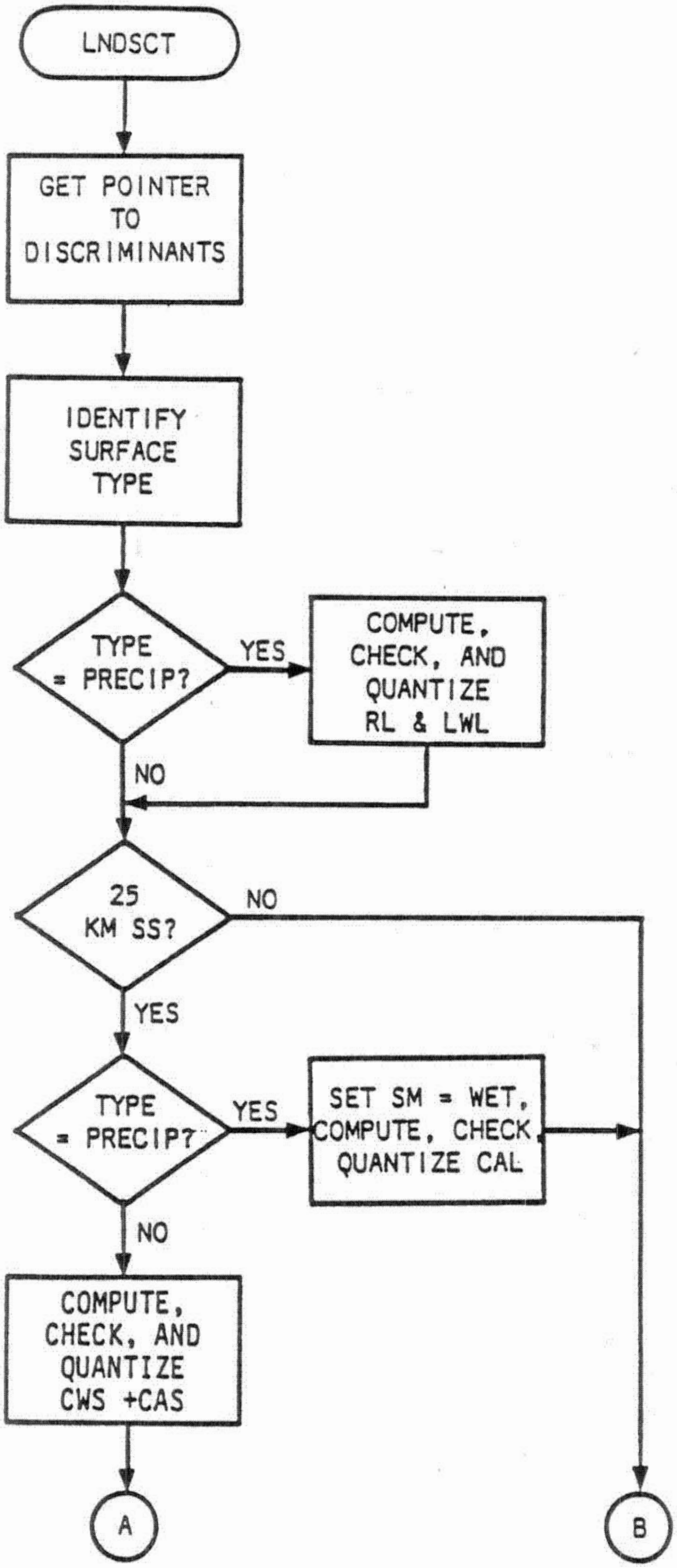

FIGURE 4.3-6 LNDSCT FLOW CHART

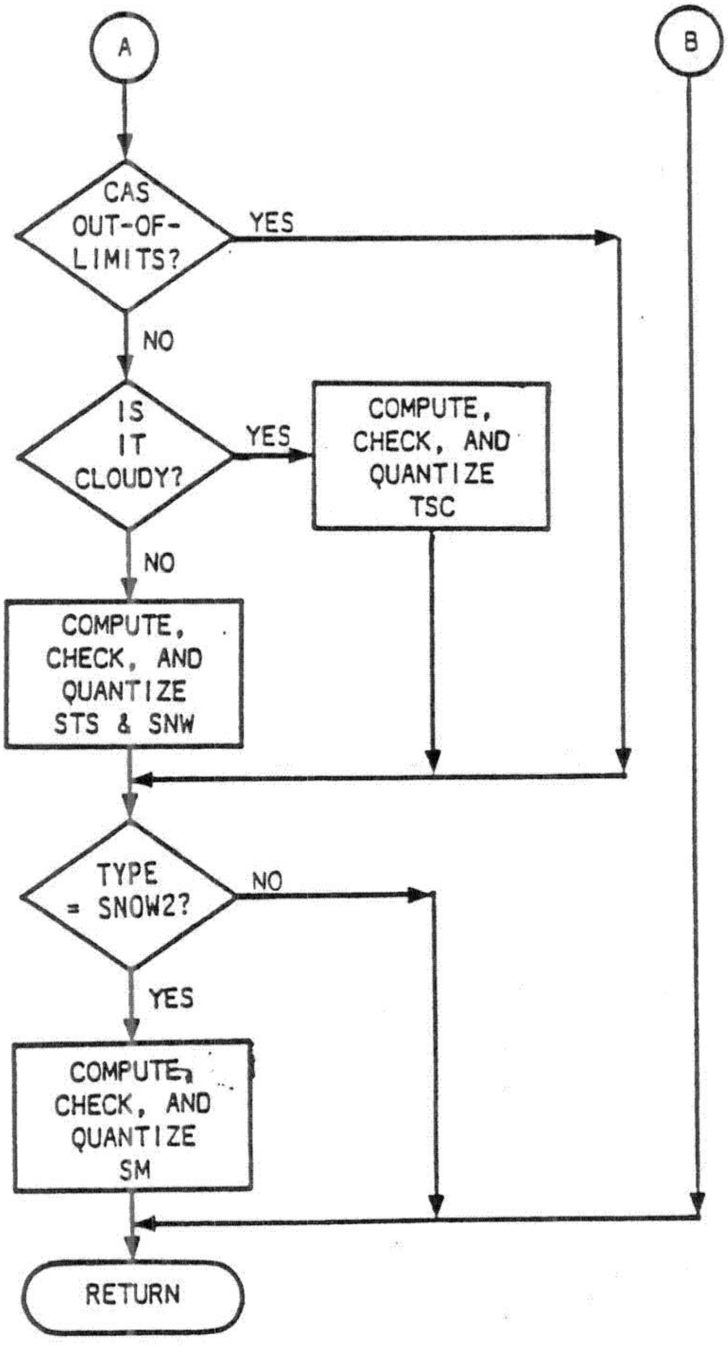

FIGURE 4.3-6 LNDSCT FLOW CHART (con't)

The module next computes cloud amount (CAL) with a call to EEUCAR. This estimate of cloud amount is used in the following logic: if the cloud amount is greater than a discriminant amount (initially 30%), surface temperature over desert (STD), over frozen ground/wet snow (STF), and over glacial surface (STG) is left indeterminate.

Like heavy vegetation, frozen ground and wet snow (they are indistinguishable by SSM/I data) appear isotropic; all the brightness temperatures are very nearly the same (typically in the mid-250's K). The brightness temperature values are, of course, much larger for vegetation than for wet snow. (The possibility of heavy vegetation was evaluated above.) The module next checks for wet snow/frozen ground:

IF: average vertical TB - average horizontal TB < discriminant (initially 3K)

THEN: the surface is frozen ground or wet snow. If rain is occurring (an unlikely event) no further parameters are estimated.

ELSE: the surface is arable soil or desert. If rain was occurring over one of these surfaces, the surface moisture parameter (SM) is set to 25%.

The LNDGND module next calculates cloud water content (CWL). It then goes on to refine the categorization of surface type. Desert (because of the lack of vegetation) has a very large polarization and, usually, a large brightness temperature.

IF: average vertical TB - average horizontal TB > discriminant (initially 20 K) AND average vertical TB > discriminant (initially 265 K)

THEN: the surface is desert. If not too cloudy, the surface temperature (STD) is estimated by a call to EEUCAR.

ELSE: the surface is arable soil - i.e., it has some reasonable amount of moisture, it is not obscured by snow or vegetation, it is not dry as a desert or frozen. Depending on the amount of cloud, an estimate of surface temperature for cloudy (TLC) or uncloudy (STL) conditions is made.

The reader may note that the inferred presence of clouds affects the logic of the parameters. Over snow surfaces, which scatter microwave radiation, clouds introduce a source of radiance which obscures the estimate of snow water content and surface temperature. Over soil surfaces, a better estimate of surface temperature can be made when 85 GHz data is incorporated in the estimation algorithm - so long as clouds do not distort that measurement. The flow chart is shown in Figure 4.3-7.

4.4 Parameter Extraction Coefficients

The coefficients used to multiply brightness temperatures in production of parameter values are shown in Table 4.4-1. The tables are a formatted printout of the parameter extraction file, made by a utility program called SMIFUM (File Utility Module). In addition to printing this report format of the coefficients, SMIFUM permits modification of the coefficient values. The coefficients shown here are the only set in existence for the SSM/I; however, up to a hundred sets can be specified in SSM/I code. This allows different coefficients for different satellites, and provides for off-line testing with alternate coefficients.

4.5 Parameter Calculations

Parameter values are calculated in the utility EEUCAR. A flow chart of EEUCAR is shown in Figure 4.5-1. As noted above, a parameter value can be based on any linear combination of brightness temperatures; in addition, a further non-linear value of the form

new value = c8 + c9 * (old value)** c10

may be computed if desired by EEUCAR.

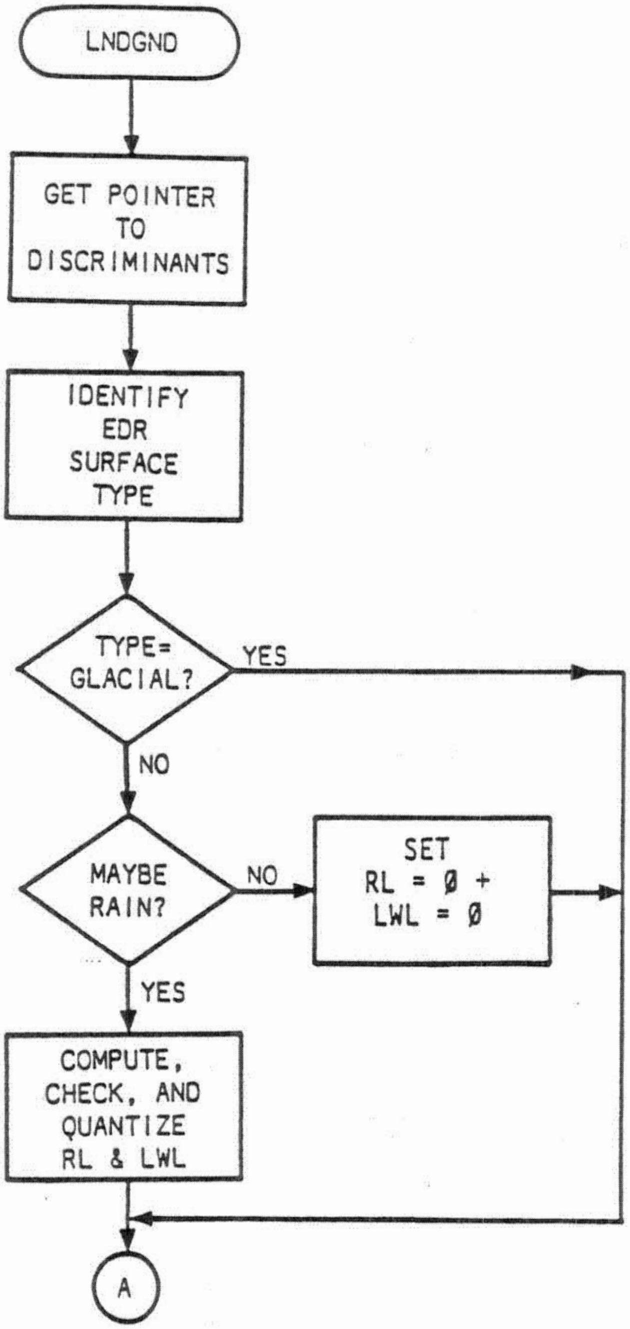

FIGURE 4.3-7 LNDGND FOW CHART

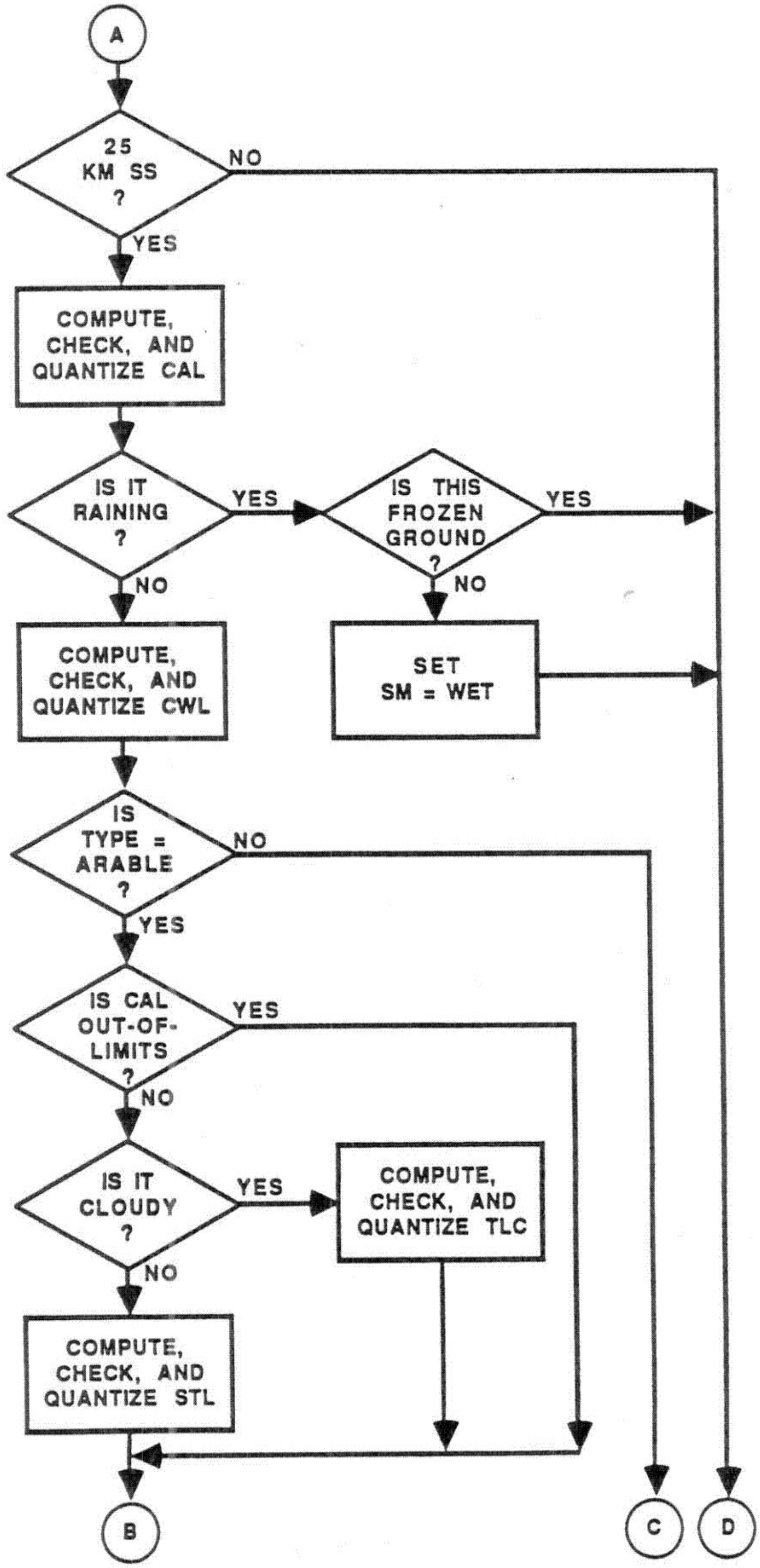

FIGURE 4.3-7 LNDGND FLOW CHART (con't)

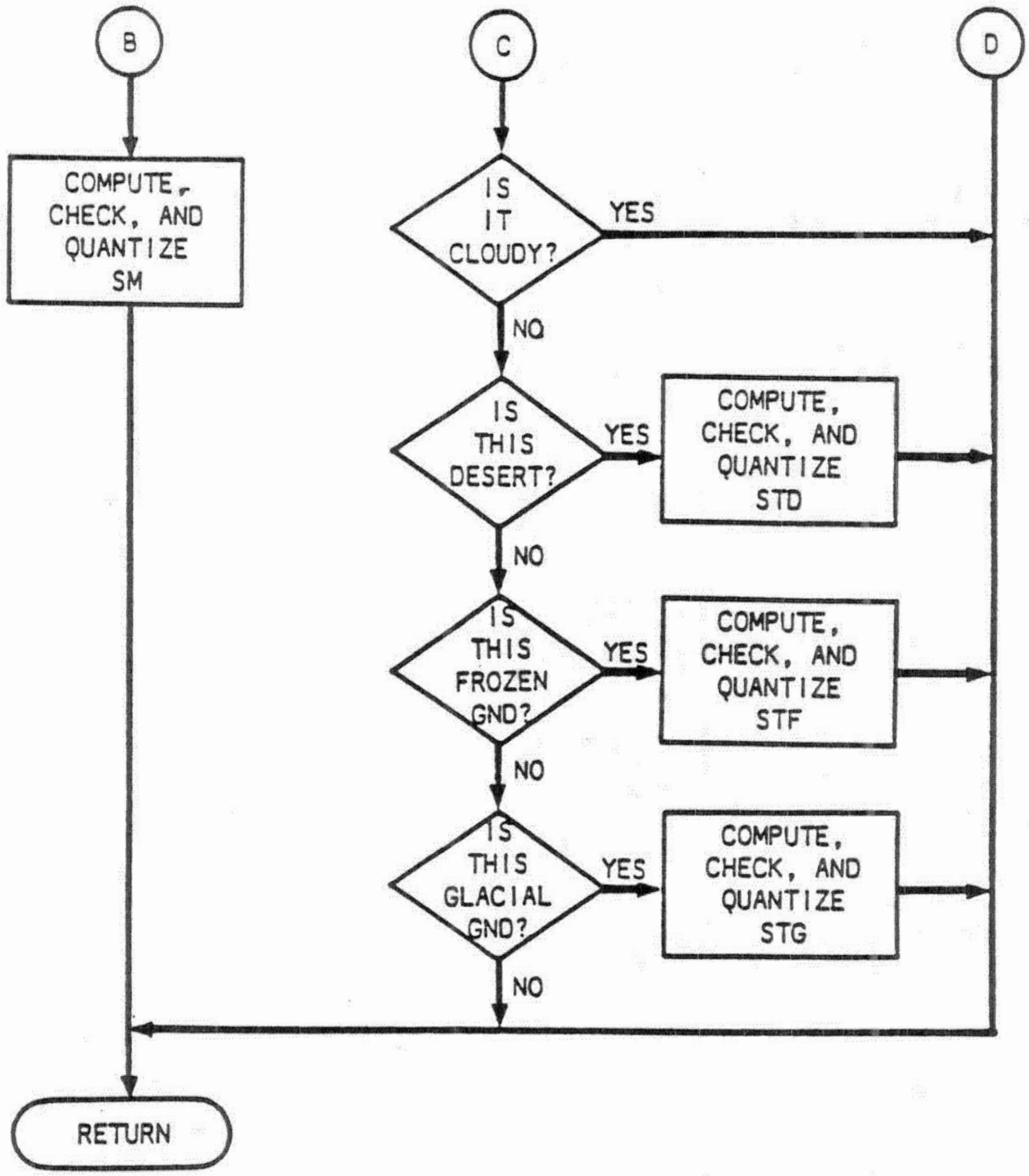

FIGURE 4.3-7 LNDGND FLOW CHART (con't)

Table 4.4-1a Parameter Extraction File for Climatic Zones (1)-(11)

CLIMATIC ZONE (1) TROPICAL - WARM

PARAM	ALG	CONST	19V	19H	22V	37V	37H	85V	85H	C8 CONST	C9 COEF	C10 EXP
RL	2	2.069+002	.000	.000	.000	-7.340-001	.000	-2.880-002	.000	.000	.000	.000
SM	2	1.213+002	-4.596-001	8.390-002	.000	.000	.000	.000	.000	.000	.000	.000
LWL	2	5.315+001	.000	.000	.000	-1.495-001	.000	-4.710-002	.000	.000	.000	.000
CWL	4	6.221-001	3.600-003	-3.100-003	.000	2.510-002	.000	-2.680-002	.000	.000	.000	.000
STD	4	-3.640+001	.000	-4.590-001	-1.270-001	1.610+000	.000	.000	6.360-002	.000	.000	.000
STF	1	.000	1.070+000	.000	.000	.000	.000	.000	.000	.000	.000	.000
STG	1	.000	1.070+000	.000	.000	.000	.000	.000	.000	.000	.000	.000
STL	4	-3.640+001	.000	-4.590-001	-1.270-001	1.610+000	.000	.000	6.360-002	.000	.000	.000
TLC	4	-1.880+001	.000	-4.840-001	4.120-001	1.670+000	.000	-5.730-001	.000	.000	.000	.000
STV	1	.000	1.090+000	.000	.000	.000	.000	.000	.000	.000	.000	.000
CAL	0	-6.389+002	.000	.000	.000	.000	-1.705+000	-2.868-001	7.457-001	.000	.000	.000
CWS	4	-1.450+000	.000	.000	-1.390-002	.000	1.770-002	2.400-004	5.250-003	.000	.000	.000
STS	4	3.210+001	2.140+000	.000	1.910+000	-1.670+000	-1.890+000	.000	.000	.000	.000	.000
TSC	4	7.580+001	.000	4.780-001	1.690+000	-2.430+000	1.060+000	.000	.000	.000	.000	.000
CAS	0	-1.895+002	.000	.000	.000	-9.710-001	7.400-001	-1.987-001	3.678-001	.000	.000	.000
SNW	4	3.200+001	5.110-001	.000	9.420-001	-1.050+000	-6.800-001	.000	.000	.000	.000	.000
RO	4	2.103+002	.000	1.217-001	-7.829-001	-1.830-001	9.980-002	.000	.000	.000	.000	.000
SW	4	1.916+002	.000	4.903-001	-4.432-001	-9.199-001	3.577-001	.000	.000	.000	.000	.000
LWO	4	5.072+001	.000	3.000-002	-1.881-001	-4.930-002	2.850-002	.000	.000	.000	.000	.000
CWO	4	-6.524+000	.000	-1.590-002	-4.400-003	4.070-002	4.500-003	.000	.000	.000	.000	.000
WVO	4	-5.681+001	-4.310-001	.000	1.531+000	-1.161+000	4.850-001	.000	.000	.000	.000	.000

DISCRIMINANTS FOR CLIMATIC ZONE (1) TROPICAL - WARM

LAND - MAYBE SNOW DELTA	: .0000
LAND - MAYBE HEAVY RAIN MIN	: 2.5500+002
LAND - FROZEN GND (SNOW) DELTA	: 3.0000+000
LAND - HEAVY VEG DELTA	: 2.0000+000
LAND - HEAVY VEG MIN	: 2.5500+002
LAND - FROZEN GND (SOIL) DELTA	: 5.0000+000
LAND - FROZEN GND (SOIL) MAX	: 2.6000+002
LAND - DESERT DELTA	: 2.0000+001
LAND - DESERT MIN	: 2.6500+002
LAND - FLOODED SOIL DELTA	: 5.0000+000
LAND - GLACIAL MAX	: 2.0000+002
LAND - CLOUD COVER MIN	: 3.0000+001
LAND - MAYBE RAIN (GND) DELTA	: .0000
LAND - MAYBE RAIN (VEG) DELTA	: .0000
BAD DATA DELTA	: -2.0000+000
OCEAN - MAYBE RAIN MIN	: 1.9000+002
OCEAN - MAYBE RAIN DELTA	: 2.5000+001
OCEAN - HEAVY RAIN DELTA	: 1.0000+001

Table 4.4-1a Parameter Extraction File for Climate Zones (1)-(11) (Con't)

CLIMATIC ZONE (2) TROPICAL - COOL

PARAM	ALG	CONST	19V	19H	22V	37V	37H	85V	85H	C8 CONST	C9 COEF	C10 EXP
RL	2	2.339+002	.000	.000	.000	-6.887-001	.000	-1.768-001	.000	.000	.000	.000
SM	2	1.088+002	-3.877-001	4.940-002	.000	.000	.000	.000	.000	.000	.000	.000
LWL	2	5.721+001	.000	.000	.000	-1.405-001	.000	-7.130-002	.000	.000	.000	.000
CWL	4	1.654+000	-8.000-004	-6.000-004	.000	3.620-002	.000	-3.840-002	.000	.000	.000	.000
STD	4	-3.640+001	.000	-4.590-001	-1.270-001	1.610+000	.000	.000	6.360-002	.000	.000	.000
STF	1	.000	1.070+000	.000	.000	.000	.000	.000	.000	.000	.000	.000
STG	1	.000	1.070+000	.000	.000	.000	.000	.000	.000	.000	.000	.000
STL	4	-3.640+001	.000	-4.590-001	-1.270-001	1.610+000	.000	.000	6.360-002	.000	.000	.000
TLC	4	-1.880+001	.000	-4.840-001	4.120-001	1.670+000	.000	-5.730-001	.000	.000	.000	.000
STV	1	.000	1.090+000	.000	.000	.000	.000	.000	.000	.000	.000	.000
CAL	0	-6.389+002	.000	.000	.000	.000	-1.705+000	-2.868-001	7.457-001	.000	.000	.000
CWS	4	-1.450+000	.000	.000	-1.390-002	.000	1.770-002	2.400-004	5.250-003	.000	.000	.000
STS	4	3.210+001	2.140+000	.000	1.910+000	-1.670+000	-1.890+000	.000	.000	.000	.000	.000
TSC	4	7.580+001	.000	4.780-001	1.690+000	-2.430+000	1.060+000	.000	.000	.000	.000	.000
CAS	0	-1.895+002	.000	.000	.000	-9.710-001	7.400-001	-1.987-001	3.678-001	.000	.000	.000
SNW	4	3.200+001	5.110-001	.000	9.420-001	-1.050+000	-6.800-001	.000	.000	.000	.000	.000
RO	4	2.152+002	.000	1.026-001	-8.059-001	-1.944-001	1.354-001	.000	.000	.000	.000	.000
SW	4	1.684+002	.000	5.366-001	-4.548-001	-7.656-001	2.635-001	.000	.000	.000	.000	.000
LWO	4	5.391+001	.000	2.590-002	-2.053-001	-4.830-002	3.740-002	.000	.000	.000	.000	.000
CWO	4	-6.529+000	.000	-1.510-002	-4.600-003	4.080-002	4.100-003	.000	.000	.000	.000	.000
WVO	4	-7.214+001	-5.185-001	.000	1.137+000	-2.810-001	5.200-002	.000	.000	.000	.000	.000

DISCRIMINANTS FOR CLIMATIC ZONE (2) TROPICAL - COOL

LAND - MAYBE SNOW DELTA	:	.0000
LAND - MAYBE HEAVY RAIN MIN	:	2.5500+002
LAND - FROZEN GND (SNOW) DELTA	:	3.0000+000
LAND - HEAVY VEG DELTA	:	2.0000+000
LAND - HEAVY VEG MIN	:	2.5500+002
LAND - FROZEN GND (SOIL) DELTA	:	5.0000+000
LAND - FROZEN GND (SOIL) MAX	:	2.6000+002
LAND - DESERT DELTA	:	2.0000+001
LAND - DESERT MIN	:	2.6500+002
LAND - FLOODED SOIL DELTA	:	5.0000+000
LAND - GLACIAL MAX	:	2.0000+002
LAND - CLOUD COVER MIN	:	3.0000+001
LAND - MAYBE RAIN (GND) DELTA	:	.0000
LAND - MAYBE RAIN (VEG) DELTA	:	.0000
BAD DATA DELTA	:	-2.0000+000
OCEAN - MAYBE RAIN MIN	:	1.9000+002
OCEAN - MAYBE RAIN DELTA	:	2.5000+001
OCEAN - HEAVY RAIN DELTA	:	1.0000+001

Table 4.4-1a Parameter Extraction File for Climate Zones (1)-(11) (Con't)

CLIMATIC ZONE (3) LOWER LAT TRANSITION - WARM

PARAM	ALG	CONST	19V	19H	22V	37V	37H	85V	85H	C8 CONST	C9 COEF	C10 EXP
RL	2	2.158+002	.000	.000	.000	-7.044-001	.000	-9.090-002	.000	.000	.000	.000
SM	2	1.096+002	-3.872-001	4.140-002	.000	.000	.000	.000	.000	.000	.000	.000
LWL	2	5.131+001	.000	.000	.000	-1.580-001	.000	-3.150-002	.000	.000	.000	.000
CWL	4	8.821-001	6.000-004	-7.000-004	.000	2.710-002	.000	-2.830-002	.000	.000	.000	.000
STD	4	-3.640+001	.000	-4.590-001	-1.270-001	1.610+000	.000	.000	6.360-002	.000	.000	.000
STF	1	.000	1.070+000	.000	.000	.000	.000	.000	.000	.000	.000	.000
STG	1	.000	1.070+000	.000	.000	.000	.000	.000	.000	.000	.000	.000
STL	4	-3.640+001	.000	-4.590-001	-1.270-001	1.610+000	.000	.000	6.360-002	.000	.000	.000
TLC	4	-1.880+001	.000	-4.840-001	4.120-001	1.670+000	.000	-5.730-001	.000	.000	.000	.000
STV	1	.000	1.090+000	.000	.000	.000	.000	.000	.000	.000	.000	.000
CAL	0	-6.389+002	.000	.000	.000	.000	-1.705+000	-2.868-001	7.457-001	.000	.000	.000
CWS	4	-1.450+000	.000	.000	-1.390-002	.000	1.770-002	2.400-004	5.250-003	.000	.000	.000
STS	4	3.210+001	2.140+000	.000	1.910+000	-1.670+000	-1.890+000	.000	.000	.000	.000	.000
TSC	4	7.580+001	.000	4.780-001	1.690+000	-2.430+000	1.060+000	.000	.000	.000	.000	.000
CAS	0	-1.895+002	.000	.000	.000	-9.710-001	7.400-001	-1.987-001	3.678-001	.000	.000	.000
SNW	4	3.200+001	5.110-001	.000	9.420-001	-1.050+000	-6.800-001	.000	.000	.000	.000	.000
RO	4	1.730+002	.000	1.938-001	-6.500-001	-2.291-001	8.080-002	.000	.000	.000	.000	.000
SW	4	1.773+002	.000	3.913-001	-2.818-001	-1.008+000	4.095-001	.000	.000	.000	.000	.000
LWO	4	4.072+001	.000	4.050-002	-1.353-001	-7.680-002	2.890-002	.000	.000	.000	.000	.000
CWO	4	-6.207+000	.000	-1.410-002	-3.800-003	3.830-002	3.500-003	.000	.000	.000	.000	.000
WVO	4	-5.681+001	-4.310-001	.000	1.531+000	-1.161+000	4.850-001	.000	.000	.000	.000	.000

DISCRIMINANTS FOR CLIMATIC ZONE (3) LOWER LAT TRANSITION - WARM

LAND - MAYBE SNOW DELTA	:	.0000
LAND - MAYBE HEAVY RAIN MIN	:	2.5500+002
LAND - FROZEN GND (SNOW) DELTA	:	3.0000+000
LAND - HEAVY VEG DELTA	:	2.0000+000
LAND - HEAVY VEG MIN	:	2.5500+002
LAND - FROZEN GND (SOIL) DELTA	:	5.0000+000
LAND - FROZEN GND (SOIL) MAX	:	2.6000+002
LAND - DESERT DELTA	:	2.0000+001
LAND - DESERT MIN	:	2.6500+002
LAND - FLOODED SOIL DELTA	:	5.0000+000
LAND - GLACIAL MAX	:	2.0000+002
LAND - CLOUD COVER MIN	:	3.0000+001
LAND - MAYBE RAIN (GND) DELTA	:	.0000
LAND - MAYBE RAIN (VEG) DELTA	:	.0000
BAD DATA DELTA	:	-2.0000+000
OCEAN - MAYBE RAIN MIN	:	1.9000+002
OCEAN - MAYBE RAIN DELTA	:	2.5000+001
OCEAN - HEAVY RAIN DELTA	:	1.0000+001

Table 4.4-1a Parameter Extraction File for Climate Zones (1)-(11) (Con't)

CLIMATIC ZONE (4) LOWER LAT TRANSITION - COOL

PARAM	ALG	CONST	19V	19H	22V	37V	37H	85V	85H	C8 CONST	C9 COEF	C10 EXP
RL	2	2.477+002	.000	.000	.000	-5.741-001	.000	-3.649-001	.000	.000	.000	.000
SM	2	8.998+001	-2.924-001	5.800-003	.000	.000	.000	.000	.000	.000	.000	.000
LWL	2	4.979+001	.000	.000	.000	-9.770-002	.000	-8.730-002	.000	.000	.000	.000
CWL	4	1.535+000	1.400-003	-3.000-003	.000	3.620-002	.000	-3.770-002	.000	.000	.000	.000
STD	4	-3.640+001	.000	-4.590-001	-1.270-001	1.610+000	.000	.000	6.360-002	.000	.000	.000
STF	1	.000	1.070+000	.000	.000	.000	.000	.000	.000	.000	.000	.000
STG	1	.000	1.070+000	.000	.000	.000	.000	.000	.000	.000	.000	.000
STL	4	-3.640+001	.000	-4.590-001	-1.270-001	1.610+000	.000	.000	6.360-002	.000	.000	.000
TLC	4	-1.880+001	.000	-4.840-001	4.120-001	1.670+000	.000	-5.730-001	.000	.000	.000	.000
STV	1	.000	1.090+000	.000	.000	.000	.000	.000	.000	.000	.000	.000
CAL	0	-6.389+002	.000	.000	.000	.000	-1.705+000	-2.868-001	7.457-001	.000	.000	.000
CWS	4	-1.450+000	.000	.000	-1.390-002	.000	1.770-002	2.400-004	5.250-003	.000	.000	.000
STS	4	3.210+001	2.140+000	.000	1.910+000	-1.670+000	-1.890+000	.000	.000	.000	.000	.000
TSC	4	7.580+001	.000	4.780-001	1.690+000	-2.430+000	1.060+000	.000	.000	.000	.000	.000
CAS	0	-1.895+002	.000	.000	.000	-9.710-001	7.400-001	-1.987-001	3.678-001	.000	.000	.000
SNW	4	3.200+001	5.110-001	.000	9.420-001	-1.050+000	-6.800-001	.000	.000	.000	.000	.000
RO	4	1.693+002	.000	1.523-001	-6.065-001	-3.531-001	2.162-001	.000	.000	.000	.000	.000
SW	4	1.478+002	.000	5.077-001	-3.547-001	-7.409-001	2.333-001	.000	.000	.000	.000	.000
LWO	4	3.946+001	.000	3.440-002	-1.226-001	-8.440-002	3.420-002	.000	.000	.000	.000	.000
CWO	4	-6.137+000	.000	-9.400-003	-5.400-003	3.980-002	-3.000-004	.000	.000	.000	.000	.000
WVO	4	-7.214+001	-5.185-001	.000	1.137+000	-2.810-001	5.200-002	.000	.000	.000	.000	.000

DISCRIMINANTS FOR CLIMATIC ZONE (4) LOWER LAT TRANSITION - COOL

LAND - MAYBE SNOW DELTA	:	.0000
LAND - MAYBE HEAVY RAIN MIN	:	2.5500+002
LAND - FROZEN GND (SNOW) DELTA	:	3.0000+000
LAND - HEAVY VEG DELTA	:	2.0000+000
LAND - HEAVY VEG MIN	:	2.5500+002
LAND - FROZEN GND (SOIL) DELTA	:	5.0000+000
LAND - FROZEN GND (SOIL) MAX	:	2.6000+002
LAND - DESERT DELTA	:	2.0000+001
LAND - DESERT MIN	:	2.6500+002
LAND - FLOODED SOIL DELTA	:	5.0000+000
LAND - GLACIAL MAX	:	2.0000+002
LAND - CLOUD COVER MIN	:	3.0000+001
LAND - MAYBE RAIN (GND) DELTA	:	.0000
LAND - MAYBE RAIN (VEG) DELTA	:	.0000
BAD DATA DELTA	:	-2.0000+000
OCEAN - MAYBE RAIN MIN	:	1.9000+002
OCEAN - MAYBE RAIN DELTA	:	2.5000+001
OCEAN - HEAVY RAIN DELTA	:	1.0000+001

Table 4.4-1a Parameter Extraction File for Climate Zones (1)-(11) (Con't)

CLIMATIC ZONE (5) MID-LAT - SPRING/FALL

PARAM	ALG	CONST	19V	19H	22V	37V	37H	85V	85H	C8 CONST	C9 COEF	C10 EXP
RL	2	2.614+002	.000	.000	.000	-4.595-001	.000	-5.170-001	.000	.000	.000	.000
SM	2	7.115+001	-1.970-001	-3.780-002	.000	.000	.000	.000	.000	.000	.000	.000
LWL	2	4.236+001	.000	.000	.000	-5.480-002	.000	-1.032-001	.000	.000	.000	.000
CWL	4	1.415+000	3.600-003	-5.400-003	.000	3.620-002	.000	-3.690-002	.000	.000	.000	.000
STD	4	-3.640+001	.000	-4.590-001	-1.270-001	1.610+000	.000	.000	6.360-002	.000	.000	.000
STF	1	.000	1.070+000	.000	.000	.000	.000	.000	.000	.000	.000	.000
STG	1	.000	1.070+000	.000	.000	.000	.000	.000	.000	.000	.000	.000
STL	4	-3.640+001	.000	-4.590-001	-1.270-001	1.610+000	.000	.000	6.360-002	.000	.000	.000
TLC	4	-1.880+001	.000	-4.840-001	4.120-001	1.670+000	.000	-5.730-001	.000	.000	.000	.000
STV	1	.000	1.090+000	.000	.000	.000	.000	.000	.000	.000	.000	.000
CAL	0	-6.389+002	.000	.000	.000	.000	-1.705+000	-2.868-001	7.457-001	.000	.000	.000
CWS	4	-1.450+000	.000	.000	-1.390-002	.000	1.770-002	2.400-004	5.250-003	.000	.000	.000
STS	4	3.210+001	2.140+000	.000	1.910+000	-1.670+000	-1.890+000	.000	.000	.000	.000	.000
TSC	4	7.580+001	.000	4.780-001	1.690+000	-2.430+000	1.060+000	.000	.000	.000	.000	.000
CAS	0	-1.895+002	.000	.000	.000	-9.710-001	7.400-001	-1.987-001	3.678-001	.000	.000	.000
SNW	4	3.200+001	5.110-001	.000	9.420-001	-1.050+000	-6.800-001	.000	.000	.000	.000	.000
RO	4	1.234+002	.000	2.019-001	-4.070-001	-5.117-001	2.969-001	.000	.000	.000	.000	.000
SW	4	1.271+002	.000	4.788-001	-2.546-001	-7.162-001	2.030-001	.000	.000	.000	.000	.000
LWO	4	2.500+001	.000	4.290-002	-3.990-002	-1.205-001	3.100-002	.000	.000	.000	.000	.000
CWO	4	-5.745+000	.000	-3.700-003	-6.200-003	3.870-002	-4.700-003	.000	.000	.000	.000	.000
WVO	4	-7.214+001	-5.185-001	.000	1.137+000	-2.810-001	5.200-002	.000	.000	.000	.000	.000

DISCRIMINANTS FOR CLIMATIC ZONE (5) MID-LAT - SPRING/FALL

LAND - MAYBE SNOW DELTA	: .0000
LAND - MAYBE HEAVY RAIN MIN	: 2.5500+002
LAND - FROZEN GND (SNOW) DELTA	: 3.0000+000
LAND - HEAVY VEG DELTA	: 2.0000+000
LAND - HEAVY VEG MIN	: 2.5500+002
LAND - FROZEN GND (SOIL) DELTA	: 5.0000+000
LAND - FROZEN GND (SOIL) MAX	: 2.6000+002
LAND - DESERT DELTA	: 2.0000+001
LAND - DESERT MIN	: 2.6500+002
LAND - FLOODED SOIL DELTA	: 5.0000+000
LAND - GLACIAL MAX	: 2.0000+002
LAND - CLOUD COVER MIN	: 3.0000+001
LAND - MAYBE RAIN (GND) DELTA	: .0000
LAND - MAYBE RAIN (VEG) DELTA	: .0000
BAD DATA DELTA	: -2.0000+000
OCEAN - MAYBE RAIN MIN	: 1.9000+002
OCEAN - MAYBE RAIN DELTA	: 2.5000+001
OCEAN - HEAVY RAIN DELTA	: 1.0000+001

Table 4.4-1a Parameter Extraction File for Climate Zones (1)-(11) (Con't)

CLIMATIC ZONE (6) MID-LAT - SUMMER

PARAM	ALG	CONST	19V	19H	22V	37V	37H	85V	85H	C8 CONST	C9 COEF	C10 EXP
RL	2	2.246+002	.000	.000	.000	-6.747-001	.000	-1.529-001	.000	.000	.000	.000
SM	2	9.787+001	-3.148-001	-1.100-003	.000	.000	.000	.000	.000	.000	.000	.000
LWL	2	4.947+001	.000	.000	.000	-1.665-001	.000	-1.580-002	.000	.000	.000	.000
CWL	4	1.142+000	-2.400-003	1.700-003	.000	2.900-002	.000	-2.980-002	.000	.000	.000	.000
STD	4	-3.640+001	.000	-4.590-001	-1.270-001	1.610+000	.000	.000	6.360-002	.000	.000	.000
STF	1	.000	1.070+000	.000	.000	.000	.000	.000	.000	.000	.000	.000
STG	1	.000	1.070+000	.000	.000	.000	.000	.000	.000	.000	.000	.000
STL	4	-3.640+001	.000	-4.590-001	-1.270-001	1.610+000	.000	.000	6.360-002	.000	.000	.000
TLC	4	-1.880+001	.000	-4.840-001	4.120-001	1.670+000	.000	-5.730-001	.000	.000	.000	.000
STV	1	.000	1.090+000	.000	.000	.000	.000	.000	.000	.000	.000	.000
CAL	0	-6.389+002	.000	.000	.000	.000	-1.705+000	-2.868-001	7.457-001	.000	.000	.000
CWS	4	-1.450+000	.000	.000	-1.390-002	.000	1.770-002	2.400-004	5.250-003	.000	.000	.000
STS	4	3.210+001	2.140+000	.000	1.910+000	-1.670+000	-1.890+000	.000	.000	.000	.000	.000
TSC	4	7.580+001	.000	4.780-001	1.690+000	-2.430+000	1.060+000	.000	.000	.000	.000	.000
CAS	0	-1.895+002	.000	.000	.000	-9.710-001	7.400-001	-1.987-001	3.678-001	.000	.000	.000
SNW	4	3.200+001	5.110-001	.000	9.420-001	-1.050+000	-6.800-001	.000	.000	.000	.000	.000
RO	4	1.358+002	.000	2.659-001	-5.170-001	-2.751-001	6.180-002	.000	.000	.000	.000	.000
SW	4	1.631+002	.000	2.923-001	-1.204-001	-1.097+000	4.612-001	.000	.000	.000	.000	.000
LWO	4	3.072+001	.000	5.100-002	-8.240-002	-1.043-001	2.930-002	.000	.000	.000	.000	.000
CWO	4	-5.890+000	.000	-1.230-002	-3.100-003	3.580-002	2.500-003	.000	.000	.000	.000	.000
WVO	4	-7.214+001	-5.185-001	.000	1.137+000	-2.810-001	5.200-002	.000	.000	.000	.000	.000

DISCRIMINANTS FOR CLIMATIC ZONE (6) MID-LAT - SUMMER

LAND - MAYBE SNOW DELTA : .0000
LAND - MAYBE HEAVY RAIN MIN : 2.5500+002
LAND - FROZEN GND (SNOW) DELTA : 3.0000+000
LAND - HEAVY VEG DELTA : 2.0000+000
LAND - HEAVY VEG MIN : 2.5500+002
LAND - FROZEN GND (SOIL) DELTA : 5.0000+000
LAND - FROZEN GND (SOIL) MAX : 2.6000+002
LAND - DESERT DELTA : 2.0000+001
LAND - DESERT MIN : 2.6500+002
LAND - FLOODED SOIL DELTA : 5.0000+000
LAND - GLACIAL MAX : 2.0000+002
LAND - CLOUD COVER MIN : 3.0000+001
LAND - MAYBE RAIN (GND) DELTA : .0000
LAND - MAYBE RAIN (VEG) DELTA : .0000
BAD DATA DELTA : -2.0000+000
OCEAN - MAYBE RAIN MIN : 1.9000+002
OCEAN - MAYBE RAIN DELTA : 2.5000+001
OCEAN - HEAVY RAIN DELTA : 1.0000+001

Table 4.4-1a Parameter Extraction File for Climate Zones (1)-(11) (Con't)

CLIMATIC ZONE (7) MID-LAT - WINTER

PARAM	ALG	CONST	19V	19H	22V	37V	37H	85V	85H	C8 CONST	C9 COEF	C10 EXP
RL	2	2.907+002	.000	.000	.000	-3.868-001	.000	-7.026-001	.000	.000	.000	.000
SM	2	8.584+001	-2.818-001	-4.000-003	.000	.000	.000	.000	.000	.000	.000	.000
LWL	2	5.225+001	.000	.000	.000	-6.870-002	.000	-1.278-001	.000	.000	.000	.000
CWL	4	1.208+000	-5.000-003	3.300-003	.000	4.150-002	.000	-4.010-002	.000	.000	.000	.000
STD	4	-3.640+001	.000	-4.590-001	-1.270-001	1.610+000	.000	.000	6.360-002	.000	.000	.000
STF	1	.000	1.070+000	.000	.000	.000	.000	.000	.000	.000	.000	.000
STG	1	.000	1.070+000	.000	.000	.000	.000	.000	.000	.000	.000	.000
STL	4	-3.640+001	.000	-4.590-001	-1.270-001	1.610+000	.000	.000	6.360-002	.000	.000	.000
TLC	4	-1.880+001	.000	-4.840-001	4.120-001	1.670+000	.000	-5.730-001	.000	.000	.000	.000
STV	1	.000	1.090+000	.000	.000	.000	.000	.000	.000	.000	.000	.000
CAL	0	-6.389+002	.000	.000	.000	.000	-1.705+000	-2.868-001	7.457-001	.000	.000	.000
CWS	4	-1.450+000	.000	.000	-1.390-002	.000	1.770-002	2.400-004	5.250-003	.000	.000	.000
STS	4	3.210+001	2.140+000	.000	1.910+000	-1.670+000	-1.890+000	.000	.000	.000	.000	.000
TSC	4	7.580+001	.000	4.780-001	1.690+000	-2.430+000	1.060+000	.000	.000	.000	.000	.000
CAS	0	-1.895+002	.000	.000	.000	-9.710-001	7.400-001	-1.987-001	3.678-001	.000	.000	.000
SNW	4	3.200+001	5.110-001	.000	9.420-001	-1.050+000	-6.800-001	.000	.000	.000	.000	.000
RO	4	1.146+002	.000	2.708-001	-6.228-001	-2.836-001	2.521-001	.000	.000	.000	.000	.000
SW	4	9.599+001	.000	6.106-001	-3.034-001	-4.638-001	1.920-002	.000	.000	.000	.000	.000
LWO	4	3.462+001	.000	4.740-002	-5.920-002	-1.749-001	6.230-002	.000	.000	.000	.000	.000
CWO	4	-6.141+000	.000	-7.000-004	-6.100-003	3.950-002	-5.900-003	.000	.000	.000	.000	.000
WVO	4	-7.681+001	-6.020-001	.000	8.850-001	2.270-001	-1.890-001	.000	.000	.000	.000	.000

DISCRIMINANTS FOR CLIMATIC ZONE (7) MID-LAT - WINTER

LAND - MAYBE SNOW DELTA	: .0000
LAND - MAYBE HEAVY RAIN MIN	: 2.5500+002
LAND - FROZEN GND (SNOW) DELTA	: 3.0000+000
LAND - HEAVY VEG DELTA	: 2.0000+000
LAND - HEAVY VEG MIN	: 2.5500+002
LAND - FROZEN GND (SOIL) DELTA	: 5.0000+000
LAND - FROZEN GND (SOIL) MAX	: 2.6000+002
LAND - DESERT DELTA	: 2.0000+001
LAND - DESERT MIN	: 2.6500+002
LAND - FLOODED SOIL DELTA	: 5.0000+000
LAND - GLACIAL MAX	: 2.0000+002
LAND - CLOUD COVER MIN	: 3.0000+001
LAND - MAYBE RAIN (GND) DELTA	: .0000
LAND - MAYBE RAIN (VEG) DELTA	: .0000
BAD DATA DELTA	: -2.0000+000
OCEAN - MAYBE RAIN MIN	: 1.9000+002
OCEAN - MAYBE RAIN DELTA	: 2.5000+001
OCEAN - HEAVY RAIN DELTA	: 1.0000+001

Table 4.4-1a Parameter Extraction File for Climate Zones (1)-(11) (Con't)

CLIMATIC ZONE (8) UPPER LAT TRANSITION - COOL

PARAM	ALG	CONST	19V	19H	22V	37V	37H	85V	85H	C8 CONST.	C9 COEF	C10 EXP
RL	2	2.393+002	.000	.000	.000	-4.323-001	.000	-4.595-001	.000	.000	.000	.000
SM	2	6.737+001	-1.483-001	-8.740-002	.000	.000	.000	.000	.000	.000	.000	.000
LWL	2	2.974+001	.000	.000	.000	-3.810-002	.000	-7.250-002	.000	.000	.000	.000
CWL	4	1.537+000	2.000-004	-1.900-003	.000	3.280-002	.000	-3.420-002	.000	.000	.000	.000
STD	4	-3.640+001	.000	-4.590-001	-1.270-001	1.610+000	.000	.000	6.360-002	.000	.000	.000
STF	1	.000	1.070+000	.000	.000	.000	.000	.000	.000	.000	.000	.000
STG	1	.000	1.070+000	.000	.000	.000	.000	.000	.000	.000	.000	.000
STL	4	-3.640+001	.000	-4.590-001	-1.270-001	1.610+000	.000	.000	6.360-002	.000	.000	.000
TLC	4	-1.880+001	.000	-4.840-001	4.120-001	1.670+000	.000	-5.730-001	.000	.000	.000	.000
STV	1	.000	1.090+000	.000	.000	.000	.000	.000	.000	.000	.000	.000
CAL	0	-6.389+002	.000	.000	.000	.000	-1.705+000	-2.868-001	7.457-001	.000	.000	.000
CWS	4	-1.450+000	.000	.000	-1.390-002	.000	1.770-002	2.400-004	5.250-003	.000	.000	.000
STS	4	3.210+001	2.140+000	.000	1.910+000	-1.670+000	-1.890+000	.000	.000	.000	.000	.000
TSC	4	7.580+001	.000	4.780-001	1.690+000	-2.430+000	1.060+000	.000	.000	.000	.000	.000
CAS	0	-1.895+002	.000	.000	.000	-9.710-001	7.400-001	-1.987-001	3.678-001	.000	.000	.000
SNW	4	3.200+001	5.110-001	.000	9.420-001	-1.050+000	-6.800-001	.000	.000	.000	.000	.000
RO	4	9.543+000	.000	1.796-001	-2.109-001	1.214-001	-7.530-002	.000	.000	.000	.000	.000
SW	4	1.304+002	.000	3.676-001	-1.580-001	-8.400-001	3.056-001	.000	.000	.000	.000	.000
LWO	4	3.091-001	.000	2.090-002	-4.900-003	3.700-003	-1.420-002	.000	.000	.000	.000	.000
CWO	4	-4.098+000	.000	-6.600-003	-1.300-003	2.300-002	2.000-003	.000	.000	.000	.000	.000
WVO	4	-7.214+001	-5.185-001	.000	1.137+000	-2.810-001	5.200-002	.000	.000	.000	.000	.000

DISCRIMINANTS FOR CLIMATIC ZONE (8) UPPER LAT TRANSITION - COOL

LAND - MAYBE SNOW DELTA	:	.0000
LAND - MAYBE HEAVY RAIN MIN	:	2.5500+002
LAND - FROZEN GND (SNOW) DELTA	:	3.0000+000
LAND - HEAVY VEG DELTA	:	2.0000+000
LAND - HEAVY VEG MIN	:	2.5500+002
LAND - FROZEN GND (SOIL) DELTA	:	5.0000+000
LAND - FROZEN GND (SOIL) MAX	:	2.6000+002
LAND - DESERT DELTA	:	2.0000+001
LAND - DESERT MIN	:	2.6500+002
LAND - FLOODED SOIL DELTA	:	5.0000+000
LAND - GLACIAL MAX	:	2.0000+002
LAND - CLOUD COVER MIN	:	3.0000+001
LAND - MAYBE RAIN (GND) DELTA	:	.0000
LAND - MAYBE RAIN (VEG) DELTA	:	.0000
BAD DATA DELTA	:	-2.0000+000
OCEAN - MAYBE RAIN MIN	:	1.9000+002
OCEAN - MAYBE RAIN DELTA	:	2.5000+001
OCEAN - HEAVY RAIN DELTA	:	1.0000+001

Table 4.4-1a Parameter Extraction File for Climate Zones (1)-(11) (Con't)

CLIMATIC ZONE (9) UPPER LAT TRANSITION - COLD

PARAM	ALG	CONST	19V	19H	22V	37V	37H	85V	85H	C8 CONST	C9 COEF	C10 EXP
RL	2	.000	.000	.000	.000	.000	.000	.000	.000	.000	.000	.000
SM	2	.000	.000	.000	.000	.000	.000	.000	.000	.000	.000	.000
LWL	2	.000	.000	.000	.000	.000	.000	.000	.000	.000	.000	.000
CWL	4	9.329-001	-4.500-003	2.800-003	.000	3.510-002	.000	-3.330-002	.000	.000	.000	.000
STD	4	-3.640+001	.000	-4.590-001	-1.270-001	1.610+000	.000	.000	6.360-002	.000	.000	.000
STF	1	.000	1.070+000	.000	.000	.000	.000	.000	.000	.000	.000	.000
STG	1	.000	1.070+000	.000	.000	.000	.000	.000	.000	.000	.000	.000
STL	4	-3.640+001	.000	-4.590-001	-1.270-001	1.610+000	.000	.000	6.360-002	.000	.000	.000
TLC	4	-1.880+001	.000	-4.840-001	4.120-001	1.670+000	.000	-5.730-001	.000	.000	.000	.000
STV	1	.000	1.090+000	.000	.000	.000	.000	.000	.000	.000	.000	.000
CAL	0	-6.389+002	.000	.000	.000	.000	-1.705+000	-2.868-001	7.457-001	.000	.000	.000
CWS	4	-1.450+000	.000	.000	-1.390-002	.000	1.770-002	2.400-004	5.250-003	.000	.000	.000
STS	4	3.210+001	2.140+000	.000	1.910+000	-1.670+000	-1.890+000	.000	.000	.000	.000	.000
TSC	4	7.580+001	.000	4.780-001	1.690+000	-2.430+000	1.060+000	.000	.000	.000	.000	.000
CAS	0	-1.895+002	.000	.000	.000	-9.710-001	7.400-001	-1.987-001	3.678-001	.000	.000	.000
SNW	4	3.200+001	5.110-001	.000	9.420-001	-1.050+000	-6.800-001	.000	.000	.000	.000	.000
RO	4	2.410+001	.000	8.250-002	1.367-001	-3.411-001	8.430-002	.000	.000	.000	.000	.000
SW	4	1.176+002	.000	4.225-001	-1.899-001	-7.096-001	2.081-001	.000	.000	.000	.000	.000
LWO	4	-8.477-001	.000	4.800-003	1.770-002	-1.370-002	-1.400-003	.000	.000	.000	.000	.000
CWO	4	-3.629+000	.000	-4.700-003	-2.100-003	2.120-002	1.100-003	.000	.000	.000	.000	.000
WVO	4	-7.681+001	-6.020-001	.000	8.850-001	2.270-001	-1.890-001	.000	.000	.000	.000	.000

DISCRIMINANTS FOR CLIMATIC ZONE (9) UPPER LAT TRANSITION - COLD

LAND - MAYBE SNOW DELTA	:	.0000
LAND - MAYBE HEAVY RAIN MIN	:	2.5500+002
LAND - FROZEN GND (SNOW) DELTA	:	3.0000+000
LAND - HEAVY VEG DELTA	:	2.0000+000
LAND - HEAVY VEG MIN	:	2.5500+002
LAND - FROZEN GND (SOIL) DELTA	:	5.0000+000
LAND - FROZEN GND (SOIL) MAX	:	2.6000+002
LAND - DESERT DELTA	:	2.0000+001
LAND - DESERT MIN	:	2.6500+002
LAND - FLOODED SOIL DELTA	:	5.0000+000
LAND - GLACIAL MAX	:	2.0000+002
LAND - CLOUD COVER MIN	:	3.0000+001
LAND - MAYBE RAIN (GND) DELTA	:	.0000
LAND - MAYBE RAIN (VEG) DELTA	:	.0000
BAD DATA DELTA	:	-2.0000+000
OCEAN - MAYBE RAIN MIN	:	1.9000+002
OCEAN - MAYBE RAIN DELTA	:	2.5000+001
OCEAN - HEAVY RAIN DELTA	:	1.0000+001

Table 4.4-1a Parameter Extraction File for Climate Zones (1)-(11) (Con't)

CLIMATIC ZONE (10) POLAR - COOL

PARAM	ALG	CONST	19V	19H	22V	37V	37H	85V	85H	C8 CONST	C9 COEF	C10 EXP
RL	2	2.172+002	.000	.000	.000	-4.050-001	.000	-4.020-001	.000	.000	.000	.000
SM	2	6.359+001	-9.950-002	-1.370-001	.000	.000	.000	.000	.000	.000	.000	.000
LWL	2	1.711+001	.000	.000	.000	-2.130-002	.000	-4.170-002	.000	.000	.000	.000
CWL	4	1.658+000	-3.300-003	1.700-003	.000	2.940-002	.000	-3.140-002	.000	.000	.000	.000
STD	4	-3.640+001	.000	-4.590-001	-1.270-001	1.610+000	.000	.000	6.360-002	.000	.000	.000
STF	1	.000	1.070+000	.000	.000	.000	.000	.000	.000	.000	.000	.000
STG	1	.000	1.070+000	.000	.000	.000	.000	.000	.000	.000	.000	.000
STL	4	-3.640+001	.000	-4.590-001	-1.270-001	1.610+000	.000	.000	6.360-002	.000	.000	.000
TLC	4	-1.880+001	.000	-4.840-001	4.120-001	1.670+000	.000	-5.730-001	.000	.000	.000	.000
STV	1	.000	1.090+000	.000	.000	.000	.000	.000	.000	.000	.000	.000
CAL	0	-6.389+002	.000	.000	.000	.000	-1.705+000	-2.868-001	7.457-001	.000	.000	.000
CWS	4	-1.450+000	.000	.000	-1.390-002	.000	1.770-002	2.400-004	5.250-003	.000	.000	.000
STS	4	3.210+001	2.140+000	.000	1.910+000	-1.670+000	-1.890+000	.000	.000	.000	.000	.000
TSC	4	7.580+001	.000	4.780-001	1.690+000	-2.430+000	1.060+000	.000	.000	.000	.000	.000
CAS	0	-1.895+002	.000	.000	.000	-9.710-001	7.400-001	-1.987-001	3.678-001	.000	.000	.000
SNW	4	3.200+001	5.110-001	.000	9.420-001	-1.050+000	-6.800-001	.000	.000	.000	.000	.000
RO	4	9.543+000	.000	1.796-001	-2.109-001	1.214-001	-7.530-002	.000	.000	.000	.000	.000
SW	4	1.304+002	.000	3.676-001	-1.580-001	-8.400-001	3.056-001	.000	.000	.000	.000	.000
LWO	4	3.091-001	.000	2.090-002	-4.900-003	3.700-003	-1.420-002	.000	.000	.000	.000	.000
CWO	4	-4.098+000	.000	-6.600-003	-1.300-003	2.300-002	2.000-003	.000	.000	.000	.000	.000
WVO	4	-7.681+001	-6.020-001	.000	8.850-001	2.270-001	-1.890-001	.000	.000	.000	.000	.000

DISCRIMINANTS FOR CLIMATIC ZONE (10) POLAR - COOL

LAND - MAYBE SNOW DELTA	:	.0000
LAND - MAYBE HEAVY RAIN MIN	:	2.5500+002
LAND - FROZEN GND (SNOW) DELTA	:	3.0000+000
LAND - HEAVY VEG DELTA	:	2.0000+000
LAND - HEAVY VEG MIN	:	2.5500+002
LAND - FROZEN GND (SOIL) DELTA	:	5.0000+000
LAND - FROZEN GND (SOIL) MAX	:	2.6000+002
LAND - DESERT DELTA	:	2.0000+001
LAND - DESERT MIN	:	2.6500+002
LAND - FLOODED SOIL DELTA	:	5.0000+000
LAND - GLACIAL MAX	:	2.0000+002
LAND - CLOUD COVER MIN	:	3.0000+001
LAND - MAYBE RAIN (GND) DELTA	:	.0000
LAND - MAYBE RAIN (VEG) DELTA	:	.0000
BAD DATA DELTA	:	-2.0000+000
OCEAN - MAYBE RAIN MIN	:	1.9000+002
OCEAN - MAYBE RAIN DELTA	:	2.5000+001
OCEAN - HEAVY RAIN DELTA	:	1.0000+001

Table 4.4-1a Parameter Extraction File for Climate Zones (1)-(11) (Con't)

CLIMATIC ZONE (11) POLAR - COLD

PARAM	ALG	CONST	19V	19H	22V	37V	37H	85V	85H	C8 CONST	C9 COEF	C10 EXP
RL	2	.000	.000	.000	.000	.000	.000	.000	.000	.000	.000	.000
SM	2	.000	.000	.000	.000	.000	.000	.000	.000	.000	.000	.000
LWL	2	.000	.000	.000	.000	.000	.000	.000	.000	.000	.000	.000
CWL	4	6.579-001	-4.000-003	2.300-003	.000	2.860-002	.000	-2.650-002	.000	.000	.000	.000
STD	4	-3.640+001	.000	-4.590-001	-1.270-001	1.610+000	.000	.000	6.360-002	.000	.000	.000
STF	1	.000	1.070+000	.000	.000	.000	.000	.000	.000	.000	.000	.000
STG	1	.000	1.070+000	.000	.000	.000	.000	.000	.000	.000	.000	.000
STL	4	-3.640+001	.000	-4.590-001	-1.270-001	1.610+000	.000	.000	6.360-002	.000	.000	.000
TLC	4	-1.880+001	.000	-4.840-001	4.120-001	1.670+000	.000	-5.730-001	.000	.000	.000	.000
STV	1	.000	1.090+000	.000	.000	.000	.000	.000	.000	.000	.000	.000
CAL	0	-6.389+002	.000	.000	.000	.000	-1.705+000	-2.868-001	7.457-001	.000	.000	.000
CWS	4	-1.450+000	.000	.000	-1.390-002	.000	1.770-002	2.400-004	5.250-003	.000	.000	.000
STS	4	3.210+001	2.140+000	.000	1.910+000	-1.670+000	-1.890+000	.000	.000	.000	.000	.000
TSC	4	7.580+001	.000	4.780-001	1.690+000	-2.430+000	1.060+000	.000	.000	.000	.000	.000
CAS	0	-1.895+002	.000	.000	.000	-9.710-001	7.400-001	-1.987-001	3.678-001	.000	.000	.000
SNW	4	3.200+001	5.110-001	.000	9.420-001	-1.050+000	-6.800-001	.000	.000	.000	.000	.000
RO	4	2.410+001	.000	8.250-002	1.367-001	-3.411-001	8.430-002	.000	.000	.000	.000	.000
SW	4	1.176+002	.000	4.225-001	-1.899-001	-7.096-001	2.081-001	.000	.000	.000	.000	.000
LWO	4	-8.477-001	.000	4.800-003	1.770-002	-1.370-002	-1.400-003	.000	.000	.000	.000	.000
CWO	4	-3.629+000	.000	-4.700-003	-2.100-003	2.120-002	1.100-003	.000	.000	.000	.000	.000
WVO	4	-7.681+001	-6.020-001	.000	8.850-001	2.270-001	-1.890-001	.000	.000	.000	.000	.000

DISCRIMINANTS FOR CLIMATIC ZONE (11) POLAR - COLD

LAND - MAYBE SNOW DELTA	: .0000
LAND - MAYBE HEAVY RAIN MIN	: 2.5500+002
LAND - FROZEN GND (SNOW) DELTA	: 3.0000+000
LAND - HEAVY VEG DELTA	: 2.0000+000
LAND - HEAVY VEG MIN	: 2.5500+002
LAND - FROZEN GND (SOIL) DELTA	: 5.0000+000
LAND - FROZEN GND (SOIL) MAX	: 2.6000+002
LAND - DESERT DELTA	: 2.0000+001
LAND - DESERT MIN	: 2.6500+002
LAND - FLOODED SOIL DELTA	: 5.0000+000
LAND - GLACIAL MAX	: 2.0000+002
LAND - CLOUD COVER MIN	: 3.0000+001
LAND - MAYBE RAIN (GND) DELTA	: .0000
LAND - MAYBE RAIN (VEG) DELTA	: .0000
BAD DATA DELTA	: -2.0000+000
OCEAN - MAYBE RAIN MIN	: 1.9000+002
OCEAN - MAYBE RAIN DELTA	: 2.5000+001
OCEAN - HEAVY RAIN DELTA	: 1.0000+001

Table 4.4-1b Parameter Extraction File: Transmissivities for Climate Zones (12)-(17)

CLIMATIC ZONE (12) TROPICAL - WARM

CHANNEL/SURFACE TYPE	CONST	19V	19H	22V	37V	37H	85V	85H
19GHZ-LAND	-1.109+000	8.846-003	-7.580-003	2.487-003	-3.427-003	8.739-004	1.311-003	2.565-003
22GHZ-LAND	5.921-002	1.036-002	-6.866-003	-2.170-003	-5.149-003	-2.869-003	3.560-003	3.247-003
37GHZ-LAND	-2.538+000	6.392-003	-5.867-003	2.147-003	-2.078-002	1.014-002	9.089-003	8.681-003
85GHZ-LAND	1.199+000	4.471-003	-3.958-003	1.488-003	-2.007-002	-5.855-003	1.096-002	8.296-003
19GHZ-OCN	-4.226-001	5.302-004	-1.124-002	1.223-002	-1.967-002	1.441-002	1.704-002	-1.135-002
22GHZ-OCN	4.129-001	4.266-003	-9.388-003	1.291-003	-1.620-002	1.218-002	1.650-002	-1.009-002
37GHZ-OCN	6.202-001	-1.311-002	-8.473-004	9.841-003	-1.573-002	7.464-003	1.776-002	-7.780-003
85GHZ-OCN	7.945-001	-1.393-003	-1.851-003	4.649-003	-1.852-002	8.234-003	2.155-002	-1.594-002
19GHZ-ICE	.000	.000	.000	.000	.000	.000	.000	.000
22GHZ-ICE	.000	.000	.000	.000	.000	.000	.000	.000
37GHZ-ICE	.000	.000	.000	.000	.000	.000	.000	.000
85GHZ-ICE	.000	.000	.000	.000	.000	.000	.000	.000

CLIMATIC ZONE (13) TROPICAL - COOL

CHANNEL/SURFACE TYPE	CONST	19V	19H	22V	37V	37H	85V	85H
19GHZ-LAND	-9.842-001	9.053-003	-8.350-003	3.401-003	1.997-003	-3.327-003	-7.966-004	2.499-003
22GHZ-LAND	-1.282-001	1.195-002	-7.762-003	-2.683-003	-3.135-003	-2.623-003	2.185-003	2.771-003
37GHZ-LAND	-2.179+000	6.901-003	-7.097-003	4.084-003	-3.833-003	-5.815-003	7.214-003	6.812-003
85GHZ-LAND	1.223+000	8.058-003	-5.481-003	-1.016-003	-2.004-002	-5.304-003	1.124-002	7.453-003
19GHZ-OCN	-3.927-001	-4.484-004	-9.948-003	8.899-003	-1.735-002	1.375-002	1.914-002	-1.202-002
22GHZ-OCN	5.813-001	3.449-003	-8.440-003	-1.095-003	-1.530-002	1.191-002	1.728-002	-9.756-003
37GHZ-OCN	3.528-001	-1.119-002	-1.475-003	8.350-003	-1.641-002	8.222-003	2.081-002	-9.644-003
85GHZ-OCN	1.431+000	-3.327-005	-2.459-003	3.540-003	-2.137-002	9.061-003	1.895-002	-1.337-002
19GHZ-ICE	.000	.000	.000	.000	.000	.000	.000	.000
22GHZ-ICE	.000	.000	.000	.000	.000	.000	.000	.000
37GHZ-ICE	.000	.000	.000	.000	.000	.000	.000	.000
85GHZ-ICE	.000	.000	.000	.000	.000	.000	.000	.000

Table 4.4-1b Parameter Extraction File: Transmissivities for Climate Zones (12)-(17) (Con't)

CLIMATIC ZONE (14) MID-LAT - SPRING/FALL

CHANNEL/SURFACE TYPE	CONST	19V	19H	22V	37V	37H	85V	85H
19GHZ-LAND	5.522-001	7.958-003	-4.684-003	-1.558-003	-1.091-002	5.067-003	3.082-004	3.668-003
22GHZ-LAND	1.100+000	1.402-002	-5.180-003	-8.505-003	-9.669-003	1.351-003	1.868-003	3.309-003
37GHZ-LAND	-1.285-001	7.410-003	-4.777-003	-4.163-004	-1.808-002	3.023-003	6.272-003	8.014-003
85GHZ-LAND	3.310-001	1.260-002	-2.390-003	-1.140-002	-1.897-002	-1.191-002	1.861-002	1.193-002
19GHZ-OCN	2.014+000	-1.340-002	1.734-004	3.342-003	-5.970-003	5.121-003	7.905-003	-3.708-003
22GHZ-OCN	1.895+000	-8.205-003	2.189-004	-3.962-003	-6.747-003	5.665-003	1.108-002	-4.513-003
37GHZ-OCN	2.289+000	-1.860-002	4.883-003	3.259-003	-1.062-002	2.710-003	1.405-002	-4.259-003
85GHZ-OCN	2.712+000	-4.297-003	1.908-003	2.860-004	-1.968-002	5.596-003	1.433-002	-8.577-003
19GHZ-ICE	9.264-001	2.187-003	1.918-003	-3.855-003	5.329-005	-2.712-003	1.277-002	-1.054-002
22GHZ-ICE	1.130+000	5.324-003	1.447-003	-8.911-003	-2.301-003	1.139-003	2.030-002	-1.825-002
37GHZ-ICE	4.188-001	2.394-003	6.634-003	-4.988-003	3.145-003	-1.334-002	3.337-002	-2.628-002
85GHZ-ICE	2.889-001	4.290-003	3.699-003	-7.166-003	2.957-003	-8.955-003	6.793-002	-6.297-002

CLIMATIC ZONE (15) MID-LAT - SUMMER

CHANNEL/SURFACE TYPE	CONST	19V	19H	22V	37V	37H	85V	85H
19GHZ-LAND	-1.460+000	8.256-003	-5.225-003	-1.632-003	-3.414-003	3.880-003	4.793-003	3.399-004
22GHZ-LAND	-4.860-001	1.290-002	-5.387-003	-8.134-003	-2.433-003	-2.588-003	6.420-003	1.904-003
37GHZ-LAND	-2.059+000	6.353-003	-4.478-003	-5.060-004	-7.378-003	-1.715-003	1.096-002	5.255-003
85GHZ-LAND	1.020+000	7.638-003	-4.185-003	-2.348-003	-1.586-002	-1.346-002	1.360-002	1.035-002
19GHZ-OCN	1.194+000	-6.473-003	-6.517-003	6.154-003	-1.358-002	1.112-002	1.291-002	-7.577-003
22GHZ-OCN	9.633-001	3.909-004	-5.799-003	-3.007-003	-1.307-002	1.007-002	1.548-002	-7.334-003
37GHZ-OCN	1.401+000	-1.809-002	3.838-003	4.608-003	-8.265-003	2.814-003	1.640-002	-6.498-003
85GHZ-OCN	1.554+000	-7.969-004	-1.342-003	1.368-003	-1.913-002	7.508-003	1.859-002	-1.236-002
19GHZ-ICE	9.264-001	2.187-003	1.918-003	-3.855-003	5.329-005	-2.712-003	1.277-002	-1.054-002
22GHZ-ICE	1.130+000	5.324-003	1.447-003	-8.911-003	-2.301-003	1.139-003	2.030-002	-1.825-002
37GHZ-ICE	4.188-001	2.394-003	6.634-003	-4.988-003	3.145-003	-1.334-002	3.337-002	-2.628-002
85GHZ-ICE	2.889-001	4.290-003	3.699-003	-7.166-003	2.957-003	-8.955-003	6.793-002	-6.297-002

Table 4.4-1b Parameter Extraction File: Transmissivities for Climate Zones (12)-(17) (Con't)

CLIMATIC ZONE (16) MID-LAT - WINTER

CHANNEL/SURFACE TYPE	CONST	19V	19H	22V	37V	37H	85V	85H
19GHZ-LAND	1.072+000	2.540-003	-2.033-003	3.206-004	-1.832-003	-7.001-003	5.391-003	1.027-003
22GHZ-LAND	1.509+000	7.299-003	-2.279-003	-4.963-003	-2.655-003	-9.400-003	8.165-003	5.139-005
37GHZ-LAND	4.095-001	3.514-003	-2.460-003	2.212-005	-1.252-002	-7.250-003	1.145-002	6.974-003
85GHZ-LAND	7.195-001	1.085-002	-1.752-003	-9.709-003	-3.205-002	-2.666-003	1.844-002	1.381-002
19GHZ-OCN	2.411+000	-1.321-002	-8.232-004	3.826-003	-8.247-003	6.435-003	7.167-003	-3.447-003
22GHZ-OCN	2.458+000	-9.258-003	-4.598-004	-2.470-003	-8.474-003	6.587-003	9.214-003	-3.994-003
37GHZ-OCN	2.943+000	-1.941-002	5.158-003	2.791-003	-1.123-002	2.887-003	1.191-002	-3.289-003
85GHZ-OCN	3.217+000	-5.240-003	2.082-003	1.539-004	-2.009-002	5.989-003	1.317-002	-8.522-003
19GHZ-ICE	1.006+000	6.166-004	7.450-004	-1.154-003	-2.444-003	1.706-003	9.809-003	-9.615-003
22GHZ-ICE	1.211+000	4.041-003	-1.276-003	-5.190-003	-6.695-003	9.510-003	1.519-002	-1.690-002
37GHZ-ICE	6.846-001	-1.746-003	5.523-003	6.262-004	-1.904-003	-5.772-003	2.697-002	-2.349-002
85GHZ-ICE	6.418-001	-1.552-004	3.984-003	-1.318-003	-8.254-003	3.428-003	6.173-002	-6.042-002

CLIMATIC ZONE (17) POLAR - COOL

CHANNEL/SURFACE TYPE	CONST	19V	19H	22V	37V	37H	85V	85H
19GHZ-LAND	5.282-001	1.494-003	-1.942-003	2.274-003	2.575-003	-1.338-002	1.615-003	7.742-003
22GHZ-LAND	1.368+000	2.789-003	-2.330-003	1.255-003	1.139-003	-1.613-002	1.536-003	8.349-003
37GHZ-LAND	-5.260-001	2.830-003	-2.571-003	2.111-003	2.929-003	-2.320-002	8.322-003	1.280-002
85GHZ-LAND	4.051-001	7.132-003	-1.354-003	-6.150-003	-1.649-002	-1.478-002	1.559-002	1.453-002
19GHZ-OCN	2.056+000	-1.002-002	2.303-003	-5.660-005	-3.339-003	1.497-003	4.936-003	-1.325-003
22GHZ-OCN	1.927+000	-2.143-003	4.537-003	-1.012-002	-2.209-003	-1.238-003	6.169-003	-2.566-004
37GHZ-OCN	2.887+000	-1.765-002	5.818-003	1.196-003	-1.105-002	1.572-003	1.172-002	-2.431-003
85GHZ-OCN	4.407+000	-7.839-003	4.691-003	-4.330-005	-1.665-002	2.183-003	4.806-003	-4.008-003
19GHZ-ICE	9.264-001	2.187-003	1.918-003	-3.855-003	5.329-005	-2.712-003	1.277-002	-1.054-002
22GHZ-ICE	1.130+000	5.324-003	1.447-003	-8.911-003	-2.301-003	1.139-003	2.030-002	-1.825-002
37GHZ-ICE	4.188-001	2.394-003	6.634-003	-4.988-003	3.145-003	-1.334-002	3.337-002	-2.628-002
85GHZ-ICE	2.889-001	4.290-003	3.699-003	-7.166-003	2.957-003	-8.955-003	6.793-002	-6.297-002

Table 4.4-1c Parameter Extraction File: Sea Ice

CLIMATIC ZONE (18) POLAR - COLD

CHANNEL/SURFACE TYPE	CONST	19V	19H	22V	37V	37H	85V	85H
19GHZ-LAND	9.996-001	2.253-003	-2.009-004	-2.117-003	-3.143-003	-2.605-003	2.754-003	2.432-003
22GHZ-LAND	1.276+000	6.305-003	-2.462-004	-6.521-003	-6.325-003	-1.032-003	3.825-003	1.989-003
37GHZ-LAND	5.402-001	2.798-003	-6.599-004	-1.842-003	-7.586-003	-1.031-002	8.293-003	9.148-003
85GHZ-LAND	5.593-001	1.128-002	-1.507-003	-9.672-003	-1.933-002	-1.949-002	1.815-002	1.794-002
19GHZ-OCN	1.946+000	-1.294-002	1.792-003	2.363-004	-4.602-003	3.550-003	8.889-003	-3.128-003
22GHZ-OCN	2.310+000	-1.086-002	2.464-003	-5.102-003	-3.777-003	3.380-003	8.947-003	-3.119-003
37GHZ-OCN	3.120+000	-1.937-002	5.240-003	1.185-003	-1.173-002	3.096-003	1.305-002	-3.650-003
85GHZ-OCN	5.184+000	-1.381-002	6.377-003	-3.852-004	-1.515-002	1.733-003	4.317-003	-3.681-003
19GHZ-ICE	1.006+000	6.166-004	7.450-004	-1.154-003	-2.444-003	1.706-003	9.809-003	-9.615-003
22GHZ-ICE	1.211+000	4.041-003	-1.276-003	-5.190-003	-6.695-003	9.510-003	1.519-002	-1.690-002
37GHZ-ICE	6.846-001	-1.746-003	5.523-003	6.262-004	-1.904-003	-5.772-003	2.697-002	-2.349-002
85GHZ-ICE	6.418-001	-1.552-004	3.984-003	-1.318-003	-8.254-003	3.428-003	6.173-002	-6.042-002

CLIMATIC ZONE (19) POLAR - COOL

PARAM	ALG	CONST	19V	19H	22V	37V	37H	85V	85H	C8 CONST	C9 COEF	C10 EXP
IC	2	1.188+000	.000	.000	.000	-1.760-002	1.760-002	.000	.000	.000	.000	.000
IA	0	-2.191+002	.000	.000	.000	1.105+000	.000	.000	.000	1.936+002	.000	.000
CWI	4	3.415-001	-1.000-003	-4.800-003	.000	-6.670-002	7.440-002	.000	.000	.000	.000	.000

DISCRIMINANTS FOR CLIMATIC ZONE (19) POLAR - COOL

MULTI-YEAR LEVEL : 2.2800+002

CLIMATIC ZONE (20) POLAR - COLD

PARAM	ALG	CONST	19V	19H	22V	37V	37H	85V	85H	C8 CONST	C9 COEF	C10 EXP
IC	2	1.178+000	.000	.000	.000	-1.760-002	1.760-002	.000	.000	.000	.000	.000
IA	0	-2.177+002	.000	.000	.000	1.105+000	.000	.000	.000	1.923+002	.000	.000
CWI	4	-2.082-001	-3.000-004	-1.210-002	.000	-3.200-002	4.680-002	.000	.000	.000	.000	.000

DISCRIMINANTS FOR CLIMATIC ZONE (20) POLAR - COLD

MULTI-YEAR LEVEL : 2.1800+002

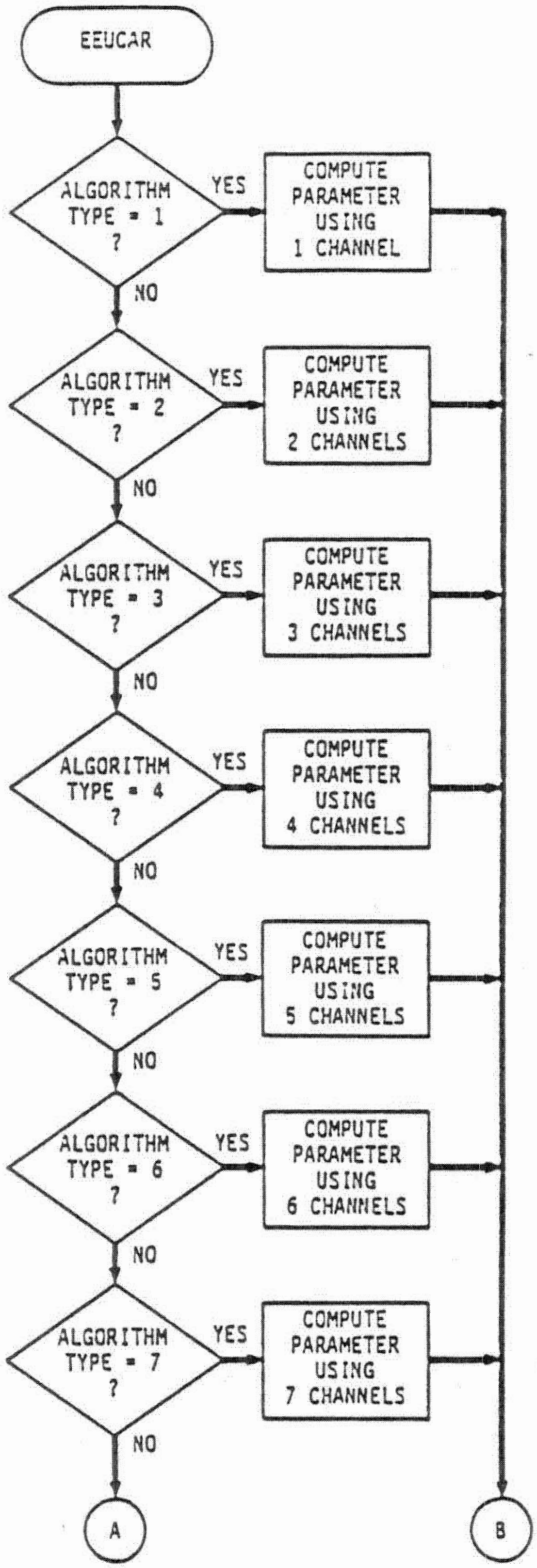

FIGURE 4.5-1 EEUCAR FLOW CHART

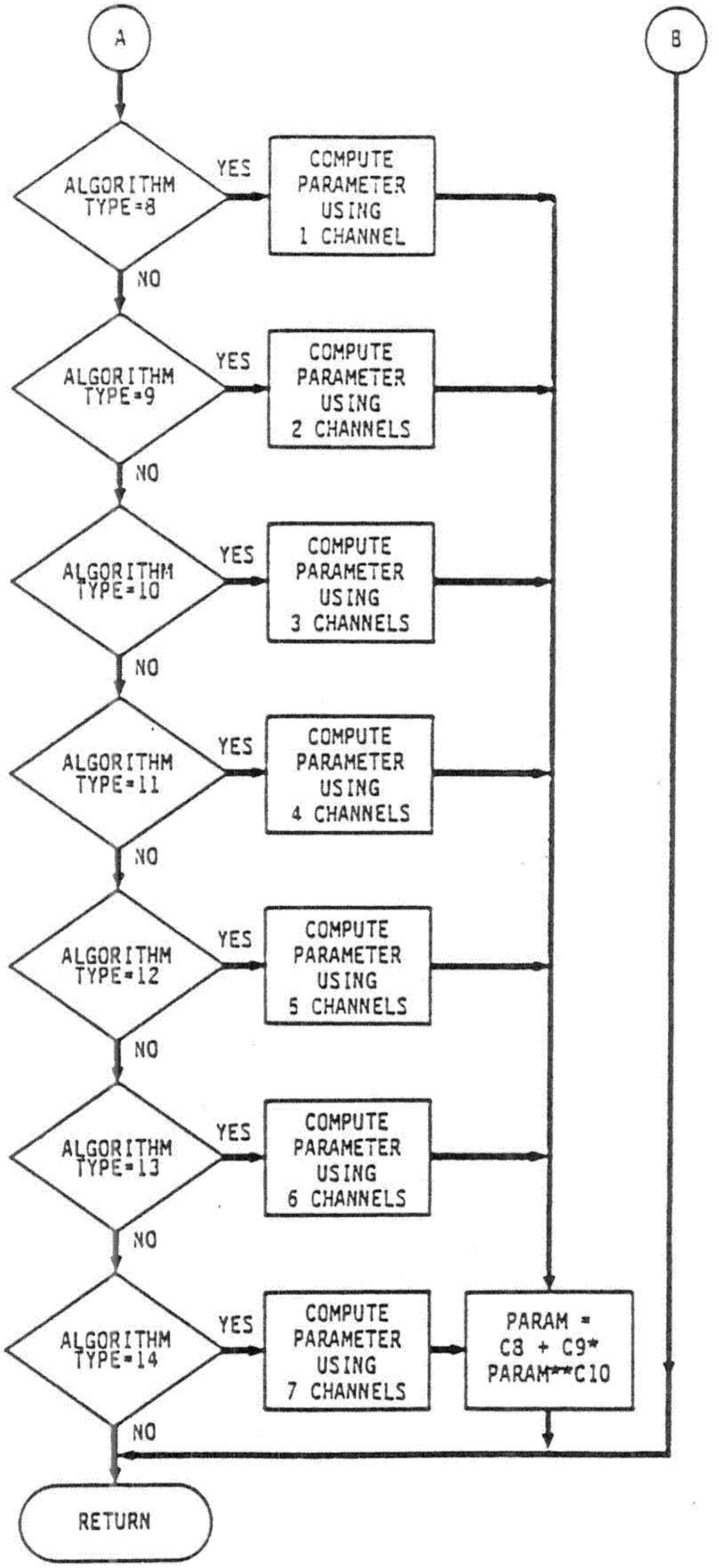

FIGURE 4.5-1 EEUCAR FLOW CHART (Con't)

5.0 SENSOR HEALTH STATISTICS

The SSM/I Sensor Health Module (SMISHM) CPC provides to the user statistical information for use in monitoring the stability of the SSM/I sensor. Three types of information are provided: calibration data, from the SSM/I Temperature Data Record (TDR) File; brightness temperatures (TBS) data, from the SSM/I Sensor Data Record (SDR) File and the Out-of-Limits File; and environmental data, from the Out-of-Limits File. SMISHM gathers the information from the files, calculates statistics, checks the statistics against fixed limits, and provides pertinent information to the user in two forms: a printed report format and a permanent Data Exchange Format (DEF) File. The DEF File made by SMISHM is called the Quality Data Record (QDR) File.

The QDR File contains QDRs for the last twenty SSM/I readouts processed. Each QDR is made up of four data blocks: the Calibration Data block, the TBS Header block, the TBS Data block, and the Environmental Data block. The Calibration Data block contains TDR header information, TDR calibration statistics, limits for these statistics and a calibration out-of-limits flag indicating how many calibration parameters have been determined to be out-of-limits. The TBS Header block contains SDR header data, quality data checks, and a TBS out-of-limits flag indicating how many TBS parameters have been determined to be out-of-limits. The TBS Data block contains SDR brightness temperature statistics and limits for these statistics. The Environmental Data block contains Out-of-Limits File header information and counts, maximum limits for the counts, and an environmental out-of-limits flag indicating the number of environmental counts determined to be out-of-limits. The QDR File format is shown in Figure 5-1.

The SMISHM component is normally run serially after SMISDP and SMIEPE execution. SMISHM calls for special operator attention in instances when certain statistics have been determined to be outside of specified limits causing the program to abort. Figure 5-2 shows the structure of the SMISHM CPC.

To perform the above functions, SMISHM first sets up the processing environment. This involves reading the user overrides and setting the print

PRODUCT IDENTIFICATION BLOCK (28 BYTES)
DATA SEQUENCE BLOCK (32 BYTES)
CALIBRATION DATA DESCRIPTION BLOCK (1318 BYTES)
TBS HEADER DATA DESCRIPTION BLOCK (94 BYTES)
TBS DATA DESCRIPTION BLOCK (478 BYTES)
ENVIRONMENTAL DATA DESCRIPTION BLOCK (622 BYTES)
CALIBRATION DATA BLOCK (232 BYTES)
TBS HEADER DATA BLOCK (32 BYTES)
TBS DATA BLOCK (786 BYTES)
ENVIRONMENTAL DATA BLOCK (208 BYTES)
(CALIBRATION, TBS HEADER, TBS AND ENVIRONMENTAL DATA BLOCKS REPEATED 19 TIMES)
END OF PRODUCT BLOCK (6 BYTES)

FIGURE 5-1 QDR FILE FORMAT

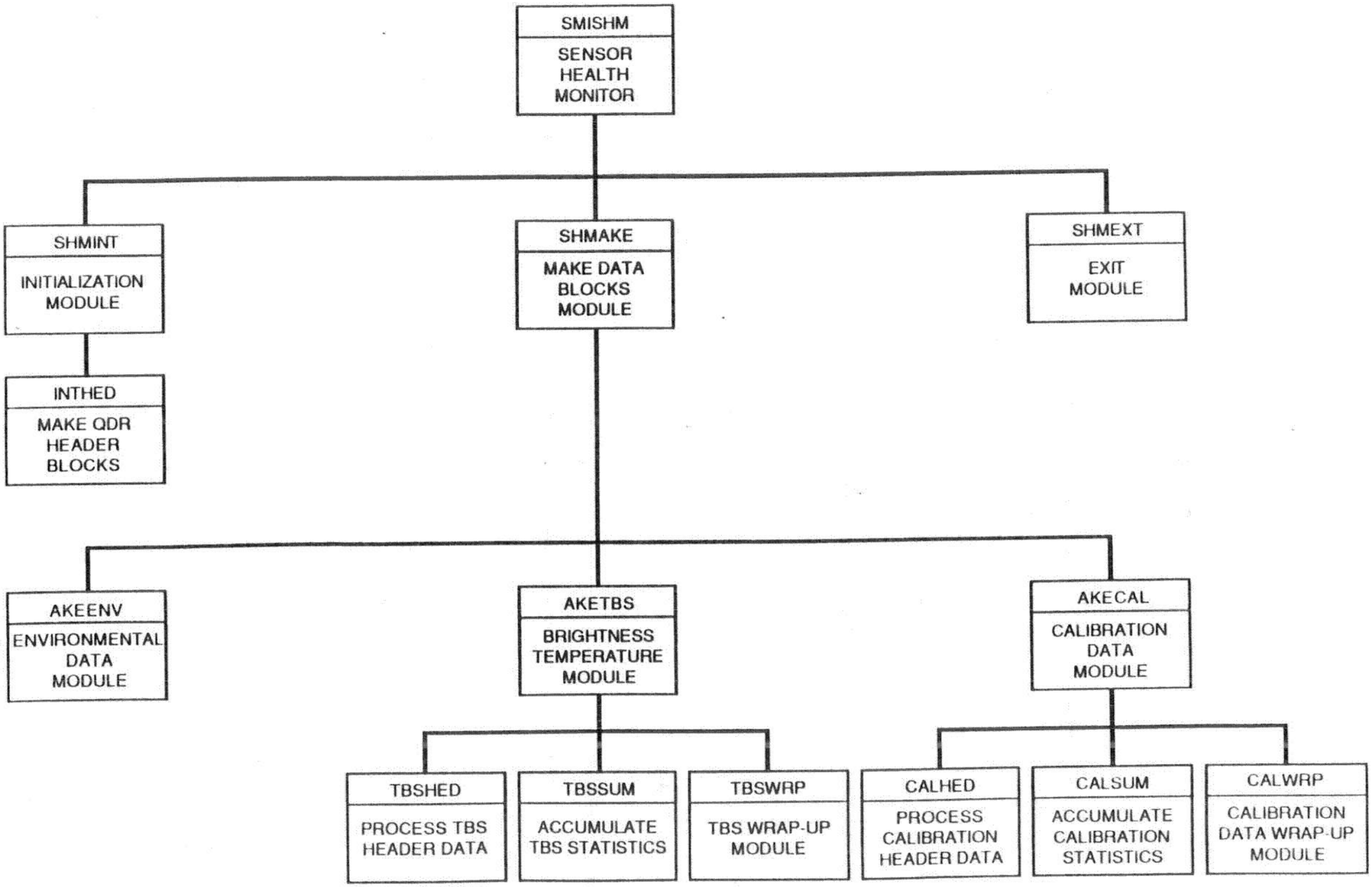

FIGURE 5-2 SMISHM STRUCTURE CHART

diagnostic flags if the user has indicated diagnostics are desired. The user may choose to print diagnostics by setting the option, OP5, in the NAMELIST and one or both of the following suboptions:

1. OP5CAL - to print calibration diagnostics.
2. OP5TBS - to print brightness temperature diagnostics.

To finish initialization of the processing environment, SHISHM sets up the QDR buffer. This is done by either: (1) reading the pre-existing QDR File into the buffer, and setting up the buffer so that the oldest QDR is deleted and a new QDR can be inserted; or by (2) requesting a new permanent file, making the QDR DEF header blocks and packing them into the QDR buffer.

Once the processing environment has been established, the primary functions of SMISHM begin. Each type of data is separately processed. First processed is the environmental data. The local Out-of-Limits File written by SMISDP and SMIEPE is read. The environmental data contained in the file are header information (i.e., spacecraft ID, rev header number, beginning scan start time, and ending scan start time) and counts for each of the 23 environmental parameters. The counts are the number of calculated values that have been determined by SMIEPE to be out-of-limits for a particular environmental parameter. The counts are checked against maximum count limits. If the count is determined to be greater than or equal to its limit, the environmental out-of-limits flag is incremented. (This flag is processed later in SMISHM wrapup functions.) To conclude environmental data processing, the Environmental Data block is made and an environmental processing summary is printed.

TBS data are then processed by SHISHM. The header information contained in the SDR File is read and two data quality checks from the Out-of-Limits File are read. These data are stored in the TBS Header block. No limit checks or statistics are made on these data; it is provided for information purposes only. The "All SDRs" flag contained in the header information is checked to determine whether the TBS data are to be processed. Only SDR Files with all SDRs processed are processed by SMISHM. Next, every all-channel scene station in the SDR File is checked to determine if it falls into one of the specified latitude and longitude areas defined in Table 5-1. If it does, the brightness temperature values for the scene station are accumulated. This allows the mean and variance brightness temperature for each of the SSM/I channels for each area to be determined later. Once each scene station is processed, the final statistics are calculated and checked against set limits. If the mean and/or variance for a parameter is determined to be outside of the set limits, the TBS out-of-limits flag is incremented. To conclude TBS data processing, the TBS Data block is made and a TBS processing summary is printed.

Table 5-1 Latitude-Longitude Areas Selected for Statistical Analyses

		LAT (O=S. POLE)	LONG (+EAST)	SURFACE TYPE
1.	Doldrums	89 - 91	0 - 360	Ocean
2.	Antarctic Ocean	30 - 32	0 - 360	Ocean
3.	Antarctic Glacier	0 - 15	0 - 360	Antarctica
4.	Arctic Ice Pack	165 - 180	90 - 230	Ice
5.	Congo Ran Forest	90 - 91	10 - 30	Veg. Land
6.	Amazon Rain Forest	90 - 91	280 - 310	Veg. Land
7.	Greenland	160 - 170	310 - 330	Veg. Land
8.	Sahara/Sudan Desert	113 - 114	345 - 30	Land
9.	Australian Desert	66 - 67	120 - 145	Land
10.	Arabian Desert	68 - 69	42 - 58	Land

Calibration data are then processed. SHISHM reads the TDR File and stores the header information for making the Calibration Data block. Then every tenth scan of the TDR File is read and processed. The calibration data are read, unpacked, and accumulated in order to calculate the following parameters:

(a) Mean and variance of spin period over entire readout.

(b) Mean and variance of hot load thermistor temperature for each scan read and the average of these statistics for the entire readout.

(c) For each channel: mean and variance of hot load counts for each scan read and the average of these statistics for the entire readout.

(d) For each channel: mean and variance of cold load counts for each scan read and the average of these statistics for the entire readout.

(e) Mean and variance of RF mixer temperature for the entire readout.

(f) Mean and variance of forward radiator temperature for the entire readout.

(g) For each channel: mean, maximum, and minimum values for slope and offset over the entire readout.

(h) For each AGC setting: counts of level changes.

Once all the data are accumulated and the statistics determined, specified parameters are checked against set limits. If the parameters are determined to be outside these limits, the calibration out-of-limits flag is incremented. Calibration data processing is concluded by making the Calibration Data block and printing a calibration processing summary.

Lastly, SMISHM begins the termination processing. The QDR buffer is written to the QDR File in record lengths of 332 Cyber words. The file is then cataloged/extended, closed, and returned. The three out-of-limits flags are then checked. If the flags are over specified limits, a special message is written indicating such and the program is aborted. This action alerts the operator to potential sensor problems. If the flags are within limits, SMISHM ends processing with a successful termination message.

Two types of errors can occur during SMISHM processing, fatal and non-fatal. Fatal errors are classified as errors which cause an abort or force the job to termination. When a fatal error occurs, a fatal error message is issued and the job is halted. A non-fatal error causes SMISHM to issue a warning message and continue processing of the next type of QDR data.

6.0 DATA FORMATTING

Under the direction of the Federal Coordinator for Meteorological Services and Supporting Research a number of groups have been tasked with the development and documentation of standards for the exchange of weather information and protocols of communication among agencies. The objective of DEF (Data Exchange Formats) is to promote efficient exchange of information among providers and efficient application by users. The initial report, "Standard Formats for Weather Data Exchange Among Automated Weather Information Systems" (FCM-52-1982), prepared by the Task Group on Communication Interfaces and Data Exchanges, establishes standards of data formats for a number of product types. Specific file formats for SSM/I DEF files are described in SSM/I Data Requirements Document (Hughes Aircraft Co., Ref. no. FS813, February 1986).

7.0 REFERENCES AND BIBLIOGRAPHY

1. Hollinger, J. and R. C. Lo, SSM/I Project Summary Report, NRL Memo Report 5055, NRL, Washington, D.C. April 1983.

2. Lo, R. C., A Comprehensive Description of the Mission Sensor Microwave Imager (SSM/I) Environmental Parameter Extraction Algorithm, NRL Memo Report 5199, NRL, Washington, D.C. Sept. 1983.

3. Stogryn, A., " Estimate of Brightness Temperature from Scanning Radiometer Data," IEEE AP, Vol. AP-26, No. 5, Sept 1978.

4. NIMBUS 5, 6, 7 User's Guide, Goddard Space Flight Center, NASA LANDSAT/NIMBUS PROJECT, 1972, 1975, 1978.

5. Njoku,E. G., "Antenna Pattern Correction Procedures for the Scanning Multichannel Microwave Radiometer (SMMR)," Boundary-Layer Met., Vol. 18, pp. 79-98, 1980.

6. Milman, A.S., "Antenna Pattern Correction for the NIMBUS-7 SMMR," IEEE Trans. Geoscience and Remote Sensing, Vol. GE-24, No. 2, Mar. 1986.

7. Njoku, E. G., J. M. Stacey, and F. T. Barath, "The SEASAT Scanning Multichannel Microwave Radiometer SMMR): Instrument Description and Performance," IEEE J. Oceanic Eng., Vol OE-5, pp. 100-115, 1980.

8. SSM/I Program Maintenance Manual (Rev. A), Vol. I - V, Hughes Aircraft Doc. H5256-0807-0101, Feb. 1986.

9. SSM/I Sensor Acceptance Test Report, S/N 002, TIS9, Hughes Aircraft Doc. H5256-0006-1299, July 1985.

A Comprehensive Description of the Mission Sensor Microwave Imager (SSM/I) Environmental Parameter Extraction Algorithm

I. Introduction

The Mission Sensor Microwave Imager (SSM/I) is a joint Navy/Air Force project. It is a passive microwave radiometric system developed by the Hughes Aircraft Company (HAC) under the direction of the Navy Space Systems Activity (NSSA) and the Air Force Space Division to be flown on the Defense Meteorological Satellite Program (DMSP) operational spacecraft as an all weather oceanographic and meteorological sensor.

The SSM/I is a seven channel, four frequency, linearly polarized, passive microwave radiometric system. The instrument measures atmospheric/ surface brightness temperatures at 19.3, 22.2, 37.0 and 85.5 GHz (1). These data will be processed by the environmental parameter extraction (EPE) algorithm in place at the Fleet Numerical Oceanography Center (FNOC) and the Air Force Global Weather Center (AFGWC) to obtain near real time precipitation maps, sea ice morphology, marine surface wind speed, columnar integrated liquid water and soil moisture percentage. These products will be distributed to Navy and Air Force DMSP operational sites to satisfy their unique mission requirements. They will also be made available to the general scientific and industrial communities through the METSAT data archival agreement between the National Oceanic and Atmospheric Administration (NOAA) and the Department of Defense (DOD).

The SSM/I data processing algorithm was developed at Environmental Research & Technology, Inc. (ERT) under a sub-contract from HAC. The algorithm is composed of two major modules (2). The first module, SMISDP, ingests and processes raw satellite data to produce earth-located brightness temperatures (T_B's). The T_B's are then processed through the second module, SMIEPE, which is the environmental parameter extraction algorithm, to produce estimates of ocean, land, and ice parameters. Large volumes of documentation of the SSM/I data processing algorithm software and data files exist (e.g., 3,4,5).

The environmental parameter extraction module retrieves the environmental parameters using the brightness temperatures as independent variables in linear regression equations. The regression coefficients, which reside in a data file as part of the software system, are determined using geophysical models, radiative transfer models, an inversion algorithm, and climatology, which are not part of the SSM/I software. The documentation of these important components is scanty and often outdated (2,6,7,8).

The purpose of this report is to present a comprehensive digest of the EPE algorithm and the related models for those interested in the SSM/I and its applications. The substance for this report has been taken from all the previously mentioned references and a software listing of the geophysical models provided by Dr. Kenneth Hardy (9), the former leader of ERT's SSM/I team. This report includes an overview of the EPE algorithm, the geophysical models involved, and the coefficients and important criteria used in the development of the retrievals of environmental parameters.

II. The Development of the SSM/I EPE Algorithm

II.A. The D Matrix Approach

The EPE algorithm, except for ice morphology, is based on the so-called D-matrix approach. It is a statistical method which chooses the most probable atmospheric and surface properties that produce the set of measured brightness temperatures (T_B's). The formalism for the statistical approach starts with the assumption that there exists some linear combination of T_B's which will provide information about the geophysical parameters in question.

That is to say:

$$P_i^* = \sum_{j=1}^{n} D'_{ij} T_j, \qquad \text{where } i = 1, \text{---}, m \quad .$$

or in vector form

$$\underline{P}^* = D' \, \underline{T}, \qquad \text{(II.1)}$$

where P_i^* is the estimate of the i-th parameter P_i, T_j is the T_B of the j-th radiometric channel and D'_{ij} is the (i,j)-th element of the D matrix.

The $\underline{\underline{D}}$ matrix used in the SSM/I EPE algorithm is "tuned" to the average value of each parameter. This is accomplished by transforming the vector $\underline{T}$ into

$$\underline{\phi}\,(\underline{T}) = (1, T_1 - \bar{T}_1, \text{----}, T_n - \bar{T}_n). \qquad \text{(II.2)}$$

The effect of this transformation is to add a column to the D matrix which contains the ensemble averages of the parameters.

$$\underline{P}^* = \underline{\underline{D}}\, \underline{\phi}\,(\underline{T}), \qquad \text{(II.3)}$$

where $\underline{\underline{D}}$ is the new D matrix with dimensions (m, n+1).

The elements of the D matrix are defined by miminizing the mean square error between the predicted and the actual values of the parameter P_i. It can be shown that

$$\underline{\underline{D}} = \underline{\underline{C}}\,(\underline{P}, \underline{\phi})\cdot\underline{\underline{C}}^{-1}\,(\underline{\phi}, \underline{\phi}), \qquad \text{(II.4)}$$

where $\underline{\underline{C}}\,(\underline{P}, \underline{\phi})$ is the correlation matrix between $\underline{P}$ and $\underline{\phi}$ and $\underline{\underline{C}}^{-1}\,(\underline{\phi}, \underline{\phi})$ is the inverse of the auto-correlation matrix of $\underline{\phi}$.

The development of the D matrix is demonstrated in Figure II.1. Radiosonde records and climatology are compiled to define the geophysical system including the atmosphere and the earth surface for radiative transfer calculations. A list of the desired environmental parameters is given in Table II.1. The atmosphere and surface data are used to simulate T_B's and thus $\underline{\phi}(\underline{T})$ through a geophysical-radiative model. Half of the $\underline{P}$ and $\underline{\phi}$ arrays are used to calculate correlation matrices and the D matrix (See equation II.4). The other half of the $\underline{\phi}$ array is used to test the validity of the D matrix by comparing the ground truth $\underline{P}$ to the estimated values, $\underline{P}^*$ which are calculated through equation II.3. The D matrices installed at FNOC and AFGWC have been tested through this procedure.

II.B. Separate Schemes for Each Climate Zone

The assumption of linearity between $\underline{P}$ and $\underline{T}$ is not satisfied over the entire earth. Instead of adding higher order terms in the regression equations, a number of climate zones have been selected for the SSM/I EPE algorithm. For each of these zones, linearity is assumed. The climate zones are defined in Table II.2. A D matrix is developed for each of the climate zones. The D matrices of the transition zones, are averages of those of neighboring zones.

Due to the limitation of computing facilities at AFGWC, the maximum number of channels used for the retrieval of each parameter is limited to four. The channel selections for all the parameters are shown in Table II.1. For example, the regression equation for the sea surface wind speed is

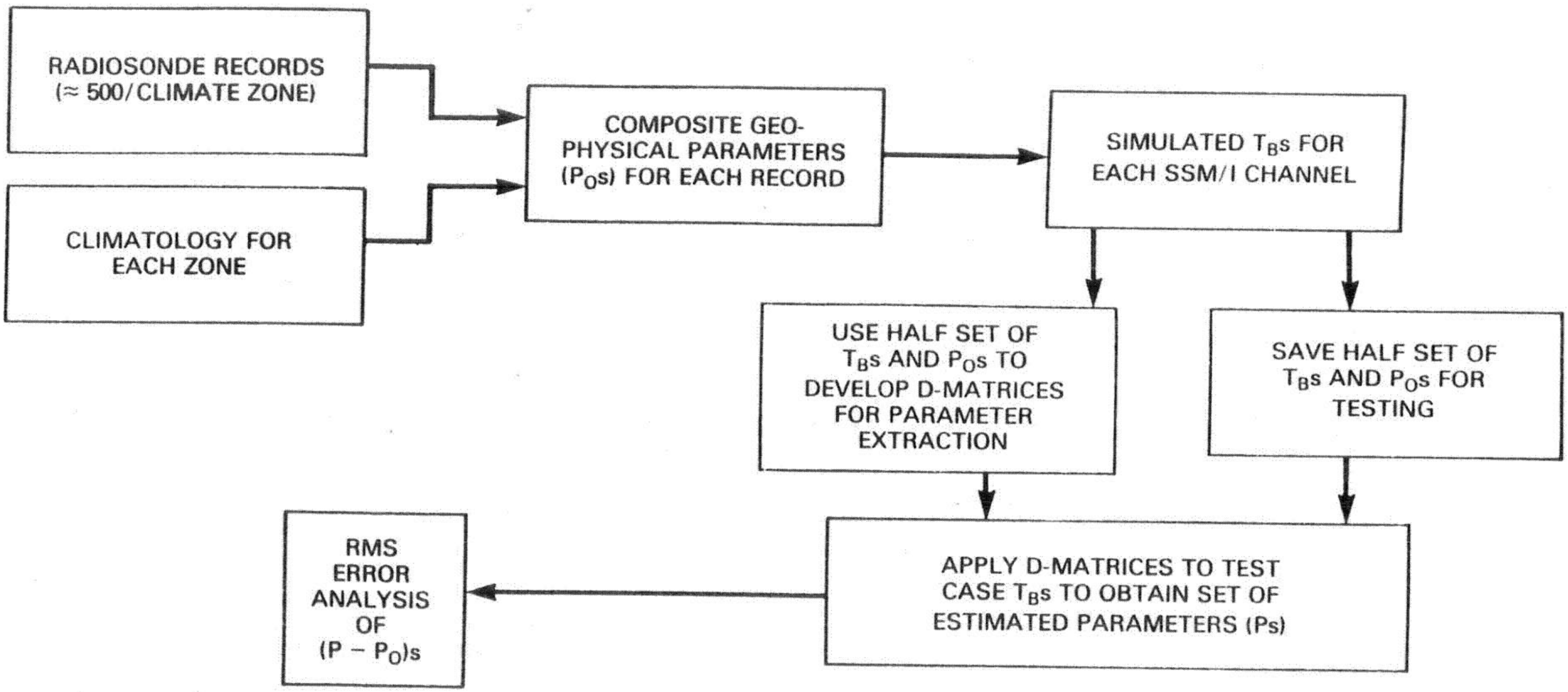

Figure II.1 SSM/I algorithm development

Table II.1 Data Channel utilization table for SSM/I

PARAMETERS		FREQUENCIES (GHz)	19 V	19 H	22 V	37 V	37 H	85 V	85 H
SW	SURFACE WIND SPEED, OCEAN			X	X	X	X		
RO	PRECIPITATION OVER OCEAN			X	X	X	X		
CWO	CLOUD WATER	OCEAN		X	X	X	X		
CWL		LAND	X	X		X		X	
LWO	LIQUID WATER	OCEAN		X	X	X	X		
LWL		LAND				X	X	X	X
SM	SOIL MOISTURE, LAND		X	X					
RL	PRECIPITATION OVER LAND					X	X	X	X
IC	SEA ICE CONDITIONS	CONCENTRATION				X	X		
IA		AGE				X			
IE		EDGE LOCATION							

TABLE II.2 Designation of SSM/I Climate Zones

		Jan	Feb	Mar	Apr	May	June	July	Aug	Sept	Oct	Nov	Dec
Trop	Land	3	3	3	3	1	1	1	1	1	1	3	3
	Ocean	4	4	4	4	2	2	2	2	2	2	2	2
Mid Lat	Land	9	9	5	5	5	7	7	7	5	5	5	9
	Ocean	10	10	6	6	6	8	8	8	6	6	6	10
Arctic	Land	13	13	13	13	11	11	11	11	11	11	13	13
	Ocean	14	14	14	14	12	12	12	12	12	12	14	14

1: tropical warm/land
2: tropical warm/ocean
3: tropical cool/land
4: tropical cool/ocean
5: mid lat spring-fall/land
6: mid lat spring-fall/ocean
7: mid lat summer/land
8: mid lat summer/ocean
9: mid lat winter/land
10: mid lat winter/ocean
11: arctic cool/land
12: arctic cool/ocean
13: arctic cold/land
14: arctic cold/ocean
15: transition zones

A. Lower Latitude transition zones (LLTS) are between tropics and mid lat.

a. LLTS warm/land
b. LLTS warm/ocean
c. LLTS cool/land
d. LLTS cool/ocean

B. Upper Latutide transition zones (ULTS) are between mid lat. and arctic

a. ULTS cool/land
b. ULTS cool/ocean
c. ULTS cold/land
d. ULTS cold/ocean

$$SW = d_o + d_1\, T_B(19H) + d_2\, T_B(22V) + d_3\, T_B(37V) + d_4\, T_B(37H),$$

where d_o, ····, d_4 are D matrix coefficients. The value of the coefficients for each environmental parameter for all climate zones will be described in Section IV.

II.C. Piecewise Scheme

Even though all the environmental parameters for each climate zone can be simultaneously extracted, the results may not be meaningful. For example, if there is heavy rain over land, the brightness temperatures will not be sensitive to the cloud water and soil moisture conditions. Similarly, when there is heavy rain over ocean, cloud water and sea surface wind retrievals would not be reliable. The SSM/I EPE algorithm employs the so-called piecewise scheme, to determine which parameters to retrieve based on the values of certain T_B observations. The piecewise schemes for ocean and land are depicted in Figures II.2 and II.3. The choice of parameters to retrieve is mainly based on rainfall. The criteria for determining whether there is no rain, light rain, or heavy rain are different for each climate zone. They are listed in Section IV.

The retrieval of ice parameters, including concentration and age, is accomplished through a deterministic approach. The ice algorithm is developed directly from physical relationships rather then through regression. The description of the physics of ice morphology and retrieval will be presented in Sections III and VI.

III. The Geophysical-Radiative Model

The radiative transfer theory is used to simulate the brightness temperature obtained by a remote sensing platform, such as a satellite, observing the earth-atmosphere system. A geophysical model which specifies the physical and electromagnetic properties of the atmospheric and the

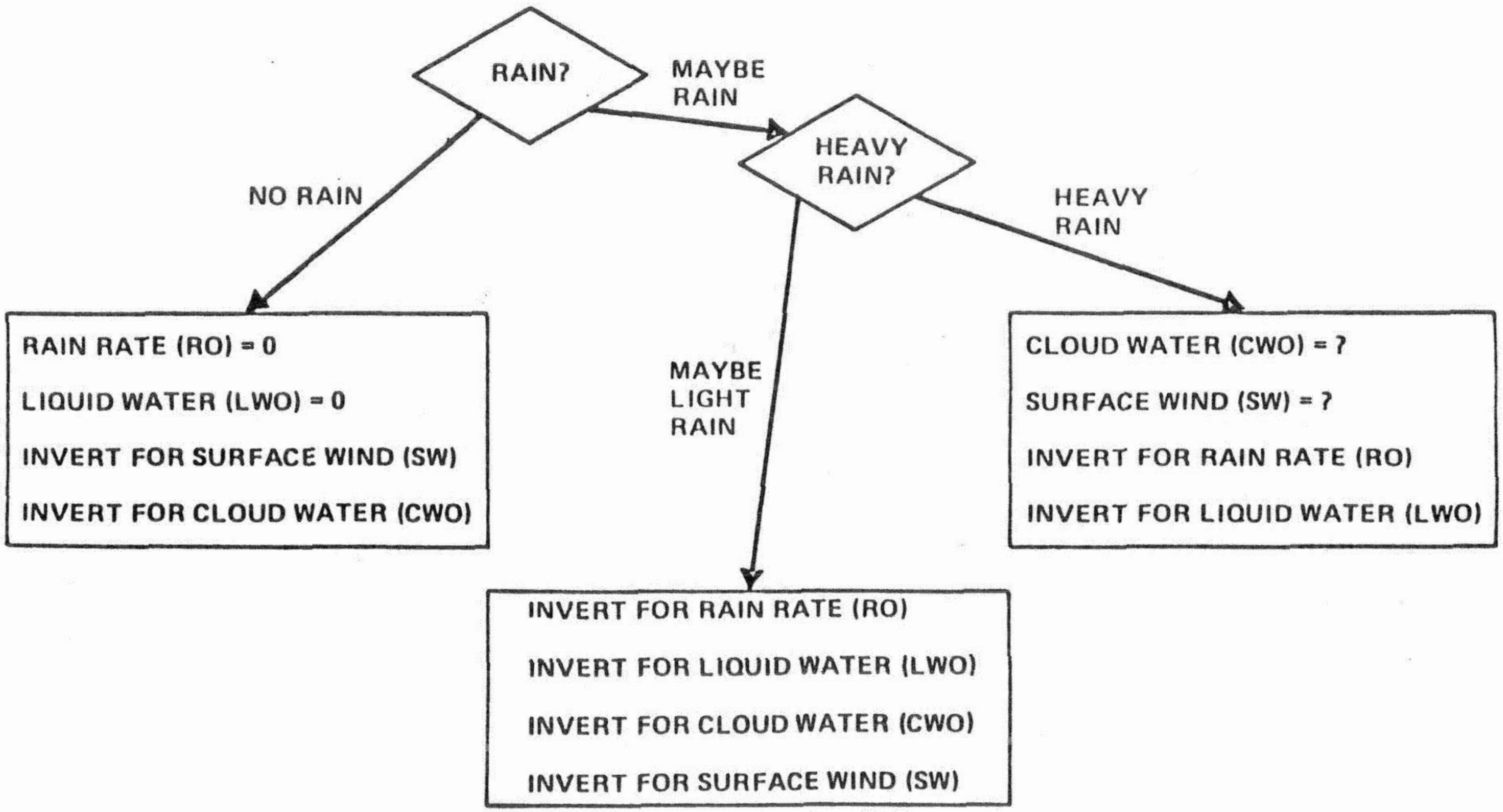

Figure II.2 Summary of piecewise algorithm over ocean

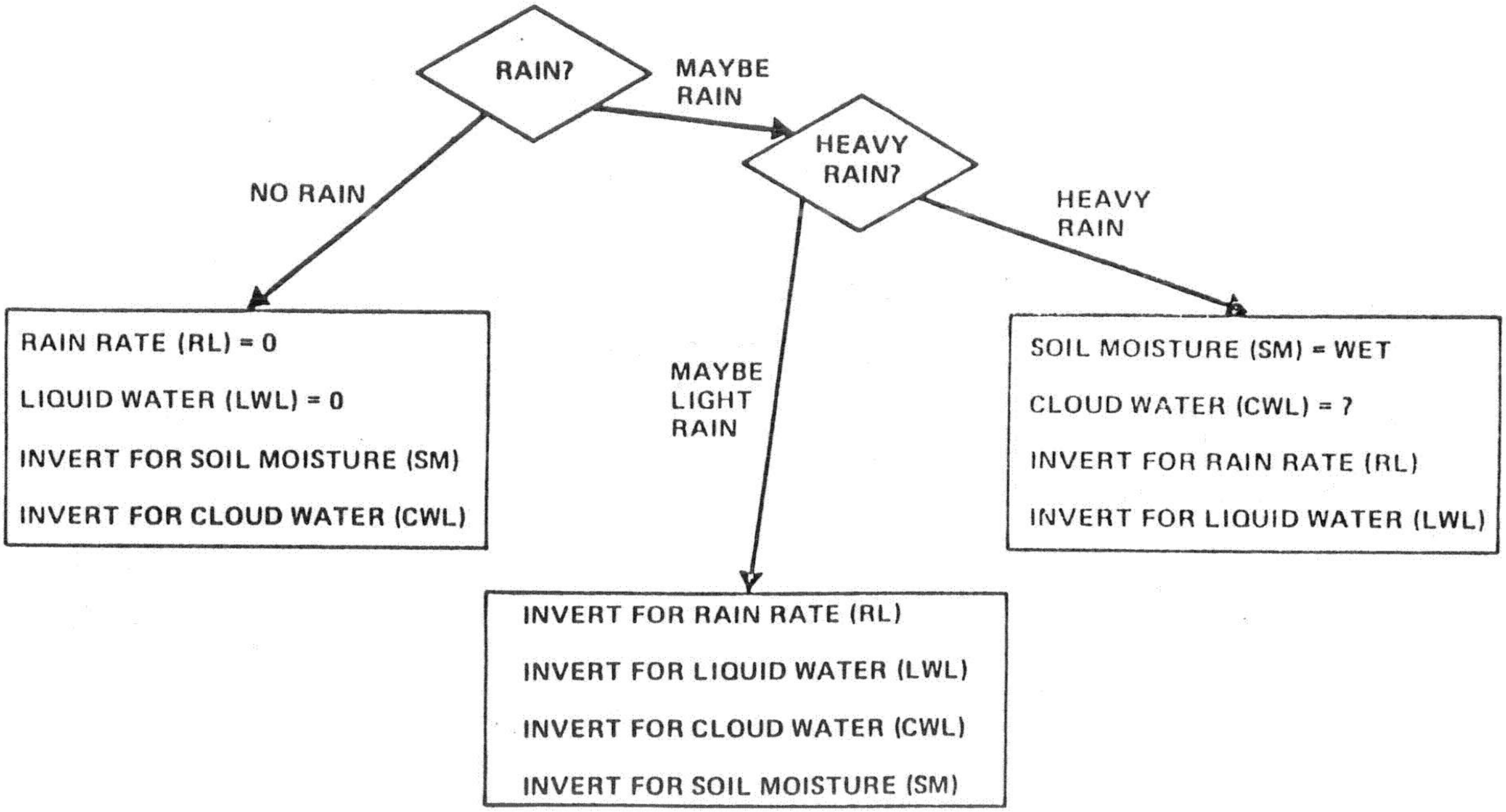

Figure II.3 Summary of piecewise algorithm over land earth's surface provides the necessary input parameters to the radiative transfer theory.

III.A The Radiative Transfer Model

For microwave radiation, the important atmosperhic parameters are water vapor, oxygen and liquid water, both in the form of cloud water and rain. The form of the liquid water governs the method of calculation for the extinction coefficient and the solution to the radiative transfer equation. When liquid water exists in small droplets such as found in clouds, the attenuation is predominantly by absorption and calculations are relatively straight forward. But in the case of rain, water drops are so large that scattering effects must be considered. The Mie theory is employed to calculate the extinction coefficient including both absorption and scattering effects. An interative algorithm is needed to solve the radiative transfer equation.

The radiative transfer equation, with the Rayleigh-Jeans long wavelength approximation, for the intensity of thermal radiation from a blackbody can be written as

$$\frac{dT_B(Z,\theta)}{d\tau} = T_B(Z,\theta) - T(Z), \qquad \text{(III.1)}$$

where T_B is the brightness temperature, a function of height, Z, and of look angle θ. T is physical temperature and τ is the opacity. In the absence of scattering, the T_B sensed by a satellite can be expressed as (9)

$$T_B(Z,\theta) = T_{B_1}(Z,\theta) + [(1-R)T_G + R\,T_{B_2}]\,e^{-\tau}, \qquad \text{(III.2)}$$

where Z is the height of the satellite, R is the effective surface reflectivity, τ is the total opacity of the atmosphere along the line of sight (nepers) and T_G is the surface temperature (K). The quantities T_{B_1} and T_{B_2} are proportional to the upward emission from the atmosphere and the downward emission from the atmosphere plus attenuated sky background radiation and are given by

$$T_{B_1} = \int_0^Z T(z)\, \gamma(z)\, e^{\left(-\int_z^Z \gamma(z')\sec\theta\, dz'\right)} \sec\theta\, dz, \qquad \text{(III.3)}$$

$$T_{B_2} = T_{sky}\, e^{-\tau} + \int_0^Z T(z)\, \gamma(z)\, e^{\left(-\int_0^z \gamma(z')\sec\theta\, dz'\right)} \sec\theta\, dz, \qquad \text{(III.4)}$$

where $\tau = \int_0^Z \gamma(z) \sec\theta\, dz$ and $\gamma(z)$ is the total opacity at height z, representing the sum of contributions from water vapor, oxygen, and cloud water droplets.

Equations III.2 thru III.4 are valid for all non-precipitating atmospheres. When precipitation is present multiple scattering effects are coupled with absorption. The Mie theory is based on the diffraction of a plane monochromatic wave by a sphere with a homogeneous, complex index of refraction. By examining the dissipation in the sphere and the scattered wave produced, it provides the information necessary for the calculation of the extinction coefficient and single scattering albedo.

The Mie efficiency factors for scattering, absorption and extinction are defined as the ratio of the actual to the geometric cross-sections.

$$Q_J = \chi_J/\pi r^2 \qquad J = S \text{ (scattering)}$$
$$\qquad A \text{ (absorption)} \qquad \text{(III.5)}$$
$$\qquad E \text{ (extinction)},$$

where χ is the actual cross-section and r is the raindrop radius. By definition $Q_E = Q_A + Q_S$. The single scattering albedo is

$$\omega_o = Q_S/Q_A \qquad \text{(III.6)}$$

The extinction coefficient is determined by integrating the efficiency factor over the drop size distribution encountered in the rain.

$$\gamma_E = \quad N(r)\, Q_E\, (\tilde{n}\, (\lambda,T),\ \lambda,r)\ r^2 dr \qquad \text{(III.7)}$$

where N(r) is the number of drops of radius r in a unit volume, λ is wavelength, $\tilde{n}$ is index of retraction and T is temperature. The radiative transfer equation for the scattering medium can be written as

$$\mu \frac{dT_B(\tau',\mu)}{d\tau'} = T_B\, (\tau',\mu) - T_S(\tau',\mu) \qquad \text{(III.8)}$$

where μ is the cosine of vertical zenith angle, $\tau' = \tau/\mu$ and T_S is the source function

$$T_S = [1 - \omega_o(\tau')]\ T(\tau',\mu) - \frac{\omega o(\tau')}{z} \int_{-1}^{1} p(\mu,\mu')\ T_B\ (\tau',\mu')\ d\mu' \qquad \text{(III.9)}$$

where P is the phase function. The integral equation for T_S with the boundaries included can be written as

$$T_S(\tau) = [1-\omega_o(\tau)]\,(T - T_{sky}\, e^{-\tau}) + \frac{\omega_o(\zeta)}{2}\int_o^{\tau^*} T_S(\tau)\, E_1\,(|\tau^* - \tau|)d\tau$$

$$+ \frac{\omega_o(\tau)}{2} E_2(\tau^* - \tau) \left[(1-R)\, T_G + R\int_o^{\tau^*} T_S(\tau)\, e^{\left[\frac{-(\tau^* - \tau)}{\mu}\right]} \frac{d\tau}{\mu}\right] \quad \text{(III.10)}$$

where τ^* is the total optical depth of the atmosphere and E_n is

$$E_n(x) = \int_o^1 e^{(-x/\mu)}\, \mu^{n-2}\, d\mu \quad \text{(III.11)}$$

For the solution of the source function T_S defined in equation (III.10) and thus the brightness temperature, a variational-iterative approach is used (10,11).

III.B The Atmosphere Model

The physical electromagnetic properties of water vapor, oxygen, and liquid water as defined in the ERT model are described in this sub-section.

III.B.1 Water Vapor

The extinction coefficient due to water vapor was described by Gaut (12). Laboratory measurements and theoretically generated data were used to examine and modify the expression formulated by Van Vleck and Weisskopf (13). For all but the highest frequency, i.e., 85.5 GHz, of the SSM/I instrument, only the absorption line at centered 22.235 GHz is considered. The extinction due to water vapor can be seen as composed of two distinct portions. They are the so-called resonance and non-resonance components, the former being the contribution from a nearby water vapor absorption line while the latter is due to the slowly varying absorption wings of more distant lines.

$$\gamma_w(z) = \gamma_{w,RES}(z) + \gamma_{w,NON}(z)$$

$$= \left\{ k_1 \rho_w(z)\, \nu^2\, T(z)^{-2.5}\, e^{[-644/T(z)]} \left[\frac{\Delta\nu}{(\nu-\nu_o)^2 + \Delta\nu^2} + \frac{\Delta\nu}{(\nu+\nu_o)^2 + \Delta\nu^2} \right] \right.$$

$$\left. + 5 \cdot k_2\, \rho_\omega(z) \nu^2\, T(z)^{-1.5} \Delta\nu \right\} \times 100 \qquad \text{(III.12)}$$

where $\gamma_\omega(z)$ is the absorption due to water vapor at height z (nepers/m), ν is frequency (GHz), ν_o is the reference frequency (22.235 GHz) and k_1, k_2 are constants.

$$k_1 = 3.5175 \times 10^{-3}; \qquad k_2 = 5.0920 \times 10^{-9}.$$

The half-width of the absorption line, $\Delta\nu$, is defined as

$$\Delta\nu = 2.62\, (P(z)/P_o)\, (T(z)/T_o)^{-0.625}\, [1 + 0.15\, \rho_w(z)\, T(z)/P(z)] \qquad \text{(III.13)}$$

where P(z) is pressure at height z (mb), P_o is 1013.25(mb), and T_o is 318.0 (K).

For 85.5 GHz, eight water vapor rotational spectral lines are included in the calculation of the absorption coefficient. The reference frequencies of these lines and other significant parameters are listed below.

i	ν_o	Stn(i)	$C_1(i)$	$C_2(i)$	$t_{exp}(i)$	$t_1(i)$	$t_2(i)$	Sp(i)
1	22.235	.0549	2.7057	.01976	.626	446.39	447.17	3
2	183.310	.1015	2.8800	.01906	.649	136.15	142.30	1
3	323.159	.0870	2.2956	.01952	.420	1283.02	1293.80	3
4	323.758	.0891	2.7876	.02050	.619	315.70	326.50	1
5	377.418	.1224	2.8440	.02102	.630	212.12	224.71	3
6	389.709	.0680	2.1060	.02035	.330	1525.31	1538.31	1
7	435.874	.0820	1.5000	.01976	.290	1045.14	1059.68	1
8	437.673	.0987	1.7700	.02253	.360	742.18	756.18	3

The resonance portion of the absorption coefficient, $\gamma_w(z)$, is given by

$$\gamma_{w,Res}(z) = \sum_{i=1}^{8} 45.5 \ \rho_w(z) \ Sp(i) \ Stn(i) \left[\frac{\nu^2}{T(z)^{1.5}}\right]$$

$$[\nu^2 - \nu_o^2(i)] \left[\frac{4\nu \cdot \Delta\nu}{(\nu^2 - \nu_o^2)^2 + 4\nu^2 \Delta\nu^2}\right] t_m(i) \quad , \qquad \text{(III.14)}$$

where Sp(i) is the spin mode and Stn(i) is the line strength.

$$\Delta\nu = C_1(i)\left(\frac{P(z)}{P_o}\right)\left(\frac{T_o}{T(z)}\right)^{t_{exp}(i)} \quad [1 + C_2(i) \ \rho_w(z) \ T(z)/P(z)] \ , \qquad \text{(III.15)}$$

where t_{exp} is the exponent for the temperature term and

$$tm = \exp\left[-1.43897 \ \frac{t_1(i)}{T(z)}\right] - \exp\left[-1.43879 \frac{t_2(i)}{T(z)}\right]$$

$$\text{if} \quad -1.43879 \ \frac{[t_1(i) - t_2(i)]}{T(z)} \geq 0.1, \qquad \text{(III.16a)}$$

$$tm(i) = \nu_o(i) \ \frac{0.04796}{T(z)} \ \exp\left[-1.43879\left(\frac{t_1(i)}{T(z)}\right)\right]$$

$$\text{if} \quad -1.43879 \ \frac{[t_1(i) - t_2(i)]}{T(z)} \leq 0.1. \qquad \text{(III.16b)}$$

The non-resonance term is defined as

$$\gamma_{w,Non}(z) = 1.2375 \times 10^{-9} \ \rho_w(z)\left(\frac{P(z)}{P_o}\right)\left(\frac{T_o}{T}\right)^{1.5 + \frac{\sum_{i=1}^{8} t_{exp}(i)}{8}} \cdot \nu^2, \qquad \text{(III.17)}$$

and the total absorption due to water vapor is then

$$\gamma_w(z) = \gamma_{w,Res}(z) + \gamma_{w,Non}(z). \qquad \text{(III.18)}$$

III.B.2 Oxygen

The Van Vleck and Weisskopf (13) formulation for the absorption line shape is adopted for the calculation of absorption due to oxygen.

$$\gamma_o(z) = C_1 \; P(z) \; (760/1013.25) \; T(z)^{-3} \cdot \nu^2$$

$$i = \sum_{1,45,2} \left\{ f_i^+[i(2i+3)/(i+1)] + f_i^-[(i+1)(2i-1)/i] + 2f_o[(i^2+i+1)(2i+1)/(i(i+1))] \right\} \cdot$$

$$e^{-2.06844\; i(i+1)/T(z)} \; , \qquad \text{(III.19)}$$

where $f_i^+ = \Delta\nu \left\{ 1/[(O^+(i) - \nu)^2 + \Delta\nu^2] + 1./[(O^+(i) + \nu)^2 + \Delta\nu^2] \right\}$

and

$$f_i^- = \Delta\nu \quad 1/[(O^-(i) - \nu)^2 + \Delta\nu^2] + 1./[O^-(i) + \nu)^2 + \Delta\nu^2] \; , \qquad \text{(III.20)}$$

$$\Delta\nu = \alpha \cdot P(z)(0.21 + 0.78 \; \xi)\left(\frac{300}{T(z)}\right)^{0.85} \; , \qquad \text{(III.21)}$$

where $= 0.25$ if $P(z) \geq 365.51$ mb

$= 0.75 \quad P(z) < 25.5$ mb

$= 0.25 + 0.5 \; \ln\left(\frac{365.51}{P(z)}\right) \Big/ \ln\left(\frac{365.51}{25.5}\right)$, if $25.5 \leq P(z) < 365.51$;

$f_o = \Delta\nu/(\nu^2 + \Delta\nu^2)$;

$C_1 = 0.61576 \times 10^{-3}$;

$= (1.95 \times 760/1013.25) \times 10^{-3}$,

and $O^+(i)$ and $O^-(i)$ are line shape parameters for the absorption lines. They are defined by Rosenkrantz (15) and are listed in Table III.1.

TABLE III.1 Line Shape Parameters for the Absorption Due to Oxygen

i	$0^{+}(i)$	$0^{-}(i)$
1	56.2648	118.7505
3	58.4466	62.4863
5	59.5910	60.4863
7	60.4348	59.1642
9	61.1506	58.3239
11	61.8002	57.6125
13	62.4112	56.9682
15	62.9980	56.3634
17	63.5685	55.7839
19	64.1272	55.2214
21	64.6779	54.6728
23	65.2240	54.1294
25	65.7626	53.5960
27	66.2978	53.0695
29	66.8313	52.5458
31	67.3627	52.0259
33	67.8923	51.5091
35	68.4205	50.9949
37	68.9478	50.4830
39	69.4741	49.9730
41	70.0000	49.4648
43	70.5249	48.9582
45	71.0497	48.4530

III.B.3 Liquid Water

a. Cloud droplets

The absorption coefficients of cloud droplets for all frequencies except 85.5 GHz are calculated based on the formulation by Staelin, et. al. (14). When there is no precipitation,

$$\gamma_C(z) = C_W(z)\cdot 10^{[0.0122\cdot(291-T(z)) -4.0]}/(30/\nu)^2, \qquad \text{(III.22)}$$

where $C_W(z)$ is the cloud water density at height z.

For the 85.5 GHz, the Raleigh-Jeans approximation is used for the calculation of the absorption coefficient

$$\gamma_C(z) = 1.88685 \times 10^{-3}\, C_W(z)\cdot I_f/(30/\nu), \qquad \text{(III.23)}$$

where I_f is the imaginary part of $(-m^2+1)/(m^2+2)$ and m is the complex index of the refraction of water.

The absorption of ice cloud particles is calculated according to the following formula, assuming the temperature is below freezing, or $T(z)<273.16$ K.

$$\gamma_C(z) = [0.2302585\cdot C_W(z)\cdot 10^{-(5.11 + 0.145\sqrt{273.16-T}\ )}]/(30/\nu). \qquad \text{(III.24)}$$

b. Precipitation

Precipitation is the primary contributor to atmospheric attenuation at microwave wavelengths. The attenuation results from both absorption and scattering by the hydrometeors. The magnitude of these processes depends upon wavelength, drop size distribution, and precipitation layer thickness.

In the case of light rain, when it is permissible to neglect the effect of multiple scattering, the attenuation due to precipitation can be calculated according to equation III.12 and III.18. The liquid water content and the rain rate are assumed to be related by the Marshall-Palmer distribution function

$$L_w = 1.28 \times 10^{-10}\ \pi \cdot \left(\frac{450\ RR^{.21}}{+3.67}\right)^{+4}, \qquad \text{(III.25)}$$

where L_w is liquid water content (gm/m^3) and RR is rain rate (mm/hr.)

For heavier rain, the multiple scattering effect will be included through the algorithm described in sub-section III.A, equations III.5 thru III.11. One of the essential elements for the algorithm is the drop size distribution. The empirically observed spectra of Laws and Parson (16) is used to fit the Deirmendjian drop size distribution for the SSM/I rain algorithm. The Deirmendjian distribution is defined as

$$n(r) = Ar^{C_1} e^{(-Br^{C_2})}, \qquad \text{(III.26)}$$

where n(r) is the drop size distribution ($cm^{-3}\mu m^{-1}$), r is the radius of raindrop (μm), and A and B are scale parameters.

$$A = \left(\frac{M\ C_2}{\frac{4\pi}{3}\rho_w \cdot 10^6}\right)\left(\frac{B}{r}\right)^{[(C_1 + 4)/C_2]}, \qquad \text{(III.27)}$$

where M is the total liquid water content (gm/m^3),

$$M_w = \rho_w \int_0^\infty \frac{4\pi}{3} r^3 n(r)dr, \qquad \text{(III.28)}$$

$$B = \left(\frac{C_1}{C_2}\right) r_o^{-C_2}, \qquad \text{(III.29)}$$

and r_o is the mode radius (μm). The shape parameters are C_1 and C_2. The former of these affects the distribution of the smaller radii while the latter affects the larger radii.

The analytical results from fitting the Laws-Parson empirical spectrum are:

$$M = 0.636\ (RR^{.881}) \quad (gm/cm^3), \text{ where RR is rain rate (mm/hr),}$$

$$r_o = 225 + 9.16\ (RR^{.881}), \quad (r_o)_{max} = 375 \quad (\mu m),$$

$$C_1 = 4.0, \tag{III.30}$$

$$C_2 = 0.70 - 0.00458 \quad (RR^{.881}), \quad (C_2)_{min} = .625.$$

This formulation relates the rain rate to mode radius and liquid water density. It parameterizes the distribution as a function of rain rate only and thus simplifies the solution to the Deirmendjian distribution. On the other hand, it still retains the sensitivity of scattering to drop size, which would be lost if the Marshall-Palmer distribution is used. Figure III.1 shows the good agreement between the Deirmendjian model and the Laws and Parson distributions.

For weak storms with low rain rate ($RR \leq 8$ mm/hr), the ceiling for the rain layer is assumed to be the 0 C isotherm. For more intensive convective storms, the ceiling is usually higher with a super-cooled water layer on top. The thickness of the layer, Z_{inc}, depends on the intensity of convection. In the ERT algorithm, the thickness of the supercooled layer, ΔZ, for rain rates in excess of 8 mm/hr, is given as

$$\Delta Z = (RR - 8.0)\ Z_{inc};\ \Delta Z < \Delta Z_{max}, \tag{III.31}$$

where Z_{inc} and ΔZ_{max} are determined from climatology (17). The values used are given below:

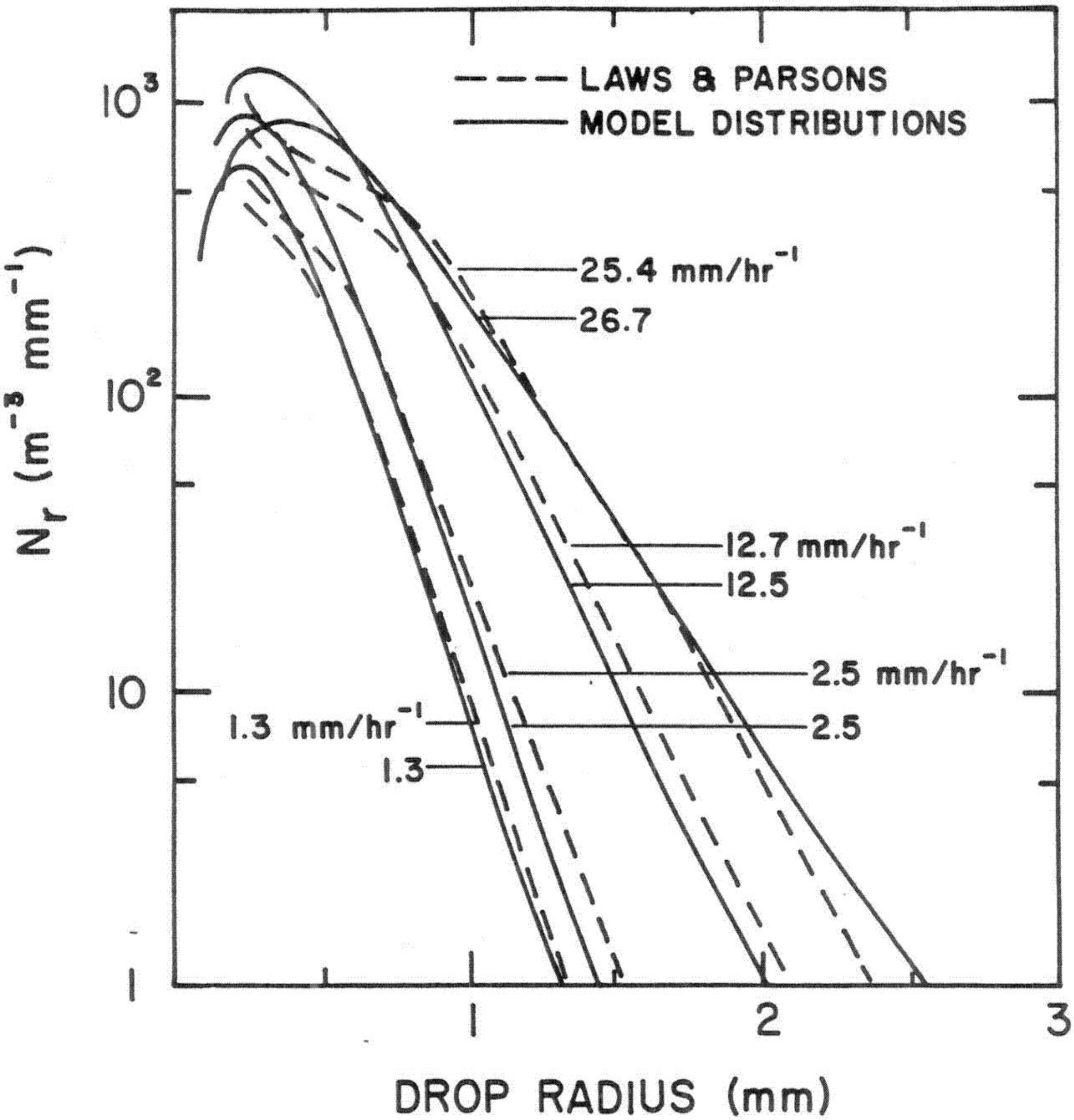

Figure III.1 The matching of the Deirmendjian raindrop size distribution used in model computations to the observed Laws and Parsons distributions.

	Z_{inc} $\frac{(m/hr)}{mm}$	ΔZ max (m)
Tropics Land	50	800
Ocean	50	800
Mid Lat Land	100	1600
Ocean	50	800
Arctic Land	25	400
Ocean	25	400

III.C The Surface Model

III.C.1 Ocean Surface

The calculation of the emissivity of a smooth water surface is relatively straightforward. The dielectric properties of sea water, derived from the measurement of Lane and Saxton (18) and expressed in analytical form by Chang and Wilheit (19) are used for the SSM/I algorithm. The Fresnel equations for a plane dielectric interface are used to calculate the emissivity of the smooth surface for a given view angle and polarization.

Wind driven waves and foam on the ocean surface both significantly alter the microwave reflectivity of the ocean surface. Wind speed is highly variable both horizontally and vertically. Marine wind speed measured from a ship is usually referenced to a standard height of 20 meters. However, the wind speed which directly relates to roughness and foam is the friction velocity at the ocean-air interface. The relationship development by Cardone (20) is used to extrapolate it to the standard 20 meter height.

The ocean surface model developed by Wilheit (21) is adopted in the SSM/I algorithm. The roughness effect is modeled after Cox and Munk (22) treating the sea surface as a collection of plane facets large compared to the observational wavelength. The variance in sea surface slope is defined as a function of wind speed and then used for calculation of emissivity assuming a Gaussian slope distribution for the facets and using the Fresnel relations. The derived wind speed dependence of the surface slope variance, σ^2, is given by

$$\sigma^2(f) = (0.3 + 0.02f)\ (0.003 + 0.48w) \qquad \text{for } f < 35 \text{ GHz;}$$
$$= 0.003 + 0.48w \qquad \text{for } f \geq 35 \text{ GHz,} \qquad \text{(III.32)}$$

where f is frequency in gigahertz (GHz) and w is the wind speed (m/sec) at 20 meter height.

Foam is treated as partially obscuring the surface in a manner independent of polarization but dependent upon frequency. The foam fraction, K, is defined as

$$K = 0.006\ (w - 7)\ (1 - e^{-f/7.5}) \qquad \text{for } w > 7 \text{ m/sec}$$
$$= 0 \qquad w \leq 7 \text{ m/sec.} \qquad \text{(III.33)}$$

This equation is based on Nordberg's (23) observation that the brightness temperature increases linearly with wind speed exceeding 7 m/sec, and that no foam forms below that wind speed.

III.C.2 Land Surface

The description of the land surface is extremely complex due to the many types of surfaces and the variation of the physical characteristics within each surface type. At present, the only land surface parameter retrieved by the SSM/I algorithm is the soil moisture for open land areas. Criteria have been developed to separate other land surface types such as forest and lakes from the open land areas.

The intensity of radiation from soil depends on the local dielectric constant and the physical temperature of the soil. Moisture produces a marked increase in both the real and the imaginary parts of the dielectric constant of soil, leading to a decrease in the soil emissivity. Experimental observations and theoretical calculations indicate that the emissivity of soil at microwave frequencies can range from >0.9 for dry soils to $\leq$0.6 for very moist soils.

A generalized incoherent layered surface model (24), was used to simulate expected SSM/I soil moisture brightness temperature signatures. Assume that there are N soil layers, with the atmospheric layer above and an infinitely deep layer, with constant temperature and moisture content, below. The brightness temperature emerging at the soil surface for the horizontal polarization, T_{BH}, is given by

$$T_{BH} = \sum_{i=1}^{N} T(i)\ W(i)\ T_{RH}(i)[1 - e^{-g(i)\ dz(i)}]\ [1 + R_H(i) \bullet g(i)\ dz(i)] \quad ,\text{(III.34)}$$

where T(i) is the temperature of the i-th layer and dz(i) is the depth of the i-th layer. The weighting function w(i), is defined as

$$w(i) = e^{-\sum_{m=1}^{i=1} g(m)\ dz(m)} \quad , \qquad \text{(III.35)}$$

where $g(m) = 4\pi\nu/c \bullet A(m)$. Here c is the speed of light and $A(m) = \epsilon_I(m)/[2\ B(m)]$, where $\epsilon_I(m)$ is the imaginary part of the dielectric constant of the m-th layer.

$$B(m) = \left\{0.5\ Y(m) \bullet [1 + (1 + (\epsilon_I(m)/Y(m))^2)^{1/2}]\right\}^{1/2} \quad , \qquad \text{(III.36)}$$

and $Y(m) = \epsilon_R(m) - \sin^2\theta$, where $\epsilon_R(m)$ is the real part of the dielectric constant of the m-th layer and θ is the incidence angle. The term, $T_{RH}(i)$, is the transmission factor of the i-th layer for horizontal polarization and is given by

$$T_{RH}(i) = [1 - R_H(1)]\ldots\ldots[1 - R_H(i-1)], \qquad \text{(III.37)}$$

where $R_H(i)$ is the horizontal extinction coefficient for the i-th layer.

$$R_H(i) = \left| \frac{C_{wv}(i) - C_{wv}(i+1)}{C_{wv}(i) + C_{wv}(i+1)} \right|^2 \quad \text{, where } C_{wv}(i) = (B(i),\ A(i)). \qquad \text{(III.38)}$$

The brightness temperature for vertical polarization, T_{BV}, emerging at the surface is

$$T_{BV} = \sum_{i=1}^{N} T(i)\ W(i)\ T_{RV}(i)\ [1 - e^{-g(i)\ dz(i)}]\ [1 + R_V(i)\ g(i)\ dz(i)]. \quad \text{(III.39)}$$

Here $T_{RV}(i)$ is the transmission factor of the i-th layer for vertical polarization;

$$T_{RV}(i) = (1 - R_V(1)\ (1 - R_V(2))\cdots\cdots(1 - R_V(i-1)), \qquad \text{(III.40)}$$

where $R_V(i)$ is the vertical extinction coefficient for the i-th layer.

$$R_V(i) = \left| \frac{\varepsilon(i)C_{wv}(i+1) - \varepsilon(i+1)\ C_{wv}(i)}{\varepsilon(i)C_{wv}(i+1) + \varepsilon(i+1)\ C_{wv}(i)} \right|^2 , \text{ where } \varepsilon(i) = (\varepsilon_R(i),\ \varepsilon_I(i)). \qquad \text{(III.41)}$$

The dielectric constant is a function of frequency and soil moisture. For the 19.35 and 22.235 GHz channels, results from the study by Wang et.al. (25) are adopted. Let SM be soil moisture in percentage. The real part of the dielectric constant, ε_R, is given by

$$\begin{aligned} SM \le 7 \qquad & \varepsilon_R = 2.67 + 0.1\ SM, \\ 7 < SM \le 19.25 \qquad & \varepsilon_R = 3.37 + 0.78\ (SM - 7), \\ 19.25 < SM \qquad & \varepsilon_R = 12.92 + 0.23\ (SM - 19.25), \end{aligned} \qquad \text{(III.42)}$$

and for the imagniary part, ε_I, by

$$\begin{aligned} SM \le 10 \qquad & \varepsilon_I = 0.08\ SM, \\ 10 < SM \le 19 \qquad & \varepsilon_I = 0.80 + 0.57\ (SM - 10), \\ 19 < SM \qquad & \varepsilon_I = 5.93 + 0.28\ (SM - 19). \end{aligned} \qquad \text{(III.43)}$$

The results from the study by Geiger and Williams (26) are adopted for the dielectric constant of soil at 37.0 and 85.5 GHz. Here

$$\varepsilon_R = (1/0.885)(-2.8426 + 1.0534\ SM - 0.033808\ SM^2 + 3.434 \times 10^{-4}\ SM^3)$$

and (III.44)

$$\varepsilon_I = (1/0.885)(-1.2981 + 0.2925\ SM + 1.79 \times 10^{-3} SM^2 - 1.465 \times 10^{-4} SM^3).$$

At the higher frequencies, there is little sensitivity to soil moisture much below the earth surface. It suffices to calculate the reflection coefficient through the Fresnel coefficients using the dielectric constants specified above.

Choudhury and Schmugge (27) have developed a simple correction factor to the reflectivity to take the surface roughness into account. The corrected reflection coefficient is given by

$$R'(\theta) = R(\theta)\, e^{(-h \cos^2\theta)}, \tag{III.45}$$

where

$$h = 4\sigma^2(2\pi/\lambda)^2.$$

σ^2 is the variance of the surface roughness, λ is the observational wavelength and h at 19.0 GHz is assumed to vary between 0 and 0.6.

III.C.3 Sea Ice

The upwelling brightness temperature of a scene containing sea water and various amounts of sea ice is a function of the ice concentration, ice emissivity, the physical temperatures of the ice components, and the amount of water vapor and liquid water in the atmosphere (6,7). The ice can be composed of first year (FY), multi-year (MY) or first-year thin ice (FT). The vertically polarized up-welling brightness temperature sensed by the SSM/I radiometer is expressed as

$$\begin{aligned} T_{BV} = e^{-\tau}\ [&C\cdot F(\varepsilon_{fv}T_f + (1-\varepsilon_{fv})T_s) + C\cdot M(\varepsilon_{mv}T_m + (1-\varepsilon_{mv})T_s) \\ &+ C(1-F-M)(\varepsilon_{tv}T_t + (1-\varepsilon_{tv})T_s) + (1-C)(\varepsilon_{wv}T_w + (1-\varepsilon_{wv})T_s)] \\ &+ T_{atm}, \end{aligned} \tag{III.46}$$

where τ = total atmospheric opacity,

C = fraction of sea ice (includes all types within field of view),

F = fraction of FY ice relative to total ice present,

M = fraction of MY ice relative to total ice present,

$\epsilon_{fv}, \epsilon_{mv}, \epsilon_{tv}$ = vertically polarized surface emissivities of FY, MY and FT ice,

$_{wv}$ = vertically polarized surface emissivity of sea water,

T_f, T_m, T_t = surface temperature of FY, MY and FT ice,

T_w = surface temperature of sea water,

T_s = incident sky temperature at the surface due to atmospheric downward self-emission, and

T_{atm} = contribution from atmospheric upward self-smission.

An approximate expression for τ at a 50^o earth incidence angle for (ν = 6.6 to 37 GHz) is

$$\tau = \frac{2.384}{\lambda^2} L, \qquad \text{(III.47)}$$

where λ is the observational wavelength (cm) and L is the integrated vertical column of liquid water and water vapor (cm). An expression similar to equation III.46 exists for horizontal polarization. Ideally all SSM/I frequencies with different sea ice dependencies can be used to solve for C, F, and M simultaneously. However, limitations at the AFGWC computing facility prevent the use of all the SSM/I channels in a single algorithm. A simpler but reliable algorithm was developed.

Results from a study on ice emissivities (28) are presented in Table III.2. The difference between the vertical and horizontal emissivities at 37 GHz exhibits significantly less dependence on ice type than does the

Table III.2 Emissivity of ice

ICE TYPE	MY		FY ICE		FY THIN ICE		WATER CALM SEA	
POLARIZATION**	V	H	V	H	V	H	V	H
FREQ, GHZ								
19.35	0.86	0.73	0.97	0.84	0.96	0.78	0.60	0.33
37	0.69	0.64	0.97	0.95	0.96	0.87	0.70	0.40
37 (V-H)	0.05		0.02		0.09		0.30	

**V – VERTICAL; H – HORIZONTAL; 50° EARTH INCIDENCE ANGLE polarization difference at 19.35 GHz. Furthermore, the polarization difference at 37 GHz is less sensitive to ice type than either the 37.0 GHz vertical or horizontal brightness temperatures. Therefore, the difference $T_{BV}(37) - T_{BH}(37)$ can be employed to obtain accurate estimates of ice concentration.

A sensitivity study was performed to determine the uncertainty of ice concentration using only the two 37 GHz channels (6,7). For winter conditions

$$T_f = T_t = 260 \pm 10^{o}K \qquad \Delta\varepsilon = \varepsilon_v - \varepsilon_h = 0.05 \pm 0.05$$
$$T_m = 250 \pm 10^{o}K \qquad \lambda = 0.81 \text{ cm}$$
$$T_w = 271K$$
$$L = 0.025 \pm 0.025 \text{ cm},$$

and for instrument noise contributions of $\Delta T = 0$ K and $\Delta T = 1$ K, ice concentration retrieval accuracy ranges from 7% when C = 100% to 6% for low ice concentrations. The uncertainty for low ice concentration arises mainly from atmospheric variability, while for high ice concentration, variability in ice emissivity is the main source of uncertainty. These analyses indicate that the 37 GHz channels will provide an adequate margin for ice concentration measurements. Thus, the proposed algorithm to retrieve ice concentration, IC, is

$$IC = A_o + A_1 \, [T_{BV}(37) - T_{BH}(37)], \qquad \text{(III.48)}$$

where A_o and A_1 are constants computed using equations III.46 and III.47 for the vertical polarization and equivalent equations for T_{BH}. Climatologically significant mean values of ice temperatures, atmospheric liquid water content, and mean values of ice emissivities are used as input to these equations. A_o and A_1 vary with season. They are presented in Section IV.

Dr. Rene Ramseier of the Atmospheric Environment Service of Canada has conducted many experiments to test the SSM/I ice algorithm using NIMBUS-7 SMMR 37.0 GHz data. Slight adjustments of coefficients were made to accommodate the difference in satellite geometry. Results from this study shows good agreement in ice concentration and ice edge between SSM/I ice

TABLE IV.1 Definition of Climate Codes

Climate Code No.	Definition
1	Tropical-warm
2	Tropical-cool
3	Lower Latitude Transition-warm
4	Lower Latitude Transition-cool
5	Mid. Lat.-Spring/Fall
6	Mid. Lat.-Summer
7	Mid. Lat.-Winter
8	Upper Lat. Transition-cool
9	Upper Lat. Transition-cold
10	Polar-cool
11	Polar-cold

determine which parameters to retrieve and which not to. It is designed to avoid meaningless retrievals and to use computing facilities most effectively. The criteria given for ocean cases include the critical temperature of the 19.35 H brightness temperature for the 'maybe rain' case CMRO, and the critical brightness temperature difference between the two polarizations of the 37 GHz frequency for 'maybe rain', CMRDO. When either of the two criteria is met, i.e., when T_B (19H) is greater than CMRO or when $T_B(37V) - T_B(37H)$ is less than CMRDO, the algorithm assumes that there is rain. The criterion for 'heavy rain' over the ocean, CHRDO, is also based on the difference in T_B between the two 37.0 GHz channels. When $T_B(37V) - T_B(37H)$ is less than CHRDO, the 'heavy rain' condition is assumed.

For land retrievals, there is a criterion, CFGL, defined to test for frozen ground. If $T_B(37V)$ is less than CFGL, the algorithm assumes frozen ground and considers soil moisture retrieval impossible. The retrieval algorithm also examines the 37 GHz brightness temperatures for 'heavy rain' using the criteria CHRL and CHRDL. The vertical channel brightness temperature is checked against the criterion CHRL. If it is less than CHRL and the difference between the two polarizations is less than CHRDL, 'heavy rain' is assumed and both the soil moisture and the cloud liquid water over land will not be retrieved. If the 'heavy rain' condition is not met, the algorithm then checks the 37 GHz brightness temperatures using criteria CMRL and CMRDL in a similar way to CHRL and CHRDL for the 'maybe rain' condition. If no rain is indicated, the rain rate over land and the liquid water over land are set to zero. The piecewise algorithm criteria are listed in Table IV.2 for the eleven climates.

IV.B Ocean Retrievals

IV.B.1 Ocean Surface Wind Speed (SW)

The response of brightness temperature at 19.35 H & V, 22.235 V, and 37 V & H to ocean surface wind speed is demonstrated in Figure IV.1 for a tropical clear atmosphere. The calculations are made at the look angle of the SSM/I. Note that the horizontal channels are more sensitive to wind

TABLE IV.2 Criteria for the Piecewise Algorithm

Climate Code	CMRO	CMRDO	CHRDO	CFGL	CHRL	CHRDL	CMRL	CMRDL
1	190	25	10	150	273	10	263	5
2	190	25	10	150	273	10	263	5
3	190	25	10	150	273	10	263	5
4	190	25	10	150	273	10	263	5
5	170	25	20	240	270	10	240	--
6	190	25	15	150	270	10	263	5
7	160	30	20	240	270	10	240	--
8	150	35	20	240	270	10	240	--
9	140	35	20	270	270	--	270	--
10	150	35	20	240	270	10	240	--
11	140	35	20	270	270	--	270	--

CMRO = Criterion for maybe rain over ocean for $T_B(19H)$

CMRDO = Criterion for maybe rain over ocean for $T_B(37V) - T_B(37H)$

CHRDO = Criterion for heavy rain over ocean for $T_B(37V) - T_B(37H)$

CFGL = Criterion for frozen ground for $T_B(37V)$

CHRL = Criterion for heavy rain over land for $T_B(37V)$

CHRDL = Criterion for heavy rain over land for $T_B(37V) - T_B(37H)$

CMRL = Criterion for maybe rain over land for $T_B(37V)$

CMRDL = Criterion for maybe rain over land for $T_B(37V) - T_B(37H)$

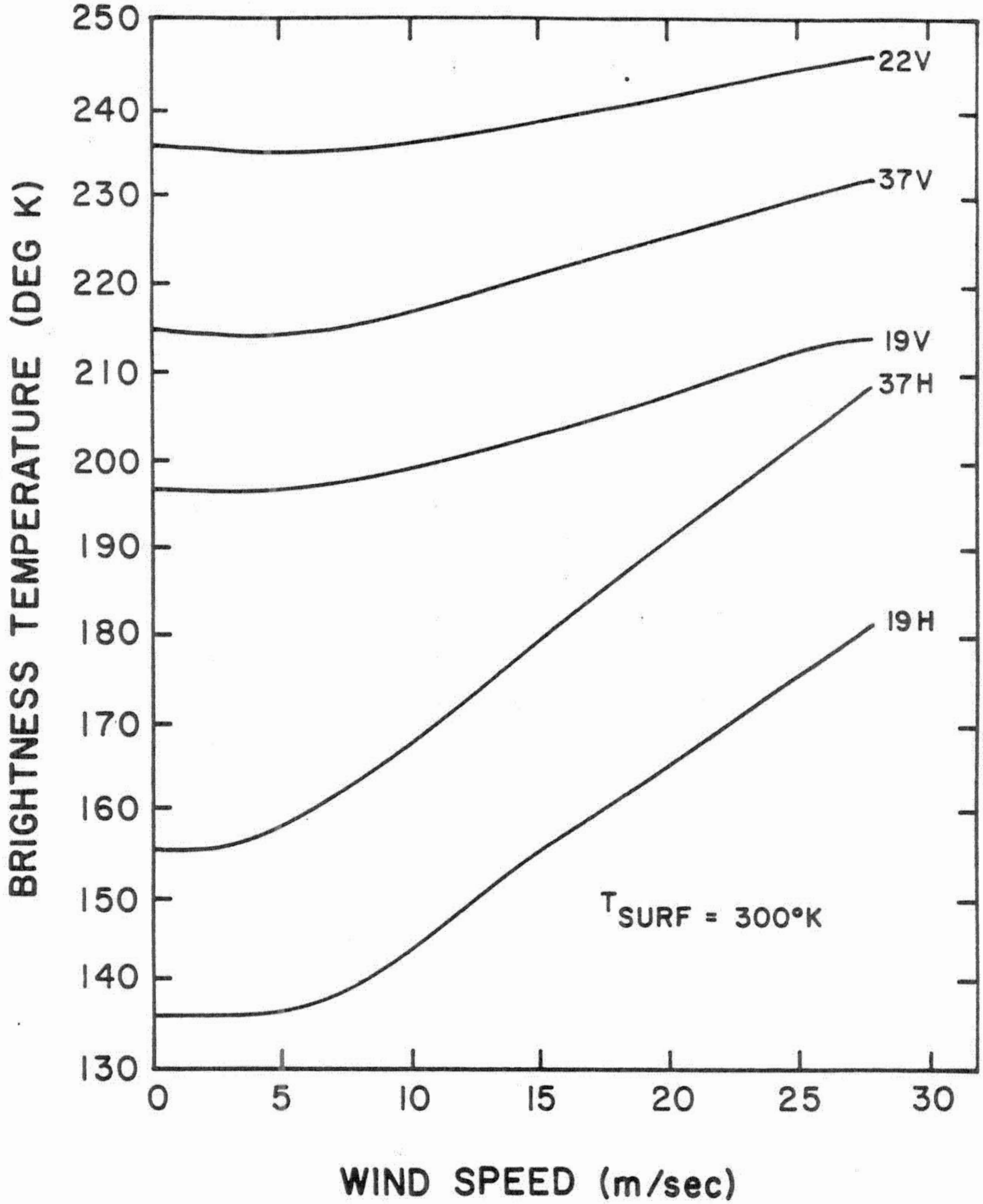

Figure IV.1 Brightness temperature as function of frequency and wind speed.

speed than the vertical channels. The SSM/I wind speed retrieval algorithm is given by

$$SW = C_{sw,o} + C_{sw,1} T_B(19H) + C_{sw,2} T_B(22V) \quad \text{(IV.1)}$$

$$+ C_{sw,3} T_B(37V) + C_{sw,4} T_B(37H),$$

where SW is surface wind speed. The coefficients for all eleven climates are listed below:

Climate Code	$C_{sw,o}$	$C_{sw,1}$	$C_{sw,2}$	$C_{sw,3}$	$C_{sw,4}$
1	191.5600	.4903	-.4432	-.9199	.3577
2	168.3900	.5366	-.4548	-.7656	.2635
3	177.3150	.3913	-.2818	-1.0083	.4095
4	147.7600	.5077	-.3547	-.7409	.2333
5	127.1300	.4788	-.2546	-.7162	.2030
6	163.0700	.2923	-.1204	-1.0967	.4612
7	95.9940	.6106	-.3034	-.4638	.0192
8	130.4200	.3676	-.1508	-.8400	.3056
9	117.5900	.4225	-.1899	-.7096	.2081
10	130.4200	.3676	-.1580	-.8400	.3056
11	117.5900	.4225	-.1899	-.7096	.2081

IV.B.2 Precipitation Over Ocean (RO)

At lower frequencies, such as 19.35 GHz, rain is highly absorptive and results in an apparent warm brightness temperature over a cold background such as the ocean. With increasing rain rate, the difference in brightness temperature between the two polarizations at a given frequency tend to decrease. These two characteristics are demonstrated in Figure IV.2.

The SSM/I data channels selected for retrieval of rain over ocean are 19.35H, 22.235V, 37.0 V & H. The algorithm for the retrieval is given by

$$RO = C_{ro,o} + C_{ro,1} T_B(19H) + C_{ro,2} T_B(22V) \quad \text{(IV.2)}$$

$$+ C_{ro,3} T_B(37V) + C_{ro,4} T_B(37H).$$

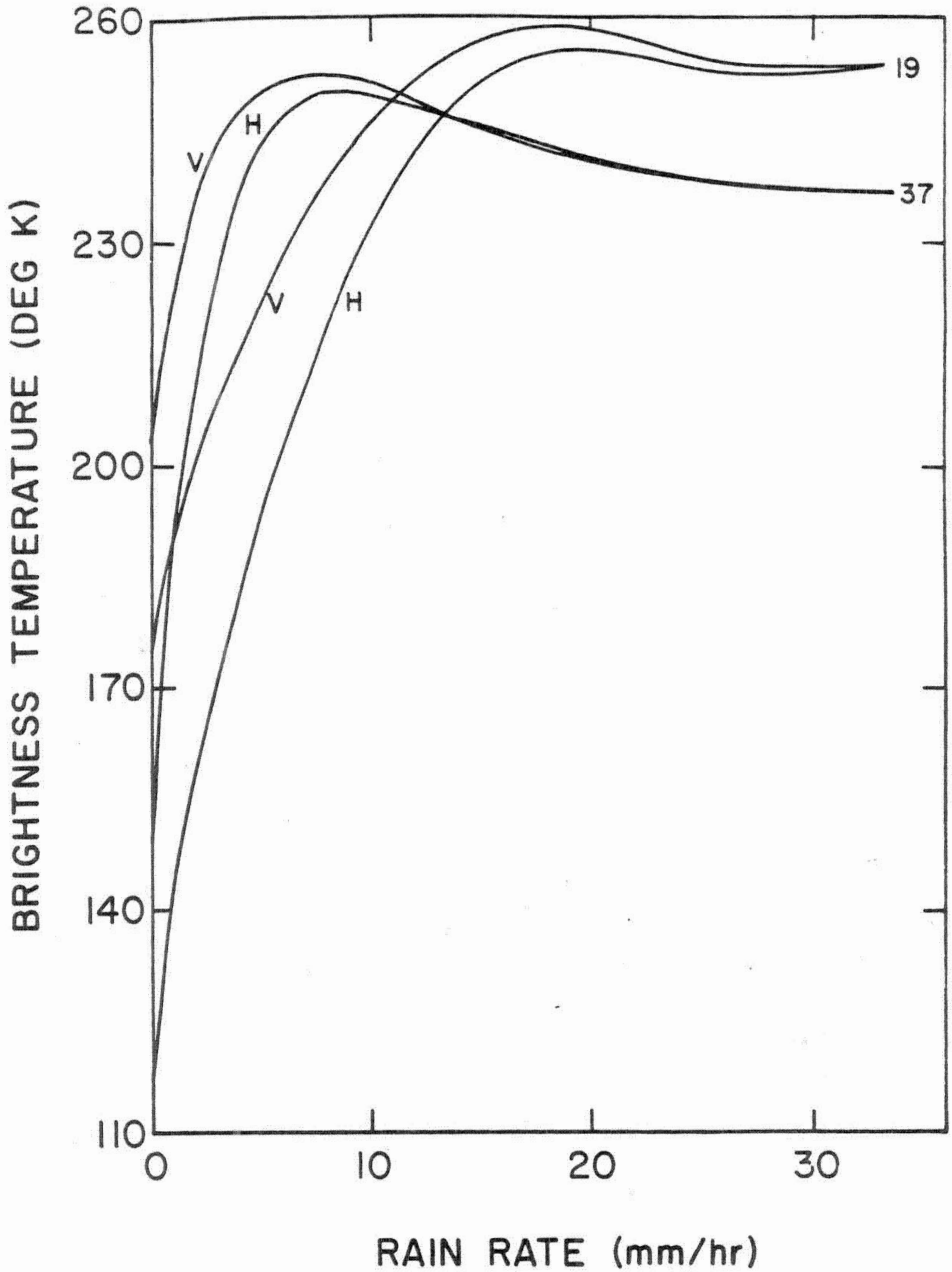

Figure IV.2 Brightness temperature vs. rain rate over mid-latitude ocean at 19 and 37 GHz

The coefficents for all climates are:

Climate code	$C_{ro,o}$	$C_{ro,1}$	$C_{ro,2}$	$C_{ro,3}$	$C_{ro,4}$
1	210.2800	.1217	-.7829	-.1830	.0998
2	215.1800	.1026	-.8059	-.1944	.1354
3	173.0400	.1938	-.6500	-.2291	.0808
4	169.2900	.1523	-.6065	-.3531	.2162
5	123.4000	.2019	-.4070	-.5117	.2969
6	135.8000	.2659	-.5170	-.2751	.0618
7	114.5500	.2708	-.6228	-.2836	.2521
8	9.5432	.1796	-.2109	.1214	-.0753
9	24.1020	.0825	.1367	-.3411	.0843
10	9.5432	.1796	-.2109	.1214	-.0753
11	24.1020	.0825	.1367	-.3411	.0843.

IV.B.3 Cloud Water (CWO) and Liquid Water (LWO) Over Ocean

The SSM/I retrieval algorithm for liquid water in the atmosphere includes two separate components. One of these, CWO, retrieves the amount of liquid water contained in cloud droplets, defined to be less than 100 m in diameter. The dominant radiative process for droplets of this size range is absorption for the SSM/I frequencies. The response at 19.35, 22.235 and 37 GHz to integrated cloud water over a mid-latitude ocean background is shown in Figure IV.3. The data channels selected for the retrieval of CWO are the same as for all the other ocean parameters, i.e., 19.35 H, 22.235 V, 37H and V.

$$CWO = C_{cwo,o} + C_{cwo,1} T_B(19H) + C_{cwo,2} T_B(22V) + C_{cwo,3} T_B(37V) + C_{cwo,4} T_B(37H). \tag{IV.3}$$

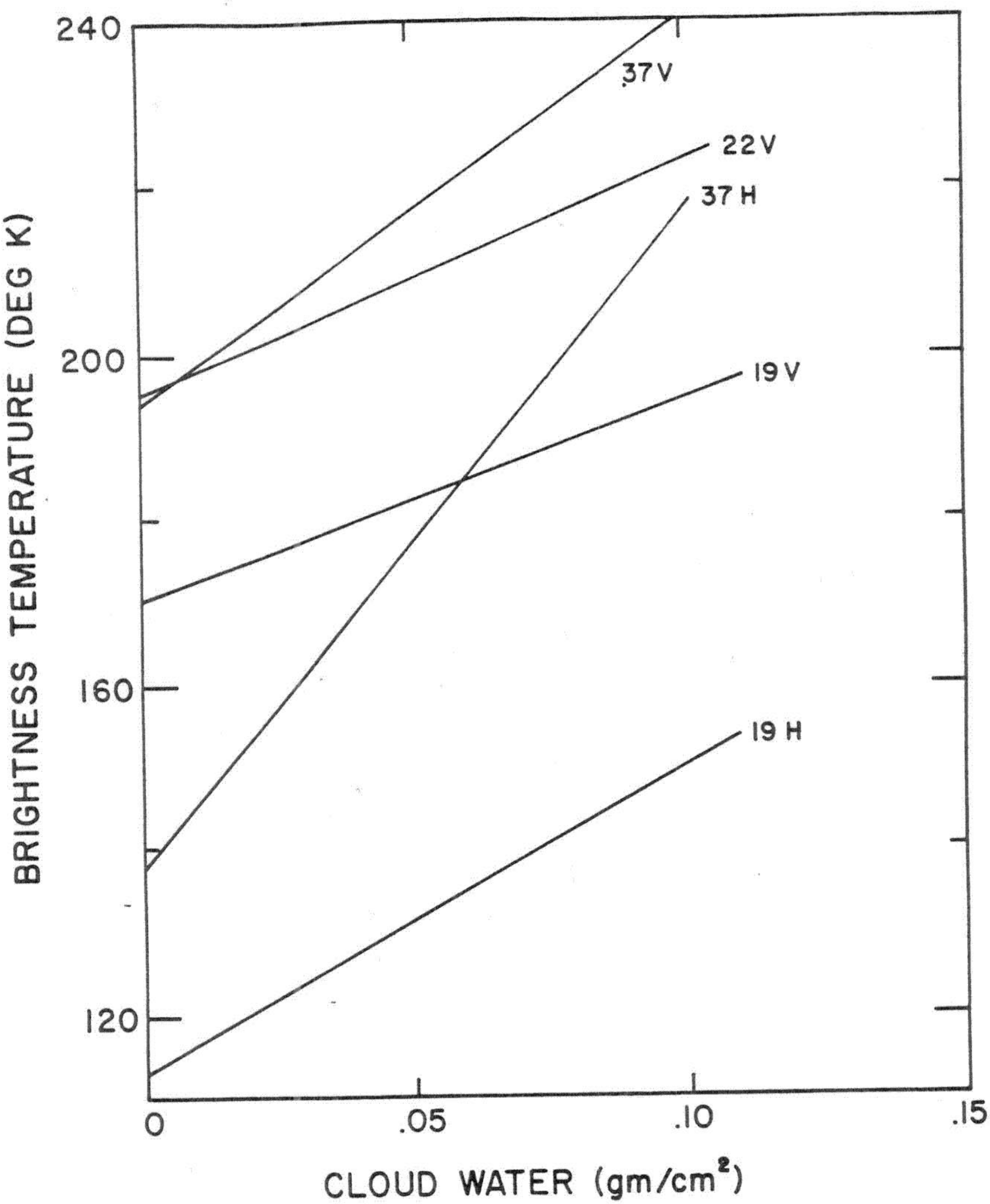

Figure IV.3 Brightness temperature vs. cloud water over mid-latitude ocean at 19, 22 and 37 GHz

The coefficients for all the climate codes are listed below:

Climate Code	$C_{cwo,o}$	$C_{cwo,1}$	$C_{cwo,2}$	$C_{cwo,3}$	$C_{cwo,4}$
1	-6.5240	-.0159	-.0044	.0407	.0045
2	-6.5292	-.0151	-.0046	.0408	.0041
3	-6.2070	-.0141	-.0038	.0383	.0035
4	-6.1372	-.0094	-.0054	.0398	-.0003
5	-5.7451	-.0037	-.0062	.0387	-.0047
6	-5.8903	-.0123	-.0031	.0358	.0025
7	-6.1411	-.0007	-.0061	.0395	-.0059
8	-4.0977	-.0066	-.0013	.0230	.0020
9	-3.6289	-.0047	-.0021	.0212	.0011
10	-4.0977	-.0066	-.0013	.0230	.0020
11	-3.6289	-.0047	-.0021	.0212	.0011

The other liquid water retrieval algorithm for the ocean is designed to retrieve the integrated liquid water contained in drops of diameter greater than 100 m, i.e., the dimensions of rain drops. The regression equation for the retrieval of LWO is

$$LWO = C_{lwo,o} + C_{lwo,1}\, T_B(19H) + C_{lwo,2}\, T_B(22V) + C_{lwo,3}\, T_B(37V) + C_{lwo,4}\, T_B(37H), \qquad (IV.4)$$

where the coefficient for the eleven climates are as follows:

Climate Code	$C_{lwo,o}$	$C_{lwo,1}$	$C_{lwo,2}$	$C_{lwo,3}$	$C_{lwo,4}$
1	50.7180	.0300	-.1881	-.0493	.0285
2	53.9140	.0259	-.2053	-.4830	.0374
3	40.7175	.0405	-.1353	-.0768	.0289
4	39.4580	.0344	-.1226	-.0844	.0342
5	25.0010	.0429	-.0399	-.1205	.0310
6	30.7170	.0510	-.0824	-.1043	.0293
7	34.6250	.0474	-.0592	-.1749	.0623
8	.3091	.0209	-.0049	-.0037*	-.0142
9	-.8477	.0048	.0177	-.0137	-.0014
10	.3091	.0209	-.0049	.0037*	-.0142
11	-.8477	.0048	.0177	-.0137	-.0014

*The difference in sign of the two numbers with asterisks is apparently a mistake. The Fleet Numerical Oceanography Center and subsequently Hughes Aircraft Company have been notified of this error.

IV.C Land Retrievals

IV.C.1 Soil Moisture (SM)

The emissivity of soil for various surface soil moisture contents is shown in Figure IV.4 for the 1.43, 19 and 37 GHz frequencies. The 19.35 V & H GHz channels are selected for the retrieval of soil moisture. The retrieval algorithm for soil moisture is given by

$$SM = C_{sm,0} + C_{sm,1} T_B(19V) + C_{sm,2} T_B(19H). \qquad (IV.5)$$

The coefficients for all the climate codes are defined as follows:

Climate Code	$C_{sm,o}$	$C_{sm,1}$	$C_{sm,2}$
1	121.3000	-0.4596	0.0839
2	108.8100	-0.3877	0.0494
3	109.5830	-0.3872	0.0414
4	89.9820	-0.2924	0.0058
5	71.1540	-0.1970	-0.0378
6	97.8660	-0.3148	-0.0011
7	85.8390	-0.2818	-0.0040
8	67.3730	-0.1483	-0.0874
9	0	0	0
10	63.5920	-0.0995	-0.1370
11	0	0	0

For the polar cold season and the upper-latitude cold season transition zones (Climate Code 11 and 9), land is regarded as frozen and soil moisture is not retrieved.

IV.C.2 Precipitation Over Land (RL)

The calculated brightness temperature at 37 and 85.5 GHz due to rain over land at mid-latitudes is given in figure IV.5. Rain causes a reduction in the apparent brightness temperature over the warm land background because the back scatter of the cold upper atmosphere begins to dominate the forward scatter from the land surface and the self emission from the atmosphere. This effect is absent over the ocean due to the much lower ocean background

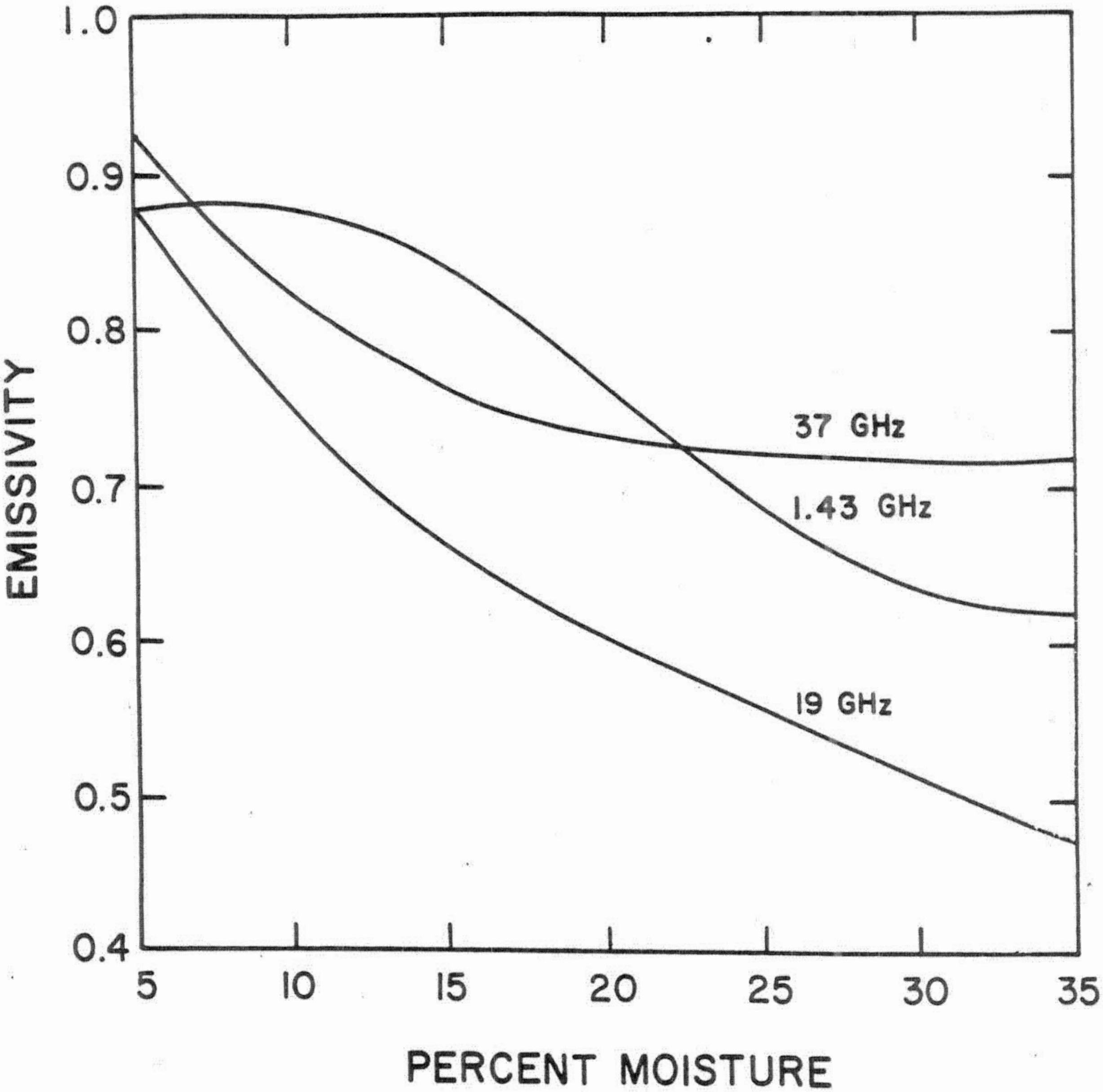

Figure IV.4 Emissivity at 1.43, 18 and 37 GHz vs. soil moisture

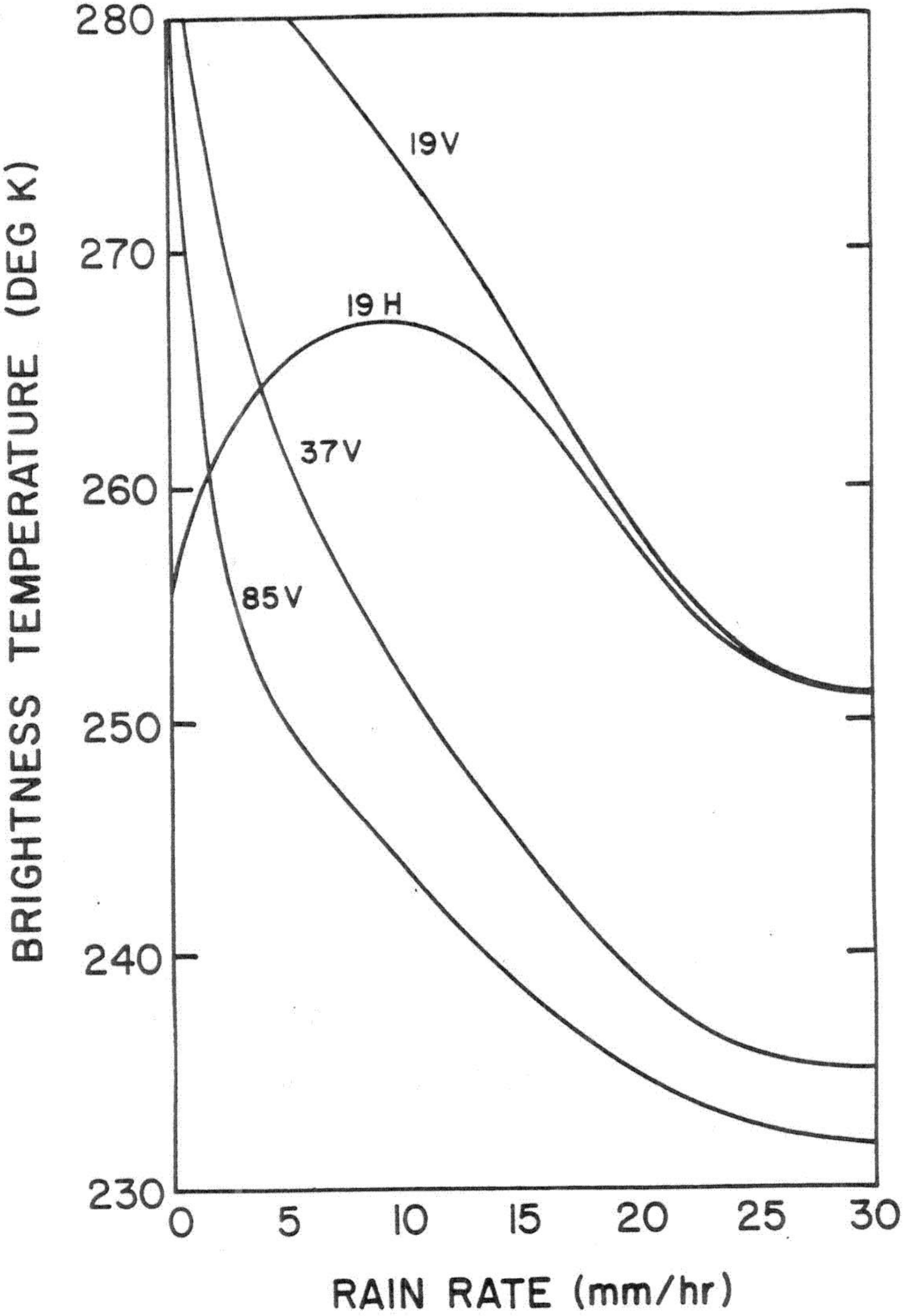

Figure IV.5 Brightness temperature vs. rain rate over mid-latitude land at 19, 37 and 85 GHz temperature. The 85.5 GHz channels have a higher resolution and greater sensitivity to the scattering effect of rain drops, as evidenced in Figure IV.5, then any previous satellite radiometer and should provide more reliable rain retrievals over land than here-to-for possible. The 37.0 and 85.5 GHz channels are proposed for the retrieval of precipitation over land.

$$RL = C_{rl,0} + C_{rl,1} T_B(37V) + C_{rl,2} T_B(85V). \qquad (IV.6)$$

The coefficients of equation (IV.6) for all the climates are listed below.

Climate Code	$C_{rl,0}$	$C_{rl,1}$	$C_{rl,2}$
1	208.8900	-0.7340	-0.0288
2	233.9200	-0.6887	-0.1768
3	215.7650	-0.7044	-0.0909
4	247.6550	-0.5741	-0.3469
5	261.3900	-0.4595	-0.5170
6	224.6400	-0.6747	-0.1529
7	290.6600	-0.3868	-0.7026
8	239.3100	-0.4323	-0.4595
9	0	0	0
10	217.2200	-0.4050	-0.4020
11	0	0	0

Only snow is considered possible during the cold season at the polar region (Climate code 11 and 9).

IV.C.3 Liquid Water Over Land (LWL)

The data channels selected for the retrieval of liquid water contained in rain are the same as those in the retrieval of rain rate, i.e., the vertical polarization channels of the 37 and the 85.5 GHz frequencies. Here

$$LWL = C_{lwl,0} + C_{lwl,1} T_B(37V) + C_{lwl,2} T_B(85V), \qquad (IV.7)$$

and the coefficients are listed below:

Climate Code	$C_{lwl,0}$	$C_{lwl,1}$	$C_{lwl,2}$
1	53.1520	-0.1495	-0.0471
2	57.2120	-0.1405	-0.0713
3	51.3090	-0.1580	-0.0315
4	49.7870	-0.0977	-0.0873
5	42.3610	-0.0548	-0.1032
6	49.4650	-0.1665	-0.0158
7	52.2480	-0.0687	-0.1278
8	29.7660	-0.0381	-0.0725
9	0	0	0
10	17.1110	-0.0213	-0.0417
11	0	0	0

Since liquid water does not generally exist in polar and sub-polar regions during the cold season, liquid water over land is not retrieved for climate codes 11 and 9.

IV.C.4 Cloud Water Over Land (CWL)

Cloud water over land is much more difficult to retrieve than cloud water over the ocean (6,7) because the land background is much warmer than the ocean. As a result, at the lower frequencies there is little sensitivity to cloud water. Besides, the land background is more variable (7) than the ocean. The brightness variation due to cloud water is of the same order of magnitude as the noise level of the land surfaces. On the other hand, the higher frequency channels tend to be so sensitive to cloud water that they serve better as indicators of the existence of clouds than of cloud water content (6). The algorithm developed for the SSM/I retrieval of CWL is given by

$$CWL = C_{cwl,o} + C_{cwl,1}\, T_B(19V) + C_{cwl,2}\, T_B(19H) \qquad (IV.8)$$

$$+ C_{cwl,3}\, T_B(37V) + C_{cwl,4}\, T_B(85V).$$

The coefficients used in retrieval for all the climates are defined below:

Climate Code	$C_{cwl,o}$	$C_{cwl,1}$	$C_{cwl,2}$	$C_{cwl,3}$	$C_{cwl,4}$
1	.6221	.0036	-.0031	.0251	-.0268
2	1.6545	-.0008	-.0006	.0362	-.0384
3	.8821	.0006	-.0007	.0271	-.0283
4	1.5350	.0014	-.0030	.0362	-.0377
5	1.4154	.0036	-.0054	.0362	-.0369
6	1.1421	-.0024	.0017	.0290	-.0298
7	1.2078	-.0050	.0033	.0415	-.0401
8	1.5366	.0002	-.0019	.0328	-.0342
9	.9329	-.0045	.0028	.0351	-.0333
10	1.6578	-.0033	.0017	.0294	-.0314
11	.6579	-.0040	.0023	.0286	-.0265

IV.D Ice Retrievals

The SSM/I retrieval algorithm for ice is derived differently than those for ocean and land retrievals. Certain relationship among the brightness temperatures and ice parameters were predetermined (See Equations III.48-50), and coefficients of these relationship are derived through analytic expressions and climatological data as described in subsection III.C.3. The coefficients A_o and A_1 from equation III.4.8 and C_o, C_1, C_2 from equation III.50 for the derivation of ice concentration, IC, and the effective average ice brightness temperature, T_x, are listed below:

	A_o	A_1	C_o	C_1	C_2	T_c(MY)
Polar-cool	1.1880	-0.0176	-219.0600	1.1050	193.6400	228.00
Polar-cold	1.1780	-0.0176	-217.7000	1.1050	192.2800	218.00

where T_c(MY) is the critical temperature for the determination of ice type. If T_x is greater than T_c(MY), the ice is defined to be first year, otherwise it is designated to be MY ice.

Cloud water over ice (CWI) is retrieved by the SSM/I algorithm even though it is not required by the specifications. The data channels employed are 19.35 V & H and 37.0 V & H.

$$CWI = C_{cwi,o} + C_{cwi,1}\, T_B(19V) + C_{cwi,2}\, T_B(19H) + C_{cwi,3}\, T_B(37V) + C_{cwi,4}\, T_B(37H). \tag{IV.9}$$

The coefficients employed are listed below.

	$C_{cwi,o}$	$C_{cwi,1}$	$C_{cwi,2}$	$C_{cwi,3}$	$C_{cwi,4}$
Polar-cool	.3415	-.0010	-.0048	-.0667	.0744
Polar-cold	-.2082	-.0003	-.0121	-.0320	.0468.

REFERENCES

1. Hollinger, J. P., and R. C. Lo, "SSM/I Project Summary Report", Naval Research Laboratory, Technical Memorandum Report 5055; April 1983.

2. "Special Sensor Microwave/Imager (SSM/I) Critical Design Review, Vol. II. Ground Segment", Contract No. F04701-79-C-0061, Hughes Aircraft Company, March 1980.

3. "Special Sensor Microwave/Imager (SSM/I) Computer Program Development Specification (Rev.B) (Specification for FNWC)", Contract No. F04701-79-C-0061, CDRL Item No. 016A2, Hughes Aircraft Company, July 1980.

4. "Special Sensor Microwave/Imager (SSM/I) Computer Program Product Specification (Specification for FNOC), Volume III Environmental Parameter Extraction, Computer Program Component (SMIEPE)", Contract No. F04701-79-C-0061, CDRL Item No. 018A2, Hughes Aircraft Company, December 1980.

5. "Special Sensor Microwave/Imager (SSM/I) Data Requirement Document DRD for AFGWC", Contract No. F04701-79-C-0061, CDRL Item No. 028A2, Hughes Aircraft Company, January 1981.

6. "Proposal for Microwave Environmental Sensor System (SSM/I), Vol. I Technical Proposal", RFP No. F0471-78-R-0094, Hughes Aircraft Company, January 1979.

7. Burke, H, K., and K. C. Jones, "Models of Environmental Parameters for the SSM/I Program", Environmental Research and Technology, Inc., February 1980.

8. Burke, H. K., et.al., "Inversion Algorithms for Environmental Parameter Extraction of the SSM/I Program", Environmental Research and Technology, Inc., February 1980.

9. Gaut, N. T., and Reifenstein III, "Interaction Model of Microwave Energy and Atmospheric Variables", Final Report, Environmental Research and Technology, Inc., Concord, Massachusetts, 1971.

10. Sze, N. D., "Variational Methods in Radiative Transfer Problems", J. Current Spectro. Radiat. Transfer, Vol. 16, 1976.

11. Burke, H. K., and N. D. Sze, "A Comparison of Variational and Discrete Ordinate Methods for Solving Radiative Transfer Problems", J. Current Spectro. Radiat. Transfer, Vol. 17, 1977.

12. Gaut, N. E., "Studies of Atmospheric Water Vapor by Means of Passive Microwave Techniques", Research Laboratory for Electronics, Tech. Report 467, Massachussetts Institute of Technology, 1968.

13. Van Vleck, J. H., and V. F. Weisskopf, "On the Shape of Collision Broadened Lines", Rev. Mod. Phys., Vol. 17, 1945.

14. Staelin, D. H., et.al., "Remote Sensing of Atmospheric Water Vapor and Liquid Water with the NIMBUS-5 Microwave Spectrometer", J. Appl. Met, Vol. 15, pp. 1203-1214, 1976.

15. Rosenkranz, P. W., "Shape of the 5 mm Oxygen Band in the Atmosphere", IEEE Trans. Antenna and Propagation, Vol. AP-23, No. 4, 1975.

16. Lewis, J. O., and D. A. Parson, "The Relation of Raindrop Size to Intensity", Trans. American Geophys. Union, Vol. 24, p. 452, 1943.

17. Burke, H. K., and K. C. Jones, "Models of Environmental Parameters for the SSM/I Program", Environmental Research and Technology, Inc., February 1980.

18. Lane, J. A., and J. A. Saxton, "Dielectric Dispersion in Pure Polar Liquids at Very High Radio Frequencies", Proc. Roy. Soc., London A, 214, pp. 531-545, 1952.

19. Chang, A. T. C., and T. Wilheit, "Remote Sensing of Atmospheric Water Vapor, Liquid Water, and Wind Speed at the Ocean Surface by Passive Microwave Techniques from the NIMBUS-5 Satellite", Radio Science, 1979.

20. Cardone, V. J., "Specification of the Wind Field Distribution in the Marine Boundary Layer for Wave Forecasting", Report TR 69-1, Geophysical. Sci. Lab., New York University, 1969.

21. Wilheit, T. T., "A Model for the Microwave Emissivity of the Ocean's Surface as a Function of Wind Speed", NASA TM 80278, 1979.

22. Cox, C. and W. Munk, "Measurement of the Roughness of the Sea Surface from Photographs of the Sun's Glitter", J. Optical Society of America, Vol. 44, No. 11, 1955.

23. Stogryn, A., "The Brightness Temperature of a Vertically Structured Medium", Radio Science, Vol. 5, No. 12, pp. 1397-1406, 1970.

24. Burke, W. J., and J. F. Paris, "A Radiative Transfer Model for Microwave Emission from Bare Agricultural Soils", NASA Tech. Memo. X-58166, NASA Johnson Space Center, Houston, Tex., 1975.

25. Wang, J., et.at., "Dielectric Constants of Soil Microwave Frequencies, II", NASA Tech. Pap. TP-1238, 1978.

26. Geiger, F., and D. Williams, "Dielectric Constants of Soils at Microwave Frequencies", Contract NASA X-652-72-238, NASA Goddard Space Flight Center, Greenbelt, Maryland, 1972.

27. Choudhury, B. J., T. J. Schmugge, A. Cheng, and R. W. Newton, "Effect of Surface Roughness on the Microwave Emission from Soil", J. of Geophy. Res., Vol. 84, No. C9, 1979.

28. Gloerson, P., et.al., "Time-Dependence of Sea-Ice Concentration and Multiyear Ice Fraction in the Arctic Basis", J. Boundary-Layer Met., Vol. 13, 1978.

29. "Special Sensor Microwave/Imager (SSM/I) Data Requirement Document DRD for AFGWC", Hughes Aircraft Company, Contract No. F04701-79-C-0061, CDRL Item No. 028A2, January 1981.

9.0 APPENDIX B: CURRENT SSM/I SENSOR CONSTANT FILE

The radiometric sensor constants used to derive the SSM/I brightness temperatures (SDRs) and the alignment coefficients needed to earth locate the SSM/I pixels are included herein. The antenna pattern correction coefficients and sensor alignment constants are subject to change depending on the results obtained in the SSM/I calibration/validation. The final coefficients will be documented in the final Cal/Val report.

```
*DECK SMID08
*IF DEF FTN
      BLOCK DATA SMID08
*
***********************************************************************
*     THIS SUBPROGRAM CONTAINS THE USER DATA VALUES FOR SMISENCA08
***********************************************************************
*
*CALL $SENCON
*CALL $APCCOF
*
***********************************************************************
*     EQUIVALENCE THE A ARRAY FOR EASIER USER IDENTIFICATION
***********************************************************************
*
      REAL HL1(6), HL2(6), HL3(6), RFMT(6), RADTMP(6)
      EQUIVALENCE (A(1,1),HL1(1)),(A(1,2),HL2(1)),(A(1,3),HL3(1)),
     1(A(1,4),RFMT(1)),(A(1,5),RADTMP(1))
*
***********************************************************************
*                          SENSOR CONSTANTS DATA                      *
***********************************************************************
*
***** ALIGNMENT TERMS 0-3 & EL OFFSET ANGLE & SENSOR SCAN PERIOD
*
      DATA EPS0  / 0.999999619/, EPS1  / 0.000000000/,
     1     EPS2  / 0.000000000/, EPS3  / 0.000872664/,
     2     ELOFF / 0.004363323/, TIMPER/ 1.899000000/
*
***** SENSOR SCAN DIRECTION & SENSOR INTEG TIME & REF VOLTAGE 1-2
*
      DATA SCNDIR/ 0.000000000/, TIMINT/ 0.004220000/,
     1     VR1   / 6.666670000/, VR2   / 0.000000000/
*
***** HOT LOAD 1 A0-A5
*
      DATA HL1   / 1.948787000E+02,  2.565077000E-02,  1.392114000E-06,
     1             4.350713000E-10,  0.0, 0.0/
*
***** HOT LOAD 2 A0-A5
*
      DATA HL2   / 1.949334100E+02,  2.566807000E-02,  1.402542000E-06,
     1             4.330412000E-10,  0.0, 0.0/
*
***** HOT LOAD 3 A0-A5
*
      DATA HL3   / 1.950729600E+02,  2.569616000E-02,  1.416201000E-06,
     1             4.316454000E-10,  0.0, 0.0/
*
***** RF MIXER TEMP A0-A5
*
      DATA RFMT  / 2.204095100E+02,  9.321052000E-02, -5.633346000E-05,
     1             2.247464000E-08,  0.0, 0.0/
*
***** RAD TEMP A0-A5
*
      DATA RADTMP/ 2.212535500E+02,  9.196866000E-02, -5.615105000E-05,
     1             2.261029000E-08,  0.0, 0.0/
*
***** HOT LOAD GRAD COEF & ON/OFF PLAT SEN 1-3
*
      DATA ALPHA / 0.010000000/,  ON1   / 1.000000000/,
     1     ON2   / 1.000000000/,  ON3   / 1.000000000/
*
***** COLD LOAD TEMP CHANNELS 1-7 & SCAN WIDTH HI BAND
*
      DATA TC    / 2.700000000,  2.700000000,  2.700000000,
```

```
     1              2.700000000,  2.700000000,  2.700000000,
     2              2.700000000/, SCNWDT / 0.013962640/
*
***** 19H TO 22H CNVR SLOPE & 19H TO 22H CNVR OFFST
*
      DATA SLP22H/ 0.653000000/, OFF22H/ 96.60000000/
*
***** ORBIT PERIOD & EARTH ROTATION FACTOR
*
      DATA ORBPER/ 6094.400000/, EARROT/ 0.004375300/
*
***** 10-16 PT CONVR LAT
*
      DATA B10T16/ 60.00000000/, DELAY / 0.356900000/
*
***** LOGICAL SPACECRAFT ID & SENSOR ID
*
      DATA LOGSAT  /1/, IDSEN / 6/
*
***** C0 COEF - B0(7,5) & C1 COEF - B1(7,5)
*
      DATA C0    / 35*0.000000000/, C1     / 35*0.000000000/
*
*
**********************************************************************
*                 ANTENNA PATTERN CORRECTION COEFFICIENTS            *
**********************************************************************
*
***** REGION 1 MAX POS #
*
      DATA NREG1 / 20/
*
***** REGION 1 19V C1-C6
                         C1          C2          C3
      DATA R1T1C / 1.047100, -0.004900, -0.007300,
     1                -0.002900,  0.000000,  0.000000/
*                        C4          C5          C6
***** REGION 1 19V N1-N6
*
      DATA I1T1N / 1, 0, 0, 0/
*
***** REGION 1 19H C1-C6
*
      DATA R1T2C / 1.047200, -0.004300, -0.008000,
     1                -0.002800,  0.000000,  0.000000/
*
***** REGION 1 19H N1-N6
*
      DATA I1T2N / 1, 0, 0, 0/
*
***** REGION 1 22V C1-C6
*
      DATA R1T3C / 1.051300, -0.011100, -0.008000,
     1                -0.005500,  0.000000,  0.000000/
*
***** REGION 1 22V N1-N6
*
      DATA I1T3N / 1, 0, 0, 0/
*
***** REGION 1 37V C1-C6
*
      DATA R1T4C / 1.042200, -0.022500, -0.003200,
     1                -0.002200,  0.000000,  0.000000/
*
***** REGION 1 37V N1-N6
*
      DATA I1T4N / 1, 0, 0, 0/
```

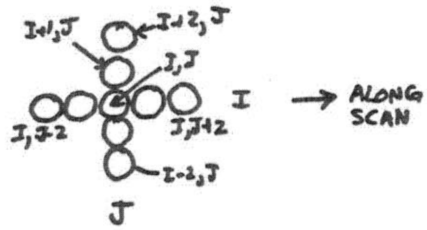

C_1 I,J CO-POL
C_2 I,J X-POL
C_3 I,J-N1 CO-POL
C_4 I,J+N1 "
C_5 (I-N2,J+N3) "
C_6 (I+N3,J-N4) "

```
*
***** REGION 1 37H C1-C6
*
      DATA R1T5C / 1.042800, -0.027200, -0.001000,
     1             -0.000400,  0.000000,  0.000000/
*
***** REGION 1 37H N1-N6
*
      DATA I1T5N / 1, 0, 0, 0/
*
***** REGION 1 85V C1-C6
*
      DATA R1T6C / 1.034100, -0.014200, -0.004000,
     1             -0.003700,  0.000000,  0.000000/
*
***** REGION 1 85V N1-N6
*
      DATA I1T6N / 1, 0, 0, 0/
*
***** REGION 1 85H C1-C6
*
      DATA R1T7C / 1.035900, -0.020100, -0.002700,
     1             -0.000900,  0.000000,  0.000000/
*
***** REGION 1 85H N1-N6
*
      DATA I1T7N / 1, 0, 0, 0/
*
***** REGION 2 MAX POS #
*
      DATA NREG2 / 32/
*
***** REGION 2 19V C1-C6
*
      DATA R2T1C / 1.047100, -0.004900, -0.007300,
     1             -0.002900,  0.000000,  0.000000/
*
***** REGION 2 19V N1-N6
*
      DATA I2T1N / 1, 0, 0, 0/
*
***** REGION 2 19H C1-C6
*
      DATA R2T2C / 1.047200, -0.004300, -0.008000,
     1             -0.002800,  0.000000,  0.000000/
*
***** REGION 2 19H N1-N6
*
      DATA I2T2N / 1, 0, 0, 0/
*
***** REGION 2 22V C1-C6
*
      DATA R2T3C / 1.051300, -0.011100, -0.008000,
     1             -0.005500,  0.000000,  0.000000/
*
***** REGION 2 22V N1-N6
*
      DATA I2T3N / 1, 0, 0, 0/
*
***** REGION 2 37V C1-C6
*
      DATA R2T4C / 1.042200, -0.022500, -0.003200,
     1             -0.002200,  0.000000,  0.000000/
*
***** REGION 2 37V N1-N6
*
      DATA I2T4N / 1, 0, 0, 0/
```

```
*
***** REGION 2 37H C1-C6
*
      DATA R2T5C / 1.042800, -0.027200, -0.001000,
     1             -0.000400,  0.000000,  0.000000/
*
***** REGION 2 37H N1-N6
*
      DATA I2T5N / 1, 0, 0, 0/
*
***** REGION 2 85V C1-C6
*
      DATA R2T6C / 1.034100, -0.014200, -0.004000,
     1             -0.003700,  0.000000,  0.000000/
*
***** REGION 2 85V N1-N6
*
      DATA I2T6N / 1, 0, 0, 0/
*
***** REGION 2 85H C1-C6
*
      DATA R2T7C / 1.035900, -0.020100, -0.002700,
     1             -0.000900,  0.000000,  0.000000/
*
***** REGION 2 85H N1-N6
*
      DATA I2T7N / 1, 0, 0, 0/
*
***** REGION 3 MAX POS #
*
      DATA NREG3 / 96/
*
***** REGION 3 19V C1-C6
*
      DATA R3T1C / 1.047100, -0.004900, -0.007300,
     1             -0.002900,  0.000000,  0.000000/
*
***** REGION 3 19V N1-N6
*
      DATA I3T1N / 1, 0, 0, 0/
*
***** REGION 3 19H C1-C6
*
      DATA R3T2C / 1.047200, -0.004300, -0.008000,
     1             -0.002800,  0.000000,  0.000000/
*
***** REGION 3 19H N1-N6
*
      DATA I3T2N / 1, 0, 0, 0/
*
***** REGION 3 22V C1-C6
*
      DATA R3T3C / 1.051300, -0.011100, -0.008000,
     1             -0.005500,  0.000000,  0.000000/
*
***** REGION 3 22V N1-N6
*
      DATA I3T3N / 1, 0, 0, 0/
*
***** REGION 3 37V C1-C6
*
      DATA R3T4C / 1.042200, -0.022500, -0.003200,
     1             -0.002200,  0.000000,  0.000000/
*
***** REGION 3 37V N1-N6
*
      DATA I3T4N / 1, 0, 0, 0/
```

```
*
***** REGION 3 37H C1-C6
*
      DATA R3T5C / 1.042800, -0.027200, -0.001000,
     1             -0.000400,  0.000000,  0.000000/
*
***** REGION 3 37H N1-N6
*
      DATA I3T5N / 1, 0, 0, 0/
*
***** REGION 3 85V C1-C6
*
      DATA R3T6C / 1.034100, -0.014200, -0.004000,
     1             -0.003700,  0.000000,  0.000000/
*
***** REGION 3 85V N1-N6
*
      DATA I3T6N / 1, 0, 0, 0/
*
***** REGION 3 85H C1-C6
*
      DATA R3T7C / 1.035900, -0.020100, -0.002700,
     1             -0.000900,  0.000000,  0.000000/
*
***** REGION 3 85H N1-N6
*
      DATA I3T7N / 1, 0, 0, 0/
*
***** REGION 4 MAX POS #
*
      DATA NREG4 /108/
*
***** REGION 4 19V C1-C6
*
      DATA R4T1C / 1.047100, -0.004900, -0.007300,
     1             -0.002900,  0.000000,  0.000000/
*
***** REGION 4 19V N1-N6
*
      DATA I4T1N / 1, 0, 0, 0/
*
***** REGION 4 19H C1-C6
*
      DATA R4T2C / 1.047200, -0.004300, -0.008000,
     1             -0.002800,  0.000000,  0.000000/
*
***** REGION 4 19H N1-N6
*
      DATA I4T2N / 1, 0, 0, 0/
*
***** REGION 4 22V C1-C6
*
      DATA R4T3C / 1.051300, -0.011100, -0.008000,
     1             -0.005500,  0.000000,  0.000000/
*
***** REGION 4 22V N1-N6
*
      DATA I4T3N / 1, 0, 0, 0/
*
***** REGION 4 37V C1-C6
*
      DATA R4T4C / 1.042200, -0.022500, -0.003200,
     1             -0.002200,  0.000000,  0.000000/
*
***** REGION 4 37V N1-N6
*
      DATA I4T4N / 1, 0, 0, 0/
```

```
*
***** REGION 4 37H C1-C6
*
      DATA R4T5C / 1.042800, -0.027200, -0.001000,
     1             -0.000400,  0.000000,  0.000000/
*
***** REGION 4 37H N1-N6
*
      DATA I4T5N / 1, 0, 0, 0/
*
***** REGION 4 85V C1-C6
*
      DATA R4T6C / 1.034100, -0.014200, -0.004000,
     1             -0.003700,  0.000000,  0.000000/
*
***** REGION 4 85V N1-N6
*
      DATA I4T6N / 1, 0, 0, 0/
*
***** REGION 4 85H C1-C6
*
      DATA R4T7C / 1.035900, -0.020100, -0.002700,
     1             -0.000900,  0.000000,  0.000000/
*
***** REGION 4 85H N1-N6
*
      DATA I4T7N / 1, 0, 0, 0/
*
***** REGION 5 MAX POS #
*
      DATA NREG5 /128/
*
***** REGION 5 19V C1-C6
*
      DATA R5T1C / 1.047100, -0.004900, -0.007300,
     1             -0.002900,  0.000000,  0.000000/
*
***** REGION 5 19V N1-N6
*
      DATA I5T1N / 1, 0, 0, 0/
*
***** REGION 5 19H C1-C6
*
      DATA R5T2C / 1.047200, -0.004300, -0.008000,
     1             -0.002800,  0.000000,  0.000000/
*
***** REGION 5 19H N1-N6
*
      DATA I5T2N / 1, 0, 0, 0/
*
***** REGION 5 22V C1-C6
*
      DATA R5T3C / 1.051300, -0.011100, -0.008000,
     1             -0.005500,  0.000000,  0.000000/
*
***** REGION 5 22V N1-N6
*
      DATA I5T3N / 1, 0, 0, 0/
*
***** REGION 5 37V C1-C6
*
      DATA R5T4C / 1.042200, -0.022500, -0.003200,
     1             -0.002200,  0.000000,  0.000000/
*
***** REGION 5 37V N1-N6
*
      DATA I5T4N / 1, 0, 0, 0/
```

```
*
***** REGION 5 37H C1-C6
*
      DATA R5T5C / 1.042800, -0.027200, -0.001000,
     1             -0.000400,  0.000000,  0.000000/
*
***** REGION 5 37H N1-N6
*
      DATA I5T5N / 1, 0, 0, 0/
*
***** REGION 5 85V C1-C6
*
      DATA R5T6C / 1.034100, -0.014200, -0.004000,
     1             -0.003700,  0.000000,  0.000000/
*
***** REGION 5 85V N1-N6
*
      DATA I5T6N / 1, 0, 0, 0/
*
***** REGION 5 85H C1-C6
*
      DATA R5T7C / 1.035900, -0.020100, -0.002700,
     1             -0.000900,  0.000000,  0.000000/
*
***** REGION 5 85H N1-N6
*
      DATA I5T7N / 1, 0, 0, 0/
*
      END
*ENDIF
```